Identification of novel MONOPTEROS target genes in embryonic root initiation

Barbara Karoline Möller

Thesis committee

Thesis supervisor
Prof. dr. S.C. de Vries
Professor of Biochemistry
Wageningen University

Thesis co-supervisor
Dr. D. Weijers
Department of Biochemistry
Wageningen University

Other members
Prof. T. Bisseling, Wageningen University
Dr. R. Heidstra, Utrecht University
Dr. S. Sabatini, Sapienza University of Rome, Italy
Prof. dr. T. Beeckman, VIB, Ghent University, Belgium

This research was conducted under the auspices of the Graduate School of Experimental Plant Sciences.

Identification of novel MONOPTEROS target genes in embryonic root initiation

Barbara Karoline Möller

Thesis
submitted in fulfilment of the requirements for the degree of doctor
at Wageningen University
by the authority of the Rector Magnificus
Prof. dr. M. J. Kropff,
in the presence of the
Thesis Committee appointed by the Academic Board
to be defended in public
on Friday 1 June 2012
at 4 p.m. in the Aula.

Barbara K. Möller
Identification of novel MONOPTEROS target genes in embryonic root initiation
189 pages

Thesis, Wageningen University, Wageningen, NL (2012)
With references and summaries in English and Dutch
ISBN 978-94-6173-239-2

Contents

Chapter 1

Auxin control of embryo patterning

Barbara Möller and Dolf Weijers

Cold Spring Harb Perspect Biol. 1(5):a001545.

Laboratory of Biochemistry, Wageningen University, Dreijenlaan 3, 6703HA Wageningen, the Netherlands

Abstract

Plants start their life as a single cell which, during the process of embryogenesis, is transformed into a mature embryo with all organs necessary to support further growth and development. Therefore, each basic cell type is first specified in the early embryo, making this stage of development excellently suited to study mechanisms of coordinated cell specification – pattern formation. In recent years it has emerged that the plant hormone auxin plays a prominent role in embryo development. Most pattern formation steps in the early Arabidopsis embryo depend on auxin biosynthesis, transport and response. In this chapter we will describe those embryo patterning steps that involve auxin activity, and we will review recent data that shed light on the molecular mechanisms of auxin action during this phase of plant development.

Establishment of the embryo body plan

All plants start as a zygote and generate a mature embryo with one or two cotyledons, an embryonic stem and embryonic root. However, the trajectories of cell divisions leading to the final shape can be dramatically different between species (Johri *et al*., 1992). As the division patterns, and hence cell ontogeny relationships are particularly regular in Arabidopsis, this species has been used as a model for most embryogenesis research. For this reason we will focus our discussion on Arabidopsis.

Two axes are formed during embryogenesis: the apical-basal (upper-lower) and radial (outer-inner) axes, and each serves as a reference for post-embryonic development. The future apical-basal axis is already apparent before fertilization by the intrinsic polarity of the egg cell (Mansfield and Briarty 1991; Laux and Jürgens 1997). This cell has its nucleus and most of the cytoplasm at one side of the cell and a large vacuole at the opposite end. After fertilization, the zygote elongates and divides asymmetrically in a smaller apical cell and a larger, highly vacuolated basal cell. The apical cell goes through two rounds of longitudinal divisions followed by a transverse division to form the 8-cell proembryo. A number of transverse divisions of the basal cell produce a cell file called the suspensor (Figure 1). At the 8-cell stage three regions can be distinguished along the apical-basal axis: the upper tier of the proembryo, the lower tier of the proembryo, and the extra-embryonic suspensor cells. The apical tier of the proembryo will give rise to the shoot meristem and most of the cotyledons, while the lower tier of the proembryo will form the abaxial part of the cotyledons, the hypocotyl, root and root meristem initials. The suspensor pushes the embryo into the lumen of the ovule and serves as connection between the developing embryo and the maternal tissues.

The radial axis emerges when cells of the 8-cell proembryo divide periclinally to give rise to the protoderm and ground tissue lineages (Jürgens 1995). The proembryo now consists of 16 cells and is at the dermatogen stage. At the 32-cell globular stage the uppermost suspensor cell, called the hypophysis, divides asymmetrically to form an upper lens-shaped cell and a lower cell. These cells will be incorporated into the embryo to form the quiescent center and the columella root cap cells, respectively. At the transition-stage of embryogenesis, the radial symmetry of the apical region of the embryo changes into a bilateral symmetry when the cotyledons arise from the flanks of the apical domain. At approximately the same time the shoot meristem is established between the emerging cotyledons.

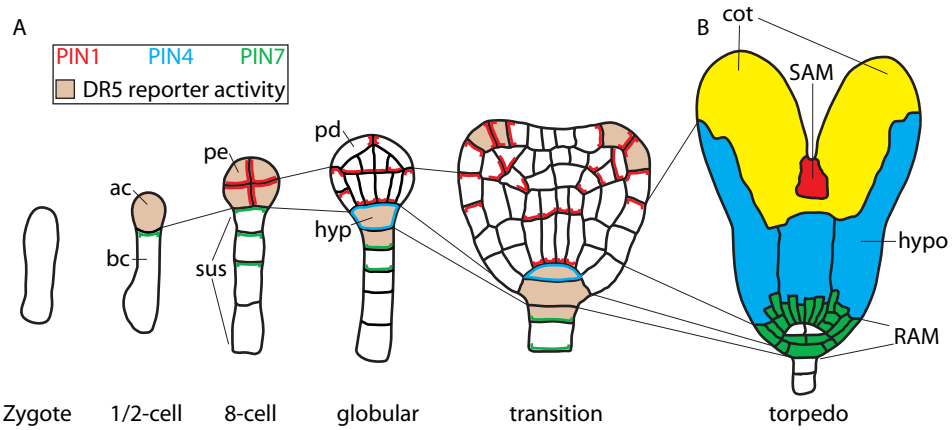

Figure 1: Cell lineages, PIN protein localization and auxin response maxima during Arabidopsis embryogenesis. Arabidopsis embryos follow a regular cell division pattern, for which a stereotype is depicted. Lineages are indicated by thin lines between individual stages. PIN protein localization at membranes is marked with red (PIN1), blue (PIN4) and green (PIN7) lines and DR5 reporter activity is indicated by pink color. (A) After division of the zygote, the 1-cell embryo (same for 2-cell embryo) expresses PIN7 in the basal daughter cell (bc), the protein pointing toward the apical cell (ac), which expresses the DR5 reporter. Subsequently, after two more cell division rounds, all proembryo (pe) cells express PIN1, without apparent polarity, and show DR5 reporter activity. Basal suspensor (sus) cells express PIN7, which is polarly localized pointing towards the proembryo. At the globular stage, basal PIN1 polarity is established in the central lower cells of the proembryo, while PIN1 localizes apically in outer protoderm (pd) cells. At the same time, PIN7 polarity reverses in suspensor cells, and PIN4 is activated in the uppermost suspensor cell. This cell now expresses the DR5 reporter, and is specified as hypophysis (hyp). During the transition stage, PIN1 polarity at the flanks of apical embryo half converges in adjacent cells, which is accompanied by the appearance of new DR5 maxima. These sites mark the initiation of the cotyledons. (B) At the torpedo stage, primordial for each of the seedling organs can be distinguished. Discrete regions of the embryo give rise to the root apical mersitem (RAM, green; note, white cells correspond to the future queiescent center), the hypopcotyl (hypo, blue), the cotyledons (cot, yellow) and the shoot apical meristem (SAM, red).

Mechanisms of pattern formation

Embryogenesis starts with a single cell, the zygote, and ends with a mature embryo in which all cells have acquired a specific fate. The organized division and specification of cells during embryogenesis is called pattern formation. The processes that generate all of these different cell types from the zygote remain largely unknown. The highly organized cell divisions observed during embryogenesis in Arabidopsis do not seem to be critically important for axis formation and cell fate specification, as embryos mutant for the *FASS* gene have a completely altered pattern of cell divisions but still contain all cell types that build the basic body plan, and show a relatively normal axis (Torres-Ruiz and Jürgens 1994). What mechanisms are involved in pattern formation? Conceptually, when focusing on those patterning steps that involve asymmetric cell divisions, two mechanisms of pattern formation can be envisioned (Laux and Jürgens 1997). Firstly, a cell with intrinsic polarity divides to generate two different daughter cells. Given the strong polarity of the egg cell and the hypophysis, this scenario could well apply to the division of these cells. Alternatively, initially identical daughter cells acquire different identities after division. This type of pattern formation requires cell-cell communication to ensure that the position, rather than lineage, of a cell determines its fate. The latter mechanism could also work over longer distances, to pattern fields of cells. In this context, an ever-increasing body of evidence shows that the plant hormone auxin is required for pattern formation (see Jenik *et al*., 2007 for a recent review). Importantly, all processes required for auxin activity - biosynthesis and transport, auxin perception by its receptor and auxin response - are each required for pattern formation. In this chapter we will review the patterning steps that require auxin activity, focusing on recent findings that illuminate the mechanism of auxin action.

Auxin controls major cell specification events during embryogenesis

Mutations in genes involved in auxin biosynthesis, transport and response all result in embryo defects that can be grouped in a number of distinct phenotypes. These phenotypes reveal specific cell divisions and cell specification events that are controlled by auxin during embryogenesis and are summarized in Figure 2. The auxin-related phenotypes occur around three developmental stages. The first anomaly observed in a number of "auxin" mutants is the aberrant transverse division of the apical daughter cell just after zygote division. The second patterning step affected in "auxin" mutants is hypophysis division at the 32-cell stage. At the same time the vascular precursor cells of the proembryo divide irregularly in a subset of auxin signaling mutants. Finally, from the transition-stage onwards, the initiation, outgrowth and correct separation of cotyledons is affected in many

"auxin" mutants. Furthermore, the hypophysis defect often results in rootless seedlings while the cotyledon initiation and separation defects result in seedlings with fused cotyledons, an aberrant number of cotyledons, asymmetric cotyledons or the complete absence of cotyledons.

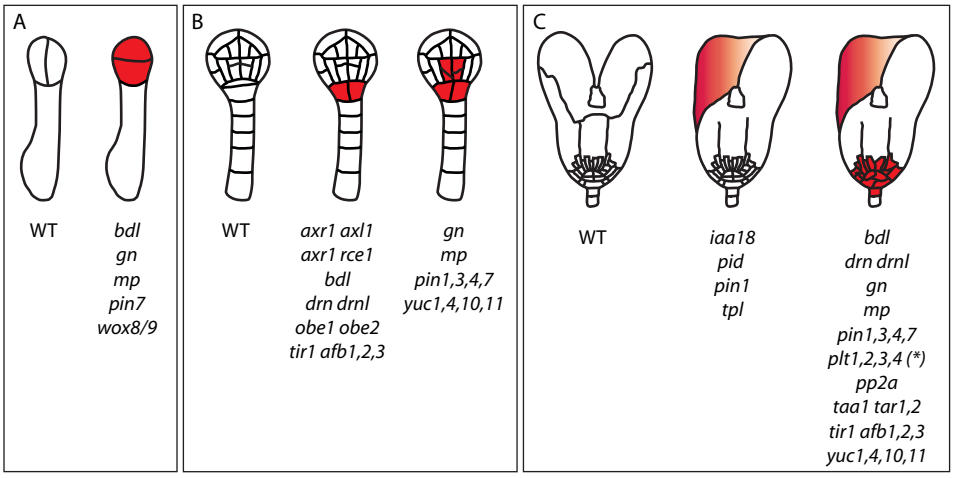

Figure 2: Distinctive embryo phenotypes of auxin mutants. Characteristic defects of auxin-related mutants at three different stages of embryo development. The figures show examples of defects (red) that can occur at each developmental stage. (A) Transverse, instead of longitudinal division of the apical cell at the 1-cell stage. (B) At the globular-stage, two phenotypes can be distinguished. Either (left), the hypophysis divides aberrantly, resulting in a rootless seedling, or in addition also vascular divisions are incorrect. (C) At the heart-stage, embryo cotyledon formation and/or separation are impaired, resulting in cotyledon fusion, an aberrant cotyledon number or complete absence of cotyledons. Other auxin related mutants have both cotyledon and root meristem defects. The root meristem defects in such mutants are the result of aberrant hypophysis division, except for the *plt1 plt2 plt3 plt4* mutant (*) where the hypophysis descendants divide abnormally.

Auxin concentrations cannot be visualized directly, which greatly hampers the understanding of auxin-dependent pattern formation. However, auxin induces the expression of the gene expression reporter DR5. Despite the shortcomings discussed below, DR5 reporter activity can be used to infer sites of auxin activity during embryogenesis (Friml *et al*., 2003; Figure 1). DR5 is first expressed in the apical cell after zygote division. DR5 expression rapidly increases in the descendants of the apical cell until the 32-cell stage, then the maximum of DR5 activity shifts basally into the uppermost suspensor cells including the hypophysis. At the transition-stage of embryogenesis DR5 maxima appear at the flanks of the apical domain where the cotyledons initiate. The sites of DR5 activity align very well with the defective cell divisions in "auxin mutants" (Figure 2), suggesting that

the DR5 reporter does indeed reveal auxin responses that are relevant for pattern formation in the embryo.
In summary, regulated auxin maxima and activity are required for the organization of both the apical and basal embryo domains and are therefore critical for the establishment of the embryo pattern.

Role of auxin biosynthesis in embryo development
Auxin is synthesized from indole via tryptophan, or independent of tryptophan (Tao *et al*., 2008). Of the two, the Trp-dependent route is most well-understood, and bifurcates into at least three routes (Figure 3A). Biosynthetic enzymes in two of these routes have non-redundant roles in embryogenesis. *TRYPTOPHAN AMINOTRANSFERASE OF ARABIDOPSIS* (*TAA1*) and its closest homologs *TRYPTOPHAN AMINOTRANSFERASE RELATED (TAR)1* and *2* function in one of these two Trp-dependent IAA biosynthesis routes (Stepanova *et al*., 2008; Tao *et al*., 2008). The other branch of the Trp-dependent IAA biosynthesis pathway is represented by the *YUCCA (YUC)* family of flavin mono-oxygenases. Arabidopsis has 11 functionally equivalent *YUC* genes of which *YUC1*, *4*, *10* and *11* have been shown to be expressed in the embryo in overlapping patterns (Cheng *et al*., 2007). Both *TAR1* and *YUC1*, *4*, *10* and *11* are expressed from the globular stage on in the apical embryo region. Embryo defects in the *yuc1 yuc4 yuc10 yuc11* quadruple mutant and in the *taa1 tar1 tar2* triple mutant occur as early as the globular stage when the hypophysis divides abnormally. Seedlings do not have a root, a strongly reduced or no hypocotyl and most of the seedlings have only one cotyledon.
Interestingly, mutations in either of the two IAA biosynthesis pathways cause similar embryonic phenotypes (Figure 2), suggesting that both IAA biosynthesis routes are required to provide sufficient auxin for correct regulation of division patterns in the apical and basal region of the embryo. While defects in *yuc1 yuc4 yuc10 yuc11* quadruple and *taa1 tar1 tar2* triple mutants are observed in both apical and basal patterning, the genes are most prominently, if not exclusively, expressed in the embryo apex. The basal embryo phenotype could be explained by low but significant *YUC* and *TAA/TAR* gene expression in the basal half of the embryo. Alternatively, and perhaps more likely, auxin produced in the apical half of the embryo may be transported to elicit auxin responses in the lower half of the embryo.

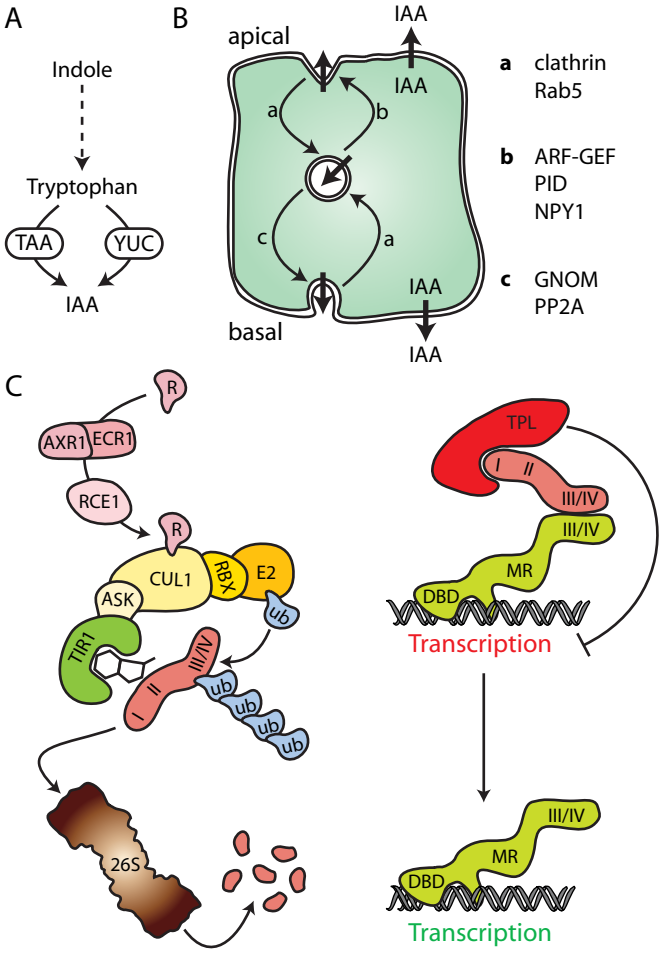

Figure 3: Auxin signaling involves auxin biosynthesis, transport, perception and response. (A) In Arabidopsis, the auxin IAA (Indole-3-acetic acid) is synthesized from indole through tryptophan or in a tryptophan-independent way. Biosynthetic enzymes in two tryptophan-dependent routes of IAA biosynthesis - the TAA and YUC proteins - have non-redundant roles in embryo development. (B) Auxin transport is mediated by the polar membrane localization of the PIN proteins (Arrows), which in turn is regulated by several factors. The endocytosis of PIN proteins from the membrane to endosomes is clathrin-dependent (a), while the targeting of PIN proteins to the apical membrane depends on a (yet unknown) ARF-GEF and the kinase PID (b). The recycling of PIN proteins to the basal membrane depends on the ARF-GEF GNOM and the PP2A phosphatases (c). (C) When auxin is perceived by its receptor TIR1, the affinity for the Aux/IAA proteins increases. The Aux/IAAs are subsequently ubiquitinated and degraded by the 26S proteasome. The ubiquitination of Aux/IAAs in Arabidopsis involves an ubiquitin activating enzyme (E1, not shown), an ubiquitin conjugating enzyme (E2) and the ubiquitin ligase (E3) SCF^{TIR1} that consists of a cullin protein, an RBX protein, the ASK proteins and the F-Box protein TIR1. Under low auxin concentrations the Aux/IAA proteins bind and inhibit the ARF proteins by recruiting the TPL co-repressor. When auxin levels rise the Aux/IAA proteins are ubiquitinated and degraded, thereby releasing the ARF proteins to exert their function as transcriptional activators or repressors.

Role of auxin transport in embryogenesis

Auxin is unique among plant hormones as it has a dedicated transport system. The direction of auxin transport is determined by the asymmetric membrane localization of the efflux carriers, the PIN proteins. Already prior to the identification of the PIN proteins, it was shown that pharmacological inhibition of auxin transport interferes with normal embryo patterning in several plant species (Liu *et al*., 1993; Hadfi *et al*., 1998), demonstrating a role for auxin transport in embryo patterning. At least four PIN proteins are dynamically expressed during embryogenesis (Friml *et al*., 2003; Figure 1). Immediately after the division of the zygote, PIN7 is localized to the apical side of the basal cell and its derivatives, presumably driving auxin transport into the apical cell. At the 32-cell stage PIN7 polarity reverses to the basal membranes of the suspensor cells, probably resulting in auxin transport into the suspensor cells. PIN1 is expressed without any polarity in the embryo from the one-cell to the 16-cell stage. At the 32-cell stage PIN1 becomes polarly localized to the basal membranes in the provascular cells next to the hypophysis, and transports auxin into the hypophysis. At the transition-stage of embryogenesis PIN1 becomes polarly localized towards the flanks of the apical embryo domain which likely results in auxin maxima at these sites. The PIN4 protein is expressed in the hypophysis cell and after division, in its uppermost daughter cell. The expression of PIN3 starts relatively late at the heart-stage in the columella precursors.

The direction of auxin flow predicted by PIN protein localization corresponds well to the expression pattern of the auxin response reporter, suggesting that auxin response maxima reflect the concentration of auxin, and that this concentration pattern follows from active transport. Indeed *pin7* mutant embryos are affected in the DR5 activity in the early embryo and display associated cell division defects, suggesting that a proper auxin distribution and response is required for correct cell specification in the early embryo. Loss of PIN functionality disrupts embryo formation in a quantitative manner: the more PIN proteins are lost, the stronger the embryo phenotype (Figure 2).

Several factors are important for correct PIN gene expression and protein localization (Figure 3B). Mutations that cause altered PIN gene expression affect the same patterning processes described above in more or less predictable ways (Izhaki and Bowman 2007; Ploense *et al*., 2009). It was found that PIN proteins are not statically localized in the membrane, but rather cycle between membrane and intracellular vesicles through endo- and exocytosis. The endocytosis of PIN proteins from the plasma membrane to endosomes is clathrin-dependent (Dhonukshe *et al*., 2007; Dhonukshe *et al*., 2008). The recycling of PIN proteins from endosomes to the basal plasma membrane requires the ARF-GEF protein GNOM

(Mayer *et al*., 1993; Geldner *et al*., 2003). Other ARF-GEFs control the recycling of proteins to the apical plasma membrane (Kleine-Vehn *et al*., 2008). The serine-threonine kinase *PINOID (PID)* and the *PROTEIN PHOSPHATASE 2A (PP2A)* antagonistically control the phosphorylation status of PIN proteins (Bennett *et al*., 1995; Benjamins *et al*., 2001; Friml *et al*., 2004; Michniewicz *et al*., 2007). Phosphoryated PIN proteins are targeted to the apical plasma membrane, while dephosphorylated PIN proteins are targeted to the basal plasma membrane. There are at least three PID homologs which are also expressed during embryogenesis (Cheng *et al*., 2008).
Interference with any of these processes results in abnormal PIN polarity and altered expression patterns of the auxin response reporter DR5. The phenotypes associated with mutants that affect PIN localization are very similar to the phenotypes of the auxin efflux carrier mutants (Figure 2). Although mutation in each of these components has a different effect on PIN protein distribution, generally defects correspond well with the predicted auxin mis-distribution that would follow. In summary, changes in PIN expression or localization result in an altered auxin distribution which in turn causes defects in embryo specification.

Auxin perception

Auxin elicits gene expression responses by binding to the F-box protein TIR1, hence increasing the affinity of TIR1 for the Aux/IAA family of transcriptional inhibitors. When the auxin concentration is high, auxin resides in the binding pocket of TIR1 and serves as a molecular glue to bring the Aux/IAAs and the auxin receptor together *(*Dharmasiri *et al.,* 2005a; Kepinski and Leyser, 2005; Tan *et al*., 2007). Once bound to the auxin receptor, Aux/IAAs are ubiquitinated and subsequently degraded by the 26S proteasome (Figure 3C). In Arabidopsis TIR1 functions in the SCF^{TIR1} complex, which consists of the F-Box-protein TIR1, the ring finger protein RBX1, the cullin protein CUL1, and the ASK proteins (Gray *et al*., 2002; Shen *et al*., 2002; Liu *et al*., 2004). Related-to-ubiquitin (RUB) modification of the CUL1 subunit of the SCF complex is important for its function (Dharmasiri *et al*., 2003) and involves the activity of a heterodimeric RUB activating enzyme composed of ECR1 and AXR1 or the redundantly acting AXL, a RUB conjugating enzyme RCE1 and the RBX1 protein of the SCF complex which serves as a RUB ligase (Figure 3C; Gray *et al*., 2002; Dharmasiri *et al*., 2007).
Mutations in the TIR1 subunit of the SCF^{TIR1} complex are not affected in embryo development due to redundancy with the closely related *AUXIN SIGNALING F-BOX PROTEINS (AFB) 1*, *2* and *3* (Dharmasiri *et al*., 2005b). Expression of *TIR1* and *AFB1*, *2* and *3* is detected throughout embryogenesis starting in the preglobular embryo. The *tir1/afb1/afb2/afb3* quadruple mutant often fails to make a root

and hypocotyl and frequently has only one cotyledon (Figure 2). As expected, levels of Aux/IAA proteins like IAA12/BDL are increased in the *tir1 afb2 afb3* triple mutant (described below).
The Arabidopsis genome encodes approximately 700 different F-box proteins (Gagne *et al*., 2002), of which four have been shown to bind to the Aux/IAA proteins. The other subunits of the SCF complex are not specific for auxin signaling. Nonetheless, all subunits of the SCF complex as well as the RUB modification of the cullin subunit are important for proper embryo development. The phenotypes of ubiquitin-ligase SCF complex mutants and mutants affecting RUB modification of CUL1 include defects in auxin regulated processes (Figure 2). Collectively, these results show that auxin perception by its receptor and the subsequent degradation of Aux/IAAs are required for embryogenesis, and the defects observed when these components are inactive are the same as when biosynthesis or transport are impaired.

Auxin response in the embryo is mediated by Auxin Response Factors
Auxin promotes the degradation of Aux/IAA proteins, short-lived nuclear proteins. When sufficiently abundant, Aux/IAA proteins bind to and inhibit the activity of another class of auxin response transcriptional regulators, the AUXIN RESPONSE FACTORS (ARFs). When auxin is perceived by its receptor, Aux/IAAs are degraded thereby releasing the ARFs to exert their function as activators or repressors of transcription. Among the 23 ARFs in Arabidopsis, five have been shown to be transcriptional activators in carrot protoplasts, whereas the remaining 18 ARFs may act as repressors (Ulmasov *et al*., 1999; Tiwari *et al*., 2003). The transcriptional activator MONOPTEROS (MP)/ARF5 is critical for embryogenesis since the *mp* loss-of-function mutant shows defects in most auxin-dependent embryo patterning processes (Figure 2). In addition, ARF7 and ARF17 contribute somewhat to cotyledon development, and it is possible that there is further redundancy between other members of the family. However, most of the defects seen in auxin biosynthesis, transport or receptor mutants can be explained by the altered activity of MP/ARF5, which defines a complete pathway for auxin-dependent embryo development, from synthesis of the hormone to the activation of transcription.
In the next sections, we will discuss in more detail the two auxin-dependent processes that have been studied in most detail: root meristem formation and the specification of the shoot apical meristem and cotyledons.

Role of auxin response in root initiation

MP activity is required to specify the hypophysis, and a loss-of-function *mp* mutant shows aberrant hypophysis division resulting in a rootless phenotype (Berleth and Jürgens 1993; Weijers *et al*., 2006; Figure 2). The gain-of-function *bdl/iaa12* mutant encoding a stabilized version of BDL/IAA12 has the same phenotype (Hamann *et al*., 1999; Hamann *et al*., 2002; Figure 2). It was shown that BDL binds to MP and inhibits its transcriptional activity. In the early globular stage embryo MP and BDL proteins accumulate in all sub-epidermal cells, but not in the hypophysis. (Weijers *et al*., 2006). Hence, MP acts non-autonomously in hypophysis specification as MP activity is required in the cells adjacent to the hypophysis to specify this cell (Figure 4). Interestingly, among the non-autonomous signals that could mediate MP-dependent cell communication in hypophysis specification is auxin itself. DR5 activity in the hypophysis is lost in the *mp* mutant and PIN1 levels are reduced in the *mp* mutant. However, since exogenous auxin treatments do not restore hypophysis specification in *mp* or *bdl* mutant embryos, auxin alone does not seem sufficient for specifying the uppermost suspensor cell as hypophysis. Therefore, auxin is unlikely to be the only signal downstream of *MP*. The nature of the other signal(s) is currently unknown. The fact that auxin elicits a response in the future hypophysis suggests that there must be another auxin machinery consisting of an ARF and an Aux/IAA in this cell (Figure 4).

Exactly how MP activity is restricted to the cells adjacent to the hypophysis and what genes are activated by MP is currently unknown. In part, MP activity is controlled by the activity of BDL. It was recently shown that BDL interacts with TOPLESS (TPL), a transcriptional co-repressor (Long *et al*., 2002; Long *et al*., 2006; Szemenyei *et al*., 2008). Importantly, the rootless phenotype of the *bdl* mutant is suppressed by mutations in the ubiquitously expressed *TPL* gene. Expression of a fusion protein containing the carboxy terminus of TPL and the C-terminal dimerization domain of BDL under the control of the *BDL* promoter results in *mp*-like phenotypes. This demonstrates that BDL inhibits MP by recruiting the TPL co-repressor (Figure 3C). *tpl* mutant embryos either lack cotyledons (Figure 2) or show a transformation of the apical pole into a second root. The formation of a second root is not dependent on *MP*. So far there is no good explanation for the *tpl* phenotypes, but it is likely that TPL represses root-promoting genes.

There is only a limited number of genes whose function has been suggested to act downstream of MP in root initiation. Among the few are the *PLETHORA (PLT)* genes. Mutations in two or more of these AP2-type transcription factors *PLT*, *PLT2*, *PLT3* and *PLT4/BABY BOOM (BBM)* interfere with divisions of the hypophyseal derivatives, resulting in the absence of a quiescent center (QC) at early

heart stage (Aida *et al*., 2004; Galinha *et al*., 2007; Figure 2). DR5 expression is not affected in *plt1 plt2* double mutants, indicating that auxin response is not impaired. Being activated hours after auxin treatment, the *PLT* genes appear to be late auxin response genes and are therefore probably not direct targets of an ARF. Nonetheless, the expression of the *PLT* genes is partially dependent on MP activity, as *PLT1* and *PLT2* expression is lost in globular and heart-stage *mp* embryos, but not in the octant-stage *mp* embryo. Post-embryonically, ectopic *PLT* expression induces the formation of ectopic roots in the shoot. Therefore, *PLT* genes are master genes in root meristem development and are part of the developmental program that is activated by auxin during root initation.

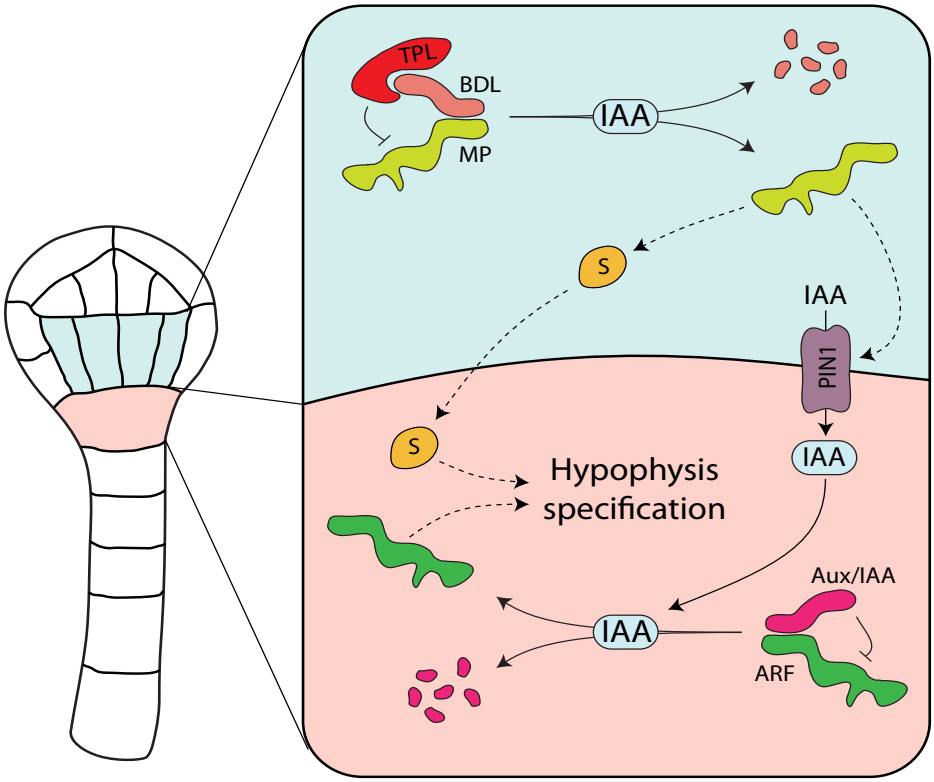

Figure 4: Hypophysis specification in the globular-stage embryo. MP activity is required non-cell autonomously in the provascular cells (light blue) adjacent to the uppermost suspensor cell (pink) to specify this cell as hypophysis. In the provascular cells, high auxin levels release MP from its inhibitor, the Aux/IAA protein BDL and the co-repressor TPL. Subsequently, MP induces the expression of *PIN1* in the provascular cells, resulting in auxin transport to the uppermost suspensor cell. MP also promotes the transport of a hypothetical signal (S) to the future hypophysis. Here, auxin releases another yet unidentified ARF from a so far unknown Aux/IAA protein to elicit an auxin response that converges with S to specify the hypophysis fate.

Correct control of MP-dependent root initiation may also involve chromatin regulation, as mutations in the plant homeodomain finger (PHD) proteins *OBERON (OBE) 1* and *2* affect root meristem initiation (Saiga *et al*., 2008; Thomas *et al*., 2009). *obe1 obe2* double mutants show aberrant hypophysis division and are rootless (Figure 2), have a disorganized shoot meristem and leaf formation arrests before or after the formation of the first pair of leaves. PHD finger proteins specifically recognize a modification of histone H3 that marks active genes. *OBE1* and *2* are expressed throughout the embryo from the four-cell stage on. The expression of the *PLT* genes but not *MP* is lost in the *obe1 obe2* double mutant. Furthermore, *MP* is epistatic to *OBE*, but is not required for *OBE* expression. The establishment of auxin response maxima in *obe1 obe2* double mutant embryos is largely similar to the wild-type pattern. This suggests that OBE functions downstream of MP to control root meristem development. It is possible that *OBE* modifies the chromatin at MP target loci to make the promoters more accessible.

Role of auxin in shoot meristem formation and cotyledon formation

At the transition-stage of embryogenesis the cotyledons initiate at the flanks of the apical embryo domain at the sites where the auxin response reporter DR5 is highly expressed (Benkova *et al*., 2003). In between, the shoot meristem is specified (Mayer *et al*., 1998). The *CUP-SHAPED COTYLEDON (CUC)* genes *1* and *2* redundantly regulate the initiation of the shoot meristem and the separation of cotyledons together with *SHOOT MERISTEMLESS (STM)* (Barton and Poethig 1993; Aida *et al*., 1997; Aida *et al*., 1999). *CUC1, CUC2* and *STM* are expressed between the presumptive cotyledon primordia in the globular stage embryo. At the bending-cotyledon stage, *CUC1* and *2* expression is restricted to the cotyledon margins while *STM* is only expressed in the SAM.

Mutations in *MP*, *PID* and *PIN1* all affect cotyledon separation and the bilateral symmetry of the cotyledons (Figure 2). Examination of the *CUC* gene expression in *mp* , *pin1 and pin1 pid* embryos revealed that all these genes are required for the activation of *CUC2* in cotyledon boundaries and the repression of CUC1 in cotyledons (Aida *et al*., 2002; Furutani *et al*., 2004). Importantly, mutation of *CUC1* in the *pin1pid* double mutant partially restores cotyledon development, suggesting that the cotyledon formation defect is at least in part the consequence of ectopic *CUC1* activity. Presumably, *PIN1* and *PID* ensure the generation of an auxin maximum that is required control *CUC* gene expression during cotyledon initiation and separation. It is unclear if MP directly regulates the *CUC* genes in response to the auxin peak supplied by PID/PIN, or whether MP mainly acts to promote proper *PIN1* gene expression.

As indicated earlier, few (potential) target genes of auxin response machinery in

the embryo are known. Recently it was shown that *DORNRÖSCHEN (DRN)* is such a direct target (Chandler *et al*., 2007; Cole *et al*., 2009). DRN encodes an AP2-type transcription factor and acts redundantly with its paralog *DRN-LIKE (DRNL)* in cotyledon development. Double homozygous *drn drnl* embryos have pin-like structures without cotyledons (Figure 2). DRN has a very dynamic expression pattern in embryo development. From the two-cell till the 16-cell stage DRN is expressed throughout the embryo, then becomes restricted to the apical domain at the sites where the cotyledon primordia will emerge and finally is expressed at the tips of the cotyledons in the heart-stage embryo. The expression of the auxin response reporter DR5 and the localization of the PIN1 protein are changed in *drn drnl* double mutant embryos. Since *DRN* is an MP target, but also itself controls auxin transport, this gene acts both downstream of auxin and upstream of auxin transport. Even though MP and DRN expression overlap to a large extent, *DRN* expression only depends on MP in the tips of the cotyledons. *drn drnl* embryos also show hypophyseal cell defects (Figure 2) although the genes are not expressed in the basal region of the embryo. The non-autonomous action of these genes in root formation may depend on their influence on auxin transport.
Gain-of-function mutations in two Aux/IAA proteins also result in cotyledon defects. The gain-of-function *iaa18* mutation that stabilizes IAA18 causes aberrant cotyledon outgrowth in three to eight percent of the embryos (Ploense *et al*., 2009; Figure 2). *IAA18* is expressed in the apical domain of the embryo from the 16-cell stage on. In the gain-of-function *iaa18* mutant *PIN1* is asymmetrically expressed with stronger expression in one side of the embryo. This probably contributes to the cotyledon defects in *iaa18* embryos. IAA18 can inhibit MP activity when ectopically expressed in the embryo, and overexpression of *MP* rescues several postembryonic leaf defects in the *iaa18* mutant. However, MP can not be the only target of IAA18 as *mp iaa18* mutants are more severe than the single mutants. The gain-of-function *bdl* mutant also has cotyledon defects. Likewise, *mp bdl* embryos have cotyledon defects, indicating that BDL must have other targets in addition to MP (Hamann *et al*., 1999).

Convergence of *ARF* and *WOX* transcription factor activities in early embryogenesis. The prominent role of auxin in patterning the early embryo is becoming increasingly clear. However, several other pathways have also been shown to operate in patterning. It will be interesting to see how these are interwoven at the molecular level. One example of such integration is the convergence of MP and WOX functions. The members of the *WUSCHEL related homeobox (WOX)* transcription factor gene family are differently expressed in the early embryo (Haecker *et al*. 2004). *WOX2* and *WOX8* are both expressed in the egg cell

and the zygote. After the division of the zygote, expression of *WOX2* marks the apical cell whereas *WOX8* is expressed in the basal cell. In the 8-cell embryo *WOX2*, *WOX8* and *WOX9* are expressed in four different regions. The apical tier of the proembryo expresses *WOX2*, the lower tier of the proembryo expresses *WOX9*, the uppermost suspensor cell expresses both WOX8 and WOX9 and the other suspensor cells express only *WOX8*.
From the 8-cell stage to the 16-cell stage *WOX9* expression expands in the descendents of the lower tier of the 8-cell proembryo and is lost in the uppermost suspensor cell. This shift of *WOX9* expression from the uppermost suspensor cell to the embryo does not occur in *mp* embryos, indicating that MP is required for both activation of WOX9 in embryo cells and downregulation of WOX9 in the hypophysis (Breuninger *et al*. 2008). There are more points of convergence between MP and WOX genes. The *wox2* mutant shows defects in cell divisions in the apical embryo domain, and this is strongly enhanced in the *wox2 mp* mutant. Similarly, the *mp wox8 wox9* triple mutant shows synergistic phenotypes. The *wox8 wox9* double mutant shows strong defects in both the apical and the basal cell lineage (Figure 2), in part because the expression of *WOX2* is lost. This is accompanied by loss of PIN1 expression and ubiquitous DR5 activity. These results show that WOX2, 8 and 9 and MP control the same embryo patterning processes. Therefore, embryo patterning is controlled by auxin in concert with other, potentially auxin-independent pathways.

Role of auxin in pattern formation

As detailed above, auxin controls several cell specification and pattern formation processes in the early embryo. The obvious question is how a molecule that is structurally so simple can elicit such different responses. In post-embryonic auxin-dependent growth and patterning, auxin has been proposed to accumulate in concentration gradients, with cells converting different threshold concentrations to distinct responses (Galinha *et al*., 2007). However evidence for concentration-dependent readout is still lacking. The other conceptual extreme of auxin activity would be that of a trigger that would elicit a predefined response above a certain threshold. While in the former scenario, multiple distinct responses are specified by the perceived auxin concentration, in the latter, there would be an “all-or-nothing” response. While no definite answer can be given at this moment, it appears that alterations in auxin concentrations can not bypass the predefined cell fate in the embryo. For example, when auxin levels are ubiquitously increased through expression of a biosynthesis gene and inhibition of transport, DR5 is activated throughout the embryo (Weijers *et al*., 2005). However, this is associated with fusion of cotyledons, but no ectopic specification of pattern elements. Likewise,

removal of auxin causes a failure to specify the root or cotyledons, but no cell fate transformations. A plausible scenario is that a prepattern determines the developmental potential that can be triggered by auxin, where the concentration of auxin could determine response amplitude. However, reality may not be so simple, since a recent report suggests that inappropriate accumulation of auxin in cotyledon tips – either through expression of dominant-negative Rab5 or apolar PIN1 - is sufficient to convert these cells to root identity (Dhonukshe *et al*., 2008). Nonetheless, a critical open question in auxin-dependent embryo patterning remains the mode of auxin action. The size of the Aux/IAA and ARF families, as well as the presence of 5 TIR1/AFB receptors would allow enormous combinatorial complexity to equip each cell with a unique response machinery to enable unique cellular auxin responses. Systematic analysis of Aux/IAA and ARF functions in the embryo, as well as identification of target genes and processes of auxin in the embryo will provide critical insight into the prominent role of auxin as an embryo patterning molecule.

Acknowledgements

We apologize to those, whose valuable contributions we could not include due to space constraints. We wish to thank Cristina Llavata Peris, Annemarie Lokerse and Eike Rademacher for helpful comments on this manuscript. This work was supported by a grant from the Dutch Organization for Scientific Research (NWO; ALW-VIDI 864.06.012).

References

Aida M, Beis D, Heidstra R, Willemsen V, Blilou I, Galinha C, Nussaume L, Noh YS, Amasino R and Scheres B. (2004). The *PLETHORA* genes mediate patterning of the Arabidopsis root stem cell niche. Cell. 119(1): 109-120.

Aida M, Ishida T, Fukaki H, Fujisawa H and Tasaka M. (1997). Genes involved in organ separation in Arabidopsis: an analysis of the cup-shaped cotyledon mutant. Plant Cell. 9(6): 841-857.

Aida M, Ishida T and Tasaka M. (1999). Shoot apical meristem and cotyledon formation during Arabidopsis embryogenesis: interaction among the *CUP-SHAPED COTYLEDON* and *SHOOT MERISTEMLESS* genes. Development. 126(8): 1563-1570.

Aida M, Vernoux T, Furutani M, Traas J and Tasaka M. (2002). Roles of PIN-FORMED1 and MONOPTEROS in pattern formation of the apical region of the Arabidopsis embryo. Development. 129(17): 3965-3974.

Barton MK and Poethig RS. (1993). Formation of the shoot apical mersitem in *Arabidopsis thaliana*: an analysis of development in the wild type and in the *shoot meristemless* mutant. Develop-

ment. 119: 823-831.

Benjamins R, Quint A, Weijers D, Hooykaas P, and Offringa R. (2001). The PINOID protein kinase regulates organ development in Arabidopsis by enhancing polar auxin transport. Development. 128(20): 4057-4067.

Benková E, Michniewicz M, Sauer M, Teichmann T, Seifertová D, Jürgens G and Friml J. (2003). Local, efflux-dependent auxin gradients as a common module for plant organ formation. Cell. 115(5): 591-602.

Bennett RM, Alvarez J, Bossinger G and Smyth DR. (1995). Morphogenesis in *pinoid* mutants in *Arabidopsis thaliana.* Plant J. 8: 505-520.

Berleth T and Jürgens G. (1993). The role of the *MONOPTEROS* gene in organizing the basal body region of the Arabidopsis embryo. Development. 118: 575-587.

Breuninger H, Rikirsch E, Hermann M, Ueda M and Laux T. (2008). Differential expression of *WOX* genes mediates apical-basal axis formation in the Arabidopsis embryo. Dev Cell. 14(6): 867-876.

Chandler JW, Cole M, Flier A, Grewe B and Werr W. (2007). The AP2 transcription factors DORNRÖSCHEN and DORNRÖSCHEN-LIKE redundantly control Arabidopsis embryo patterning via interaction with PHAVOLUTA. Development. 134(9): 1653-1662.

Cheng Y, Dai X and Zhao Y. (2007). Auxin synthesized by the YUCCA flavin monooxygenases is essential for embryogenesis and leaf formation in Arabidopsis. Plant Cell. 19(8): 2430-2439

Cheng Y, Qin G, Dai X and Zhao Y. (2008). *NPY* genes and *AGC* kinases define two key steps in auxin-mediated organogenesis in Arabidopsis. Proc Natl Acad Sci USA. 105(52): 21017-21022.

Cole M, Chandler J, Weijers D, Jacobs B, Comelli P and Werr W. (2009). *DORNRÖSCHEN* is a direct target of the auxin response factor MONOPTEROS in the Arabidopsis embryo. Development. 136(10): 1643-1651

Dharmasiri N, Dharmasiri S and Estelle M. (2005a). The F-box protein TIR1 is an auxin receptor. Nature. 435(7041): 441-445.

Dharmasiri S, Dharmasiri N, Hellmann H and Estelle M. (2003). The RUB/Nedd8 conjugation pathway is required for early development in Arabidopsis. EMBO J. 22(8): 1762-1770.

Dharmasiri N, Dharmasiri S, Weijers D, Karunarathna N, Jürgens G and Estelle M. (2007). *AXL* and *AXR1* have redundant functions in RUB conjugation and growth and development in Arabidopsis. Plant J. 52(1): 114-123.

Dharmasiri N, Dharmasiri S, Weijers D, Lechner E, Yamada M, Hobbie L, Ehrismann JS, Jürgens G and Estelle M. (2005b). Plant development is regulated by a family of auxin receptor F-box proteins. Dev Cell. 9(1): 109-119.

Dhonukshe P, Aniento F, Hwang I, Robinson DG, Mravec J, Stierhof YD and Friml J. (2007). Clathrin-mediated constitutive endocytosis of PIN auxin efflux carriers in Arabidopsis. Curr Biol.

17(6): 520-527.

Dhonukshe P, Tanaka H, Goh T, Ebine K, Mahonen A.P, Prasad K, Blilou I, Geldner N, Xu J, Uemura T, Chory J, Ueda T, Nakano A, Scheres B and Friml J. (2008). Generation of cell polarity in plants links endocytosis, auxin distribution and cell fate decisions. Nature 456(7224): 962-966.

Friml J, Vieten A, Sauer M, Weijers D, Schwarz H, Hamann T, Offringa R and Jürgens G. (2003). Efflux-dependent auxin gradients establish the apical-basal axis of Arabidopsis. Nature. 426(6963): 147-153.

Friml J, Yang X, Michniewicz M, Weijers D, Quint A, Tietz O, Benjamins R, Ouwerkerk PB, Ljung K, Sandberg G, Hooykaas PJ, Palme K and Offringa R. (2004). A PINOID-dependent binary switch in apical-basal PIN polar targeting directs auxin efflux. Science. 306(5697): 862-865.

Furutani M, Vernoux T, Traas J, Kato T, Tasaka M, and Aida M. (2004). *PIN-FORMED1* and *PINOID* regulate boundary formation and cotyledon development in Arabidopsis embryogenesis. Development. 131(20): 5021-5030.

Gagne JM, Downes BP, Shiu SH, Durski AM and Vierstra RD. (2002). The F-box subunit of the SCF E3 complex is encoded by a diverse superfamily of genes in Arabidopsis. Proc Natl Acad Sci U S A. 99(17): 11519-11524.

Galinha C, Hofhuis H, Luijten M, Willemsen V, Blilou I, Heidstra R and Scheres B. (2007). PLETHORA proteins as dose-dependent master regulators of Arabidopsis root development. Nature. 449(7165): 1053-1057.

Geldner N, Anders N, Wolters H, Keicher J, Kornberger W, Muller P, Delbarre A, Ueda T, Nakano A and Jürgens G. (2003). The Arabidopsis GNOM ARF-GEF mediates endosomal recycling, auxin transport, and auxin-dependent plant growth. Cell. 112(2): 219-230.

Gray WM, Hellmann H, Dharmasiri S and Estelle M. (2002). Role of the Arabidopsis RING-H2 protein RBX1 in RUB modification and SCF function. Plant Cell. 14(9): 2137-2144.

Hadfi K, Speth V and Neuhaus G. (1998). Auxin-induced developmental patterns in *Brassica juncea* embryos. Development. 125(5): 879-887.

Haecker A, Gross-Hardt R, Geiges B, Sarkar A, Breuninger H, Herrmann M and Laux T. (2004). Expression dynamics of *WOX* genes mark cell fate decisions during early embryonic patterning in Arabidopsis thaliana. Development. 131(3): 657-668.

Hamann T, Mayer U and Jürgens G. (1999). The auxin-insensitive *bodenlos* mutation affects primary root formation and apical-basal patterning in the Arabidopsis embryo. Development. 126(7): 1387-1395.

Hamann T, Benkova E, Bäurle I, Kientz M and Jürgens G. (2002). The Arabidopsis *BODENLOS* gene encodes an auxin response protein inhibiting MONOPTEROS-mediated embryo patterning. Genes Dev. 16(13): 1610-1615.

Izhaki A and Bowman JL. (2007). *KANADI* and class III HD-Zip gene families regulate embryo patterning and modulate auxin flow during embryogenesis in Arabidopsis. Plant Cell. 19(2): 495-

508.

Jenik PD, Gillmor CS and Lukowitz W. (2007). Embryonic patterning in *Arabidopsis thaliana*. Annu Rev Cell Dev Biol. 23: 207-236.

Johri BM, Ambegaokar KB and Srivastava PS. (1992). Comparative embryology of Angiosperms. *Springer-Verlag, Berlin, Germany.*

Jürgens G. (1995). Axis formation in plant embryogenesis: cues and clues. Cell. 81(4): 467-470.

Kepinski S and Leyser O. (2005). The Arabidopsis F-box protein TIR1 is an auxin receptor. Nature. 435(7041): 446-451.

Kleine-Vehn J, Dhonukshe P, Sauer M, Brewer PB, Wisniewska J, Paciorek T, Benkova E and Friml J. (2008). ARF GEF-dependent transcytosis and polar delivery of PIN auxin carriers in Arabidopsis. Curr Biol. 18(7): 526-531.

Laux T and Jürgens G. (1997). Embryogenesis: A New Start in Life. Plant Cell. 9(7): 989-1000.

Liu C, Xu Z and Chua NH. (1993). Auxin polar transport is essential for the establishment of bilateral symmetry during early plant embryogenesis. Plant Cell. 5(6): 621-630.

Long JA, Ohno C, Smith ZR and Meyerowitz EM. (2006). TOPLESS regulates apical embryonic fate in Arabidopsis. Science. 312(5779): 1520-1523.

Long JA, Woody S, Poethig S, Meyerowitz EM and Barton MK. (2002). Transformation of shoots into roots in Arabidopsis embryos mutant at the *TOPLESS* locus. Development. 129(12): 2797-2806.

Mansfield SG and Briarty LG. (1991). Early embryogenesis in *Arabidopsis thaliana*. II. The developing embryo. Can J Bot. 69: 461-476.

Mayer KF, Schoof H, Haecker A, Lenhard M, Jürgens G and Laux T. (1998). Role of *WUSCHEL* in regulating stem cell fate in the Arabidopsis shoot meristem. Cell. 95(6): 805-815.

Mayer U, Büttner G and Jürgens G. (1993). Apical-basal pattern formation in the Arabidopsis embryo: studies on the role of the *GNOM* gene. Development. 117: 149-162.

Michniewicz M, Zago MK, Abas L, Weijers D, Schweighofer A, Meskiene I, Heisler MG, Ohno C, Zhang J, Huang F, Schwab R, Weigel D, Meyerowitz EM, Luschnig C, Offringa R and Friml J. (2007). Antagonistic regulation of PIN phosphorylation by PP2A and PINOID directs auxin flux. Cell. 130(6): 1044-1056.

Ploense SE, Wu MF, Nagpal P and Reed JW. (2009). A gain-of-function mutation in *IAA18* alters Arabidopsis embryonic apical patterning. Development. 136(9): 1509-1517.

Saiga S, Furumizu C, Yokoyama R, Kurata T, Sato S, Kato T, Tabata S, Suzuki M and Komeda Y. (2008). The Arabidopsis *OBERON1* and *OBERON2* genes encode plant homeodomain finger proteins and are required for apical meristem maintenance. Development. 135(10): 1751-1759.

Shen WH, Parmentier Y, Hellmann H, Lechner E, Dong A, Masson J, Granier F, Lepiniec L, Estelle M and Genschik P. (2002). Null mutation of *AtCUL1* causes arrest in early embryogenesis in Arabidopsis. Mol Biol Cell. 13(6): 1916-1928.

Stepanova AN, Robertson-Hoyt J, Yun J, Benavente LM, Xie DY, Dolezal K, Schlereth A, Jürgens G and Alonso JM. (2008). *TAA1*-mediated auxin biosynthesis is essential for hormone crosstalk and plant development. Cell. 133(1): 177-191.

Szemenyei H, Hannon M and Long JA. (2008). TOPLESS mediates auxin-dependent transcriptional repression during Arabidopsis embryogenesis. Science. 319(5868): 1384-1386.

Tan X, Calderon-Villalobos LI, Sharon M, Zheng C, Robinson CV, Estelle M and Zheng N. (2007). Mechanism of auxin perception by the TIR1 ubiquitin ligase. Nature. 446(7136): 640-645.

Tao Y, Ferrer JL, Ljung K, Pojer F, Hong F, Long JA, Li L, Moreno JE, Bowman ME, Ivans LJ, Cheng Y, Lim J, Zhao Y, Ballaré CL, Sandberg G, Noel JP and Chory J. (2008). Rapid synthesis of auxin via a new tryptophan-dependent pathway is required for shade avoidance in plants. Cell. 133(1): 164-176.

Thomas CL, Schmidt D, Bayer EM, Dreos R and Maule AJ. (2009). Arabidopsis plant homeodomain finger proteins operate downstream of auxin accumulation in specifying the vasculature and primary root meristem. Plant J. 59(3): 426-436.

Tiwari SB, Hagen G and Guilfoyle T. (2003). The roles of auxin response factor domains in auxin-responsive transcription. Plant Cell. 15(2): 533-543.

Torres-Ruiz RA and Jürgens G. (1994). Mutations in the *FASS* gene uncouple pattern formation and morphogenesis in Arabidopsis development. Development. 120(10): 2967-2978.

Ulmasov T, Hagen G and Guilfoyle TJ. (1999). Activation and repression of transcription by auxin-response factors. Proc Natl Acad Sci U S A. 96(10): 5844-5849.

Weijers D, Sauer M, Meurette O, Friml J, Ljung K, Sandberg G, Hooykaas P and Offringa R. (2005). Maintenance of Embryonic Auxin Distribution for Apical-Basal Patterning by PIN-FORMED-Dependent Auxin Transport in Arabidopsis. Plant Cell. 17(9): 2517-2526.

Weijers D, Schlereth A, Ehrismann JS, Schwank G, Kientz M and Jürgens G. (2006). Auxin triggers transient local signaling for cell specification in Arabidopsis embryogenesis. Dev Cell. 10(2): 265-270.

Scope of the thesis

In the early Arabidopsis embryo, the root is initiated by the coordinated specification of organizer cells and tissue-specific stem cells that collectively create the root meristem. Root initiation requires the activity of the MONOPTEROS (MP) transcription factor that is the main executer of auxin signaling during embryogenesis. MP is required to specify the precursor of the organizing cells of the root meristem. In this thesis, we investigate the diverse functions of MP during embryonic root initiation using two different approaches. On one hand, we employ transcription profiling to identify novel MP target genes that are expressed in the early embryo. Some of the direct MP target genes are studied in detail. On the other hand, we attempt to reveal putative MP interacting proteins using transcriptomics.

Chapters 2-5 deal with the identification of novel MP target genes and their roles in embryonic root initiation, while **Chapter 6** focuses on the efforts that were undertaken to find MP interacting proteins.

In **Chapter 2**, we describe the results of a microarray on seedlings that was designed to find novel MP target genes involved in setting up the root meristem in the early embryo.

Chapter 3 focuses on TARGET OF MP5 (TMO5) and its interaction partner LONESOME HIGHWAY and their role in embryonic and postembryonic vascular cells of the root to promote stem cell-like divisions.

Chapter 4 reports on the results of a microarray on embryos in which MP activity was locally inhibited in cells that will contribute to the embryonic root meristem. This microarray aimed to identify novel MP target genes that were specifically expressed in the first vascular and ground tissue cells of the embryonic root meristem.

In **Chapter 5**, we present evidence that suggests that MP is involved in the specification of the first ground tissue cells of the embryonic root meristem.

Chapter 6 informs on the optimization of an immunoprecipitation protocol aimed to identify MP interacting proteins.

Chapter 7 discusses insights obtained from this thesis and shows that MP employs novel molecular mechanisms involved in embryonic root initiation.

Chapter 2

MONOPTEROS controls embryonic root initiation by regulating a mobile transcription factor

Alexandra Schlereth[1]†, Barbara Möller[2], Weilin Liu[2], Marika Kientz[1], Jacky Flipse[2], Eike H. Rademacher[2], Markus Schmid[3], Gerd Jürgens[1] & Dolf Weijers[1,2]

Nature. (2010). 464(7290): 913-6.

[1]Entwicklungsgenetik, Zentrum für Molekularbiologie der Pflanzen (ZMBP), Universität Tübingen, Auf der Morgenstelle 3, 72076 Tübingen, Germany.

[2]Laboratory of Biochemistry, Wageningen University, Dreijenlaan 3, 6703 HA Wageningen, the Netherlands.

[3]Max Planck Institute for Developmental Biology, Department of Molecular Biology, Spemannstrasse 37–39, 72076 Tübingen, Germany.

†Present address: Syngenta Crop Protection, CH-4332 Stein, Switzerland.

Abstract

Acquisition of cell identity in plants relies strongly on positional information, hence cell–cell communication and inductive signalling are instrumental for developmental patterning (Scheres, 2001). During *Arabidopsis* embryogenesis, an extra-embryonic cell is specified to become the founder cell of the primary root meristem, hypophysis, in response to signals from adjacent embryonic cells (Hamann *et al*., 1999). The auxin-dependent transcription factor MONOPTEROS (MP) drives hypophysis specification by promoting transport of the hormone auxin from the embryo to the hypophysis precursor. However, auxin accumulation is not sufficient for hypophysis specification, indicating that additional MP-dependent signals are required (Weijers *et al*., 2006). Here we describe the microarray-based isolation of MP target genes that mediate signalling from embryo to hypophysis. Of three direct transcriptional target genes, *TARGET OF MP 5* (*TMO5*) and *TMO7* encode basic helix–loop–helix (bHLH) transcription factors that are expressed in the hypophysis-adjacent embryo cells, and are required and partially sufficient for MP-dependent root initiation. Importantly, the small TMO7 transcription factor moves from its site of synthesis in the embryo to the hypophysis precursor, thus representing a novel MP-dependent intercellular signal in embryonic root specification.

Introduction and Results

The *Arabidopsis* root system is initiated in the embryo by the specification of a single extra-embryonic suspensor cell as hypophysis. This root founder cell divides asymmetrically and generates the quiescent centre, the future organizer cells in the root meristem (Weigel and Jürgens, 2002). Hypophysis specification and embryonic root formation critically depend on the *AUXIN RESPONSE FACTOR 5* (*ARF5*)/*MP* gene (Hardtke and Berleth, 1998), which encodes a transcription factor that mediates auxin-responsive gene expression (Ulmasov *et al*., 1999a). Auxin-dependent degradation of the interacting BODENLOS (BDL) protein releases MP from inhibition and allows for the activation of target genes (Weijers *et al*., 2005, 2006; Hamann *et al*., 2002; Dharmasiri *et al*., 2005). Intriguingly, hypophysis specification requires cell-cell signalling as MP is expressed in an adjacent group of embryo cells and thus acts non cell-autonomously (Figure 1a). Auxin itself is one of the signals involved since MP promotes PIN-FORMED 1 (PIN1)-dependent auxin transport to the future hypophysis. However, auxin accumulation is neither restricted to the uppermost suspensor cell nor sufficient to promote hypophysis specification, indicating the involvement of other, yet unknown signals

(Weijers *et al*., 2006).

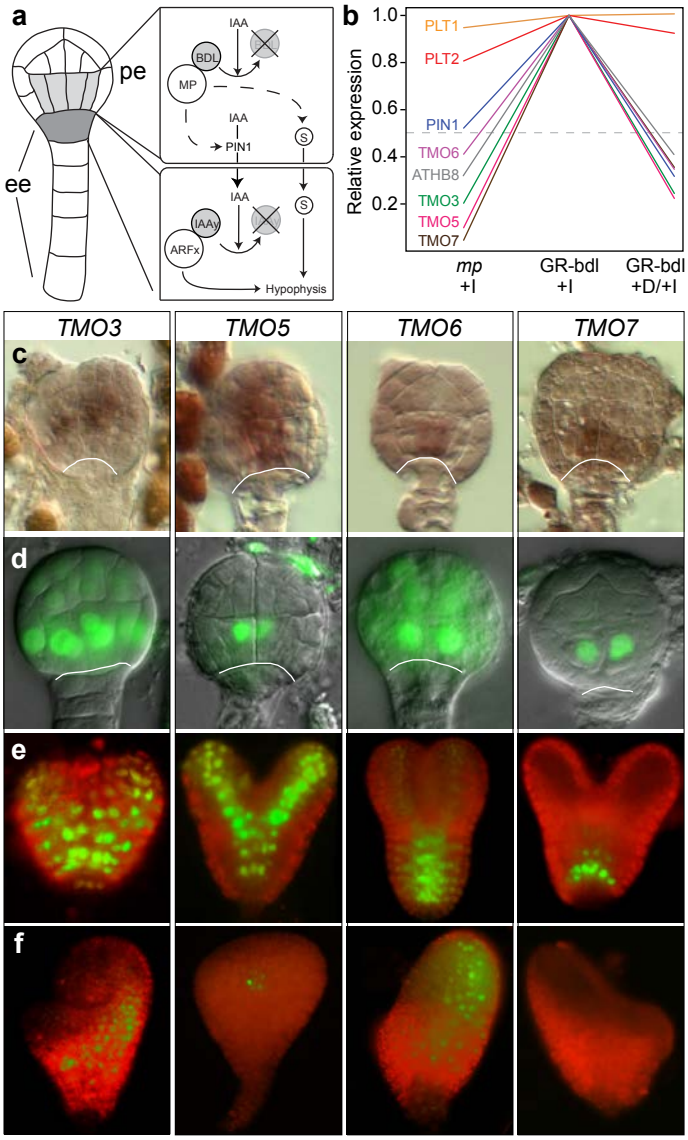

Figure 1 Identification of TARGET OF MONOPTEROS (TMO) genes. a, MP-dependent root initiation (model). In pro-embryo (pe) cells (light-grey), auxin (IAA)-induced BDL degradation allows MP to activate transport of auxin (through PIN1) and hypothetical signal (S) to the adjacent extra-embryonic (ee) cell (dark- grey). Here, an auxin-activated ARFx-IAAy pair and signal S specify hypophysis fate. b, Microarray expression of TMO and reference genes in IAA-treated seedlings: *mp* (*mp* +I), *GR–bdl* (*GR–bdl* +I; set to 1) and DEX-induced *GR–bdl* (GR–bdl +D/+I). c, *TMO* mRNA in-situ hybridization (brown) in globular embryos. d–f, *TMO* promoters driving nuclear 3xGFP in wild-type (d, e) and *mp-B4149* (f) embryos (d, globular; e and f, heart stage). White lines (c, d) mark pro-embryo-suspensor boundaries.

To dissect the mechanisms involved in root initiation and to identify novel factors in cell–cell communication, we performed microarray experiments in search of MP target genes. We compared messenger RNA from *mp* mutant seedlings and from seedlings expressing a dexamethasone (DEX)-dependent bdl mutant protein from a strong meristematic promoter (*pRPS5A::GR–bdl*; ref. 3). DEX treatment allows the nuclear translocation of otherwise cytosolic GR–bdl (Weijers *et al*., 2006). GR–bdl seedlings were either treated with DEX or mock-treated with inducer-free medium. In addition, we included auxin (IAA) in the medium to remove potential other Aux/IAA inhibitors and allow full activation of MP target genes. Optimal concentrations of IAA and DEX and duration of treatment were determined by quantitative PCR (qPCR) on several primary auxin-regulated genes (Supplementary Figure 1a–c). Based on this optimization, seedlings were pre-treated with DEX for 1 h, and subsequently treated with both DEX and IAA for another hour (Supplementary Figure 1d).

Duplicate mRNA samples were hybridized to Affymetrix ATH1 (22K) arrays and a list of differentially expressed genes was obtained after statistical analysis (>twofold changed; $P < 0{,}001$; Supplementary Table 1). The 96 differentially expressed genes represented various functional categories, including known primary auxin response genes (*GH3*, *SAUR*, *Aux/IAA* and most of the genes in the 'Others' category; Tian *et al*., 2002; Okushima *et al*., 2005), hormone homeostasis (*ACS*, *GA20OX*, *CKX7*), metabolic enzymes ('Others' category) and a relatively high number of transcription factors (16/96 = 17% versus 5% in the genome; Riechmann *et al*., 2000). The latter included the ARF7/19 targets *LBD16* and *LBD29* (Okushima *et al*., 2007), the MP target *AtHB8* (Donner *et al*., 2009; Figure 1b) and also notably five basic helix–loop–helix proteins (5/96 = 5.2% versus approximately 0.5% in the genome). Neither the *PLETHORA* genes nor *PIN* genes other than *PIN1* were significantly changed (Figure 1b and Supplementary Table 1; Galinha *et al*., 2007). After interrogation of public expression data, several genes of each functional category except the 'auxin-responsive' class, and most of the transcription factors were validated by qPCR with reverse transcription (Supplementary Table 1 and Supplementary Figure 2). Eight of these 16 genes were confirmed by qPCR and further investigated by *in-situ* hybridization in wild-type and *mp* mutant embryos. Four genes showed MP-dependent expression in cells relevant for root initiation (Figure 1b and Supplementary Figure 3). We have named these four genes (Figure 1b and Supplementary Figure 4) *TARGET OF MONOPTEROS* (*TMO*). *TMO3* (At4g23750) encodes an AP2-type transcription factor. *TMO5* (At3g25710) and *TMO7* (At1g74500) both encode basic helix–loop–helix (bHLH) transcription factors, and *TMO6* (At5g60200) encodes a

Dof-type transcription factor. During the course of our study, *TMO3* has also been described as *CRF2* (Rashotte *et al*., 2006), and *TMO7* as *PRE3* (Lee *et al*., 2006) and *ATBS1* (Wang *et al*., 2009).
The expression of the four *TMO* genes was divergent at later embryonic stages (Supplementary Figure 3a), with *TMO3* being broadly expressed, *TMO5* and *TMO6* specific for vascular tissues and *TMO7* restricted to the future root stem cells. At the globular stage, however, all four *TMO* genes were expressed in those cells adjacent to the hypophysis where MP acts (Figure 1c). *TMO* promoter-nuclear GFP reporters reflected the gene expression patterns (Figure 1d, e) and their dependence on MP (Figure 1f), indicating that the *TMO* genes are transcriptionally controlled by MP through their promoters.

TMO genes have several potential ARF-binding sites in their promoters (Figure 2a). To determine whether *TMO* genes are indeed regulated by direct binding of MP to their promoters, we devised a chromatin immunoprecipitation (ChIP) assay using a functional MP–GFP (green fluorescent protein) fusion protein expressed from a genomic fragment (Supplementary Figure 5). In these assays, *TMO3*, *5* and *7* promoter fragments were enriched using a YFP (yellow fluorescent protein) antibody, when compared to a mock control, whereas no enrichment was observed for the *TMO6* promoter (Figure 2b). Using a series of primer pairs distributed across the *TMO7* promoter, we found that MP binds in the 500 base pairs (bp) directly upstream of the ATG (Figure 2c). This window contained no canonical auxin response elements (TGTCTC; Ulmasov *et al*., 1999b) but two TGTC core elements that could mediate MP binding (Figure 2a).
Finally, to determine whether MP is not only necessary, but also limiting for the expression of the *TMO* genes, we examined *TMO3*, *5* and *7* expression in plants overexpressing MP (*35S::MP*). In these lines, we observed no change in *TMO3* and *TMO5* expression, but found that the levels of *TMO7* mRNA were significantly upregulated (Figure 2d). In conclusion, we have isolated three direct targets of MP in the embryo, of which *TMO7* can be activated by excess MP.

To determine the functional contribution of *TMO* genes to MP-dependent root formation, we expressed each *TMO* cDNA in embryos of the weak *mp-S319* allele. This allele shows a reduced penetrance of embryo defects, such that only about 30–40% of *mp-S319* homozygous seedlings are rootless (Figure 3a; Donner *et al*., 2009; Cole *et al*., 2009), allowing for quantification of changes in MP-dependent root formation. For misexpression, we used an *MP* promoter fragment that recapitulated *MP* mRNA and protein accumulation patterns (Figure 3b; compare references Weijers *et al*., 2006; Hardtke *et al*., 1998; Hamann *et al*., 2002).

Although the rootless rate was unaltered in *pMP-TMO3* lines, the embryo defect was suppressed to varying degrees in lines carrying *pMP-TMO5*, *pMP-TMO6* or *pMP-TMO7* (Figure 3a). The greatest level of rescue was observed in lines expressing TMO5 or TMO7. This result shows that TMO5 and TMO7 functions are an important output of MP activity in embryonic root formation.

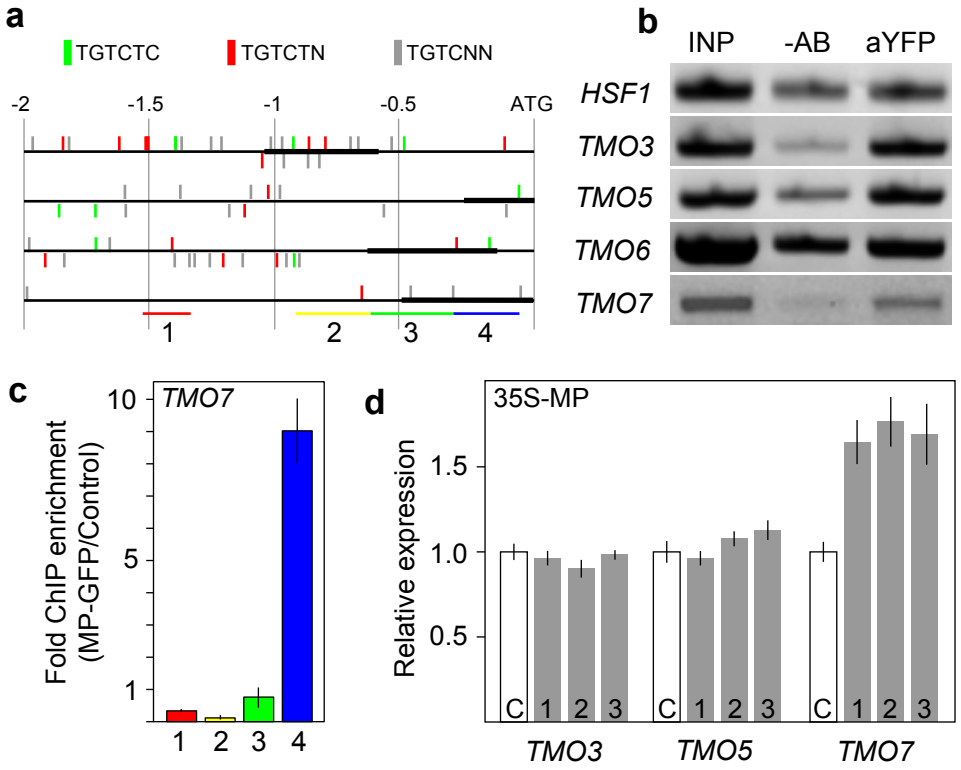

Figure 2 *TMO* genes are direct MP targets. a, Potential ARF-binding sites on the plus (upper side) and minus strand (lower side) of 2 kilobases upstream each *TMO* gene. Thick lines: fragments amplified in b (black) or c (coloured). b, PCR-amplified *TMO* promoter fragments or *HSF1* coding region from chromatin immunoprecipitation (ChIP) of MP–GFP seedlings with (aYFP) or without (−AB) anti-YFP antibody, (INP, chromatin input). c, qPCR of *TMO7* promoter fragments (as in a) in ChIP of MP–GFP seedling roots, compared to wild type. d, *TMO* qRT–PCR in three MP-overexpressing lines (*35S::MP*). Expression in wild type (C) is set to 1. Bars indicate standard deviation from the mean (n = 3).

We next investigated the function of the *TMO5* and *TMO7* genes in MP-dependent root initiation using a loss-of-function approach. Neither a T-DNA insertion mutation in *TMO5*, nor interfering RNA (RNAi) knockdown caused obvious defects in embryogenesis or plant growth (Supplementary Table 2). However, *TMO5* has several close homologues (Supplementary Figure 7), of which one (At1g68810;

TMO5-LIKE1) was co-expressed with *TMO5* in the microarray (Supplementary Table 1). Hence, redundancy with TMO5-LIKE1 may mask a potential function of TMO5 in root initiation.

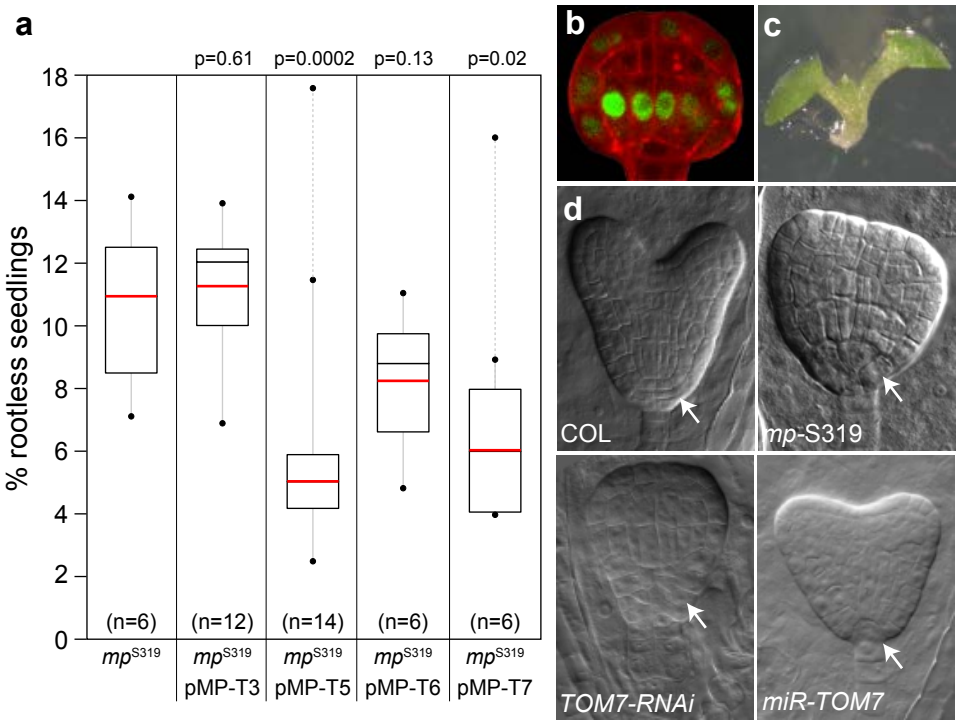

Figure 3 TMO5 and TMO7 act downstream of MP in root initiation. a, Frequencies of rootless progeny of *mp-S319* heterozygotes carrying p*MP-TMO* transgenes (n, independent lines) compared to non-transgenic mutants (n, individual plants); P-value (two-tailed unpaired Student's t-test) for difference shown above. Black dots, highest and lowest value; box, median 50%; black line, median; red line, average. The highest values for TMO5 and TMO7 were considered statistical outliers. b, Globular-stage embryo expressing nuclear 3xGFP (green) from *MP* promoter. c, Rootless *TMO7-RNAi* seedling. d, Heart-stage embryos of wild-type (COL), *mp-S319*, *TMO7-RNAi* and *miR-TMO7* plants. Note the irregular cell division pattern of hypophysis derivatives (arrow) in mutant embryos compared to wild type.

Since none of the available *TMO7* insertion mutants showed reduced mRNA levels, we generated RNAi and artificial microRNA lines to downregulate *TMO7* expression. Importantly, the closest homologue of *TMO7*, *TMO7-LIKE1* (At3g47710; also known as *PRE4*; Lee *et al*., 2006), was not represented on the ATH1 array (Supplementary Figure 7). The expression of this gene was determined using promoter–GFP fusion, and showed that *TMO7-LIKE1* is not co-expressed with

TMO7 in early embryogenesis (Supplementary Figure 6a, b), precluding functional redundancy. Both RNA suppression approaches yielded lines with *TMO7* mRNA levels that were reduced to 15–40% (Supplementary Figure 6c–e), causing aberrant divisions of the hypophysis and its descendants similar to the *mp-S319* mutant (Figure 3d and Supplementary Table 2). Consistent with these embryonic defects, rootless seedlings (Figure 3c) were found at a low frequency (between 1 and 7% in independent transgenics; Supplementary Table 2). *TMO7* RNAi increased the percentage of rootless seedlings of the weak *mp-S319* allele to over 20% (Supplementary Table 2), close to the 25% observed in strong *mp* alleles (Toledo-Ortiz *et al*., 2003). This demonstrates the requirement of *TMO7* in MP-dependent root initiation.

To determine where and when TMO5 and TMO7 proteins act in MP-dependent root initiation and whether they partake in cell–cell signalling, we constructed fusions of entire genomic fragments with carboxy-terminal GFP, or with triple-GFP to allow more sensitive visualization. Consistent with its predicted function as a transcription factor (Supplementary Figure 4b), TMO5–3×GFP protein is localized exclusively in the nucleus (Figure 4a). Likewise, TMO5 fused to a single YFP was exclusively nuclear in leaf mesophyll protoplasts (Figure 4g). Expression of TMO5–3×GFP is restricted to its transcriptional domain (Figure 4a, compare with Figure 1c-e), indicating that it mediates cell-autonomous MP functions in the pro-embryo. In contrast, TMO7–GFP protein was not only found in the nucleus, but also in the cytoplasm in its domain of transcription (Figure 4b, compare with Figure 1c-e), and the same result was obtained in leaf protoplasts (Figure 4h). Strikingly, TMO7–GFP protein was also found in cells outside its transcription domain, including the vasculature of the heart-stage embryo (Figure 4b, e). Importantly, whereas *TMO7* transcription was limited to pro-embryo cells at the globular stage (Figure 1c, d), TMO7 protein was found also in the hypophysis nucleus (Figure 4b). This indicates movement of TMO7–GFP protein from its site of synthesis into the hypophysis. Movement depended on the size of the fusion protein, since the addition of triple-GFP (84 kDa) to the 11 kDa TMO7 protein blocked movement beyond the transcriptional domain, and led to mostly cytosolic localization (Figure 4c, f). TMO7 movement at the globular stage appeared directional, because the TMO7–GFP protein was detected in the hypophysis, but not in the apical half of the embryo (Figure 4b).

TMO7 is required for root formation, sufficient to partially suppress the rootless defect in a weak *mp* mutant allele, and moves to the hypophysis in a size-dependent manner. To determine if TMO7 protein accumulation in the hypophysis con-

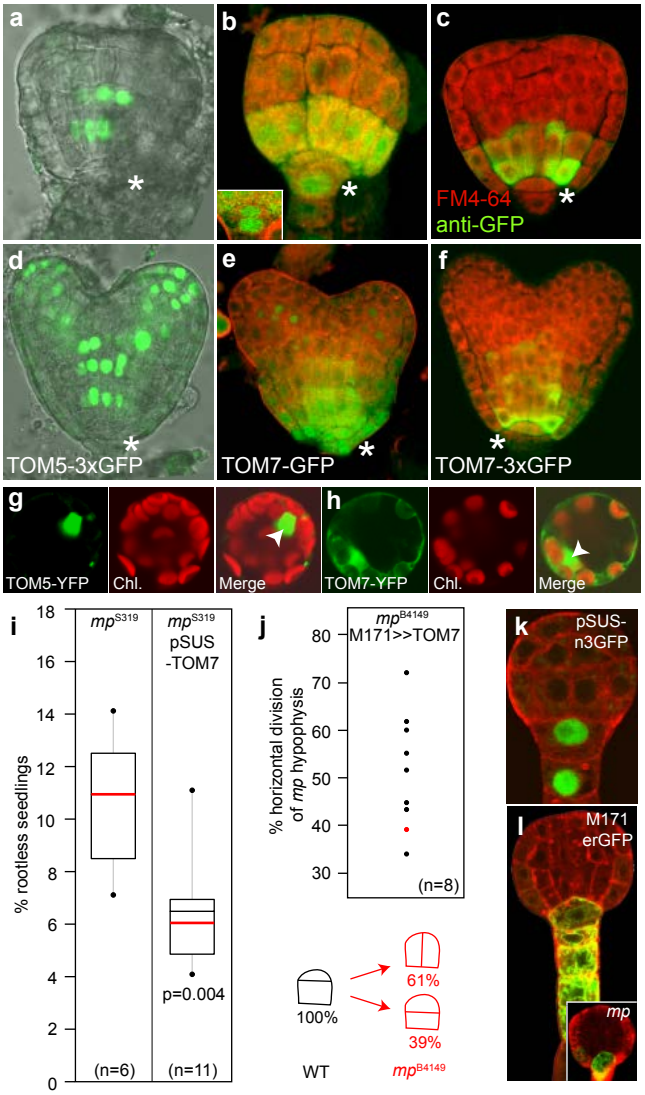

Figure 4 TMO5 and TMO7 proteins perform spatially separate functions during root formation. a–f, Globular- (a–c) and heart-stage (d–f) embryos expressing TMO5–3xGFP (a, d; green, live imaging), TMO7–GFP (b, e) or TMO7–3xGFP (c, f). b, c, e, f, Anti-GFP immunostaining (green). Asterisks, hypophysis and derivatives. Inset (b and inset), nuclear TMO7–GFP after hypophysis division and cytosolic signal in adjacent cells. g, h, Subcellular localization of TMO5–YFP (g; green) and TMO7–YFP (g, h; green) in leaf mesophyll protoplasts. Red and Chl., chlorophyll; arrowheads, nuclei. i, Frequency of rootless progeny of *mp-S319* heterozygotes with *pSUSP-TMO7* or without (same as Figure 3a, see also for boxplot and statistics). j, Percentage of horizontal hypophysis division in *mp-B4149* (red dot) and eight *M171 >> TMO7 mp-B4149* lines (black dots). Below: hypophysis division is asymmetric in wild type (WT), horizontal or vertical in mp-B4149. k, l, Extra-embryonic expression (green) of *pSUSP* promoter-nuclear 3×GFP (k), *M171–erGFP* in wild type (l) and *mp-B4149* (l, inset). Membranes are counterstained with FM4-64 (red) in b, c, e, f, k, l.

tributes to its function in root formation, TMO7 was misexpressed in *mp* mutant suspensor cells. First, TMO7 was expressed from the promoter of the *At1g34170* gene (*pSUSP-TMO7*), which drives expression in the suspensor from early stages onward (Figure 4k; data not shown).
This transgene suppressed the rootless embryo defect of the *mp-S319* mutant (Figure 4i), indicating that TMO7 acts in the future hypophysis to mediate root formation. To determine whether TMO7 function mediates hypophysis development, or a later step of root formation, we expressed *TMO7* from the suspensor-specific GAL4 driver line *M171* (Figure 4l) in the strong *mp-B4149* allele and analysed the hypophysis division plane. Whereas almost all wild-type hypophysis cells divide asymmetrically and horizontally, 40% of *mp-B4149* mutant embryos showed symmetrical horizontal division, and the remaining 60% divided vertically (Figure 4j). In contrast, in 7 out of 8 independent *mp-B4149 M171 >> TMO7* lines, we observed an increased frequency of symmetrical horizontal hypophysis division (Figure 4j). This quantitative suppression of the *mp* hypophysis defect indicates that TMO7 promotes the correct definition of the hypophysis cell division plane, and confirms that the movement of TMO7 to the hypophysis contributes to MP-dependent root formation. Whether TMO7 has a more general role in hypophysis cell specification or function, or if it specifically regulates division plane orientation in this cell remains to be addressed.
Of several direct target genes of MONOPTEROS identified here, *TMO5* and *TMO7* act downstream of MP in root initiation and encode bHLH transcriptional regulators, which indicates that MP function in root initiation is mediated by successive transcriptional steps. Whereas TMO5 acts cell-autonomously, TMO7 protein moves to the hypophysis and to vascular cells. Interestingly, the mode of TMO7 movement resembles that of SHORTROOT (SHR) in that SHR is also both cytosolic and nuclear in its transcriptional domain, but mostly nuclear in its target domain (Nakajima *et al*., 2001).
By sequence homology (Toledo-Ortiz *et al*., 2003; Supplementary Figure 4), TMO7 is predicted not to bind DNA, but might rather act as a cofactor for other bHLH transcription factors, in analogy to the animal ID (inhibitor of DNA binding/differentiation) proteins (Massari and Murre, 2000). Hence, we expect TMO7 to interact with a specific partner in the hypophysis to regulate cell division and mediate root formation. Candidates for such a partner were recently found in a yeast 2-hybrid screen with TMO7 (here referred to as ATBS1; Wang *et al*., 2009).
With auxin and TMO7, we have now identified two mobile factors whose transport or expression is activated by MP and which are both transported to the hypophysis. Interestingly, whereas auxin response is also activated in extra-embryonic cells below the future hypophysis (Weijers *et al*., 2006), TMO7 protein is restrict-

ed to the uppermost extra-embryonic cell, consistent with a model in which accumulation of both auxin and TMO7 in the same extra-embryonic cell is required for hypophysis specification. A future question is how these two signals converge during this process.

Material and Methods

Plant Material

The wild type used in all experiments was Columbia. GR–BDL and GR–bdl lines (Weijers *et al*., 2006) and *mp-B4149* (Weijers *et al*., 2005) were as described. The *mp-S319* allele corresponds to SALK_021319. Insertion lines for *TMO* genes (*tmo5-1*, SALK_013517; *tmo7-1*, SALK_058700, *tmo7-2*, SALK_080003) are from the SALK collection and were obtained through NASC. The M171 GAL4–GFP enhancer trap line (www.plantsci.cam.ac.uk/Haseloff/construction/catalogues/Mlines/ record/record_42.html) was crossed to *mp-B4149*, and plants homozygous for the transgene and heterozygous for the *mp* mutation were selected in F3/F4 generations. MP was overexpressed by fusing a C-terminally haemagglutinin (HA) epitope-tagged cDNA (Weijers *et al*., 2005) to the double-enhanced CaMV 35S promoter. Transgenic plants were used in first or second generation, and care was taken to select lines that show elevated *MP* mRNA levels in qRT–PCR.

Promoter–GFP reporters were constructed by introducing 2–2.6 kb fragments directly upstream of the ATG of the *TMO3*, *TMO5*, *TMO6*, *TMO7*, *TMO7-LIKE1*, *MP* and *At1g34170 (SUSP)* genes into pGreenII KAN SV40-3xGFP (Takada and Jürgens, 2007). A translational MP–GFP fusion was generated by introducing eGFP into a unique MscI site in the middle region of MP in a genomic fragment in pGreenII BAR. The construct was introduced into the *mp-B4149* mutant and complemented the rootless mutant phenotype. Translational fusions of TMO5 and 7 proteins to single or triple eGFP were constructed by introducing 3,789 bp (*TMO5*) and 2,454 bp (*TMO7*) genomic fragments excluding the stop codon and including 2,293 bp (*TMO5*) or 2,087 bp (*TMO7*) of upstream sequence into pGreenIIKAN GFP or pGreenIIKAN 3xGFP. Misexpression constructs for *TMO3*, *5*, *6* and *7* were generated by fusing C-terminally HA epitope-tagged cDNAs to the 4 kb *MP* promoter in pGreenII KAN. RNA interference (RNAi) constructs were generated by cloning *TMO5*- or *TMO7*-specific DNA fragments (primers are shown in Supplementary Table 3) in both orientations into pHANNIBAL (Wesley *et al*., 2001). The RNAi cassettes were then fused to the *RPS5A* promoter (Weijers *et al*., 2001) in pGreenIIKan. *TMO7* microRNA was designed according to the WMD server (http://wmd2.weigelworld.org) and constructed according to Schwab *et al* (2006).

The *TMO7* miR (*miR-TMO7*) was fused to the *TMO7* promoter in pGreenIIBAR. An *At1g34170* (*SUSP*) promoter–*TMO7* fusion was constructed by replacing the *MP* promoter in pGreenIIKan *pMP-TMO7* with a 2 kb *At1g34170* (*SUSP*) promoter fragment. *UAS-TMO7* was generated by cloning a *TMO7* cDNA excluding 5′ and 3′ UTR regions into a pGreenIIBAR vector containing a *UAS-tNOS* cassette. For protein localization in protoplasts, *TMO5* and *TMO7* cDNAs were amino-terminally fused to YFP in pMON999 (Monsanto).
All constructs were transformed into wild-type, *mp-B4149*, *mp-S319* or *mp-B4149* plants homozygous for the *M171* GAL4 driver by floral dip (Clough and Bent, 1998), using the *Agrobacterium* strain GV3101[pSoup]. The *miR-TMO7* construct was introduced into TMO7-3xGFP plants. Transgenic plants were genotyped by PCR for the insertion of the correct transgene, and for the presence of the *mp*-S319 or *mp*-B4149 mutations.

Plant growth and treatments
Plants were grown at 23 °C in a 16 h light/8 h dark cycle. Seeds were germinated on vertical half-strength MS medium with 1% sucrose and 1.5% Daichin agar (Duchefa). For dexamethasone or auxin (IAA) treatments, seedlings were transferred to liquid medium to which the appropriate concentrations of DEX and/or IAA had been added.

Microarray experiment
The microarray experiment was performed by incubating 9-day-old *mp-B4149* and GR–bdl seedlings, germinated on MS plates in duplicate (*mp-B4149*) or quadruplicate (GR–bdl) and transferred to liquid media. Dex (10 μM) was added to two of the GR–bdl cultures and to both *mp-B4149* cultures. After 1 h, 50 μM IAA was added to all cultures. RNA was isolated after 1 h using an RNeasy kit (Qiagen). Probe synthesis and array hybridizations were carried out as described (www.weigelworld.org/ resources/microarray/AtGenExpress/AtGE_probe_synthesis.pdf) at the Max Planck Institute for Developmental Biology. Affymetrix ATH1arrays were hybridized, washed and scanned in accordance with the Affymetrix guidelines, using a Hybridization oven 640, a Fluidics Station 450 and a GeneChip Scanner 3000. Array data were statistically analysed according to Van den Bosch *et al* (2007). Expression estimates of probesets were obtained by GC-robust multi-array (GCRMA) analysis (Wu *et al*., 2004). Probesets were redefined according to Dai *et al* (2005). Next, differentially expressed probesets were identified using linear models, applying moderated *t*-statistics that implement intensity-dependent Bayes regularisation of standard errors (Smyth, 2004; Sartor *et al*., 2006). Only genes with a fold-change of at least 2 and a *P*-value lower than 0.001

were considered.

ChIP

Chromatin immunoprecipitation (ChIP) was performed according to Leibfried *et al* (2005) with minor modifications. A complementing *MP–GFP* line was used to precipitate MP–GFP-bound chromatin with a custom-made affinity-purified rabbit anti-YFP antiserum bound to Protein-A-agarose, or as a control, the same Protein-A-agarose beads without the antiserum. For the ChIP-qPCR, chromatin was isolated from MP–GFP or wild type, and MP–GFP was precipitated using magnetic anti-GFP beads and microMACS columns (Miltenyi Biotec). Fold enrichment was calculated by comparing the C_t values of triplicate measurements between immunoprecipitates from MP–GFP and wild-type plants, relative to the C_t value of the chromatin input control. Primers used to detect *TMO* gene promoters or the *HSF1* coding region are listed in Supplementary Table 3.

Imaging and phenotypic analysis

GFP signals were analysed either by epifluorescence microscopy (Zeiss Axiophot), or by confocal imaging (Leica TCS-SP2 AOBS or Zeiss LSM510). Embryos were prepared out of the developing seed in PBS buffer containing 4% paraformaldehyde and 5% glycerol. FM4-64 was added at a final concentration of 1 μM to counterstain membranes. Embryo phenotypes were determined by DIC microscopy as described in Weijers *et al* (2006). Protoplasts were prepared and transfected as described in Aker *et al* (2006), and imaging was done as earlier on a Zeiss LSM510.

For analysis of rootless frequencies, plants were genotyped for *mp-S319* and the relevant transgene(s), and between 100 and 600 seedlings were plated. Those seedlings that showed complete absence of the root after 5–6 days of growth were considered rootless, and the percentage was scored.

For determining the hypophysis division plane, plants were genotyped for the *mp-B4149* mutation and for *UAS-TMO7* and *M171* transgenes. Between 50 and 150 embryos were microscopically analysed for each line, as well as for the non-transgenic control. Hypophysis division plane was scored only in embryos taken from siliques where all hypophyses had divided (transition to early heart stage), and were classified as horizontal or deviating from the horizontal plane.

RNA *in-situ* hybridization on *Arabidopsis* embryos was performed as described[7] either on wild-type siliques, or on siliques of the *mp-B4149* mutant, that segregates 25% mutant embryos. PCR oligonucleotides for amplifying gene-specific probes are listed in Supplementary Table 3. Immunofluorescence staining of GFP-tagged proteins was performed as described in Lauber *et al* (1997), using an

affinity-purified rabbit anti-YFP serum. Embryos were counterstained with 30 μM FM4-64 (Molecular Probes).

qPCR

For qRT–PCR, RNA was isolated using either TRIzol reagent (Invitrogen), or an RNeasy kit (Qiagen). cDNA was reverse-transcribed using Superscript II RT (Invitrogen). qRT–PCR reactions were performed either using Taq polymerase (ABgene) and SYBR green (Molecular Probes) on a BIO-RAD iCycler thermocycler, or with a qPCR kit (Eurogentec) on a Bio-Rad MyiQ thermocycler. Gene-specific signals were normalized relative to *ACTIN2* expression. Oligonucleotides for qRT–PCR are listed in Supplementary Table 3.

Public expression data resources

For selecting genes from the microarray experiment, we used the Atgenexpress (http://jsp.weigelworld.org/expviz/expviz.jsp) and eFP Browser (http://bbc.botany.utoronto.ca) online resources, to determine the expression of each gene in siliques or embryos, and to assess the overlap with *MP* expression.

Acknowledgements

We acknowledge P. van Oorschot, A. van Haperen and S. Heilbronner for technical assistance, C. Arsene for plant care, S. de Folter and O. Mathieu for advice on ChIP, M. Wunderlich and G. Bijl for help with qPCR, G. Hooiveld for help with statistical analysis of the microarray data and the Nottingham *Arabidopsis* Stock Centre for mutant and transgenic seeds. We thank P. Maier, S. de Vries, A. Koltunow, A. Lokerse, S. Saiga, V. Willemsen and M. Tsiantis for discussions and comments on the manuscript. This work was supported by grants from the Netherlands Organization for Scientific Research (NWO; VIDI 864.06.012 to D.W.), from the Deutsche Forschungsgemeinschaft (DFG; SFB446 to G.J.) and the Netherlands Proteomics Centre (NPC; D.W., grant awarded to S. de Vries).

Author Contributions

A.S. established conditions for the microarray experiment, which was performed together with M.S., validated the array data by qPCR, generated most transgenic lines for expression analysis and functional studies of *TMO* genes, which was done together with B.M. M.K. performed *in situ* hybridizations, J.F. and D.W. performed ChIP, and W.L. generated and analysed *TMO7* downregulation and *TMO7-LIKE1* reporter lines. B.M. performed MP overexpression, and suspensor-

specific TMO7 expression experiments, and generated *pMP–GFP* lines. E.H.R. identified the suspensor-specific *At1g34170* gene, and generated *pSUSP-GFP* lines. D.W. and G.J. conceived and supervised the study. D.W. wrote the paper with input from G.J., A.S. and B.M.

References

Aker J, Borst JW, Karlova R and De Vries S. (2006). The *Arabidopsis thaliana* AAA protein CDC48A interacts in vivo with the somatic embryogenesis receptor-like kinase 1 receptor at the plasma membrane. J Struct Biol. 156(1): 62-71.

Clough SJ and Bent AF. (1998). Floral dip: a simplified method for Agrobacterium-mediated transformation of *Arabidopsis thaliana*. Plant J. 16(6): 735-743.

Cole M, Chandler J, Weijers D, Jacobs B, Comelli P and Werr W. (2009). *DORNRÖSCHEN* is a direct target of the auxin response factor MONOPTEROS in the Arabidopsis embryo. Development. 136(10): 1643-1651

Dai M, Wang P, Boyd AD, Kostov G, Athey B, Jones EG, Bunney WE, Myers RM, Speed TP, Akil H, Watson SJ and Meng F. (2005). Evolving gene/transcript definitions significantly alter the interpretation of GeneChip data. Nucleic Acids Res. 33(20): e175.

Dharmasiri N, Dharmasiri S, Weijers D, Lechner E, Yamada M, Hobbie L, Ehrismann JS, Jürgens G and Estelle M. (2005). Plant development is regulated by a family of auxin receptor F-box proteins. Dev Cell. 9(1): 109-119.

Donner TJ, Sherr I and Scarpella E. (2009). Regulation of preprocambial cell state acquisition by auxin signaling in Arabidopsis leaves. Development. 136(19): 3235-46.

Galinha C, Hofhuis H, Luijten M, Willemsen V, Blilou I, Heidstra R and Scheres B. (2007). PLETHORA proteins as dose-dependent master regulators of Arabidopsis root development. Nature. 449(7165): 1053-7.

Hamann T, Benkova E, Bäurle I, Kientz M and Jürgens G. (2002). The Arabidopsis *BODENLOS* gene encodes an auxin response protein inhibiting MONOPTEROS-mediated embryo patterning. Genes Dev. 16(13): 1610-5.

Hamann T, Mayer U and Jürgens G. (1999). The auxin-insensitive *bodenlos* mutation affects primary root formation and apical-basal patterning in the Arabidopsis embryo. Development. 126(7): 1387-1395.

Hardtke CS and Berleth T. (1998). The Arabidopsis gene *MONOPTEROS* encodes a transcription factor mediating embryo axis formation and vascular development. EMBO J. 17(5): 1405-1411.

Lauber MH, Waizenegger I, Steinmann T, Schwarz H, Mayer U, Hwang I, Lukowitz W and Jürgens G. (1997). The Arabidopsis KNOLLE protein is a cytokinesis-specific syntaxin. J Cell Biol. 139(6): 1485-93.

Lee S, Lee S, Yang KY, Kim YM, Park SY, Kim SY and Soh MS. (2006). Overexpression of *PRE1* and its homologous genes activates Gibberellin-dependent responses in *Arabidopsis thaliana*. Plant Cell Physiol. 47(5): 591-600.

Leibfried A, To JP, Busch W, Stehling S, Kehle A, Demar M, Kieber JJ and Lohmann JU. (2005). WUSCHEL controls meristem function by direct regulation of cytokinin-inducible response regulators. Nature. 438(7071): 1172-5.

Massari ME and Murre C. (2000). Helix-loop-helix proteins: regulators of transcription in eucaryotic organisms. Mol Cell Biol. 20(2): 429-440.

Nakajima K, Sena G, Nawy T and Benfey PN. (2001). Intercellular movement of the putative transcription factor SHR in root patterning. Nature. 413(6853): 307-311.

Okushima Y, Fukaki H, Onoda M, Theologis A and Tasaka M. (2007). ARF7 and ARF19 regulate lateral root formation via direct activation of *LBD/ASL* genes in Arabidopsis. Plant Cell. 19(1): 118-130.

Okushima Y, Overvoorde PJ, Arima K, Alonso JM, Chan A, Chang C, Ecker JR, Hughes B, Lui A, Nguyen D, Onodera C, Quach H, Smith A, Yu G and Theologis A. (2005). Functional genomic analysis of the *AUXIN RESPONSE FACTOR* gene family members in *Arabidopsis thaliana*: unique and overlapping functions of ARF7 and ARF19. Plant Cell. 17(2): 444-463.

Rashotte AM, Mason MG, Hutchison CE, Ferreira FJ, Schaller GE and Kieber JJ. (2006). A subset of Arabidopsis AP2 transcription factors mediates cytokinin responses in concert with a two-component pathway. Proc Natl Acad Sci U S A. 103(29): 11081-11085.

Riechmann JL, Heard J, Martin G, Reuber L, Jiang C, Keddie J, Adam L, Pineda O, Ratcliffe OJ, Samaha RR, Creelman R, Pilgrim M, Broun P, Zhang JZ, Ghandehari D, Sherman BK and Yu G. (2000). Arabidopsis transcription factors: genome-wide comparative analysis among eukaryotes. Science. 290(5499): 2105-2110.

Schwab R, Ossowski S, Riester M, Warthmann N and Weigel D. (2006). Highly specific gene silencing by artificial microRNAs in Arabidopsis. Plant Cell. 18(5): 1121-1133.

Sartor MA, Tomlinson CR, Wesselkamper SC, Sivaganesan S, Leikauf GD and Medvedovic M. (2006). Intensity-based hierarchical Bayes method improves testing for differentially expressed genes in microarray experiments. BMC Bioinformatics. 7: 538.

Scheres B. (2001). Plant cell identity. The role of position and lineage. Plant Physiol. 125(1): 112-114.

Smyth GK. (2004). Linear models and empirical bayes methods for assessing differential expression in microarray experiments. Stat Appl Genet Mol Biol. 3: Article3.

Takada S and Jürgens G. (2007). Transcriptional regulation of epidermal cell fate in the Arabidopsis embryo. Development. 134(6): 1141-1150.

Tian Q, Uhlir NJ and Reed JW. (2002). Arabidopsis SHY2/IAA3 inhibits auxin-regulated gene expression. Plant Cell. 14(2): 301-319.

Toledo-Ortiz G, Huq E and Quail PH. (2003). The Arabidopsis basic/helix-loop-helix transcription factor family. Plant Cell. 15(8): 1749-1770.

Ulmasov T, Hagen G and Guilfoyle TJ. (1999a). Activation and repression of transcription by auxin-response factors. Proc Natl Acad Sci U S A. 96(10): 5844-5849.

Ulmasov T, Hagen G and Guilfoyle TJ. (1999b). Dimerization and DNA binding of auxin response factors. Plant J. 19(3): 309-319.

Van den Bosch HM, Bünger M, de Groot PJ, van der Meijde J, Hooiveld GJ and Müller M. (2007). Gene expression of transporters and phase I/II metabolic enzymes in murine small intestine during fasting. BMC Genomics. 8:267.

Wang H, Zhu Y, Fujioka S, Asami T, Li J and Li J. (2009). Regulation of Arabidopsis brassinosteroid signaling by atypical basic helix-loop-helix proteins. Plant Cell. 21(12): 3781-3791.

Weigel D and Jürgens G. (2002). Stem cells that make stems. Nature. 415(6873): 751-754.

Weijers D, Benkova E, Jäger KE, Schlereth A, Hamann T, Kientz M, Wilmoth JC, Reed JW and Jürgens G. (2005). Developmental specificity of auxin response by pairs of ARF and Aux/IAA transcriptional regulators. EMBO J. 24(10): 1874-1885.

Weijers D, Franke-van Dijk M, Vencken RJ, Quint A, Hooykaas P and Offringa R. (2001). An Arabidopsis Minute-like phenotype caused by a semi-dominant mutation in a *RIBOSOMAL PROTEIN S5* gene. Development. 128(21): 4289-4299.

Weijers D, Schlereth A, Ehrismann JS, Schwank G, Kientz M and Jürgens G. (2006). Auxin triggers transient local signaling for cell specification in Arabidopsis embryogenesis. Dev Cell. 10(2): 265-270.

Wesley SV, Helliwell CA, Smith NA, Wang MB, Rouse DT, Liu Q, Gooding PS, Singh SP, Abbott D, Stoutjesdijk PA, Robinson SP, Gleave AP, Green AG and Waterhouse PM. (2001). Construct design for efficient, effective and high-throughput gene silencing in plants. Plant J. 27(6): 581-590.

Wu Z, Irizarry RA, Gentleman R, Martinez-Murillo F and Spencer F. (2004). A model-based background adjustment for oligonucleotide expression arrays. J Am Stat Assoc. 99: 909-917.

Supplementary Information

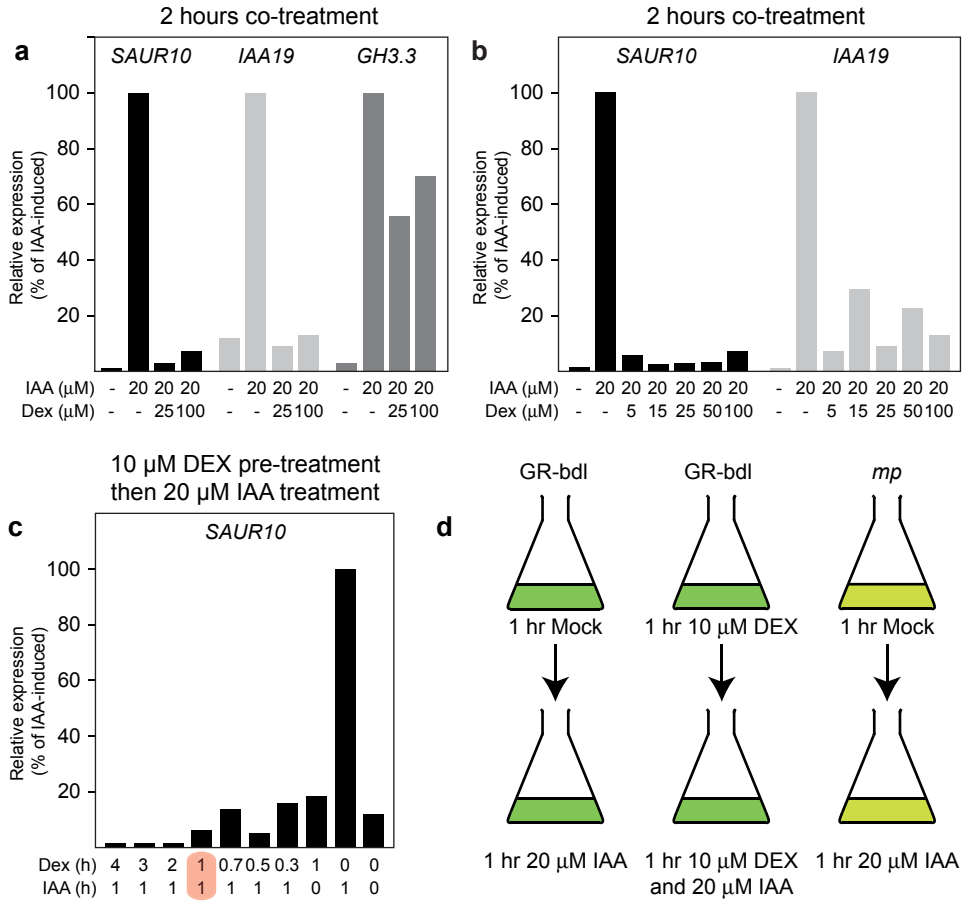

Figure S1: qRT-PCR based optimization of IAA and DEX treatments for microarray. To determine the optimal treatment for repressing ARF-dependent gene activation in RPS5A::Myc-GR-bdl seedlings, several schemes were applied and the expression of model primary auxin-responsive (potentially ARF-dependent) genes was quantified by qRT-PCR. In the initial experiment (**a**), the *SAUR10*, *IAA19* and *GH3.3* genes were selected because of their reported fast response to auxin (Reference 10). Seedlings were treated with 20 µM indole acetic acid (IAA) in the presence or absence of dexamethasone (DEX, applied at two different concentrations – 25 and 100 µM), during 2 hours. Expression of all three genes is strongly activated by IAA. This induction is almost completely abrogated by co-treatment with DEX for both *SAUR10* and *IAA19* genes, but to a much lesser extent for the *GH3.3* gene. (**b**) To determine optimal concentrations of DEX for complete ARF inhibition, the expression level of *SAUR10* and *IAA19* was determined after 2 hours of treatment with 20 µM IAA and varying concentrations of DEX (0, 5, 15, 25, 50, 100 µM). The strong IAA induction of *SAUR10* and *IAA19* expression is reduced almost to background levels by treatment with 5 µM DEX, and the extent of reduction varies a bit with increasing concentrations.

Based on this result, the optimal DEX concentration to (almost) completely inhibit ARF-dependent gene activation was chosen to be 10 µM. (**c**) Finally, to determine the minimal time required to achieve complete inhibition of ARF-dependent gene activation, we analyzed IAA-induced expression of the *SAUR10* gene after various pretreatments with 10 µM DEX. *SAUR10* was chosen since it responded most robustly to DEX-treatment in the experiments in (a) and (b). Seedlings were pretreated with DEX for a duration ranging between 20 minutes (0.3 hours) and 4 hours, followed by a 1-hour treatment with IAA and DEX. DEX pretreatment as brief as 20 minutes already strongly inhibited IAA-induced *SAUR10* expression, and longer treatments reduced this further, even below non-IAA-treated control levels (compare left-most 3 columns with right-most column). A 1-hour pre-treatment with 10 µM DEX, followed by a 1-hour treatment with 20 µM IAA was chosen as optimal for the microarray, since expression of *SAUR10* was reduced effectively to levels in untreated seedlings. (**d**) Set-up of the microarray experiment. Plate grown seedlings of the GR-bdl or *mp-B4149* genotype were transferred to liquid cultures and pretreated for 1 hour with 10 µM DEX or treated with mock medium. Subsequently, 20 µM IAA was added to all cultures for another hour of treatment before RNA extraction.

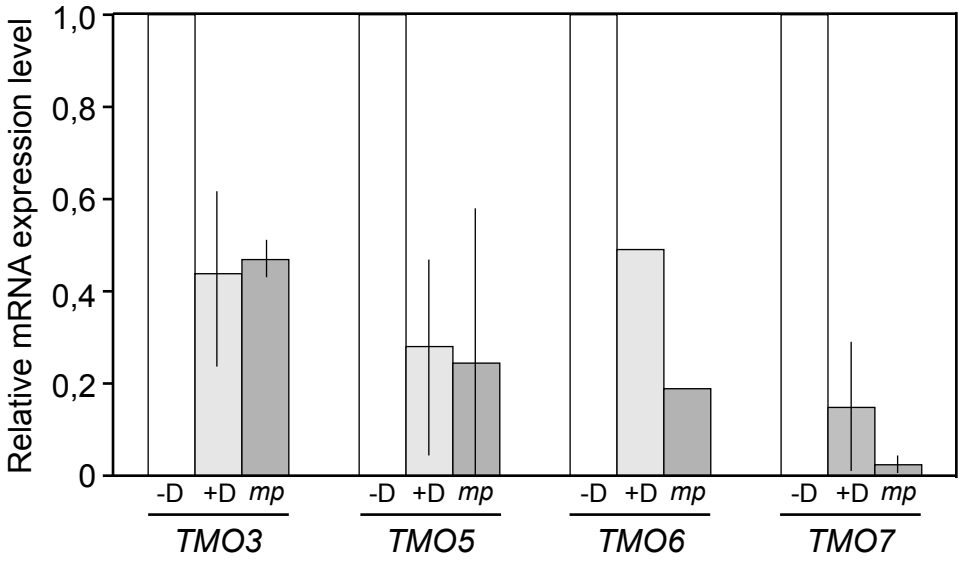

Figure S2: qRT-PCR verification of MP-dependent *TMO* gene expression as detected on microarrays. Selected genes indicated in Table S1 were subjected to qRT-PCR with mRNAs isolated independently from seedlings as in the microarray experiment (-D: GR-bdl +IAA-DEX; +D: GR-bdl +IAA+DEX; *mp*: *mp-B4149* +IAA). Shown here are relative expression values of *TMO3, 5, 6* and *7*. Expression in the (-D) mRNA sample is set to 1. The bar shows the average relative expression and standard deviation for 3 (*TMO5*), 2 (*TMO3*, *TMO7*) and 1 (*TMO6*) independent experiments. The qRT-PCR experiment recapitulates the downregulation seen in the microarray experiment in all cases.

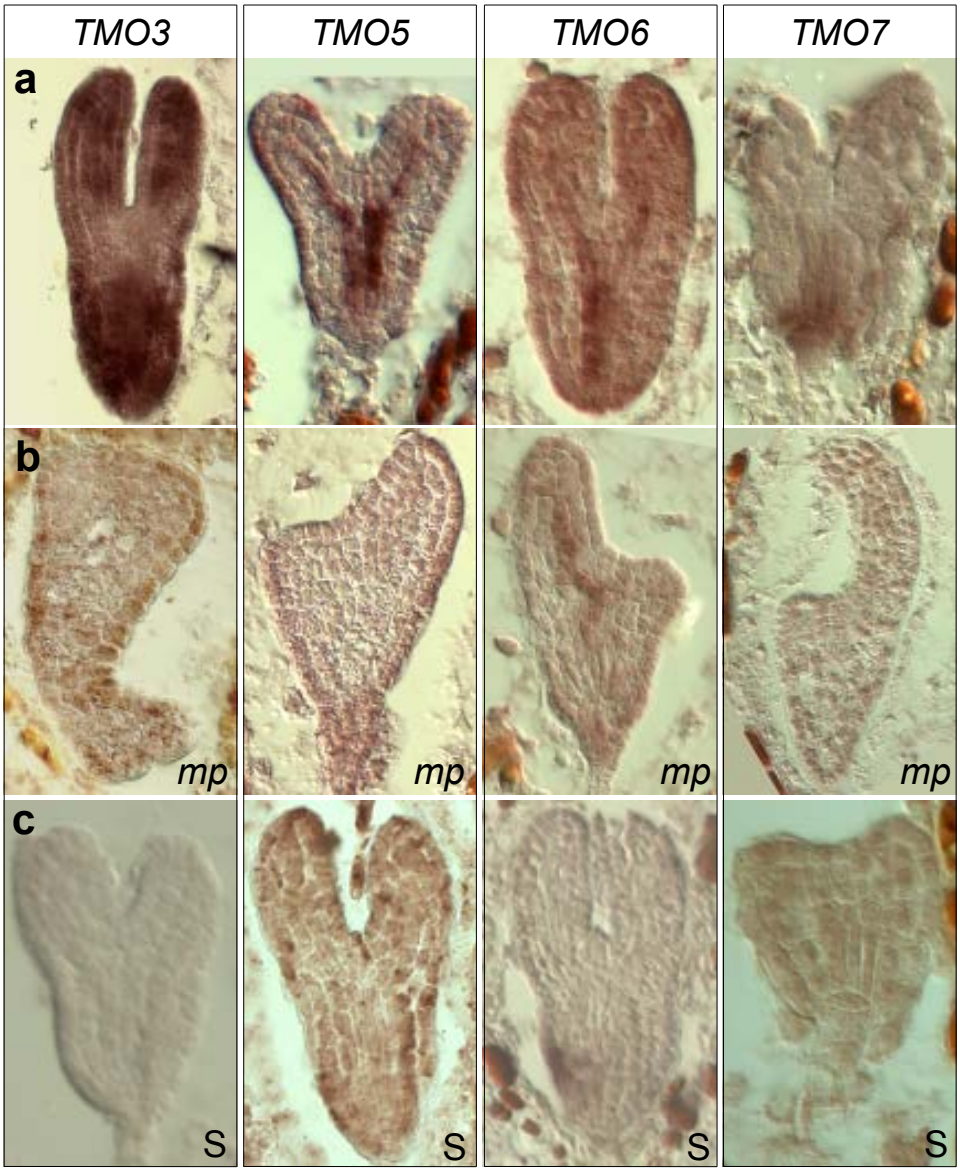

Figure S3: MP-dependent transcription patterns of *TMO* genes. (a,b) mRNA in-situ hybridization with antisense probes specific for *TMO3, 5, 6* or *7* on late heart-stage wild-type (a) or *mp-B4149* mutant (b) embryos. Red-brown colour indicates mRNA expression. Note that *TMO3* is ubiquitous, *TMO5* and *6* are vascular and *TMO7* is restricted to root stem cells, yet most expression depends on MP, since all but the vascular *TMO6* expression in the cotyledons is lost in the *mp* mutant. (c) Sense control (S) hybridizations for *TMO3, 5 ,6* and *7* on wild-type late heart-stage embryos.

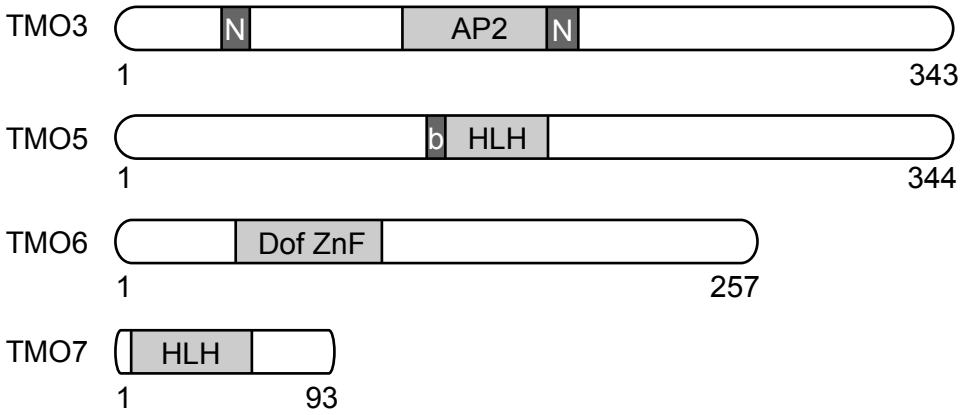

Figure S4: Domain organization of TMO proteins. Position 1 corresponds to the N-terminus, the number on the C-terminus indicates the length of each protein. Light-grey boxes show the conserved APETALA2 (AP2)-type domain of TMO3, the basic Helix-Loop-Helix (bHLH) domain of TMO5, the Dof-type Zinc-Finger (Dof ZnF) domain of TMO6 and the Helix-Loop-Helix (HLH) domain of TMO7. Predicted nuclear localization signals (NLS) are indicated in dark grey ("N" in TMO3). The basic region of the bHLH domain in TMO5 is predicted to contain an NLS. No canonical NLS is predicted for TMO6 and 7. Note that the basic region is missing from the HLH in TMO7.

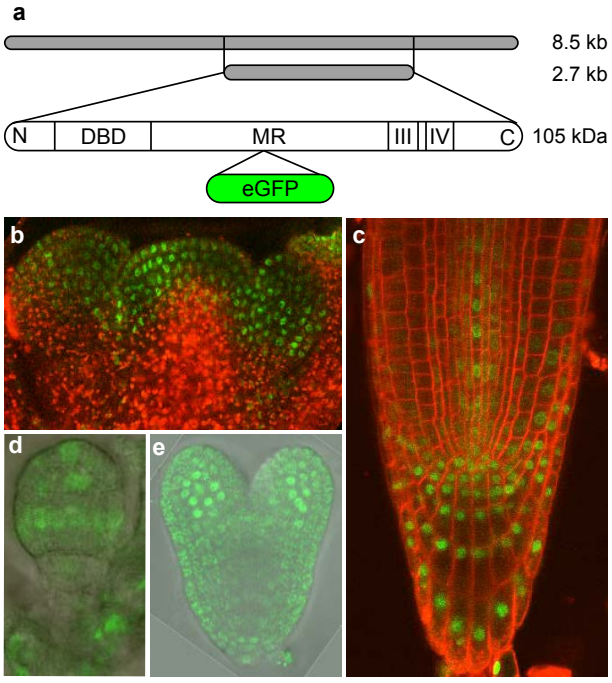

Figure S5: Expression and localization of MP-GFP. (a) A genomic fragment of 8.5 kb encompassing the *MP* locus that was previously shown to complement the *mp* mutant (Reference 3) was used to generate an MP-GFP fusion protein. The *MP* locus generates a cDNA containing the 2.7 kb open

reading frame that encodes the 105 kDa MP protein. The MP protein consists of a conserved N-terminal B3-type DNA-binding domain (DBD), a non-conserved Middle Region (MR) that mediates transcriptional activation, and C-terminal domains III and IV responsible for homotypic (ARF-ARF) and heterotypic (ARF-Aux/IAA e.g. MP-BDL) protein interactions. eGFP was inserted into the non-conserved Middle Region (MR) and the construct was introduced into the *mp-B4149* mutant. The transgene completely restored wild-type development (not shown). (b-e) Expression of the MP-GFP fusion protein in the shoot apical meristem and flower primordia (b), in the root tip (c), a globular-stage embryo (d) and in a heart-stage embryo (e). Note that MP-GFP is nuclear in all instances. Red signal in (b) is chlorophyll autofluorescence, in (c) FM4-64. The small green fluorescent particles in the embryo in (e) are autofluorescent plastids.

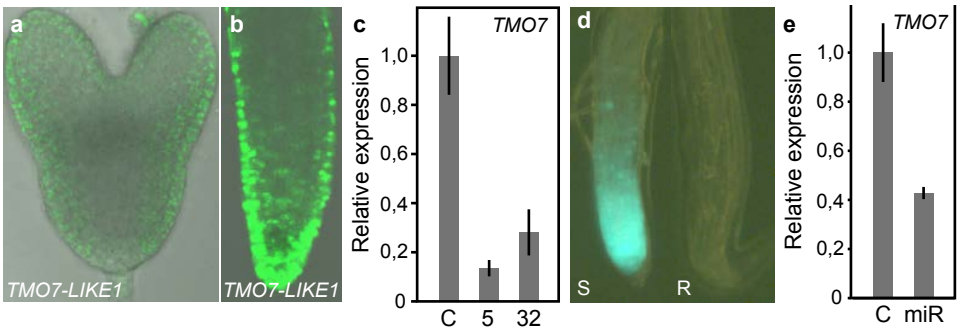

Figure S6: Downregulation of *TMO7* expression in RNAi and microRNA lines. (a,b) Expression of *pTMO7-LIKE1-n3GFP* in a heart-stage embryo (a) and in a root tip (b). Note that nuclear green fluorescence is absent from the embryo and present in the outer cell layer of the root tip. (c) qRT-PCR showing the relative expression level of TMO7 transcript in seedlings of wild-type (C) and two independent *pRPS5A::TMO7-RNAi* lines (#5 and #32). Expression in wild-type is set to 1, and error bars show standard deviation (SD) from the mean in 3-4 measurements. (d) *pTMO7::TMO7-3xGFP* (green) is strongly expressed in primary roots of wild-type (S; PPT sensitive) seedlings, but almost completely absent from segregating *pTMO7::miR-TMO7* (R; PPT resistant) seedling roots. These images are representative for at least 40 analyzed individuals in 2 independent lines. (e) qRT-PCR experiment showing the relative expression of *TMO7* transcript in seedling roots of the parental TMO7-3xGFP line (C) and of the *pTMO7::miR-TMO7* line (miR). Expression in the control is set to 1, and error bars represent the SD in three replicas.

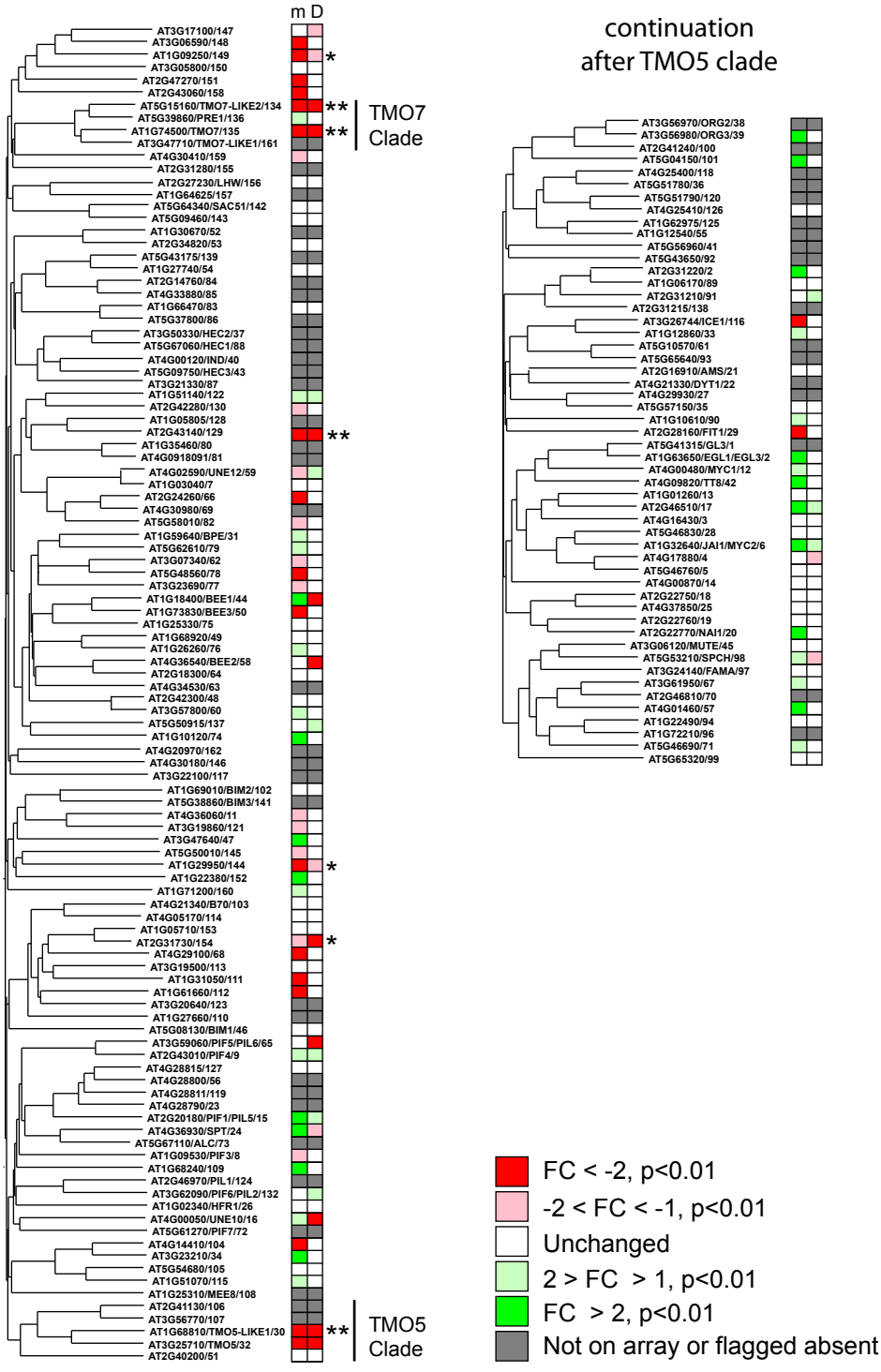
m D
AT3G17100/147
AT3G06590/148
AT1G09250/149
AT3G05800/150
AT2G47270/151
AT2G43060/158
AT5G15160/TMO7-LIKE2/134
AT5G39860/PRE1/136
AT1G74500/TMO7/135
AT3G47710/TMO7-LIKE1/161
AT4G30410/159
AT2G31280/155
AT2G27230/LHW/156
AT1G64625/157
AT5G64340/SAC51/142
AT5G09460/143
AT1G30670/52
AT2G34820/53
AT5G43175/139
AT1G27740/54
AT2G14760/84
AT4G33880/85
AT1G66470/83
AT5G37800/86
AT3G50330/HEC2/37
AT5G67060/HEC1/88
AT4G00120/IND/40
AT5G09750/HEC3/43
AT3G21330/87
AT1G51140/122
AT2G42280/130
AT1G05805/128
AT2G43140/129
AT1G35460/80
AT4G0918091/81
AT4G02590/UNE12/59
AT1G03040/7
AT2G24260/66
AT4G30980/69
AT5G58010/82
AT1G59640/BPE/31
AT5G62610/79
AT3G07340/62
AT5G48560/78
AT3G23690/77
AT1G18400/BEE1/44
AT1G73830/BEE3/50
AT1G25330/75
AT1G68920/49
AT1G26260/76
AT4G36540/BEE2/58
AT2G18300/64
AT4G34530/63
AT2G42300/48
AT3G57800/60
AT5G50915/137
AT1G10120/74
AT4G20970/162
AT4G30180/146
AT3G22100/117
AT1G69010/BIM2/102
AT5G38860/BIM3/141
AT4G36060/11
AT3G19860/121
AT3G47640/47
AT5G50010/145
AT1G29950/144
AT1G22380/152
AT1G71200/160
AT4G21340/B70/103
AT4G05170/114
AT1G05710/153
AT2G31730/154
AT4G29100/68
AT3G19500/113
AT1G31050/111
AT1G61660/112
AT3G20640/123
AT1G27660/110
AT5G08130/BIM1/46
AT3G59060/PIF5/PIL6/65
AT2G43010/PIF4/9
AT4G28815/127
AT4G28800/56
AT4G28811/119
AT4G28790/23
AT2G20180/PIF1/PIL5/15
AT4G36930/SPT/24
AT5G67110/ALC/73
AT1G09530/PIF3/8
AT1G68240/109
AT2G46970/PIL1/124
AT3G62090/PIF6/PIL2/132
AT1G02340/HFR1/26
AT4G00050/UNE10/16
AT5G61270/PIF7/72
AT4G14410/104
AT3G23210/34
AT5G54680/105
AT1G51070/115
AT1G25310/MEE8/108
AT2G41130/106
AT3G56770/107
AT1G68810/TMO5-LIKE1/30
AT3G25710/TMO5/32
AT2G40200/51
*
**
**
TMO7
Clade
**
*
*
**
TMO5
Clade

continuation
after TMO5 clade
AT3G56970/ORG2/38
AT3G56980/ORG3/39
AT2G41240/100
AT5G04150/101
AT4G25400/118
AT5G51780/36
AT5G51790/120
AT4G25410/126
AT1G62975/125
AT1G12540/55
AT5G56960/41
AT5G43650/92
AT2G31220/2
AT1G06170/89
AT2G31210/91
AT2G31215/138
AT3G26744/ICE1/116
AT1G12860/33
AT5G10570/61
AT5G65640/93
AT2G16910/AMS/21
AT4G21330/DYT1/22
AT4G29930/27
AT5G57150/35
AT1G10610/90
AT2G28160/FIT1/29
AT5G41315/GL3/1
AT1G63650/EGL1/EGL3/2
AT4G00480/MYC1/12
AT4G09820/TT8/42
AT1G01260/13
AT2G46510/17
AT4G16430/3
AT5G46830/28
AT1G32640/JAI1/MYC2/6
AT4G17880/4
AT5G46760/5
AT4G00870/14
AT2G22750/18
AT4G37850/25
AT2G22760/19
AT2G22770/NAI1/20
AT3G06120/MUTE/45
AT5G53210/SPCH/98
AT3G24140/FAMA/97
AT3G61950/67
AT2G46810/70
AT4G01460/57
AT1G22490/94
AT1G72210/96
AT5G46690/71
AT5G65320/99

FC < -2, p<0.01
-2 < FC < -1, p<0.01
Unchanged
2 > FC > 1, p<0.01
FC > 2, p<0.01
Not on array or flagged absent

Figure S7: Phylogenetic relationship of *Arabidopsis* bHLH proteins and expression profiles in the microarray. The sequences of all predicted *Arabidopsis* bHLH proteins (http://www.arabidopsis.org/ browse/genefamily/blhm.jsp) were downloaded and aligned using ClustalW. An unrooted phylogenetic tree was constructed and drawn with Treeview. The AGI number (e,g, At3g24140), a common name (when available; e.g. FAMA) and the bHLH number (Reference 21; e.g. 97) are given for each protein. The expression profile in the microarray experiment is represented on a colour scale in two boxes for each *bHLH* gene. The left box (m) depicts the fold-change (FC) between *mp* mutant seedlings and non-DEX treated *GR-bdl* seedlings. The right box (D) shows the FC between DEX treated and non-DEX treated *GR-bdl* seedlings. The FC's are only shown for those comparisons where the p-value is equal to or lower than 0.01. If the expression is not significantly different ($p>0.01$), the box is white. Negative FC (downregulation) is shown in different intensities of red (bright red if FC<-2 and pale red if FC is between -2 and -1), while positive FC (upregulation) is depicted in intensities of green (bright green if FC>2 and pale green if FC is between 1 and 2). Genes that are not represented on the ATH1 array, that were eliminated because of probe re-annotation, or that were flagged absent are shown with grey boxes. Those genes that fulfil the statistical criteria used in our analysis (FC < - 2 in both comparisons and $p<0.01$) are marked with two asterisks (**), and genes that show the same tendency, but FC between -2 and -1 are marked with one asterisk (*). The clades to which *TMO5* and *TMO7* belong are highlighted. Note that both *TMO5* and its closest homolog (*TMO5-LIKE1*) are significantly 2-fold downregulated in both comparisons (**). Likewise, *TMO7* and a close relative in the same clade (*TMO7-LIKE2*) are differential (**), while the closest *TMO7* homologue (*TMO7-LIKE1*) is not present in the dataset.

Table S1: List of genes that were differentially expressed between GR-bdl (-DEX), GR-bdl (+DEX) and *mp* seedlings. Shown are the fold-change (FC) of normalized (gcRMA) expression values between *mp* and *GR-bdl* –DEX or between *GR-bdl* +DEX and –DEX. The normalized expression values represent the average of two independent biological replicas. Differential expression was statistically tested by a regularized t-test, and the raw p-value is shown. Those genes that show at least 2-fold change in both comparisons are shown. Genes are listed according to their functional category. For comparison, the *PIN-FORMED* (*PIN*) and *PLETHORA* (*PLT*) genes are included. The genes selected for qRT-PCR (qPCR) are indicated, and those that were further selected for in-situ hybridization on embryos are also shown (ISH).

AGI	Description	FC mp/-Dex	p-value	FC +Dex/-Dex	p-value	qPCR	ISH
Auxin-responsive							
AT4G34770	*SAUR*	-6.1	1.1E-09	-2.1	1.0E-05		
AT2G14960	*GH3.1*	-4.8	1.1E-08	-6.1	2.3E-09		
AT5G54510	*GH3.6*	-2.4	7.2E-08	-2.7	1.3E-08		
AT3G15540	*IAA19*	-2.7	6.3E-07	-7.3	4.1E-10		
AT1G04240	*IAA3*	-2.1	1.1E-04	-2.5	1.9E-05		
AT1G15580	*IAA5*	-5.5	5.6E-08	-61.5	3.4E-12		
AT1G52830	*IAA6*	-6.9	4.5E-09	-7.9	2.2E-09		
AT5G55250	*IAMT1*	-2.2	8.5E-05	-2.5	2.1E-05		
AT2G21050	*LAX2*	-3.3	5.0E-07	-4.6	4.3E-08		
AT1G29490	*SAUR*	-14.1	5.8E-11	-19.8	1.5E-11		
AT2G45210	*SAUR*	-11.7	1.5E-10	-4.0	8.3E-08		
AT4G36110	*SAUR*	-11.0	3.7E-10	-3.5	3.9E-07		
AT5G18060	*SAUR*	-4.9	8.4E-09	-10.5	1.2E-10		
AT2G18010	*SAUR*	-4.4	1.2E-07	-23.2	3.3E-11		
AT1G29440	*SAUR*	-4.2	5.9E-08	-21.8	1.3E-11		
AT1G29450	*SAUR*	-3.1	4.8E-07	-4.6	2.2E-08		
AT3G03830	*SAUR*	-2.7	1.4E-06	-7.6	7.8E-10		
AT3G03840	*SAUR*	-2.2	1.4E-03	-5.5	1.7E-06		
AT4G38850	*SAUR*	-2.0	2.7E-05	-6.8	9.3E-10		
Other Hormones							
AT3G63440	Cytokinin – *CKX6*	-3.3	1.5E-06	-13.8	3.3E-10		
AT4G08040	Ethylene - *ACS11*	-3.0	2.0E-07	-2.2	4.9E-06		
AT2G22810	Ethylene - *ACS4*	-2.8	1.2E-06	-33.3	2.0E-12	Y	
AT5G65800	Ethylene - *ACS5*	-4.0	2.9E-09	-4.4	1.4E-09	Y	
AT4G11280	Ethylene - *ACS6*	-4.5	1.5E-06	-5.0	7.3E-07		
AT4G37770	Ethylene - *ACS8*	-7.6	1.6E-09	-6.7	3.2E-09		
AT3G25900	Ethylene - HMT	-4.7	7.0E-08	-3.5	6.6E-07		
AT5G51810	Gibberellin - *GA20OX2*	-2.7	1.7E-06	-3.2	3.3E-07		
AT4G21200	Gibberellin - *GA2OX8*	-9.1	8.5E-10	-5.8	1.0E-08	Y	
AT1G72450	Jasmonic acid (*JAZ6*)	-2.1	3.9E-05	-3.3	2.8E-07		
Transcription Factors							
AT4G23750	AP2 (*CRF2/TMO3*)	-4.9	4.1E-08	-4.1	1.5E-07	Y	Y
AT5G15160	bHLH (*TMO7-LIKE2*)	-4.9	1.3E-06	-4.3	3.3E-06	Y	Y
AT2G43140	bHLH	-3.2	9.7E-07	-5.3	2.2E-08	Y	
AT3G25710	bHLH (*TMO5*)	-10.1	3.2E-10	-4.5	3.6E-08	Y	Y
AT1G68810	bHLH (*TMO5-LIKE1*)	-8.4	3.9E-09	-2.0	2.0E-04		
AT1G74500	bHLH (*TMO7*)	-21.7	2.0E-11	-2.8	2.3E-06	Y	Y
AT5G28770	bZIP (*bZIP63*)	-3.6	8.9E-07	-2.0	2.6E-04		
AT3G58120	bZIP (*bZIP61*)	-2.5	2.6E-06	-3.3	2.0E-07	Y	
AT5G60200	Dof-type (*TMO6*)	-2.4	2.9E-05	-2.9	5.6E-06	Y	Y
AT5G61600	AP2 (*ERF104*)	-4.0	1.6E-06	-4.5	7.3E-07		
AT4G17460	HD (*HAT1*)	-11.5	1.8E-09	-4.4	4.0E-07	Y	
AT4G32880	HD-Zip (*AtHB8*)	-3.2	1.4E-05	-2.4	1.4E-04		
AT2G42430	LBD (*LBD16*)	-2.7	5.7E-05	-2.9	2.8E-05		
AT3g58190	LBD (*LBD29*)	-7.8	3.1E-08	-2.4	1.5E-04		
AT2G45680	TCP-type (*TCP9*)	-2.0	4.9E-05	-2.4	6.5E-06		
AT5G43170	ZF (*AZF3*)	-13.6	3.8E-11	-2.7	1.0E-06	Y	Y
Other							
AT5G56220	ATP Synthase	-2.9	1.5E-06	-2.3	2.0E-05		
AT2G40330	Bet V I allergen	-3.4	1.1E-07	-2.1	1.4E-05		
AT4G32810	Carotenoid Cleavage Dioxygenase (*MAX4*)	-3.2	1.3E-05	-2.4	1.5E-04		
AT3G48970	Copper-binding protein	-6.1	2.7E-07	-2.5	1.9E-04		
AT2G27690	CYP450 (*CYP94C1*)	-3.3	3.6E-07	-2.0	6.6E-05		
AT5G54490	EF-Hand protein (*PBP1*)	-10.0	3.2E-08	-2.6	1.7E-04		
AT1G69530	Expansin (*EXP1*)	-7.1	1.3E-09	-2.3	1.0E-05	Y	

AT2G40610	Expansin (*EXP8*)	-5.1	2.3E-08	-4.3	7.4E-08		
AT1G06830	Glutaredoxin	-7.4	1.5E-09	-3.1	6.8E-07		
AT4G15680	Glutaredoxin	-6.0	2.1E-07	-2.1	9.5E-04		
AT4G01950	Glycerol-3P acyltransferase (*GPAT3*)	-2.2	1.1E-04	-2.1	1.6E-04		
AT1G80280	Hydrolase	-5.6	7.7E-09	-2.3	1.4E-05		
AT1G65390	Lectin (*ATPP2-A5*)	-2.1	5.1E-06	-2.9	1.1E-07		
AT1G02660	Lipase	-11.9	2.3E-09	-2.9	1.4E-05		
AT5G05160	LRR-RLK	-3.4	6.4E-07	-2.0	1.3E-04		
AT1G78970	Lupeol synthase (*LUP1)*	-10.1	8.3E-10	-3.9	2.3E-07		
AT3G23550	MATE efflux protein	-2.7	1.2E-05	-2.1	1.3E-04		
AT3G06370	Na/H pump (*NHX4*)	-2.5	2.4E-06	-2.4	3.7E-06		
AT3G18200	MtN21 Nodulin-like protein	-10.5	3.4E-08	-2.5	2.9E-04		
AT5G14120	Nodulin-like protein	-2.2	3.4E-08	-2.1	6.5E-08		
AT5G06930	Nucleolar protein	-2.6	2.3E-05	-2.9	7.9E-06		
AT4G24120	Oligopeptide transporter (*YSL1*)	-3.7	8.4E-07	-2.6	1.8E-05		
AT4G27730	Oligopeptide transporter (*OPT6*)	-2.4	7.0E-06	-3.3	2.5E-07		
AT3G07010	Pectate lyase	-3.7	1.7E-08	-2.1	4.2E-06		
AT4G00080	Pectinesterase inhibitor (*UNE11*)	-11.7	9.5E-08	-2.3	2.1E-03		
AT5G04190	Phytochrome kinase substrate (*PKS4*)	-3.2	1.2E-06	-3.6	4.5E-07		
AT4G18290	Potassium channel (*KAT2*)	-2.3	1.0E-05	-2.6	3.8E-06		
AT1G17700	Prenylated Rab acceptor (*PRA1.F1*)	-5.5	1.3E-07	-2.0	5.2E-04		
AT4G23200	Protein kinase	-4.8	8.5E-07	-2.2	3.8E-04		
AT5G59010	Protein kinase	-2.6	2.7E-06	-3.3	3.6E-07		
AT5G18930	SAM decarboxylase (*BUD2*)	-2.5	2.7E-06	-2.2	1.3E-05		
AT5G22860	serine carboxypeptidase S28	-4.5	7.3E-09	-2.2	5.9E-06		
AT3G26760	Short-chain dehydrogenase	-3.2	1.2E-06	-3.3	9.5E-07		
AT5G19530	Spermine synthase (*ACL5*)	-7.4	1.5E-09	-5.5	8.9E-09		
AT1G23090	Sulphate transporter (*SULTR3*)	-7.9	2.3E-10	-5.3	2.5E-09		
AT5G07010	Sulphotransferase (*ST2A*)	-72.7	2.6E-13	-2.1	3.2E-05		
AT5G07000	Sulphotransferase (*ST2B*)	-3.7	1.2E-07	-2.3	9.2E-06		
AT1G72920	TIR-NBS Disease resistance	-4.6	4.2E-09	-2.2	3.9E-06		
AT1G78120	TPR-protein	-3.7	4.6E-07	-2.2	6.6E-05		
AT4G31910	Transferase	-11.0	1.6E-08	-3.2	2.7E-05		
AT2G22190	Trehalose phosphatase	-3.6	3.7E-07	-2.6	6.3E-06		
AT5G58750	Wound-responsive	-5.0	2.7E-09	-2.4	1.9E-06		
Unknown							
AT2G39370	Unknown	-9.8	2.3E-11	-7.7	8.3E-11		
AT3G42800	Unknown	-8.2	3.1E-09	-4.8	6.7E-08	Y	Y
AT3G47510	Unknown	-8.0	2.4E-09	-2.1	6.2E-05		
AT3G19200	Unknown	-6.3	1.3E-09	-3.9	3.6E-08	Y	Y
AT3G28420	Unknown	-3.3	3.1E-07	-6.5	2.6E-09		
AT4G09890	Unknown	-2.8	3.3E-05	-12.0	3.5E-09		
AT2G17080	Unknown	-2.6	2.9E-06	-2.2	1.6E-05		
AT4G35200	Unknown	-3.7	7.4E-09	-2.1	3.2E-06		
AT5G12050	Unknown	-2.9	3.3E-07	-6.1	1.2E-09	Y	
PIN / PLT Genes							
AT1G73590	*PIN1*	-1.9	9.8E-05	-3.2	4.1E-07		
AT5G57090	*PIN2/EIR1/AGR1/WAV6*	-2.9	2.4E-05	-1.5	0.03		
AT1G70940	*PIN3*	-1.1	0.57	-6.1	6.1E-09		
AT2G01420	*PIN4*	-1.4	4.8E-03	-2.8	6.5E-07		
AT5G16530	*PIN5*	1.2	0.13	1.2	0.05		
AT1G77110	*PIN6*	1.0	0.78	-1.0	0.87		
AT1G23080	*PIN7*	-1.8	6.8E-06	-2.1	5.7E-07		
AT3G20840	*PLT1*	-1.1	0.58	1.0	0.94		
AT1G51190	*PLT2*	-1.2	0.03	-1.1	0.39		
AT5G10510	*PLT3/AIL6*	-1.3	0.02	-1.2	0.11		
AT5G17430	*PLT4/BBM*	-1.0	0.70	1.1	0.56		

Table S2: Frequencies of rootless seedlings and defective embryos in mutants and transgenic lines. [a] Progeny from 6 plants heterozygous for the *mp-S319* mutation were independently counted to estimate the spectrum of allele penetrance. [b] These are the results from two independent *pRPS5A-TMO7-RNAi* lines.

Genotype	% rootless seedlings (N)	N	% defective embryos (stage)	N
Wild-type	<0.1 (>1000)	>1000		
mp-B4149	25 (329)	329		
mp-S319[a]	7 8 10 12 13 14	590 511 129 95 62 228		
tmo5-1	<0.5	>200		
TMO5 RNAi	<0.5	>200		
tmo7-1	<0.5	>200		
tmo7-2	<0.5	>200		
TMO7 RNAi[b]	7.4 1.1	50 93	7.2	529
miR-TMO7	<0.2 (1 rootless seedling)	>500	23 (globular-heart) 14 (torpedo-mature)	290 179
TMO7 RNAi mp-S319[b]	17 22	1697 481		

Table S3: Primers used in this study.

Primer Name	Sequence (5′-3′)
ChIP	
HSF1-S	GCTATCCACAGGTTAGATAAAGGAG
HSF1-AS	GAGAAAGATTGTGTGAGAATGAAA
TMO3-ChIP-S	GGTCGGCACTAATATCTAATTATCGAC
TMO3-ChIP-AS	AGCACATGTAATGGTAGAGAGTGACTATTT
TMO5-ChIP-S	CAATTCTCCTTGATGTGATCAAAGATAATGG
TMO5-ChIP-AS	TTTTGGTTTTTTTGGTTTTTTAGTTTTTGG
TMO6-ChIP-S	CAAGTTTTTGATGTGGTTATAGGTTTATAGCTTTAC
TMO6-ChIP-AS	GAAGCAAAAGGAAAAGCCAAGCATCTG
TMO7-ChIP-S	GAACTGCAAGGTCCGAGTGTCAAATTC
TMO7-ChIP-AS	CCAAGCTTTTTTGTAGAATATTGTTCAACAAGTAG
TMO7-ChIP-1-S	GGCCTATGAGTTTCTAAATACGGCCCTA
TMO7-ChIP-1-AS	GAGCCAAAGTATGAGTGATTTGACTGGTC
TMO7-ChIP-2-S	CATGTGTGGACGTGGTAGAGCGAA
TMO7-ChIP-2-AS	CGAACAGACATGGACGTCATGTAACAG
TMO7-ChIP-3-S	CTGTTACATGACGTCCATGTCTGTTCG
TMO7-ChIP-3-AS	GAATTATATGCCCCCTCTCCTGACAAC
TMO7-ChIP-4-S	GTTGTCAGGAGAGGGGGCATATAATTC
TMO7-ChIP-4-AS	GTAGTAAGAGTGACAGAGATAGAAGCAAAGGC
qPCR	
ACT2-S	ATTCAGATGCCCAGAAGTCTTGTTC
ACT2-AS	GCAAGTGCTGTGATTTCTTTGCTCA
MP-RT-S	CCCAGGATTCTTCAGCTGTTGTG
MP-RT-AS	GCTGCATCAAGGGACTGAACTG
TMO3-RT-S	CCGAGGAGTGAGACAGCGTCC
TMO3-RT-AS	GCTTCTTCCGCCGTGTTGTAAGTACC
TMO5-RT-S	CAGATCACCGACACGTATCAAGTCC
TMO5-RT-AS	GACGTCATGCATGAGGTCAGTCC
TMO7-RT-S	CCTAAACTCCATAACCTGTTTCACCG
TMO7-RT-AS	GAGTTTGCTAGTAACTCAGATAGCCTC
In-situ probes	
TMO3-ISH-S	TTCTGCAGAAATCTCTCATCTTCTTCCTCG
TMO3-ISH-AS	TTGGATCCCCACAACTACCAGTAACAAC
TMO5-ISH-S	TTCTGCAGACAAAGCTTCTTTGCTAGCG
TMO5-ISH-AS	TTGGATCCAAACCCAGCTCTATACATTTC
TMO6-ISH-S	TTCTGCAGTTGCTGAACAAACAACATCC
TMO6-ISH-AS	TTGATCCGACATTATATACCATTACCAAG
TMO7-ISH-S	TTCTGCAGATGTCGGGAAGAAGATCAC
TMO7-ISH-AS	TTGGATCCTTATTGGGTAAGTAAGCTTCTG
Promoters	
TMO3-PRO-S	TGTTTTTTTTGGTACCACTCAGCTCTATTGTCTG
TMO3-PRO-AS	TTTTCTTTCGTATTCTCTGTTTTTGACTCGAG
TMO5-PRO-S	GTTGAACGTCGTGTGGGCTTC
TMO5-PRO-AS	TTTTGGTTTTTTTGGTTTTTTAGTTTTTGG
TMO6-PRO-S	TCCATCCTATCAAACATGAAACGAAAGAAAGAG
TMO6-PRO-AS	AAGAGCTGAATCTGAGAAGTTGCTTGAAG
TMO7-PRO-S	AATTGTCAATAGTAAAACAATAGG
TMO7-PRO-AS	TTTTGTAGAATATTGTTCAACAAGTAG
TMO7-LIKE1-PRO-S	CGAATTCGATCTGTCAAAAGAGGAATTGTC
TMO7-LIKE1-PRO-AS	CGGATCCTATGTAATATATATGATATGGTAGAG
Translational fusions	
TMO5-CDS-AS	AGCATAATCAGGAACATCATAAGGATAATTATAACATCGA TTCACCATCTTAC
TMO7-CDS-AS	TTGGGTAAGTAAGCTTCTG
cDNAs	
TMO5-CDS-S	ATGTACGCAATGAAAGAAGAAG
TMO7-CDS-S	ATGTCGGGAAGAAGATCAC
RNAi	
TMO7-S	TTTTTTTTCTCGAGTCTAGAATGTCGGGAAGAAGATCAC
TMO7-AS	TTTTTTTTGAATTCGGATCCGGGTAAGTAAGCTTCTG
microRNA	
I-miR-T7-S	GATTCACTTAGATCATCAACCTCTCTCTCTTTTGTATTCC
II-miR-T7-AS	GAGAGGTTGATGATCTAAGTGAATCAAAGAGAATCAATGA
III-miR*-T7-S	GAGAAGTTGATGATCAAAGTGATTCACAGGTCGTGATATG
IV-miR*-T7-AS	GAATCACTTTGATCATCAACTTCTCTACATATATATTCCT

Chapter 3

Genetic control of stem cell specification in the plant embryo

Bert De Rybel[1,*], Barbara Möller[1,*], Saiko Yoshida[1], Ilona Grabowicz[1], Pierre Barbier de Reuille[2], Sjef Boeren[1], Richard S. Smith[2], Jan Willem Borst[1,3] and Dolf Weijers[1]

[1] Laboratory of Biochemistry, Wageningen University, Dreijenlaan 3, 6703HA Wageningen, the Netherlands

[2] Institute of Plant Sciences, University of Bern, Altenbergrain 21, Bern CH-3013, Switzerland

[3] Microspectroscopy Center, Wageningen University, Dreijenlaan 3, 6703HA Wageningen, the Netherlands

* These authors contributed equally

Abstract

Plants have the remarkable potential for indeterminate post-embryonic tissue growth. Stem cells for indeterminate growth are initiated in the early embryo. A major unanswered question is how the specification of embryonic stem cell populations is genetically controlled. Here, we identify a novel mechanism that controls both embryonic stem cell specification and tissue indeterminacy. Two bHLH transcription factor subfamilies, TARGET OF MONOPTEROS5 (TMO5/TMO5-LIKE) and LONESOME HIGHWAY (LHW/LHW-LIKE), are both critically required for vascular tissue initiation. Loss of either subfamily also triggers a switch to determinate tissue growth. Proteomic studies revealed that these proteins form heterodimeric complexes *in vivo*. Although both subfamilies are expressed in larger domains, overlap of TMO5 and LHW expression uniquely marks a small population of presumptive vascular stem cells. Strikingly, combined misexpression of both proteins triggers stem cell-like divisions. Our data reveals a mechanism for transcriptional control of a vascular cell population in which bHLH heterodimers specify stem cell identity for indeterminate growth.

Introduction

Vascular tissues in plants connect all organs and enable efficient transport of water, nutrients and hormones (Esau, 1965). They are mainly comprised of two specialized cell types called xylem and phloem that are both ancient and evolutionary conserved among vascular plants (Kenrick and Crane, 1997). The development of vascular tissues is regarded to be a key step in the evolution of land plants, and has allowed these organisms to increase in body size (Raven, 1993). In the last decades, much has been learned about specification, differentiation and pattern formation of cell types within the vascular tissue (Scarpella and Helariutta, 2010). The role of several hormones in these processes has been well established (Dettmer *et al.*, 2009). In contrast, very little is known about the mechanisms that initially define vascular tissues in early embryos. Furthermore, while stem cells for various tissues in the root have been identified (Bennett and Scheres, 2010), the vascular stem cell pool is poorly defined, and mechanisms of vascular indeterminacy are not clearly understood. Genetic screens have not identified components of these processes. This is presumably due to the high level of functional redundancy amongst genes in *Arabidopsis thaliana* (Cutler and McCourt, 2005), and because severe defects in vascular tissue development may be confounded by pleiotropy (Bonke *et al.*, 2003). We have recently identified targets (Chapter 2) of the auxin-dependent MONOPTEROS (MP) transcription factor (Hardtke and

Berleth, 1998), whose functions are diverse, and include vascular tissue development (Przemeck et al, 1996). Here, we have used MP and its direct targets as a starting point for dissecting the control of vascular tissue formation. We show that heterodimers of the bHLH transcription factors TARGET OF MONOPTEROS5 (TMO5) (Chapter 2) and LONESOME HIGHWAY (LHW) (Ohashi-Ito and Bergmann, 2007) control stem cell-like properties in a small population of cells defined by the overlap of their expression patterns. Hence, activation of the *TMO5* gene couples vascular tissue initiation in the early embryo to the establishment of the stem cell population that controls tissue indeterminacy.

Results

TMO5 controls vascular tissue initiation

While MP activity has been shown to be critical for vascular tissue development in post-embryonic stages (Donner *et al.*, 2009; Przemeck *et al.*, 1996), its role in the earliest steps of tissue establishment has not been studied. In previous work, several vascular tissue-specific genes (e.g. *TMO5*, *ATHB8*) have been identified as direct targets of MP (Donner *et al.*, 2009; Chapter 2). These genes are activated in vascular tissues at its first establishment, and expression is strongly downregulated in *mp* mutant embryos, opening the possibility that MP controls vascular initiation. The first vascular cells (Figure 1a) divide transverse and asymmetrically (100%, n=86; Table S1), and since these cells generate the entire vascular tissue, they can be regarded the first vascular stem cells (VSC). We analyzed VSC divisions in embryos of a strong *mp* mutant allele (*mp*-B4149) (Weijers *et al.*, 2005) in which mutant individuals could be identified by the well-described division defects of the hypophysis (Figure 1b). We found that the majority of mutant embryos displayed aberrant division plane orientations in VSC (88%, n=50; Table S1; Figure 1b), mostly switching from transverse to longitudinal. This defect was also found in a second independent *mp* allele (*mp*-S319) (Donner *et al.*, 2009; Chapter 2) with nearly identical frequencies (94%, n=53; Table S1). MP action in hypophysis specification is non cell-autonomous and requires the mobile transcription factor TMO7 (Chapter 2). MP protein is expressed both in and around vascular initial cells (Chapter 2; Weijers *et al.*, 2006), and its action in VSC specification and division could therefore also be cell non-autonomous. To determine the mode of MP action in this process, we expressed the MP inhibitor bdl/iaa12 (Hamann *et al.*, 2002) in the inner proembryo cells of the basal embryo region including the VSC using the Q0990 GAL4 driver line (Figure S1a) (Weijers *et al.*, 2006). This induced the same defects in VSC division as in *mp* mutants (Figure S1b), demonstrating that MP action in the first steps of vascular tissue formation does not

require signaling from apical or outer embryo cells.

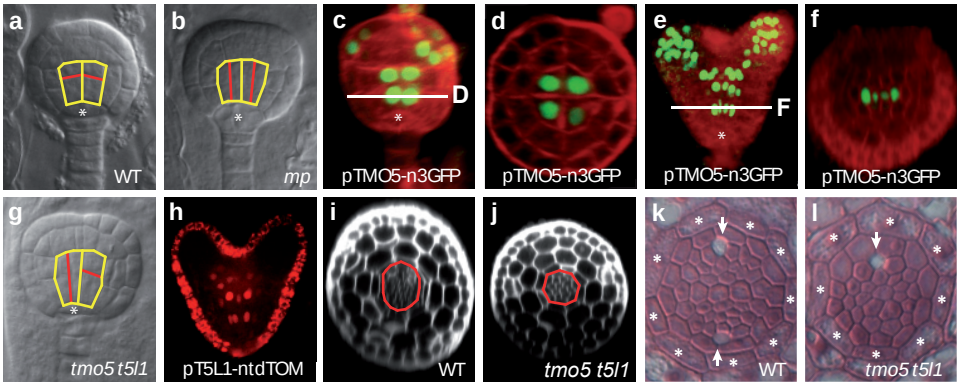

Figure 1 Vascular phenotypes of *mp* and *tmo5 tmo5-like1* double mutants. a. In wild-type globular-stage embryos, the putative vascular stem cells (VSC; yellow lines) divide transverse (red line) to produce daughter cells. In *mp* (b) and *tmo5 tmo5-like1* (g) mutant embryos, longitudinal divisions of the VSC were observed. (c-f) Expression of p*TMO5-n3GFP* (green) in globular (c, d), and heart stage (e, f) embryos, counterstained with the (red) membrane dye FM4-64. Embryos in c and e are maximum projections of 3D image stacks and D and F are cross-sections along the lines indicated. (h) Expression of p*TMO5-LIKE1-ntdTomato* in the vasculature of a heart-stage embryo. (i, j) Optical cross-sections through the root of mature wild-type (i) and *tmo5 tmo5-like1* double mutant (j) embryos show that the vascular tissue diameter is reduced in the double mutant. (k, l) Cross-sections of post-embryonic roots of wild-type (k) and *tmo5 tmo5-like1* double mutant (l) show that the normal pattern of two phloem poles (arrows) and a xylem axis in wild-type (k) is changed to a single phloem and xylem pole in the double mutant (l). Asterisks indicate lens shaped cell in (a, c, e, g); undivided hypophysis in (b) and endodermis cells in (k, l).

The MP target gene *TMO5* encodes a bHLH transcription factor that is initially expressed in all 4 vascular initials (Figures 1c, d) and later becomes restricted to xylem in both embryo (Figures 1e, f) and root (Figures S1f, g) and thus represents a good candidate for mediating MP function in vascular initiation. Indeed, restoring TMO5 expression in a weak *mp* mutant partially restores root formation (Chapter 2). As the bHLH transcription factor TMO7 shows the same initial gene expression pattern, but the protein is transported to the adjacent hypophysis (Chapter 2), we first investigated TMO5 protein localization. The accumulation of TMO5-3GFP, TMO5-tdTomato and TMO5-YFP translational fusion proteins exactly matched previously described *TMO5* mRNA and p*TMO5-n3GFP* reporter patterns in globular stage embryos (Figures S1d, e) and mature roots (Figures S1h-j). As TMO5-3GFP protein is active in complementing mutant phenotypes (see below), this suggests that TMO5 is not transported out of the VSC.

To determine the role of TMO5 in vascular tissue initiation, we analyzed insertion mutants (Figures S3a, b). As *tmo5* single mutants did not display any phenotypes (Chapter 2), we created a double mutant with its closest homolog *TMO5-LIKE1* (At1g68810). The TMO5-LIKE1 protein is 48% identical to TMO5 (Figure S2) and the gene shows MP-dependent expression in transcript profiling (Chapter 2) (Figure S8), and is expressed in the vasculature of the embryo (Figure 1h). Interestingly, at globular stage, *tmo5 tmo5-like1* double mutants displayed VSC division defects similar to the *mp* mutant, albeit at lower frequency (7,4%; Figure 1g; Table S1). At later embryonic stages, the vascular tissue was reduced in diameter in the double mutant, and contained fewer cells (Figure 1i, j). Post-embryonically, double mutant roots showed a characteristic phenotype with a reduced vascular tissue with one phloem pole and one protoxylem pole (monarch symmetry; Figure 1l), compared to two of each (diarch symmetry) in wild-type (Figure 1k). This phenotype was complemented by introduction of TMO5-3GFP fusion protein (Table S2).

To establish the relationship between TMO5 expression and vascular tissue development, we first optimized a procedure for 3D imaging and segmentation of Arabidopsis embryos. The ontogeny of the vascular system during early embryogenesis has been described, bur only at low resolution (Chapter 2), and hence the 3D-arrangement of cells and their relation is entirely unclear. 2D analysis of the small and elongated vascular cells hampers precise analysis of phenotype at tissue inception. In stead, our optimized 3D imaging method allows detailed analysis of cell divisions in fixed embryos (Figure 2a-d). In wild-type, the four vascular initial cells all divide longitudinally to give rise to two concentric cell layers (Figure 2a, b, i). Subsequently, the outer cells all divide longitudinally (Figure 2c, i). In contrast to these regular divisions, already the first transverse division of vascular initials is disturbed in *tmo5 tmo5-like1* embryos (Figures 2e-f), leading to a vascular tissue with fewer cells dividing at abnormal planes (Figures 2g-h). The occurrence of this defect immediately follows the first appearance of TMO5 expression (Figures 1c, d).
We conclude that TMO5 and TMO5-LIKE1 act downstream of MP to control the first divisions of the vascular initials (Figure 2i), and hence the establishment of the vascular tissue.

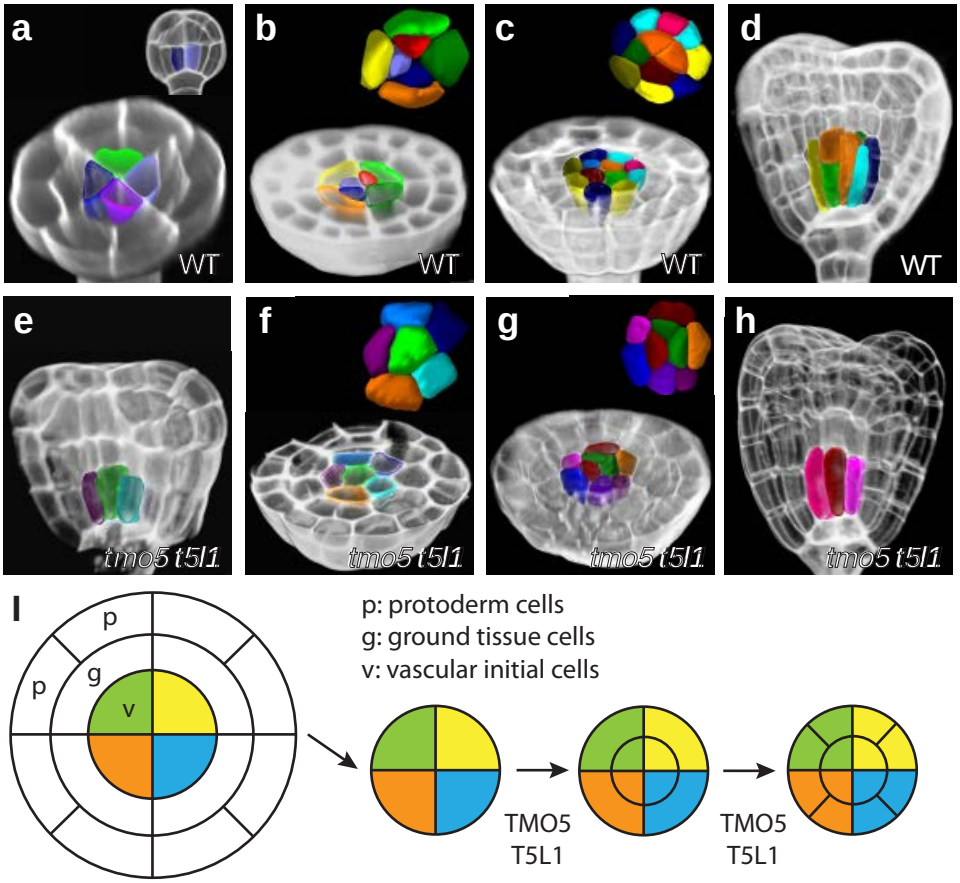

Figure 2 3D imaging of wild type and *tmo5 tmo5-like1* mutant embryos. (a-h) 3-dimensional reconstructions of wild-type (a-d) and *tmo5 tmo5-like1* mutant (e-h) embryos. Images show transversal (a-c, f, g) and longitudinal (d, e, h) sections (white). Segmented cells within the vascular lineage are shown as randomly colored volumes. Inset in (a) shows longitudinal section of the same embryo. Insets in (b, c, f, h) show a top view of the vascular cell volumes. Images in (c, d), (e, f) and (g, h) are different views of the same embryo. Note that all 4 vascular cells (a) undergo 2 stereotyped divisions in wild-type (b, c). In the *tmo5 tmo5-like1* double mutant these divisions are disturbed (f, h). (i) Schematic representation of the vascular initial cell divisions in wild type and indication of which steps are controlled by TMO5 and TMO5-LIKE1.

TMO5 forms a bHLH dimer with LHW *in vivo*

The root phenotype observed in the *tmo5 tmo5-like1* mutant had previously been described in the *lonesome highway* (*lhw*) mutant (Ohashi-Ito and Bergmann, 2007). Indeed, in our hands, phenotypes of *lhw* and *tmo5 tmo5-like1* are indistinguishable (Table S2 and Figure S4). *LHW* encodes a bHLH transcription factor that is phylogenetically distant from TMO5 (<10% identity: Figure S2), and yeast-2-hybrid screens had suggested a potential interaction between LHW and

TMO5 (Ohashi-Ito and Bergmann, 2007). To determine if TMO5-LHW dimers are formed *in vivo* during embryogenesis, we performed immunoprecipitation (IP) on TMO5-3GFP siliques followed by mass spectrometry (MS). After relative quantification and statistical analysis, we found TMO5 and GFP to be the most abundant proteins in the immunocomplex, confirming the quality of the analysis (Table S3). Importantly, LHW and LHW-LIKE2 (At2g31280) were recovered (Figure 3a; Table S3), confirming an *in planta* interaction between TMO5 and LHW/LHW-LIKE2 during embryogenesis.

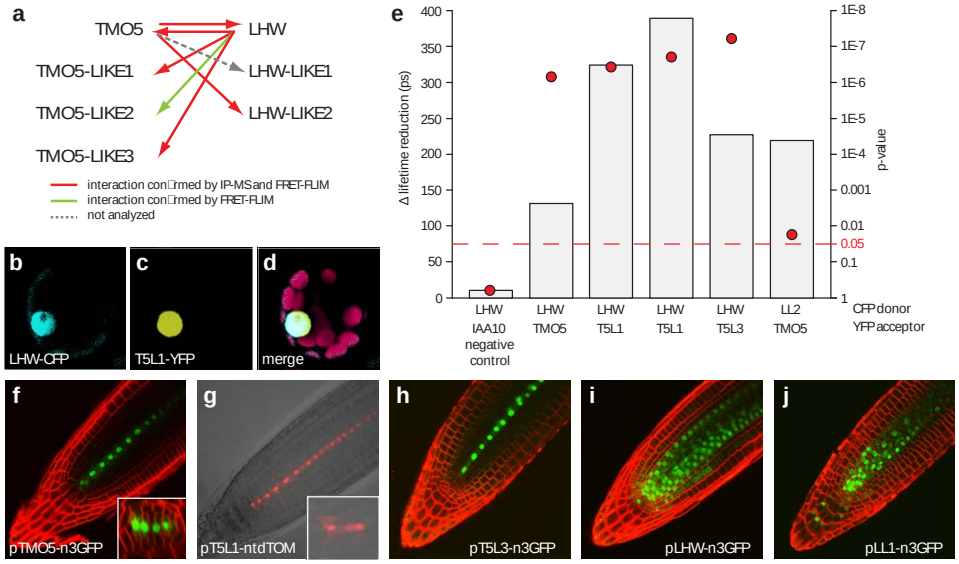

Figure 3 Members of the TMO5 and LHW subclades interact *in planta*. a. Overview of the interactions between TMO5 and LHW subclade members as determined by immunoprecipitation (IP) in combination with mass spectrometry (MS) and/or FRET-FLIM analyses. IP-MS was performed on siliques and/or seedlings expressing TMO5-3GFP or LHW-YFP protein fusion constructs. A detailed list of the interactors can be found in Table S4. b-d. Expression of YFP-tagged TMO5-LIKE1 (b) and CFP-tagged LHW (c) in protoplasts. (d) Overlay of YFP and CFP signals with chloroplast autofluorescence. Note co-localization in the nucleus of protoplasts. e. Reduction in fluorescence lifetime of the CFP donor (in picoseconds, left Y-axis) and respective p-values (right Y-axis) for tested interactions between members of the LHW and TMO5 subclades as determined by FRET-FLIM analysis. IAA10-YFP was used as negative control. f-j. Expression patterns of p*TMO5-n3GFP* (f), p*TMO5-LIKE1-ntdTomato* (g), p*TMO5-LIKE3-n3GFP* (h), p*LHW-n3GFP* (i) and p*LHW-LIKE1-n3GFP* (j) in the root meristem. Insets in f and g show confocal cross sections through the root meristem.

We next performed reciprocal IP-MS experiments on LHW-YFP siliques and seedling roots and recovered TMO5, TMO5-LIKE1 and TMO5-LIKE3 as inter-

actors (Figure 3a; Table S3).
These results demonstrate with high confidence that TMO5 and LHW form a complex *in vivo*, but the recovery of LHW-LIKE2, TMO5-LIKE1 and TMO5-LIKE3 suggest that other members of the same subclades may also interact. To test this hypothesis and to determine if the observed interactions are direct protein-protein interactions, we used a FRET-FLIM interaction analysis on CFP- and YFP-tagged proteins expressed in a transient Arabidopsis leaf mesophyll protoplast system (Figure 3b-d). In this assay, changes of the fluorescence lifetime of the donor (CFP) molecules are measured upon interactions with an YFP-tagged acceptor fusion protein (Kremers *et al.*, 2006). We detected a significant reduction of the CFP fluorescence lifetime, and hence interactions, between LHW and all TMO5 subclade members and between TMO5 and the LHW subclade members analyzed (Figure 3e). These data confirm that functional TMO5-LHW bHLH heterodimers exist *in planta*, while genetic data suggests that both partners act to positively control the same process.

TMO5-LHW dimers control vascular indeterminacy
Our protein interaction studies imply further genetic redundancy of TMO5 and TMO5-LIKE1 with TMO5-LIKE2 and TMO5-LIKE3, as well as of LHW with LHW-LIKE1 and LHW-LIKE2. To determine which of these proteins could contribute to vascular development, we analyzed the expression pattern of the interacting members of the *TMO5* and *LHW* clades. Importantly, all *TMO5* subclade members analyzed showed expression in the vasculature of the root meristem (Figures 3g, h) similar to *TMO5* (Figure 3f). In striking contrast to these highly specific expression patterns, *LHW* and *LHW-LIKE1* were more broadly expressed in embryos (Figures 4e, f) and in root meristems (Figures 3i-j), while no *LHW-LIKE2* expression could be observed in the embryo or root.
Given the co-expression and *in vivo* interaction between TMO5 and LHW subclades, we determined the consequences of further reducing the function of either of the two subclades. Therefore, we created higher-order mutants by combining alleles with strongly reduced transcript levels (Figures S3a, b). None of the double and triple mutant combinations that we generated in the TMO5 subclade, showed defects unless both *tmo5* and *tmo5-like1* mutations were present (Table S2 and Figure S4). This suggests that *TMO5* and *TMO5-LIKE1* are the main regulators of vascular development, while *TMO5-LIKE2* and *TMO5-LIKE3* do not make major contributions in an otherwise wild-type background. Interestingly however, *tmo5 tmo5-like1 tmo5-like3* triple mutants and *tmo5 tmo5-like1 tmo5-like2 tmo5-like3* quadruple mutants displayed dramatic vascular phenotypes that increased in severity upon removal of more clade members (Table S2; Figures 4a, b, d and S4).

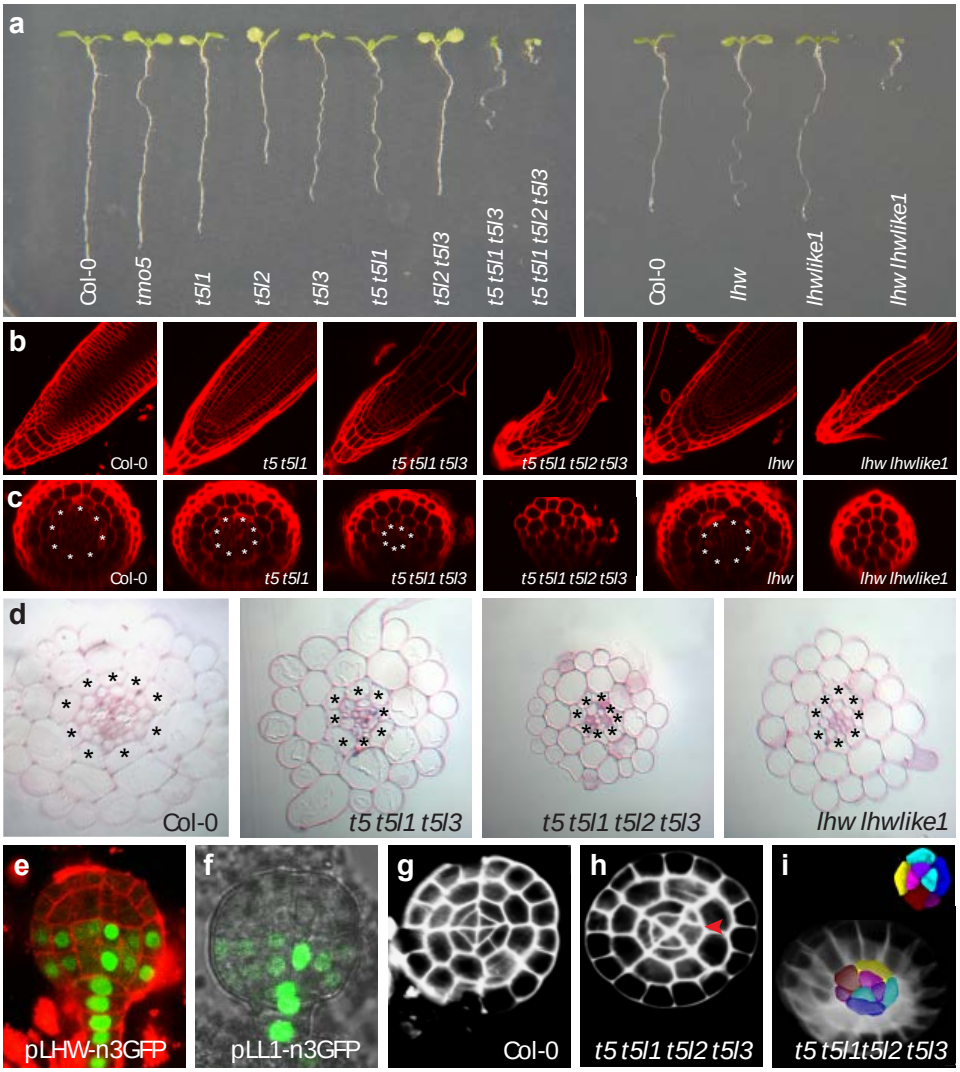

Figure 4 TMO5 and LHW are required for vascular development and indeterminacy. a. Seedling phenotypes of 7-day-old single and multiple mutants within *TMO5* and *LHW* clades. The *TMO5* clade triple and quadruple mutants, as well as the *lhw lhw-like1* double mutant, show a strong reduction of root length compared to wild-type roots. b, c. Root meristems and representative optical cross-sections through the meristem of *TMO5* and *LHW* clade single and multiple mutants. d. Histological cross-sections through mature roots of *TMO5* and *LHW* clade single and multiple mutants. e, f. Expression patterns of p*LHW-n3GFP* (e) and p*LHW-LIKE1-n3GFP* (f) in globular-stage embryos. Embryo in e was counterstained using FM4-64. (g-i) Optical transverse cross-sections (g, h) and segmented cell volumes (i) of wild-type (g) and *tmo5 tmo5-like1 tmo5-like2 tmo5-like3* quadruple mutant (h, i) embryos. Inset in (i) shows top view of vascular cell volumes. Note abnormal division plane of vascular cell in quadruple mutant (arrowhead). All image series in b, c and d were taken at same magnification. Asterisks in c-d indicate endodermis cells.

In *tmo5 tmo5-like1 tmo5-like3* triple mutants, the vascular tissue in the root meristem was reduced in size relative to the *tmo5 tmo5-like1* double mutant (Figures 4b, d and S4). Furthermore, only short stretches of differentiated vascular tissue could be observed along the entire length of the root (Figure S4). In quadruple *tmo5 tmo5-like1 tmo5-like 2 tmo5-like3* mutants, we did not observe any differentiated vascular tissue along the root (Figure S4). As a consequence of this defect, these mutants produced seedlings with a very short root (Figure 4a).
Strikingly, *lhw lhw-like1* double mutants showed identical defects compared to quadruple mutants in the *TMO5* subclade (Figures 4a, b, d and S4). In all mutants, epidermis and endodermis differentiated normally as judged by the presence of root hairs and Casparian strips (Figures 4b, d and S4); which were present even in severely affected roots. Hence, initial defects were restricted to vascular tissue, despite expression of both *LHW* and *LHW-LIKE1* in other cell types (Figures 3i, j). Analysis of initial defects in *tmo5 tmo5-like1 tmo5-like 2 tmo5-like3* quadruple mutant embryos by 3D imaging (Figures 4g-i) showed that phenotypes are indistinguishable from the *tmo5 tmo5-like1* double mutant (Figures 2e-f). Importantly, while the reduced size of the vascular tissue in *tmo5 tmo5-like1* double or *lhw* single mutants was stable and indeterminate, all higher-order mutants showed a switch to determine vascular growth with younger parts of the root having even less vascular cells than older parts of the same root (Figure S4). Hence TMO5-LHW clade heterodimers are critical for establishing vascular indeterminacy.

TMO5/LHW dimers trigger stem cell-like divisions

Genetic and proteomic data demonstrates that vascular tissue establishment and subsequent indeterminacy depends on a complex containing both TMO5 and LHW proteins. To identify precisely which cells accumulate both proteins, and are hence capable of forming such heterodimers, we generated a line expressing both TMO5-tdTomato and LHW-YFP. Even though the low abundance of these proteins precluded sensitive detection in embryos, we found nuclei in the vascular tissue of heart-stage embryos that accumulate both proteins (Figures 5a-e). Post-embryonically, LHW-YFP protein was found in all cell types of the root meristem but its abundance decreased sharply as cells were displaced further away from the QC (Figures 5g-j). In contrast, while TMO5-tdTomato protein is specific to xylem cells in the root meristem, its levels remained relatively constant along the cell file (Figures 5f, i). Quantification of signals for both proteins and determination of relative abundance revealed a steep gradient of the LHW to TMO5 ratio along the root meristem (Figures 5h and S5). The cells with high TMO5 and LHW levels are located close to the quiescent center (QC) and considering the requirement of heterodimers for vascular indeterminacy these cells may correspond to the pre-

sumptive xylem stem cells in the root meristem.

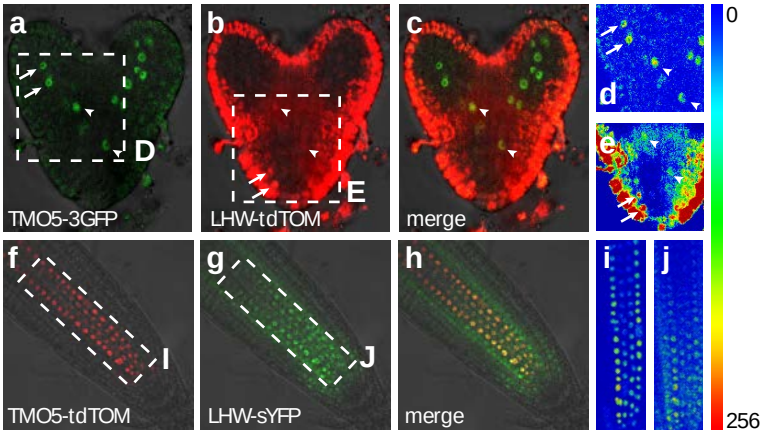

Figure 5 TMO5 and LHW co-localize in a small subset of cells in embryos and root meristems. a-c. Co-localization of TMO5-3GFP (green) and LHW-tdTomato (red) proteins driven by endogenous promoters in vascular cells of a heart-stage embryo of a double-tagged line. d, e. False color images showing TMO5 and LHW protein accumulation. Arrows in a-e indicate nuclei with TMO5 or LHW protein accumulation, while arrowheads indicate nuclei with co-localization of both proteins. f-h. Co-localization of TMO5-tdTomato (red) and LHW-YFP (green) proteins driven by endogenous promoters in the xylem cells of the root meristem. i-j. False color images showing TMO5 and LHW protein accumulation. False color scale is shown on the right.

To investigate if accumulation of TMO5-LHW dimers limits the vascular stem cell population, we individually misexpressed TMO5, LHW and their closest homologs using the strong *RPS5A* promoter (Weijers *et al.*, 2001) (Figures S3c, d). Consistent with the broader expression of LHW and LHW-LIKE1, their misexpression did not induce obvious defects (Figures 6a, b and S6e-g). In contrast, root diameter was increased in pRPS5A-TMO5 and pRPS5A-TMO5-LIKE1 lines (Figures 6a-c and S6a, b); which was in part due to an increased vascular tissue size (Figures 6i-j). This phenotype became apparent as early as the heart stage of embryogenesis (not shown), and we also observed vascular over-proliferation in late rosette leaves (Figure S6h).

While the TMO5 misexpression phenotype and loss of function defects are consistent with the TMO5-LHW heterodimer being necessary and sufficient for defining a vascular stem cell population, the data could also be explained by these proteins regulating an aspect of vascular identity. Strongly affected *tmo5 tmo5-like1 tmo5-like3* triple mutants with severely reduced vascular tissue still differentiated patches of xylem (Table S2), rendering a prominent role in vascular tissue identity unlikely. Nonetheless, we introduced markers for cell identities within the vascular tissue in TMO5 misexpression lines, and in *tmo5 tmo5-like1* double

mutants. We did not observe changes in the expression of the vascular marker Q0990 in pRPS5A-TMO5 roots (Figures 6e, f). Likewise, *TMO5* expression was still detected in the remaining cells in the xylem position in *tmo5 tmo5-like1* roots (Figures 6g, h). Hence, we conclude that TMO5 does not regulate vascular tissue identity, but rather controls stem cell-like properties within the vascular tissue.

To determine if the proposed activity of TMO5 in promoting stem cell-like properties is limited to vascular cells, we used the J0571 GAL4 driver to misexpress a functional, DEX-inducible TMO5-GR protein (Figures S6j, k) in the ground tissue, a cell type that expresses LHW (Figures 3i and 5g), but not TMO5 (Figures 3f and 5f). In J0517>>TMO5-GR seedlings grown on dexamethasone (DEX), we observed excessive longitudinal divisions in the ground tissue, resulting in additional ground tissue cell layers (Figure 6m, o). This division plane orientation is normally limited to the ground tissue stem cell (Figures 6l,n). Interestingly, the capacity to induce stem cell-like divisions was not limited to either of the two ground tissue cell types (cortex or endodermis; Figure 6o).
Finally, to determine if the TMO5-LHW heterodimer could function more generally as a stem cell-promoting complex outside of the domain that is defined by expression of *LHW* and *TMO5* genes, we misexpressed both genes using the *RPS5A* promoter. This resulted in dramatically increased root meristems, in which cells in most cell types proliferated excessively (Figures 6d, k). In addition to a multi-layered ground tissue, this also resulted in multiple layers of vascular and epidermal tissues. Hence, the TMO5-LHW heterodimer can induce stem cell-like divisions in all three major tissues in the root.
Strikingly, in these lines, excessive stem cell-like divisions were not limited to the root or vascular systems, as ectopic leaves were initiating on pre-existing leaves (Figures 6p-r and S7), leading to highly fascinated and compound leaves (Figure S7). This result suggests that TMO5-LHW heterodimers are capable of promoting stem cell-like properties in various contexts, and that their activity is normally restricted to young xylem cells by transcriptional regulation of both genes.

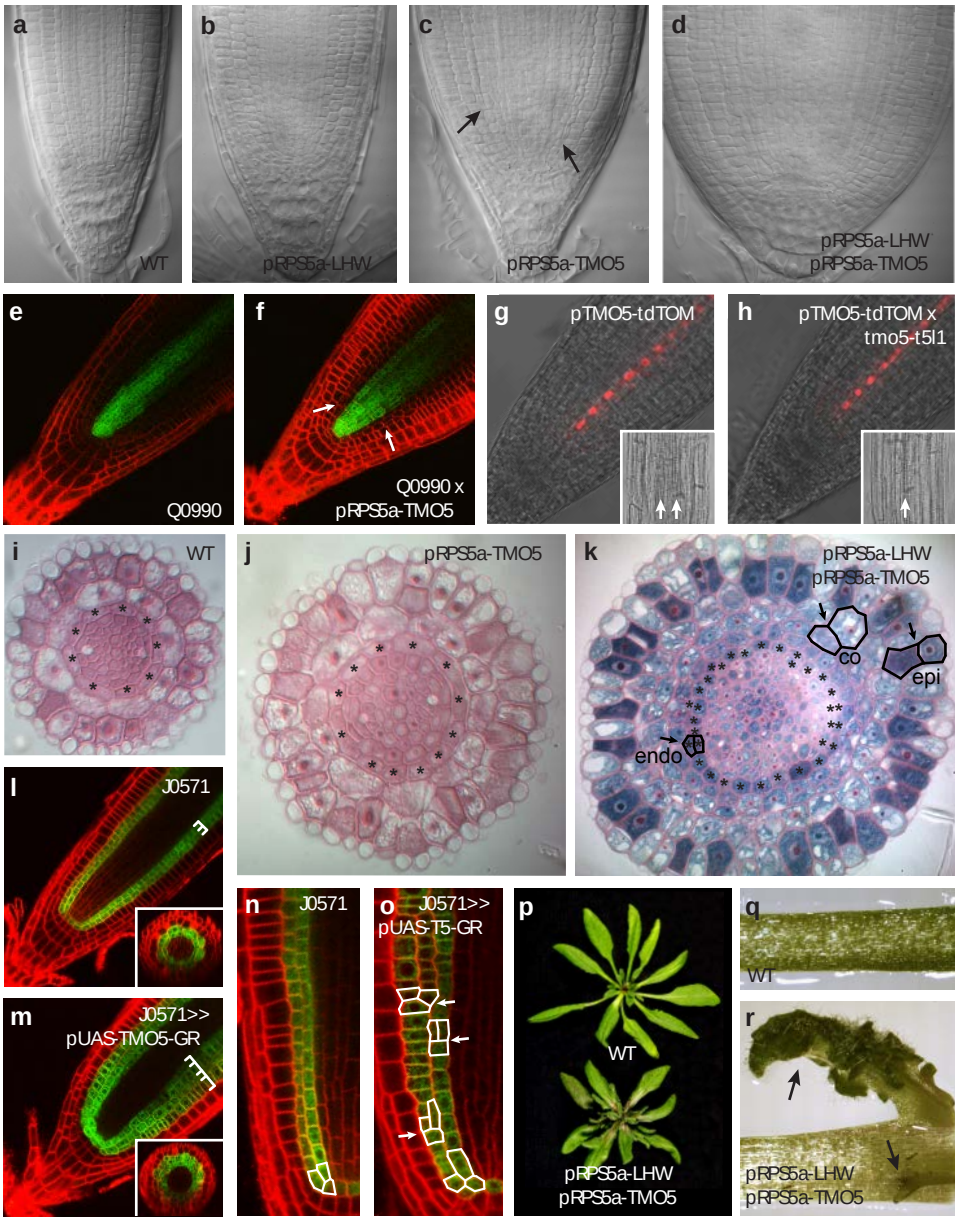

Figure 6 TMO5-LHW heterodimers trigger stem cell-like divisions. a-d. Root meristems of seedlings misexpressing LHW (b), TMO5 (c) or both TMO5 and LHW (d) driven by the RPS5A promoter. E-F. Expression of the vascular marker Q0990 (green) in wild-type (e) or pRPS5A-TMO5 (f) root tips. g-h. p*TMO5-n3GFP* expression in wild-type (g) or *tmo5 tmo5-like1* double mutant (h) root tips. i-k. Histological sections through root meristems of wild type plants (i) or plants misexpressing TMO5 (j) or both TMO5 and LHW (k) epi: epidermic, co: cortex, endo: endodermis. Histological sections were stained with rhutenium red and/or toluidine blue. l-o. Expression of ground

tissue marker J0571 (green) in wild type root tip (l, n) and in J0571>>pUAS-TMO5-GR plants grown on 10 μM dexamethasone (DEX; m, o). Note that additional layers of J0571-expressing cells (brackets) are found in (m, o). Insets show cross-sections of the root tips. P-R. Rosette phenotype of wild type plants and plants misexpressing both TMO5 and LHW (p). Detail of a leaf petiole of the same age of a wild type plant (Q) and a plant misexpressing both TMO5 and LHW (r, arrows indicate ectopic leaf primordia). q and r are details from leaf series in Figure S7. Arrows in c and f indicate ectopic divisions. Asterisks in i-k indicate endodermis cells. In all confocal images, roots were counterstained with FM4-64.

Discussion

Our study identifies key regulators of vascular tissue formation and indeterminacy in *Arabidopsis thaliana*. The TMO5-LHW bHLH heterodimer acts during the very first division of vascular cells in the early embryo. It controls both the establishment of a vascular tissue containing a sufficient number of cells and the indeterminacy of this cell population in the growing post-embryonic tissue. Based on the requirement of both TMO5 and LHW partners for indeterminacy and the sufficiency for stem cell-like divisions, we propose that the protein dimer represents a stem cell determinant within the vascular system. Although the precise mode of action of the dimer remains to be determined through the identification of its target genes, several findings suggest that the primary function is in defining a cellular state that allows indeterminate growth. The initial size of the vascular tissue is similar in double, triple and quadruple *tmo5 tmo5-like* mutants (Figure S4), but in contrast to the double mutant, triple and quadruple mutants fail to maintain this size. This observation, together with the findings that vascular identity markers are unaffected in mutants, and that combined ectopic expression of TMO5 and LHW is sufficient to induce stem cell-like divisions in various different tissue types, suggests that the dimer triggers stem cell properties. As TMO5-LHW protein co-expression is limited to the youngest xylem cells in the root (Figure 7), it is conceivable that these cells act as a local organizer that determines the size of the vascular tissue.

Our findings reveal a new mechanisms for the specification of a plant stem cell population that relies on the integration of two gene expression patterns (Figure 7). bHLH proteins are thought to require dimerization for DNA binding (Massari and Murre, 2000) and the stoichiometry between both partners is therefore essential for complex formation. For example, regulation of bHLH partner accumulation is key to the formation of transcription complexes in vertebrate myogenesis (Berkes and Tapscott, 2005), B-cell specification (Sigvardsson *et al.*, 1997) and Drosophila sex determination (Salz and Erickson, 2010). In the latter example, the difference between 1 and 2 copies of an X-linked bHLH gene is crucial in sex determination.

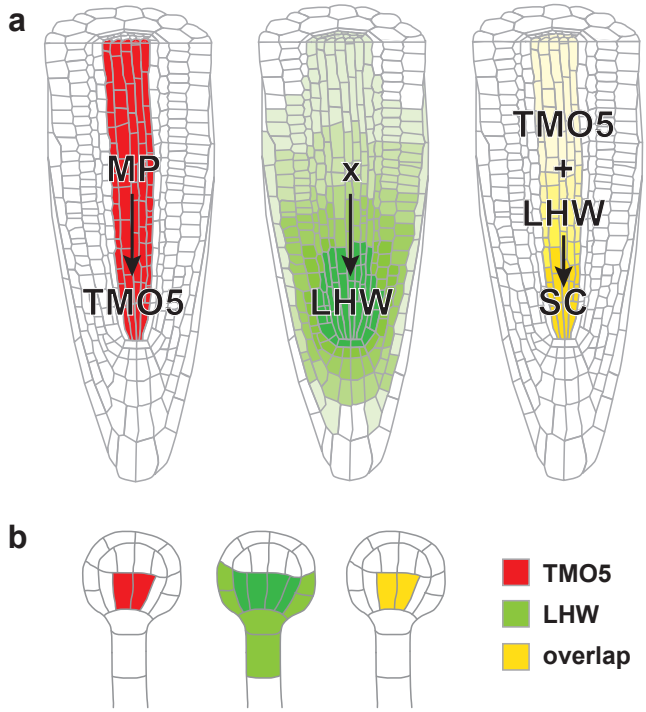

Figure 7 A model for specification of the vascular stem cell population. A MP-dependent pathway controls TMO5 expression (red) while a yet unknown pathway controls LHW (green) in roots (a) and globular stage embryos (b). A TMO5-LHW dimer is formed only in cells that accumulate both proteins (yellow). In this cell population, the transcription factor dimer promotes stem cell (SC) properties.

While TMO5 is strictly tissue-specific and protein levels remain fairly constant as cells are displaced from the distal part of the root tip, LHW accumulates in all cell types of the root meristem, but protein levels decline sharply from younger to older cells (Figure 7). These two overlapping patterns mark a small distal subpopulation of vascular cells with high levels of poth proteins. Given that the probability of heterodimer formation is proportional to the absolute quantities of both proteins, these two patterns are integrated to define a discrete domain in which heterodimers can form. Given the biological function of the heterodimer, it is conceivable that the stems for the vascular tissue are directly defined by the accumulation of these two proteins. Hence, the combinatorial regulation of these two genes allows accurate positioning of the stem cell domain by both radial (*TMO5*) and longitudinal (*LHW*) restriction. Co-accumulation of TMO5 and LHW marks the earliest vascular precursors (Figure 7), whose divisions depend on both TMO5

and LHW proteins.
Finally, the dimeric nature of TMO5-LHW complexes allows integration of different developmental and hormonal inputs in controlling the vascular stem cell population and in vascular development. *TMO5* is a direct auxin response gene (Chapter 2), while *LHW* is not (Figure S8). As such, transcriptional control of *LHW* sets a domain of competence for auxin-dependent vascular tissue formation, which is consistent with the reduced NPA-induced vascular hypertrophy in the *lhw* mutant (Ohashi-Ito and Bergmann, 2007).
In conclusion, our work has provided long-sought factors that control vascular tissue formation and indeterminacy. Both *TMO5* and *LHW* genes have homologues in sequenced genomes of all vascular plants including *Selaginella moellendorffii*, but not in the (non-vascular) moss *Physcomitrella patens* (Carretero-Paulet *et al.*, 2010; Pires and Dolan, 2010a, b). Therefore, the identification of the TMO5-LHW dimer as a stem cell factor should now allow addressing questions of vascular system evolution and stem cell identity.

Material and Methods

Plant material

All seeds were surface sterilized, sown on solid MS plates and vernalized for two days before growing at a constant temperature of 22°C in a growth room. T-DNA or Ds transposon insertion lines *tmo5-3* (GABI-KAT_143E03), *tmo5-like1* (RIKEN_12-4602-1), *tmo5-like2* (RIKEN_16-0907-1), *tmo5-like3* (SALK_109295), *lhw* (SALK_023629) and *lhw-like1* (SALK_108940), and Q0990 en J0571 GAL4 enhancer trap lines were obtained from the Arabidopsis Stock Centers (NASC-ABRC) and were genotyped using primers listed in Table S4.

Cloning

All cloning was performed using the LIC cloning system (De Rybel *et al.*, 2011) and the vectors described therein. For transcriptional fusions of pTMO5, pTMO5-LIKE1, pTMO5-LIKE3, pLHW, pLHW-LIKE1 and pLHW-LIKE2, 2-4 kb fragments upstream of the ATG were PCR-amplified from genomic DNA using Phusion Flash polymerase (Finzymes). For translational fusions, the same promoter fragment was amplified together with the genomic coding sequence excluding the stop codon. To generate pRPS5A-driven misexpression, coding sequences of all genes were amplified from cDNA clones. To generate pRPS5A-TMO5-GR, pRPS5A-TMO5-YFP and pRPS5A-LHW-YFP, GR or YFP were added to the cDNA by overlap extension PCR. All constructs were completely sequenced. Primers used are listed in Table S4.

Microscopic analysis

Differential interference contrast (DIC) microscopy, fluorescence and confocal microscopy were performed as described previously (Llavata-Peris *et al.*, 2011). For histological sections, roots were fixed overnight and embedded as described previously (De Smet *et al.*, 2004). 3D imaging of embryos was performed as described previously with minor modifications (Truernit *et al.*, 2008). Briefly, embryos were hand-dissected from ovules before fixation and Schiff-staining. Confocal image stacks were reconstructed and segmentation of cell volumes was performed in MorphoGraphX software (http://sybit.net/software/MorphoGraphX/).

IP-MS

Immunoprecipitation experiments were performed as described previously (Zwiewka *et al.*, 2011) using 3g of siliques and/or seedlings of pTMO5-TMO5-3GFP or pLHW-LHW-YFP transgenic lines in Col-0 background for each sample. Interacting proteins were isolated by applying a total protein extracts to anti-GFP coupled magnetic beads (Milteny Biotech). Three biological replicates of each sample were compared with three non-transgenic Col-0 samples (Table S3). MS and statistical analysis using MaxQuant and Perseus software was performed as described previously (Hubner *et al.*, 2010; Lu *et al.*, 2011) with minor modifications.

FRET-FLIM

FRET-FLIM analysis in Arabidopsis leaf mesophyll protoplasts was performed as described previously (Rademacher *et al.*, 2011) with minor modifications. All cloning for FRET-FLIM was done using pMON999-LIC-YFP-NOSt and pMON999-LIC-CFP-NOSt vectors modified for LIC-cloning (De Rybel *et al.*, 2011) and primers described in Table S4.

Q-RT-PCR analysis

Q-RT-PCR analysis was performed as described previously (De Rybel *et al.*, 2010). RNA was extracted with the RNeasy kit (Qiagen). Poly(dT) cDNA was prepared from 1 µg of total RNA with an iScript cDNA Synthesis Kit (Biorad) and analyzed on a CFX384 Real Time PCR detection system (BioRad) with iQ SYBR Green Supermix (BioRad) according to the manufacturer's instructions. Primer pairs were designed with the Beacon Designer 7.0 (Premier Biosoft International). All individual reactions were done in triplicate with two or three biological replicates. Data were analyzed with qBase (Hellemans *et al.*, 2007). Expression levels were normalized to those of *EEF1α4* and *CDKA1;1*. Primer sequences are listed in Table S4.

Acknowledgements and author contributions

The authors would like to thank Thomas Berleth and Yka Helariutta for sharing materials and Tom Beeckman and Sacco de Vries for helpful comments on the manuscript. This work was supported by a long-term FEBS fellowship and a Marie Curie long term FP7 Intra-European Fellowship (IEF-2009-252503) to B.D.R., by a Swiss National Science Foundation grant (CR3213_132586) and SystemsX.ch support to R.S.S., and by funding from the Netherlands Organization for Scientific Research (NWO; ALW-VIDI-864.06.012 and ALW-820.02.019 and) to D.W.
B.D.R and B.M. performed most experiments. S.Y. performed 3D imaging of TMO5 expression and vascular development. P.B.d.R. and R.S. developed MorphoGraphX software. I.G. generated FRET-FLIM data with the help of J.W.B. and B.D.R. S.B. performed nLC-MS/MS analyses. B.D.R, B.M. and D.W. conceived the study and wrote the paper with input from all authors. D.W. supervised the project. The authors declare that they have no competing financial interests.

References

Bennett T and Scheres B. (2010). Root development-two meristems for the price of one? Curr Top Dev Biol. 91:67-102.

Berkes CA and Tapscott SJ. (2005). MyoD and the transcriptional control of myogenesis. Semin Cell Dev Biol. 16(4-5): 585-95.

Bonke M, Thitamadee S, Mähönen AP, Hauser MT and Helariutta Y. (2003). APL regulates vascular tissue identity in Arabidopsis. Nature. 426(6963): 181-186.

Carretero-Paulet L, Galstyan A, Roig-Villanova I, Martínez-García JF, Bilbao-Castro JR and Robertson DL. (2010). Genome-wide classification and evolutionary analysis of the bHLH family of transcription factors in Arabidopsis, poplar, rice, moss, and algae. Plant Physiol. 153(3):1398-1412.

Cutler S and McCourt P. (2005). Dude, where's my phenotype? Dealing with redundancy in signaling networks. Plant Physiol. 138(2): 558-559.

De Rybel B, van den Berg W, Lokerse A, Liao CY, van Mourik H, Möller B, Peris CL and Weijers D. (2011). A versatile set of ligation-independent cloning vectors for functional studies in plants. Plant Physiol. 156(3): 1292-1299.

De Rybel B, Vassileva V, Parizot B, Demeulenaere M, Grunewald W, Audenaert D, Van Campenhout J, Overvoorde P, Jansen L, Vanneste S, Möller B, Wilson M, Holman T, Van Isterdael G, Brunoud G, Vuylsteke M, Vernoux T, De Veylder L, Inzé D, Weijers D, Bennett MJ and Beeckman T. (2010). A novel aux/IAA28 signaling cascade activates GATA23-dependent specification of lateral root founder cell identity. Curr Biol. 20(19): 1697-1706.

De Smet I, Chaerle P, Vanneste S, De Rycke R, Inzé D and Beeckman T. (2004). An easy and versatile embedding method for transverse sections. J Microsc. 213(Pt 1): 76-80.

Dettmer J, Elo A and Helariutta Y. (2008). Hormone interactions during vascular development. Plant Mol Biol. 69(4): 347-360.

Donner TJ, Sherr I and Scarpella E. (2009). Regulation of preprocambial cell state acquisition by auxin signaling in Arabidopsis leaves. Development. 136(19): 3235-3246.

Esau K. (1965). Plant Anatomy (2nd edition), Wiley, New York.

Hamann T, Benkova E, Bäurle I, Kientz M and Jürgens G. (2002). The Arabidopsis *BODENLOS* gene encodes an auxin response protein inhibiting MONOPTEROS-mediated embryo patterning. Genes Dev. 16(13): 1610-1615.

Hardtke CS and Berleth T. (1998). The Arabidopsis gene MONOPTEROS encodes a transcription factor mediating embryo axis formation and vascular development. EMBO J. 17(5): 1405-1411.

Hellemans J, Mortier G, De Paepe A, Speleman F and Vandesompele J. (2007). qBase relative quantification framework and software for management and automated analysis of real-time quantitative PCR data. Genome Biol. 8(2): R19.

Hubner NC, Bird AW, Cox J, Splettstoesser B, Bandilla P, Poser I, Hyman A and Mann M. (2010). Quantitative proteomics combined with BAC TransgeneOmics reveals in vivo protein interactions. J Cell Biol. 189(4): 739-754.

Kenrick P and Crane PR. (1997). The origin and early evolution of plants on land. Nature. 389: 33-39.

Kremers GJ, Goedhart J, van Munster EB, Gadella TW Jr. (2006). Cyan and yellow super fluorescent proteins with improved brightness, protein folding, and FRET Förster radius. Biochemistry. 45(21): 6570-6580.

Llavata-Peris CI, Lokerse AS, Möller B, De Rybel B and Weijers D. (2012). Imaging of phenotypes, gene expression and protein localization during embryonic root formation in Arabidopsis. Meth Mol Biol. *in press*.

Lu J, Boeren S, de Vries SC, van Valenberg HJ, Vervoort J and Hettinga K. (2011). Filter-aided sample preparation with dimethyl labeling to identify and quantify milk fat globule membrane proteins. J Proteomics. 75(1): 34-43.

Massari ME and Murre C. (2000). Helix-loop-helix proteins: regulators of transcription in eucaryotic organisms. Mol Cell Biol. 20(2): 429-440.

Ohashi-Ito K and Bergmann DC. (2007). Regulation of the Arabidopsis root vascular initial population by LONESOME HIGHWAY. Development. 134(16): 2959-2968.

Pires N and Dolan L. (2010a). Origin and diversification of basic-helix-loop-helix proteins in plants. Mol Biol Evol. 27(4): 862-874.

Pires N and Dolan L. (2010b). Early evolution of bHLH proteins in plants. Plant Signal Behav. 5(7): 911-912.

Przemeck GK, Mattsson J, Hardtke CS, Sung ZR and Berleth T. (1996). Studies on the role of the Arabidopsis gene *MONOPTEROS* in vascular development and plant cell axialization. Planta. 200(2): 229-237.

Rademacher EH, Lokerse SA, Schlereth A, Llavata-Peris CI, Bayer M, Kientz M, Freire Rios A, Borst JW, Lukowitz W, Jürgens G and Weijers D. (2012). Different auxin response machineries control distinct cell fates in the early plant embryo. Genes Dev. 22(1): 211-222.

Raven JA. (1993). The evolution of vascular plants in relation to quantitative functioning of dead water- conducting cells and stomata. Biol Rev. 68: 337-363.

Salz HK and Erickson JW. (2010). Sex determination in Drosophila: The view from the top. Fly (Austin). 4(1): 60-70.

Scarpella E and Helariutta Y. (2010). Vascular pattern formation in plants. Curr Top Dev Biol. 91: 221-265.

Scheres B, Wolkenfelt H, Willemsen V, Terlouw M, Lawson E, Dean C and Weisbeek P. (1994). Embryonic origin of the Arabidopsis primary root and root meristem initials. Development. 2475-2487.

Sigvardsson M, O'Riordan M and Grosschedl R. (1997). EBF and E47 collaborate to induce expression of the endogenous immunoglobulin surrogate light chain genes. Immunity. 7(1): 25-36.

Truernit E, Bauby H, Dubreucq B, Grandjean O, Runions J, Barthélémy J and Palauqui JC. (2008). High-resolution whole-mount imaging of three-dimensional tissue organization and gene expression enables the study of Phloem development and structure in Arabidopsis. Plant Cell. 20(6): 1494-1503.

Weijers D, Benkova E, Jäger KE, Schlereth A, Hamann T, Kientz M, Wilmoth JC, Reed JW and Jürgens G. (2005). Developmental specificity of auxin response by pairs of ARF and Aux/IAA transcriptional regulators. EMBO J. 24(10): 1874-1885.

Weijers D, Franke-van Dijk M, Vencken RJ, Quint A, Hooykaas P and Offringa R. (2001). An Arabidopsis Minute-like phenotype caused by a semi-dominant mutation in a *RIBOSOMAL PROTEIN S5* gene. Development. 128(21): 4289-4299.

Weijers D, Schlereth A, Ehrismann JS, Schwank G, Kientz M and Jürgens G. (2006). Auxin triggers transient local signaling for cell specification in Arabidopsis embryogenesis. Dev Cell. 10(2): 265-270.

Zwiewka M, Feraru E, Möller B, Hwang I, Feraru MI, Kleine-Vehn J, Weijers D and Friml J. (2011). The AP-3 adaptor complex is required for vacuolar function in Arabidopsis. Cell Res. 21(12): 1711-1722.

Supplemental Information

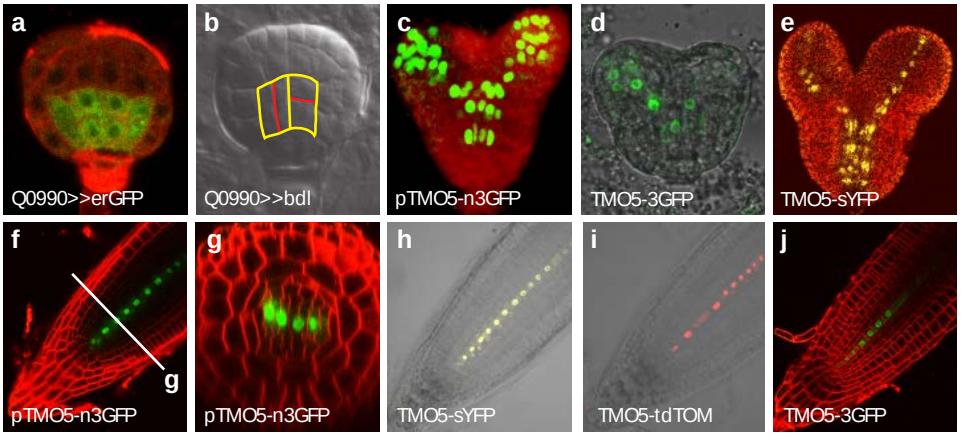

Figure S1. TMO5 expression and protein accumulation in embryo and root meristem. a. Globular stage embryo expressing erGFP driven by the Q0990 driver line. b. Aberrant provascular stem cell divisions in a globular stage embryo containing a stabilized bodenlos (bdl) version driven by the Q0990 driver line. c-j. p*TMO5-n3GFP* expression (c, f, g) and TMO5 protein localizations (d, e, h-j) in heart stage embryos (c-e) and root tips (f-j). TMO5 protein was visualized as fusions of genomic localizations (h-j) in root meristems. Embryos in (a, c, e) and roots in (f, g, j) were counterstained with FM4-64 (red).

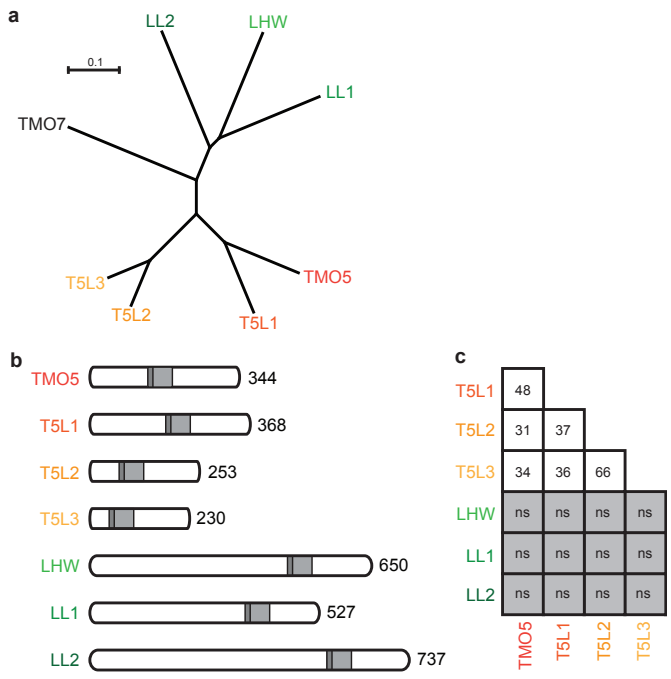

Figure S2. Phylogenetic analysis of TMO5 and LHW protein families. a. Phylogenetic tree of TMO5 and LHW subclades of the Arabidopsis bHLH family using whole protein sequences. The TMO7 protein sequence is used as outgroup. b. Schematic representation and domain structure of the TMO5 and LHW protein subclades. c. Matrix of protein identity (in percentage similarity) between members of the TMO5 and LHW subclades (ns: not significant due to highly different amino acid sequences).

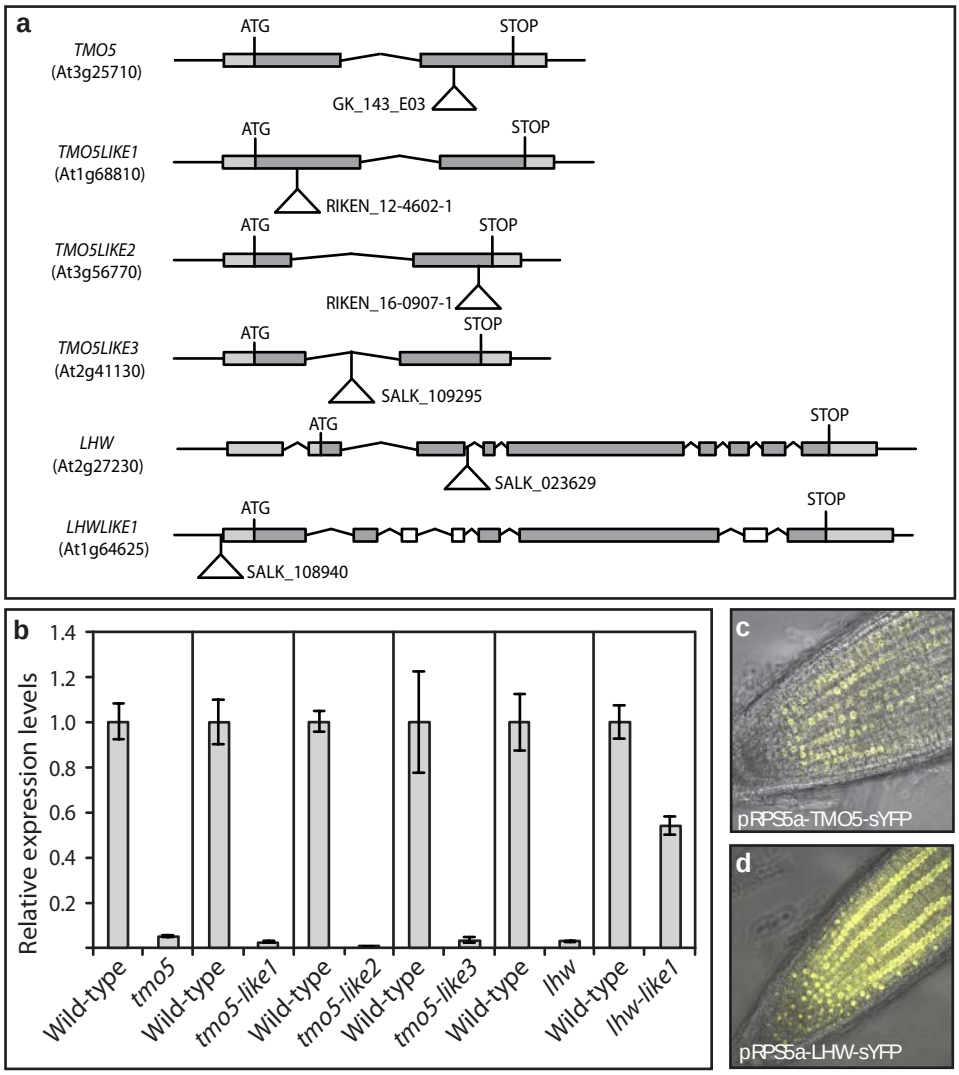

Figure S3. Characterization of insertion mutants of *TMO5* and *LHW* subclade members. a. Gene structure and location of T-DNA and transposon insertions of the insertion lines used in this study. Gene structures are shown on same scale. Boxes represent exons, and lines introns. Codes of insertion lines are given next to each triangle. b. Relative transcript levels of the respective genes in roots of the insertion lines compared to wild-type (set to 1) as determined by Q-RT-PCR. Error bars indicate standard error. c, d. Misexpression of TMO5-YFP (c) and LHW-YFP (d) in root meristem driven by the RPS5A promoter.

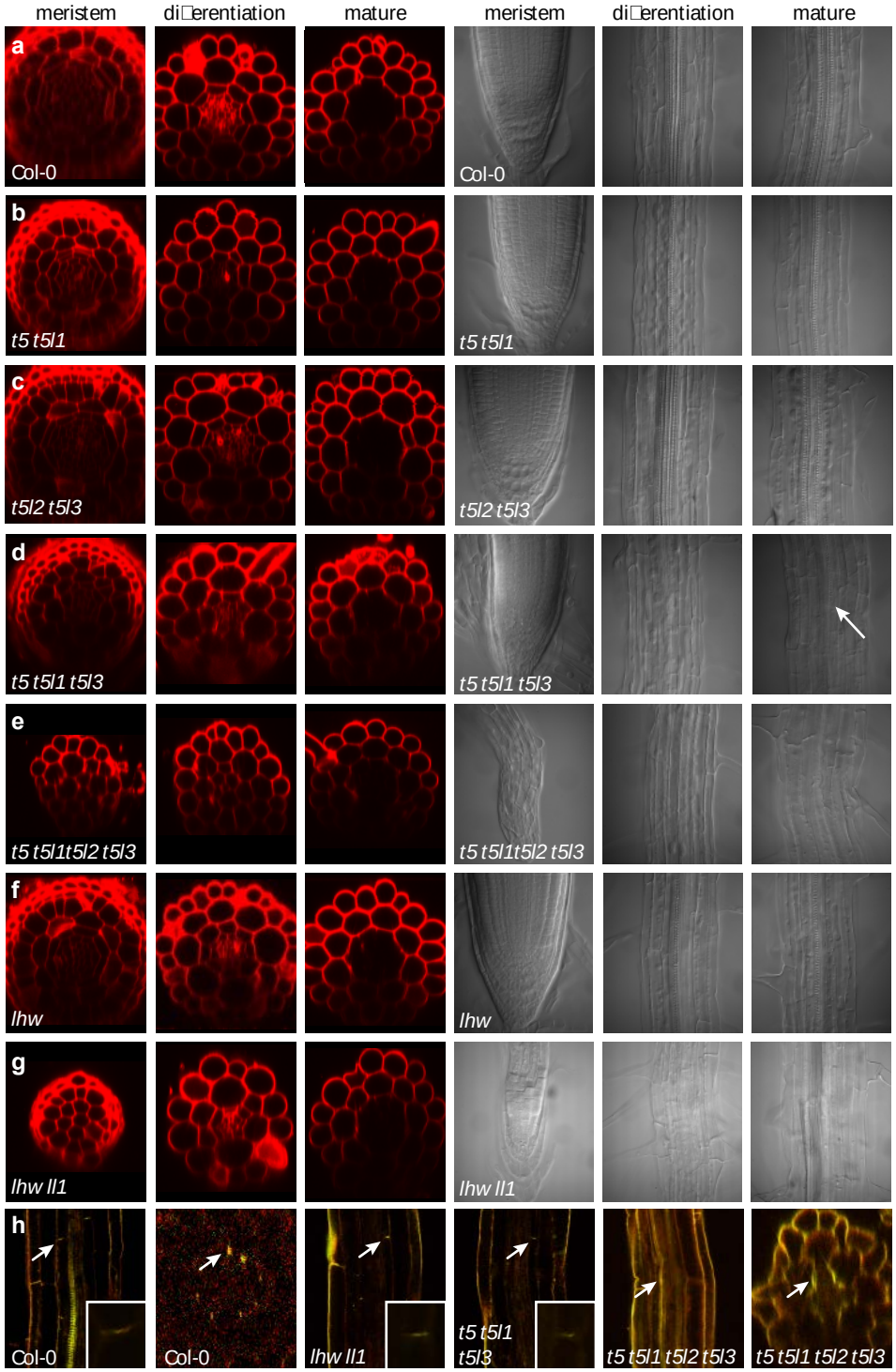
meristem
differentiation
mature
meristem
differentiation
mature
a
Col-0
Col-0
b
t5 t5l1
t5 t5l1
c
t5l2 t5l3
t5l2 t5l3
d
t5 t5l1 t5l3
t5 t5l1 t5l3
e
t5 t5l1t5l2 t5l3
t5 t5l1t5l2 t5l3
f
lhw
lhw
g
lhw ll1
lhw ll1
h
Col-0
Col-0
lhw ll1
t5 t5l1
t5l3
t5 t5l1 t5l2 t5l3
t5 t5l1 t5l2 t5l3

Figure S4. Vascular root phenotypes of *TMO5* and *LHW* higher order mutants. a-g. Optical cross-sections of propidium-iodide stained roots and Normarski DIC images of *TMO5* and *LHW* insertion mutants in the root meristem, differentiation zone, and mature root close to the hypocotyl (a. Col-0 b. *tmo5 tmo5-like1* c. *tmo5-like2 tmo5-like3* d. *tmo5 tmo5-like1 tmo5-like3* e. *tmo5 tmo5-like1 tmo5-like2 tmo5-like3* f. *lhw* g. *lhw lhw-like1*). h. Casparian strip autofluorescence in roots of Col-0, *lhw lhw-like1*, *tmo5 tmo5-like1 tmo5-like3*, and *tmo5 tmo5-like1 tmo5-like2 tmo5-like3* mutants. Arrows indicate Casparian bands and insets show a magnification.

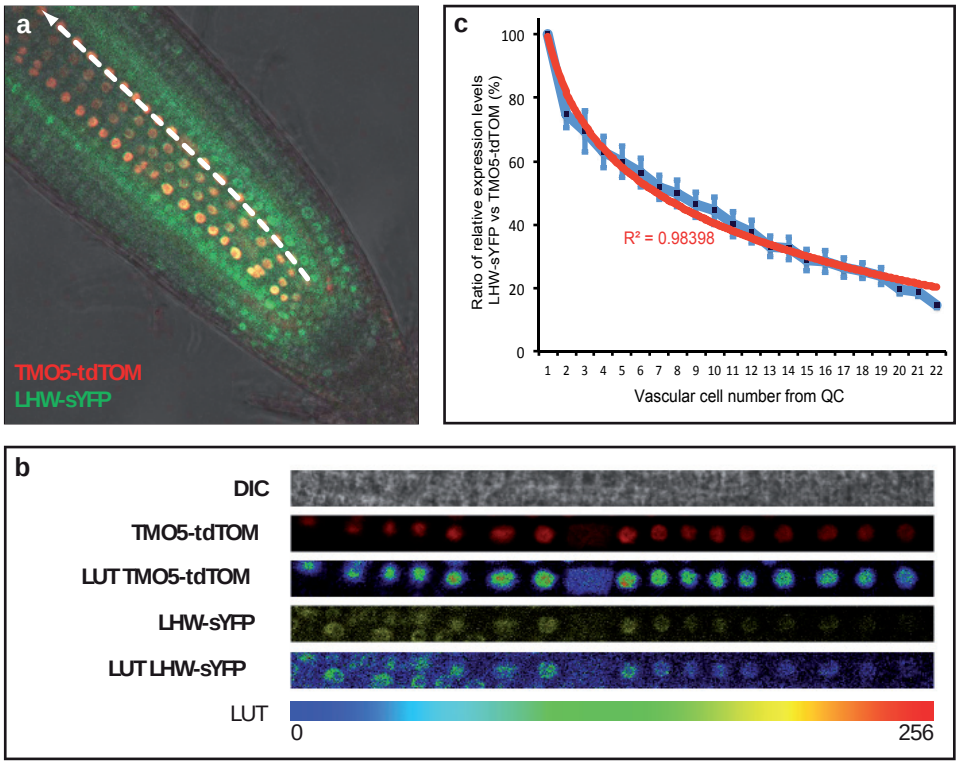

Figure S5. Ratio of TMO5 and LHW protein in xylem cells of the root meristems. a. Representative root tip of TMO5-tdTomato (red); LHW-YFP (green) line with TMO5 and LHW protein accumulation overlap in xylem cells. Both proteins are driven by endogenous promoters. b. Overview of the nuclei along the dashed line from panel a with cells close to the QC on the left, including a false color image of the same nuclei according to the false color scale at the bottom c. Ratio of the relative fluorescence intensity levels of LHW vs. TMO5 in each nucleus along the line indicated in (a). The red line fits the data points with the indicated R^2 value. Error bars indicate standard error.

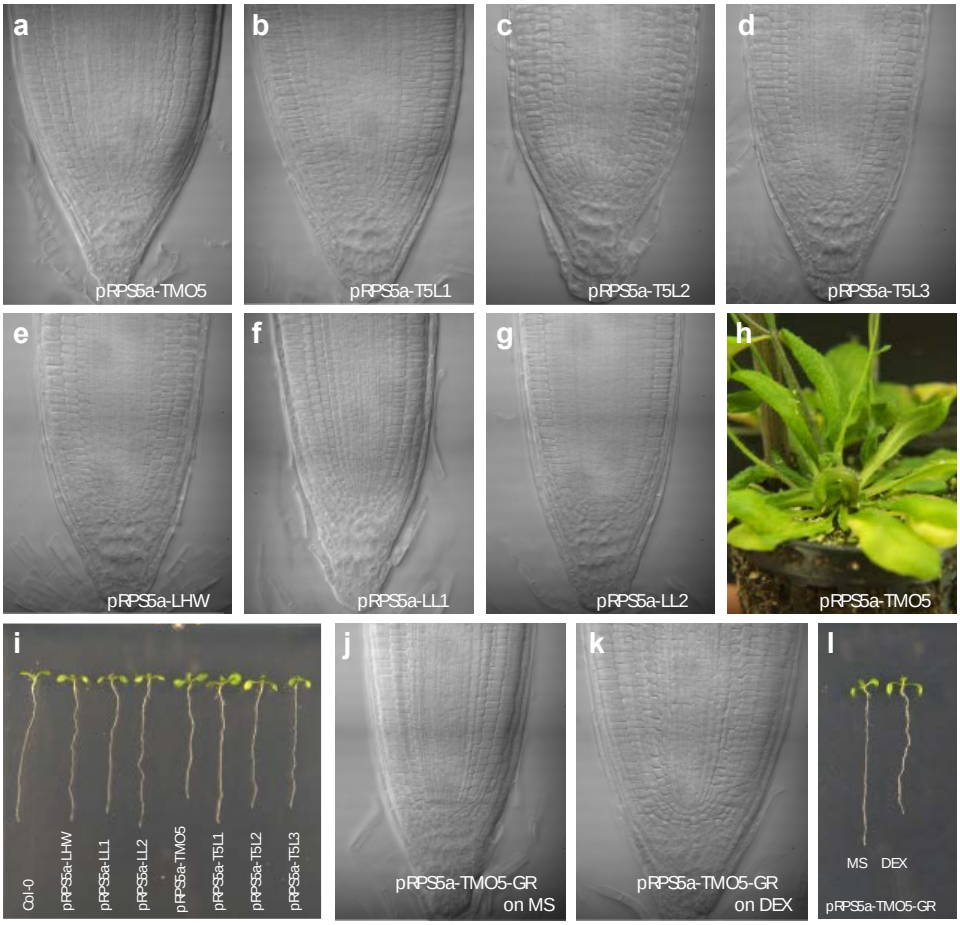

Figure S6. Misexpression of *TMO5* or *TMO5-LIKE1* causes overproliferation. a-g. Root meristems of plants misexpressing *TMO5* or *LHW* subclade members under the control of the *RPS5A* promoter. h. Rosette phenotype of a pRPS5A-TMO5 plant. i. Overview of seedlings misexpressing *TMO5* or *LHW* subclade members under the control of the RPS5A promoter. j-k. Root meristems of plants misexpressing RPS5A-TMO5-GR grown without and with dexamethasone (DEX) for 12 hours. l. Overview of seedlings misexpressing RPS5A-TMO5-GR grown with or without DEX for 12 hours.

Figure S7. Co-misexpression of TMO5 and LHW results in ectopic leaf primordium formation. Leaf series of a wild-type plant (a) and a plant expressing both TMO5 and LHW under the control of the RPS5A promoter (b). Magnification of the insets shown in A and B are shown in Manuscript Figures 6O and 6P respectively.

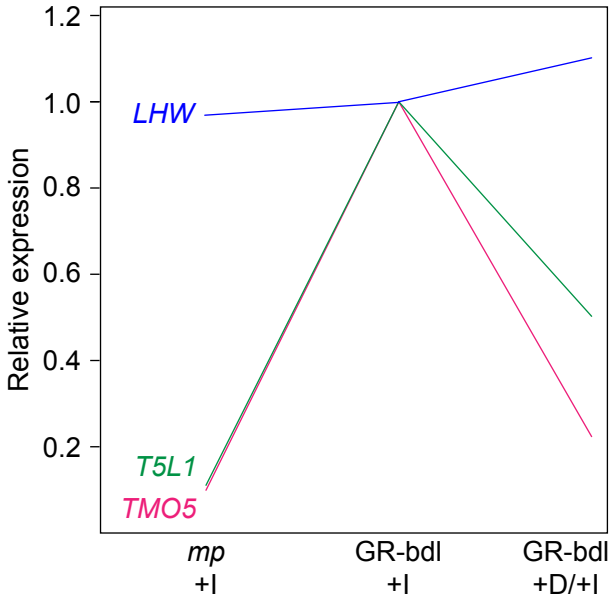

Figure S8. Auxin-regulation of *TMO5*, *T5L1* and *LHW* expression. Relative expression levels of *TMO5*, *T5L1* and *LHW* in mock-treated pRPS5A-bdl-GR (center), DEX-treated pRPS5A-bdl-GR (right) and *mp*-B4149 mutant 10 day-old seedlings. All samples were treated with 20 µM IAA to induce auxin-responsive genes. Expression levels were measured by Affymetrix ATH1 microarray hybridization, and normalized to the level in mock-treated pRPS5A-bdl-GR. Data was reproduced from Chapter 2. Note that *TMO5* and *T5L1* are strongly down-regulated in both mp mutant and DEX-treated pRPS5A-bdl-GR, while *LHW* remains unaffected in both conditions.

Table S1. Aberrant vascular stem cell (VSC) divisions in globular-stage *monopteros* (*mp*) and *tmo5 tmo5-like1* double mutant embryos. The percentage of globular-stage embryos with aberrantly divided VSC was counted; N is the number of embryos.

Genotype	% embryos with aberrant VSC	N
wild-type	0	86
mpB4149	88	50
mpS319	94,3	53
tmo5 tmo5like1	7,4	54

Table S2. Overview of vascular phenotypes in mutants of the TMO5 and LHW subclades and higher order mutant combinations. For each genotype, the percentage diarch or monarch roots, the presence of only small stretches of differentiated xylem in a monarch architecture and the percentage of roots without any differentiated xylem tissues are indicated. N is the number of roots analyzed.

Genotype	% diarch roots	% monarch roots	% roots with short stretches of one xylem pole	% roots without differentiated xylem	N
wild-type	100	0	0	0	32
tmo5	100	0	0	0	30
tmo5like1	100	0	0	0	30
tmo5like2	100	0	0	0	32
tmo5like3	100	0	0	0	31
tmo5 tmo5like1	6,9	93.1	0	0	87
tmo5 tmo5like3	100	0	0	0	70
tmo5like2 tmo5like3	100	0	0	0	80
tmo5 tmo5like1 tmo5like3	0	0	60.9	39.1	23
tmo5 tmo5like2 tmo5like3	100	0	0	0	80
tmo5 tmo5like1 tmo5like2 tmo5like3	0	0	0	100	12
lhw	0	100	0	0	32
lhwlike1	100	0	0	0	27
lhw lhwlike1	0	0	0	100	17
tmo5 tmo5like1; TMO5-3GFP (+)	100	0	0	0	51
tmo5 tmo5like1; TMO5-3GFP (-)	22	78	0	0	27

Table S3. Overview of the IP-MS results. The tables show the first 10 interactors in the list after MaxQuant and Perseus statistical analysis with an indication of the ratio WT vs. sample and p-value obtained from the three repeats. The coverage of the detected peptides in the interacting proteins is highlighted below each IP experiment.

Transgenic line used: pTMO5-TMO5-3GFP
Tissue type: 3 grams of siliques

Number	Ratio	p-value	UniProt ID	Peptides (n)	Unique peptides (n)	description
1	6963	1.5E-05	Q9LS08	22	22	bHLH32-TMO5/bait
2	2195	4.7E-06	GFP	5	5	GFP
3	455	1.5E-08	B9DGI1	5	5	bHLH156LHW
4	333	9.5E-06	Q8RY71-1	5	5	
5	202	2.4E-04	Q6NLH7	11	11	
6	134	5.7E-12	Q9FI66	1	1	
7	99	3.7E-10	Q84RJ4	2	2	bHLH155/LHWLIKE2
8	50	2.0E-02	Q940Z2	1	1	
9	39	2.8E-03	Q0WN82	3	3	
10	35	2.2E-02	B9DG49	2	2	

>TMO5 (BAIT)
MYAMKEEDCLQTFHNLQDYQDQFHLHHHPQILPWSSTSLPSFDPLHFPSNPTRYSDPVHYFNRRASSSSSSFDYNDGFV
SPPPSMDHPQNHLRILSEALGPIMRRGSSFGFDGEIMGKLSAQEVMDAKALAASKSHSEAERRRRERINTHLAKLRSILP
NTTKTDKASLLAEVIQHMKELKRQTSQITDTYQVPTECDDLTVDSSYNDEEGNLVIRASFCCQDRTDLMHDVINALKSL
RLRTLKAEIATVGGRVKNILFLSREYDDEEDHDSYRRNFDGDDVEDYDEERMMNNRVSSIEEALKAVIEKCVHNNDES
NDNNNLEKSSSGGIKRQRTSKMVNRCYN

>LHW
MGVLLREALRSMCVNNQWSYAVFWKIGCQNSSLLIWEECYNETESSSNPRRLCGLGVDTQGNEKVQLLTNRMMLNN
RIILVGEGLVGRAAFTGHHQWILANSFNRDVHPPEVINEMLLQFSAGIQTVAVFPVVPHGVVQLGSSLPIMENLGFVND
VKGLILQLGCVPGALLSENYRTYEPAADFIGVPVSRIIPSQGHKILQSSAFVAETSKQHFNSTGSSDHQMVEESPCNLVDE
HEGGWQSTTGFLTAGEVAVPSNPDAWLNQNFSCMSNVDAAEQQQIPCEDISSKRSLGSDDLFDMLGLDDKNKGCDNS
WGVSQMRTEVLTRELSDFRIIQEMDPEFGSSGYELSGTDHLLDAVVSGACSSTKQISDETSESCKTTLTKVSNSSVTTPS
HSSPQGSQLFEKKHGQPLGPSSVYGSQISSWVEQAHSLKREGSPRMVNKNETAKPANNRKRLKPGENPRPRPKDRQMI
QDRVKELREIIPNGAKCSIDALLERTIKHMLFLQNVSKHSDKLKQTGESKIMKEDGGGATWAFEVGSKSMVCPIVVEDI
NPPRIFQVEMLCEQRGFFLEIADWIRSLGLTILKGVIETRVDKIWARFTVEASRDVTRMEIFMQLVNILEQTMKCGGNSK
TILDGIKATMPLPVTGGCSM

>LHW-LIKE2
MGSTSQEILKSFCFNTDWDYAVFWQLNHRGSRMVLTLEDAYYDHHGTNMHGAHDPLGLAVAKMSYHVYSLGEGIVG
QVAVSGEHQWVFPENYNNCNSAFEFHNVWESQISAGIKTILVVAVGPCGVVVQLGSLCKVNEDVNFVNHIRHLFLALRD
PLADHAANLRQCNMNNSLCLPKMPSEGLHAEAFPDCSGEVDKAMDVEESNILTQYKTRRSDSMPYNTPSSCLVMEKA
AQVVGGREVVQGSTCGSYSGVTFGFPVDLVGAKHENQVGTNIIRDAPHVGMTSGCKDSRDLDPNLHLYMKNHVLND
TSTSALAIEAERLITSQSYPRLDSTFQATSRTDKESSYHNEVFQLSENQGNKYIKETERMLGRNCESSQFDALISSGYTFA
GSELLEALGSAFKQTNTGQEELLKSEHGSTMRPTDDMSHSQLTFDPGPENLLDAVVANVCQRDGNARDDMMSSRSVQ
SLLTNMELAEPSGQKKHNIVNPINSAMNQPPMAEVDTQQNSSDICGAFSSIGFSSTYPSSSSDQFQTSLDIPKKNKKRAKP
GESSRPRPRDRQLIQDRIKELRELVPNGSKCSIDSLLERTIKHMLFLQNVTKHAEKLSKSANEKMQQKETGMQGSSCAV
EVGGHLQVSSIIVENLNKQGMVLIEMLCEECGHFLEIANVIRSLDLVILRGFTETQGEKTWICFVTEVGSRITQFMKEIPK
QIKSQNSKVMQRMDILWSLVQIFQPKANEKG

Transgenic line used: pLHW-LHW-GFP
Tissue type: 3 grams of siliques

Number	Ratio	p-value	UniProt ID	Peptides (n)	Unique peptides (n)	description
1	18723	2.1E-06	GFP	11	11	GFP
2	14621	1.7E-06	Q9XIN0	39	39	bHLH156/LHW/bait
3	3503	3.9E-09	Q9ASX9	13	13	
4	1967	2.4E-08	Q3EC99	44	9	
5	1913	6.5E-10	C0SV80	5	5	
6	1248	3.0E-06	Q9S7C0	47	12	
7	617	7.1E-06	Q94AZ4	5	5	
8	461	1.5E-07	Q9S7Y1	3	3	bHLH30/TMO5LIKE1
9	408	2.5E-10	P56765	12	12	
10	328	3.3E-06	Q84WU2	12	4	
132	14	1.4E-05	Q9LS08	4	4	bHLH32/TMO5

>LHW (BAIT; SILIQUES)
MGVLLREALRSMCVNNQWSYAVFWKIGCQNSSLLIWEECYNETESSSNPRRLCGLGVDTQGNEKVQLLTNRMMLNN
RIILVGEGLVGRAAFTGHHQWILANSFNRDVHPPEVINEMLLQFSAGIQTVAVFPVVPHGVVQLGSSLPIMENLGFVND
VKGLILQLGCVPGALLSENYRTYEPAADFIGVPVSRIIPSQGHKILQSSAFVAETSKQHFNSTGSSDHQMVEESPCNLVDE
HEGGWQSTTGFLTAGEVAVPSNPDAWLNQNFSCMSNVDAAEQQQIPCEDISSKRSLGSDDLFDMLGLDDKNKGCDNS
WGVSQMRTEVLTRELSDFRIIQEMDPEFGSSGYELSGTDHLLDAVVSGACSSTKQISDETSESCKTTLTKVSNSSVTTPS
HSSPQGSQLFEKKHGQPLGPSSVYGSQISSWVEQAHSLKREGSPRMVNKNETAKPANNRKRLKPGENPRPRPKDRQMI
QDRVKELREIIPNGAKCSIDALLERTIKHMLFLQNVSKHSDKLKQTGESKIMKEDGGGATWAFEVGSKSMVCPIVVEDI
NPPRIFQVEMLCEQRGFFLEIADWIRSLGLTILKGVIETRVDKIWARFTVEASRDVTRMEIFMQLVNILEQTMKCGGNSK
TILDGIKATMPLPVTGGCSM

>TMO5
MYAMKEEDCLQTFHNLQDYQDQFHLHHHPQILPWSSTSLPSFDPLHFPSNPTRYSDPVHYFNRRASSSSSSFDYNDGFV
SPPPSMDHPQNHLRILSEALGPIMRRGSSFGFDGEIMGKLSAQEVMDAKALAASKSHSEAERRRRERINTHLAKLRSILP
NTTKTDKASLLAEVIQHMKELKRQTSQITDTYQVPTECDDLTVDSSYNDEEGNLVIRASFCCQDRTDLMHDVINALKSL
RLRTLKAEIATVGGRVKNILFLSREYDDEEDHDSYRRNFDGDDVEDYDEERMMNNRVSSIEEALKAVIEKCVHNNDES
NDNNNLEKSSSGGIKRQRTSKMVNRCYN

>TMO5-LIKE1
MCAKKEEEEEEEEDSSEAMNNIQNYQNDLFFHQLISHHHHHHHHDPSQSETLGASGNVGSGFTIFSQDSVSPIWSLPPPTSI
QPPFDQFPPPSSSPASFYGSFFNRSRAHHQGLQFGYEGFGGATSAAHHHHEQLRILSEALGPVVQAGSGPFGLQAELGK
MTAQEIMDAKALAASKSHSEAERRRRERINNHLAKLRSILPNTTKTDKASLLAEVIQHVKELKRETSVISETNLVPTESD
ELTVAFTEEEETGDGRFVIKASLCCEDRSDLLPDMIKTLKAMRLKTLKAEITTVGGRVKNVLFVTGEESSGEEVEEEYCI
GTIEEALKAVMEKSNVEESSSSGNAKRQRMSSHNTITIVEQQQQYNQR

Transgenic line used: pLHW-LHW-GFP
Tissue type: 3 grams of siliques

Number	Ratio	p-value	UniProt ID	Peptides (n)	Unique peptides (n)	description
1	6980	2.5E-04	Q9XIN0	38	38	bHLH156/LHW/bait 2
2	798	1.0E-07	Q9S7C0	48	8	
3	722	9.0E-08	P56759	4	4	
4	353	7.6E-07	O80674	3	3	bHLH106/TMO5LIKE3
5	189	8.2E-07	Q9XEX2	2	2	
6	141	3.9E-07	P20363	6	2	
7	101	2.0E-07	Q9LPR4	2	2	
8	99	2.1E-09	Q9FMU6	2	2	
9	92	1.8E-05	P29197	9	4	
10	87	1.4E-05	Q9LS08	6	6	bHLH32/TMO5

>LHW (BAIT; SEEDLINGS)
MGVLLREALRSMCVNNQWSYAVFWKIGCQNSSLLIWEECYNETESSSNPRRLCGLGVDTQGNEKVQLLTNRMMLNN
RIILVGEGLVGRAAFTGHHQWILANSFNRDVHPPEVINEMLLQFSAGIQTVAVFPVVPHGVVQLGSSLPIMENLGFVND
VKGLILQLGCVPGALLSENYRTYEPAADFIGVPVSRIIPSQGHKILQSSAFVAETSKQHFNSTGSSDHQMVEESPCNLVDE
HEGGWQSTTGFLTAGEVAVPSNPDAWLNQNFSCMSNVDAAEQQQIPCEDISSKRSLGSDDLFDMLGLDDKNKGCDNS
WGVSQMRTEVLTRELSDFRIIQEMDPEFGSSGYELSGTDHLLDAVVSGACSSTKQISDETSESCKTTLTKVSNSSVTTPS
HSSPQGSQLFEKKHGQPLGPSSVYGSQISSWVEQAHSLKREGSPRMVNKNETAKPANNRKRLKPGENPRPRPKDRQMI
QDRVKELREIIPNGAKCSIDALLERTIKHMLFLQNVSKHSDKLKQTGESKIMKEDGGGATWAFEVGSKSMVCPIVVEDI
NPPRIFQVEMLCEQRGFFLEIADWIRSLGLTILKGVIETRVDKIWARFTVEASRDVTRMEIFMQLVNILEQTMKCGGNSK
TILDGIKATMPLPVTGGCSM

>TMO5
MYAMKEEDCLQTFHNLQDYQDQFHLHHHPQILPWSSTSLPSFDPLHFPSNPTRYSDPVHYFNRRASSSSSSFDYNDGFV
SPPPSMDHPQNHLRILSEALGPIMRRGSSFGFDGEIMGKLSAQEVMDAKALAASKSHSEAERRRRERINTHLAKLRSILP
NTTKTDKASLLAEVIQHMKELKRQTSQITDTYQVPTECDDLTVDSSYNDEEGNLVIRASFCCQDRTDLMHDVINALKSL
RLRTLKAEIATVGGRVKNILFLSREYDDEEDHDSYRRNFDGDDVEDYDEERMMNNRVSSIEEALKAVIEKCVHNNDES
NDNNNLEKSSSGGIKRQRTSKMVNRCYN

>TMO5-LIKE3
MQPETSDQMLYSFLAGNEVGGGGYCVSGDYMTTMQSLCGSSSSTSSYYPLAISGIGETMAQDRALAALRNHKEAERR
RRERINSHLNKLRNVLSCNSKTDKATLLAKVVQRVRELKQQTLETSDSDQTLLPSETDEISVLHFGDYSNDGHIIFKASL
CCEDRSDLLPDLMEILKSLNMKTLRAEMVTIGGRTRSVLVVAADKEMHGVESVHFLQNALKSLLERSSKSLMERSSGG
GGGERSKRRRALDHIIMV

Table S4. Overview of the primers used for cloning, genotyping and Q-RT-PCR. All primer sequences are from 5' to 3'.

Insertion mutant	Forward and reverse genotyping primers for insertion lines
tmo5	TGAGTGCACAAGAAGTCATGG TCAAATCCCATTTTGCAAGTC
t5l1	ctccacatatcctgcaaaccattgg GTGGTGTTGGGTAATATGCTACGGAGC
t5l2	GCAAAAGTGGTTCAACGAGTC AAAGGCAGAACTCTTTAGGGG
t5l3	ctccggcgactacatgacgactatg CTCCACCACCAGAACTACGTTCCATC
lhw	TGAAACTCCCCAACTGTTGTC CGTTTTGTCTTTGTTTAGCCC
ll1	TTTTTCCATTGCACCAGTTTC AAAGCATACCCTTGGCCTAAG

Gene name	Construct	Forward and reverse primer used for cloning for FRET-FLIM experiments
TMO5	coding sequence	described in Schlereth *et al.*, 2010
T5L1	coding sequence	TAGTTGGAATAGGTTCatgtgcgctaagaaagaagaagaagaagaagaagaagaagacagttctgaagcc AGTATGGAGTTGGGTTCcctctgattatattgttgttgttgttcg
T5L2	coding sequence	TAGTTGGAATAGGTTCatgcaaccagagacctcagatcag AGTATGGAGTTGGGTTCcaccattatgatgtgatccagc
T5L3	coding sequence	TAGTTGGAATAGGTTCatgcagccagaggtttcagatcaaatattttatgcc AGTATGGAGTTGGGTTCgaccattatgatgtgatccagc
LHW	coding sequence	TAGTTGGAATAGGTTCatgggagttttactaagag AGTATGGAGTTGGGTTCcattgaacagccaccagtaacc
LL1	coding sequence	TAGTTGGAATAGGTTCatgggttcagagtataagc AGTATGGAGTTGGGTTCtgataataaatcatcatgtttgg
LL2	coding sequence	TAGTTGGAATAGGTTCatgggttctacttctcaagagatactg AGTATGGAGTTGGGTTCccccttctcattggcctttggttg

Gene name	Construct	Forward and reverse primer used for LIC cloning
TMO5	promoter	described in Schlereth *et al*., 2010
T5L1	promoter	TAGTTGGAATGGGTTCGAAgaacataggtccaaagtccgtctttagtc TTATGGAGTTGGGTTCGAAATCACTTGTTTCTATGAAGACATGAGAGTC
T5L3	promoter	TAGTTGGAATGGGTTCGAATCATTGTTCATGTTATTGAC TTATGGAGTTGGGTTCGAATATCTTTTGTTTGCGCCGCCT
LHW	promoter	TAGTTGGAATGGGTTCGAAgtggtcaaagtattacgatgttc TTATGGAGTTGGGTTCGAAtacttccggtaataaggaagag
LL1	promoter	TAGTTGGAATGGGTTCGAAccactttcggacacaattg TTATGGAGTTGGGTTCGAAatttaggaatccaagccggg
LL2	promoter	TAGTTGGAATGGGTTCGAAgtatggacaagttataaagttcc TTATGGAGTTGGGTTCGAAtctaaagggtaaacctcaaaaccc
TMO5	genomic sequence	TAGTTGGAATGGGTTCGAAcacaaaaatagtactcgaatccggtagc TTATGGAGTTGGGTTCGAACATTATAACATCGATTCACCATCTTACTAGTCC
LHW	genomic sequence	TAGTTGGAATGGGTTCGAAgtggtcaaagtattacgatgttc TTATGGAGTTGGGTTCGAACcattgaacagccaccagtaaccgg
TMO5	coding sequence	TAGTTGGAATAGGTTCatgtacgcaatgaaagaagaagac AGTATGGAGTTGGGTTCctaattataacatcgattcaccatc
T5L1	coding sequence	TAGTTGGAATAGGTTCatgtgcgctaagaaagaagaagaagaagaagaagaagaagacagttctgaagcc AGTATGGAGTTGGGTTCttacctctgattatattgttgttgttcg
T5L2	coding sequence	TAGTTGGAATAGGTTCatgcaaccagagacctcagatcag AGTATGGAGTTGGGTTCtcacaccattatgatgtgatccagc
T5L3	coding sequence	TAGTTGGAATAGGTTCatgcagccagaggtttcagatcaaatattttatgcc AGTATGGAGTTGGGTTCtcacaccattatgatgtgatccagc
LHW	coding sequence	TAGTTGGAATAGGTTCATGGGAGTTTTACTAAGAGAAGC AGTATGGAGTTGGGTTCTTACATTGAACAGCCACCAGTAACCGG
LL1	coding sequence	TAGTTGGAATAGGTTCatgggttcagagtataagc AGTATGGAGTTGGGTTCctatgataataaatcatcatgtttgg
LL2	coding sequence	TAGTTGGAATAGGTTCatgggttctacttctcaagagatactg AGTATGGAGTTGGGTTCttacccctctcattggcctttggttg

Chapter 4

Identification of novel putative MONOPTEROS target genes in embryonic root initiation

Barbara Möller[1], Daoquan Xiang[2], Lorena Gonzalez Lopez[1], Nerys Williams[1a], Raju Datla[2] and Dolf Weijers[1]

[1]Laboratory of Biochemistry, Wageningen University, Dreijenlaan 3, 6703HA Wageningen, the Netherlands

[2]Plant Biotechnology Institute, National Research Council, 110 Gymnasium Place, Saskatoon, Saskatchewan, Canada

[a]Present address: Hubrecht Institute, Uppsalalaan 8, 3584CT Utrecht, the Netherlands

Abstract

In plants, the root is initiated in the early embryo by the coordinated specification of tissues, stem cells and organizer cells in the root meristem. The MONOPTEROS transcription factor is required to specify the Arabidopsis root meristem, and previous work identified several *TARGET OF MP (TMO)* genes involved in root initiation. We performed a microarray on early embryos, designed to find novel MP target genes involved in the earliest specification events of the embryonic root meristem. Upon local MP inhibition in the embryo, *TMO7* was the most down-regulated gene in the dataset, validating our approach. Moreover, expression of many transcription factors and cell wall remodeling genes was affected, suggesting that MP regulates multiple processes and plays a role in the dynamic cell shape changes in early embryo development. We identified several genes specifically expressed in either the first vascular or ground tissue cells of the developing root meristem in the early embryo. Two other genes are ubiquitously expressed in the stem cell niche from early embryogenesis on. Furthermore, we showed that MP activates expression of these genes. These results suggest a role for MP to specify the first vascular and ground tissue cells of the embryonic root, and to promote cell divisions in the root stem cell niche.

Introduction

In higher plants, the basic body plan is established early in embryo development. This body plan contains stem cell niches for the root and shoot meristem, located at opposite ends of the embryo, which produce most of the adult plant (Weigel and Jürgens, 2002). Both meristems consist of an organizing center, surrounded by different types of stem cells that continuously supply new cells that are incorporated into organs. In the root, this organizing center is called the quiescent center (QC), and has been shown to be required for stem cell maintenance (Van den Berg *et al.*, 1997). Generation of these niches requires the coordinated programming of different cell types. We use root meristem initiation in the early embryo of the small weed *Arabidopsis thaliana*, as a model for coordinated stem cell and organizer specification. While this first initiation of the meristems is not well-understood, later steps in meristem establishment and maintenance are understood in some detail and some key regulators are known. *SHORTROOT (SHR)* and *SCARECROW (SCR)* are members of the GRAS family of transcription factors, required for QC maintenance and radial patterning in the postembryonic root (Di Laurenzio *et al.*, 1996; Helariutta *et al.*, 2000; Sabatini *et al.*, 2003). Both genes are expressed in embryogenesis from globular stage on. However, the earliest defects in QC

specification and radial patterning are reported at early heart stage of embryogenesis (Scheres *et al.*, 1995; Wysocka-Diller *et al.*, 2000; Helariutta *et al.*, 2000). *PLETHORA (PLT)* genes are AP2 type transcription factors required for root meristem formation (Aida *et al.*, 2004; Galinha *et al.*, 2007). They are expressed in the QC and surrounding stem cells, and have been shown to be indispensable for QC specification and the proliferating activity of the root meristem. *WUSCHEL RELATED HOMEOBOX5 (WOX5)* is a member of a subclade of the homeobox transcription factor family involved in patterning the early embryo (Sarkar *et al.*, 2007). *WOX5* is expressed in the QC and its precursor cells from early embryogenesis on. From there, it signals to the surrounding stem cells to keep them undifferentiated. In addition to these transcription factors, also small peptides called root meristem growth factors (RGFs) are required for root meristem maintenance (Matsuzaki *et al.*, 2010). These proteins all appear to act in a network that controls QC and stem cell function, but their mechanism of action and interconnections are not yet understood.

While genetic approaches have identified several regulators of meristem patterning, only few regulators of embryonic root initiation have been recovered. Those few that have been found are all implicated in action of the the plant hormone auxin (reviewed in Chapter 1). Auxin is perceived by a family of auxin receptors. Upon binding of auxin with its receptor, the affinity of the receptor for a family of transcriptional repressors, called *Aux/IAAs*, increases. Consequently, Aux/IAAs are degraded, which in turn activates another class of DNA binding transcription factors called *AUXIN RESPONSE FACTORS (ARFs)*. *MONOPTEROS (MP)/ ARF5* is one of 23 *ARF* genes in the Arabidopis genome. *mp* is the only single *arf* mutant with pronounced embryo defects. One of the earliest defects in *mp* mutants is the aberrant division of the hypophysis at early globular stage of embryo development. The hypophysis is the precursor for the QC and columella stem cells of the root meristem. In *mp* mutants, the hypophysis is not properly specified, resulting in rootless seedlings. *Aux/IAA12/BODENLOS (BDL)* binds MP to inhibit its transcriptional activity. A specific mutation in the *BDL* gene results in the production of stable bdl protein that can no longer be degraded. MP activity is constantly inhibited in these gain-of-function mutants, resulting in rootless seedlings identical to *mp* mutants. Recently, several MP target genes with important functions in root initiation have been identified by transcription profiling of seedlings in which MP activity was lost (*mp* mutant) or transiently inhibited (inducible bdl protein) (Chapters 2, 3). The newly identified genes are called *TARGET OF MONOPTEROS (TMO)* genes, of which the bHLH transctiption factors *TMO5* and *7* are so far the best studied examples. TMO7 protein has been shown to be transported from its site of expression in the proembryo to the adjacent hypophysis cell, where it

is required to specify the hypophysis (Chapter 2). *TMO5* is specifically expressed in the first vascular tissue cells of the globular stage embryo (Chapter 2). *TMO5* and its homologs were shown to be required for the activity of the vascular stem cells (Chapter 3). Moreover, we found a high frequency of division defects in the first vascular cells in early *mp* embryos (Chapter 3). These results suggest that MP activity might not only be required to specify the hypophysis, but possibly also vascular tissue cells or vascular stem cells in the early embryo. As such, MP presents a good starting point to identify genes and mechanisms that operate in embryonic root initiation, in particular in stem cell and organizer specification.
Since a previous transcription profiling study was performed using post-embryonic tissue (Chapter 2), many of the MP-dependent genes that act specifically in the embryo will have been missed. Therefore, in this study, we have performed transcription profiling on isolated, early embryos in which MP activity is locally inhibited in the first vascular and ground tissue cells. *TMO7* is the most strongly down-regulated gene in the microarray, which validates the approach. Furthermore, transcription factors and cell wall remodeling genes are overrepresented among the down-regulated genes. Expression pattern analysis of 37 down-regulated genes identified several genes with specific expression in either the first vascular or ground tissue cells of the early embryo, or in both. Furthermore, we show that MP is required to promote transcription of several genes expressed in the vascular or ground tissue initials. These results suggest that MP is involved in specifying the first vascular and ground tissue cells in the embryo.

Results

Microarray setup

We designed a microarray to identify novel MP target genes that are active in the first vascular and ground tissue cells of the early embryo. We locally inhibited MP activity in the inner basal embryo cells of the early embryo that will acquire vascular or ground tissue identity, depending on their position (Figure 1a). Consistent embryo expression patterns for *MP* have been reported with various techniques, including *in situ* hybridization, immunostaining, and the use of transcriptional and translational fusions for *MP* (Hamann *et al.*, 2002; Weijers *et al.*, 2006; Chapter 2). These all revealed near-identical *MP* mRNA and MP protein accumulation patterns, which are schematically depicted in Figure 1b-e. Accumulation of MP protein is already observed at dermatogen stage. Until early globular stage, MP protein is present in all pro-embryo cells, but not in the suspensor (Figure 1b). One division round later, MP protein accumulates additionally in the apical daughter cell of the extra-embryonic hypophysis cell (Figure 1c). During embryogenesis,

MP accumulation becomes increasingly concentrated in the vasculature and QC, although MP is still present at lower levels in the outer tissues (Figure 1b-e).

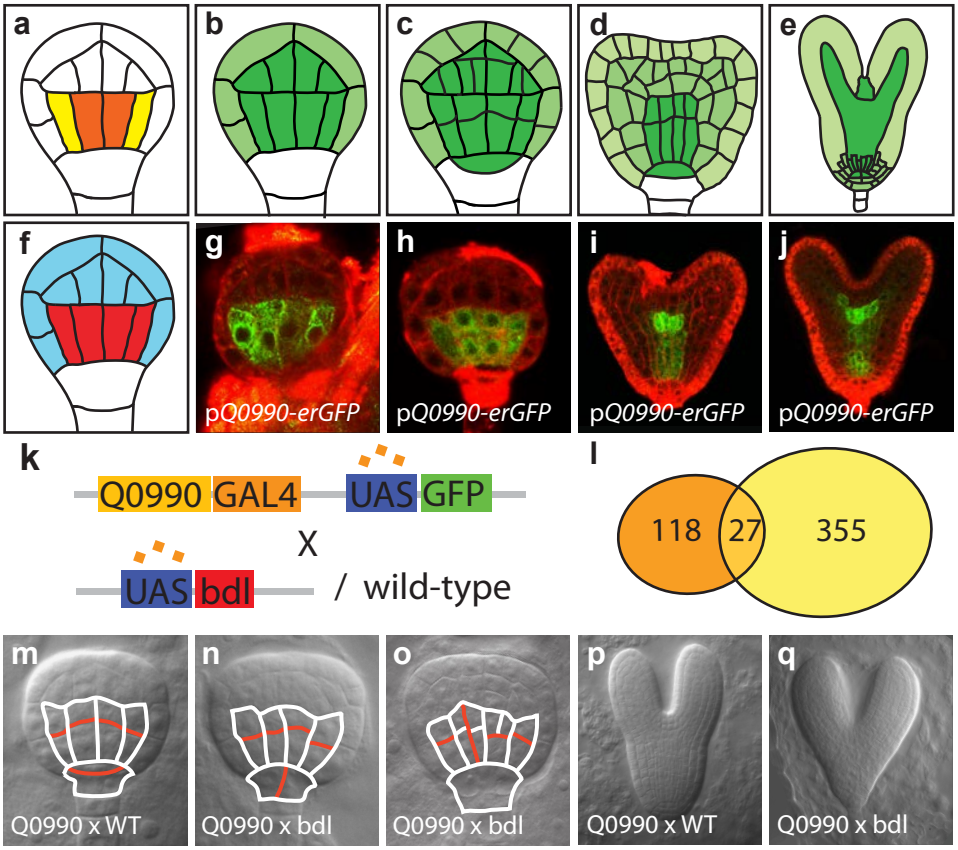

Figure 1. Explanation of a microarray on isolated embryos in which MP activity is locally inhibited in the inner basal embryo cells. a, Schematic view of a globular stage embryo with the putative first vascular (orange) and ground tissue (yellow) cells. b-e, Schematic presentation of strong (green) and weaker (lighter green) MP protein accumulation in the embryo at globular stage before (b) and after (c) division of the first vascular and ground tissue cells, transition stage (d) and heart stage (e). f, MP activity is inhibited in the putative first vascular and ground tissue cells (red) in the globular stage embryo in Q0990>>>bdl plants. MP is still active in the surrounding embryo cells (blue). g-j, p*Q0990-erGFP* expression in the embryo at globular stage before (g) and after (h) division of the first vascular and ground tissue cells, transition stage (i) and heart stage (j). k, Schematic presentation of constructs that were used to cross p*Q0990-GAL4* containing plants with p*UAS-bdl* plants. Two independent microarrays were performed with either globular or heart stage embryos resulting from these crosses. Embryos of similar age, dissected from crosses between p*Q0990-GAL4* and wild-type plants, were used as control. l, Venn diagram showing the overlap (light orange, 27 genes) of down-regulated genes in the microarrays on globular (dark orange) and heart stage embryos (yellow). m-q, Phenotypes of embryos expressing Q0990>>>bdl at globular (n-o) and heart stage (q). m and p show wild-type globular and heart stage embryos, respectively.

Since it had previously been shown that MP expression in a small domain in the basal half of the embryo marked by the Q0990 GAL4-GFP enhancer trap is sufficient to restore the *mp* mutant phenotype (Weijers *et al.*, 2006), we designed an experiment to inhibit MP activity only in these cells (Figure 1f). This strategy would allow uncoupling of MP activity in root meristem initiation from its activity in cotyledon formation (Hardtke *et al.*, 2004). Since Q0990-driven bdl expression perfectly phenocopies the root initiation defects in *mp* mutants (Weijers *et al.*, 2006), this can be used as a genetically dominant tool for local MP inhibition. Other ARFs are co-expressed with MP at this stage of development, most notably ARF1 , ARF6 and ARF18 (Rademacher *et al.*, 2011). However, since Q0990-bdl induces the *mp* phenotype, we consider MP to be the major target of bdl inhibition. p*Q0990-GFP* expression is detected in the inner basal embryo cells of the globular stage embryo (Figure 1g, h). Around heart stage, *Q0990* expression becomes restricted to the vasculature (Figure 1i, j). To first determine the efficiency of MP inhibition, Q0990-GAL4 (henceforth Q0990) were crossed to *UAS-bdl* plants, or to wild-type plants as control (Fig. 1k, l). Indeed, Q0990-bdl embryos displayed *mp*-like defects in hypophysis and stem cell divisions, and these became apparent at the time these cells normally divide (Figure 1n, o). We determined that three days after pollination, most embryos had reached globular stage (Figure 1m-o). After six days, the majority of embryos were at late heart stage (Figure 1p, q). Based on these findings, three and six days after pollination were chosen as the time points for embryo dissection.

Early globular stage embryos and heart stage embryos were isolated and used as samples for the microarray. Plant embryos are fully enclosed by their surrounding tissue which makes them difficult to isolate. Therefore, embryos were manually dissected from ovules using fine forceps (Xiang *et al.*, 2011). This technique eliminates any interference of the embryo surrounding tissue on the embryo expression profiles. We separately isolated [Q0990 x bdl] and [Q0990 x wild-type] embryos three and six days post pollination, extracted, amplified and labeled their RNA, followed by hybridization to long (70-mer) oligonucleotide arrays representing approximately 29,000 genes (Operon-Qiagen; http://ag.arizona.edu/microarray/) using 4 replicates of each isolation. Expression data were normalized and statistically analyzed using Limma Software (Smyth, 2004).

Microarray analysis

Before we analyzed the microarray data, we verified if *BDL* expression was up-regulated as a result of activation by the Q0990 promoter. Indeed, *BDL* expression was 2,6-2,7 times up-regulated in the datasets of globular stage and heart stage embryos. To analyze the microarray datasets, we initially defined an arbitrary

threshold of a two-fold, significant change in gene expression in all four replicates (p= 0,05). Using these criteria, 145 genes were down-regulated in the dataset from early globular stage embryos (Table 1), while 412 genes were up-regulated. The dataset of heart stage embryos showed a considerable increase in the number of down-regulated genes with 382 entries, while only 147 genes were up-regulated. We initially focused on the down-regulated genes, because most MP target genes that have been identified so far, are activated by MP (Cole *et al.*, 2009; Donner *et al.*, 2009, Chapter 2). Nonetheless, the high number of up-regulated genes in these datasets suggest that MP might also function as transcriptional repressor. 27 genes were down-regulated in both datasets (Figure 1l, Table 1). Of the 145 ≥2-fold downregulated genes in globular embryos, only 6 had previously passed the threshold criteria (≥2-fold downregulated both in *mp* mutant and in induced bdl-GR) in the seedling microarray (Chapter 2, Table 1). Strikingly, one of these genes is the known MP target gene *TMO7*, which is the most down-regulated gene in the dataset of early globular stage embryos. Therefore, while this new dataset validates known MP targets, our approach could also identify novel MP target genes.

To select genes that might be active in the first vascular and ground tissue cells, we focused on the dataset of early globular stage embryos for several reasons. First of all, based on lineage analysis (Scheres *et al.*, 1994), vascular and ground tissue specification are more likely to occur at early globular stage compared to heart stage. Secondly, the dataset of early globular stage embryos is more likely to include direct MP target genes, compared to the dataset of heart stage embryos. Thirdly, phenotypic severity increased in heart stage embryos compared to globular stage embryos (Figure 1m-q), such that root meristem organization is completely lost at heart stage (Figure 1q). Therefore, the dataset of heart stage embryos is complex and probably includes many genes that are misregulated as a result of phenotypic defects.
Since many of the genes that are downregulated have not been characterized, we found that Gene Ontology term enrichment did not help identify over-represented functions. However, among the 145 down-regulated genes in the dataset of early globular stage embryos are 36 transcription factors, which corresponds to ~25% of the down-regulated genes (Table 1). This is a considerable enrichment compared to the ~5% transcription in the Arabidopsis genome (Riechmann *et al.*, 2000), and is consistent with a role for MP as regulator of multiple different processes in embryogenesis. We also found that ~14% of the genes in the list of down-regulated genes has predicted or demonstrated cell wall remodeling activity (Table 2). This finding is not surprising in light of the dynamic changes in cell shape during early embryo development, and suggests that MP might influence these rather

directly. Furthermore, several genes implicated in auxin signaling are down-regulated (Table 1). Among these are the primary auxin response genes *Aux/IAA19* and *30*, genes involved in auxin biosynthesis or conjugation like *TAA1*, *YUCCA8*, and *BRU6*, and auxin transporters such as *PIN4* and *LAX2* (Tiwari *et al.*, 2001; Stepanova *et al.*, 2008; Tao *et al.*, 2008; Cheng *et al.*, 2007; Staswick *et al.*, 2005; Friml *et al.*, 2003; Ugartechea-Chirino *et al.*, 2010). The downregulation of genes involved in auxin signaling suggests that MP is normally required to promote their expression during embryo development.

We next selected genes for examining their expression pattern to verify if they could be novel MP target genes during embryonic root initiation (Table 1). Our selection criteria were (1) The role of these genes in embryo development is not yet characterized; (2) Expression of these genes is significantly down-regulated in the dataset of globular stage embryos; (3) Gene function: most of these genes belong to transcription factor families (27 genes) or are predicted to be involved in signal transduction; (4) The predicted root expression pattern according to the publicly available data (Winter *et al.*, 2007; Brady *et al.*, 2007) shows expression in inner root meristem tissues. However, for the majority of genes, the eFP Browser displayed expression in several root zones, or the expression level was too low to be informative; (5) Since forward-genetic screens have not recovered these genes, it is likely that functions are redundant. Therefore, the presence of closely related genes in the dataset that were also down-regulated was taken into consideration; (6) Expression of these genes was enriched in the pro-embryo compared to the suspensor in globular stage embryos according to publicly available data from Laser Capture Microdissection (LCM) (Le *et al.*, 2010). According to these criteria, we selected a subset of 37 genes that fulfill at least several, for further study.

Expression analysis of candidate MP target genes during root initiation

We examined embryo expression patterns of 37 selected genes from the microarray dataset on globular stage embryos, to verify if they could be MP target genes. We generated transcriptional fusions, consisting of a 2kb fragment upstream of the ATG, and a sensitive nuclear triple GFP reporter (Takada and Jürgens, 2007), for each of these genes. Although gene regulation through elements outside 2 kb upstream is common, this region often gives a good approximation of the expression pattern (Megraw *et al*., 2006). Subsequently, these constructs were transformed into wild-type. We analyzed root meristem expression patterns for approximately 25 independent T1 transgenic seedlings per gene. This approach demonstrated that the majority of genes displayed a uniform root expression pattern among multiple independent transformants, while several genes did not appear to be expressed in the root tip. We selected on average four lines with strong expression

in the root tip for the embryo expression analysis. This increased the chance to visualize gene expression in the embryo, which is in general low compared to expression levels in the postembryonic root. For genes whose expression was undetectable in the root, we analyzed embryo expression in approximately eight independent lines. In total, expression of 14 genes was not detectable in the embryo using the 2kb promoter-n3GFP fusion (Table 2). Nine of these genes showed no or weak expression in the proximal meristematic region of the postembryonic root (Table 2). In addition, four other genes showed variable embryo expression patterns between different lines (Table 2). Although each microarray experiment generates false positive data, there might be several explanations for these findings. The easiest explanation is that these genes are expressed in the embryo, but our analysis method failed to detect their expression due to low expression levels. Alternatively, the 2kb promoter fragment did not contain all necessary regulatory elements to faithfully record the expression pattern of some genes. This probably caused the variable expression patterns observed in multiple independent lines transformed with the same construct.

Category A: ambiguous genes

The remaining 23 genes showed identical embryo expression patterns in at least two, but usually four, of the preselected lines. For 11 of these genes, expression was found outside of the MP expression domain, and is difficult to reconcile with local MP inhibition in vascular and ground tissue cells of the globular stage embryo (Table 2). The expression patterns of these genes can be divided in several groups. *WRKY21* and *TET10* are expressed in both the apical and basal parts of the embryo, including the hypophysis and its descendents (Figure 2a-d, Table 2). The down-regulation of these genes in the microarray can be explained by local down-regulation of gene expression in those cells where MP activity is inhibited. The expression pattern of *WRKY21* exactly matches that of *MP* during embryo development (Figure 2a, b, compare with Figure 1b-e), except for the suspensor expression, and *WRKY21* might hence be a MP target gene. Four other genes are expressed in the hypophysis and epidermis of the globular stage embryo (Figure 2e-p, Table 2). *GATA8* and *PUB22* are only expressed in the hypophysis and epidermis, while *WRKY17* is also expressed in ground tissue cells and *IQD16* in all future root meristem cells of the globular stage embryo. Another four genes are exclusively expressed in the apical embryo region after globular stage of embryogenesis (Figure 2q-t, Table 2). These expression patterns could be explained by misregulation of genes as a result of phenotypic defects in globular stage embryos in which MP activity is inhibited. For example, the hypophysis is not properly specified in embryos lacking MP activity in the cells adjacent to the hypophysis

(Figure 1o). Therefore, genes normally expressed in the hypophysis are expected to be misregulated. In summary, expression patterns of 29 out of 37 analyzed genes, did not match with a role for these genes in vascular or ground tissue specification downstream of MP.

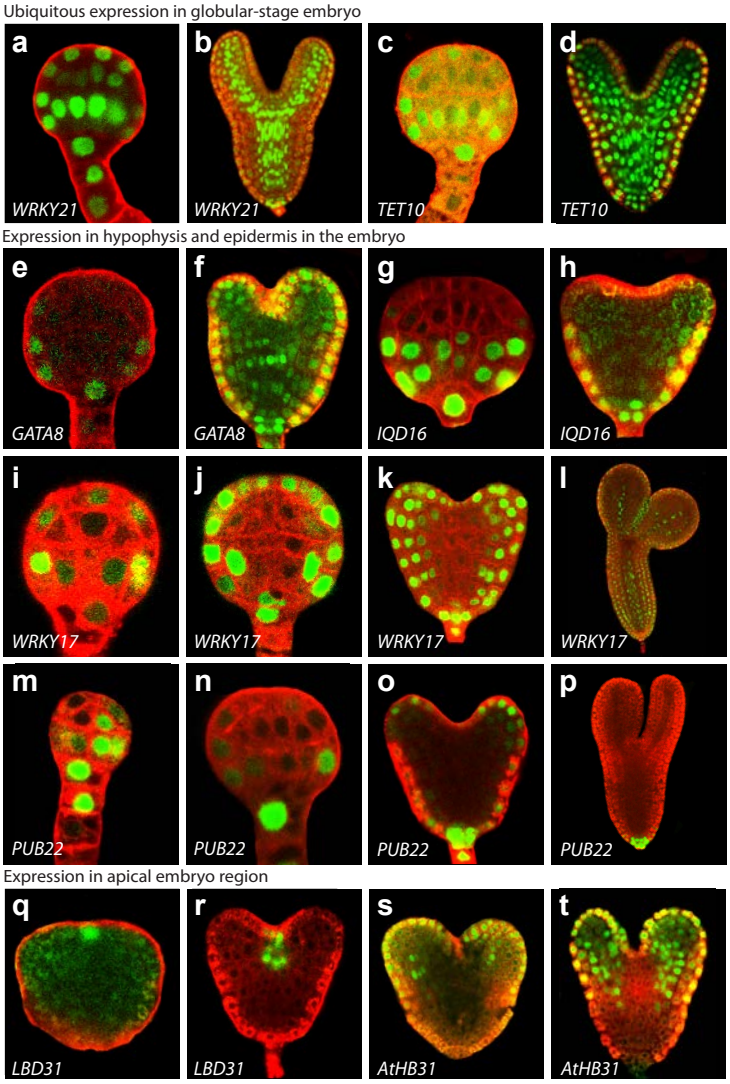

Figure 2. Expression patterns of down-regulated genes in the microarray dataset of globular stage embryos in which MP activity was locally inhibited. Ubiquitous expression of p*WRKY21-n3GFP* (a, b) and p*TET10-n3GFP* (c, d), hypophysis and epidermis expression of p*GATA8-n3GFP* (e, f), p*IQD16-n3GFP* (g, h), p*WRKY17-n3GFP* (i-l), and p*PUB22-n3GFP* (m-p), and apical expression of p*LBD31-n3GFP* (q, r) and p*AtHB31-n3GFP* (s, t) in pre-globular (i, m), globular (a, c, e, g, j, n), transition (q, s), heart (b, d, f, h, k, o, r, t), and torpedo (l, p) stage embryos.

Category B: Genes expressed in future root meristem cells in the globular stage embryo

SPATULA (SPT)/ *bHLH24* and the U-box-containing E3 Ubiquitin ligase *PUB25* are expressed in all basal embryo cells of the globular stage embryo (Figure 3a, b, f, g; Table 2). Both genes are not expressed in the hypophysis before its division (Figure 3a, f), but are expressed in hypophysis descendents, like *MP* (Fig. 1c-e). *PUB25* appears to be expressed in both daughter cells of the hypophysis (Figure 3g-i), while *SPT* is only expressed in the apical daughter cell that will form the QC (Figure 3c, d). Interestingly, while *PUB25* is expressed in the vascular tissue initials before their division, it is no longer detected in the apical daughter cells after division (Figure 3g-h), providing evidence that this division is asymmetric with regards to cell identity. Postembryonically, *PUB25* and *SPT* are strongly expressed in the root meristem, while their expression quickly decreases in cells displaced further away from the QC. The expression level of *PUB25* drops faster than that of *SPT*. These genes could be MP target genes as they are expressed in the same cells as MP protein (Fig. 1b-e). The *mei2*-like RNA binding protein *MCT1* is only expressed in the inner basal embryo cells of the globular stage embryo (Fig. 3k, l, Table 2), but not in the hypophysis or its descendents. Strikingly, the expression of *MCT1* is lost in the root meristem after globular stage (Figure 3m-o), and expression is activated in the shoot meristem of heart stage embryos (Figure 3n). In conclusion, these three genes could be MP target genes involved in root initiation, based on their expression patterns, but neither is specific to a single cell type.

Category C: Genes expressed in the first vascular tissue cells of the globular stage embryo

IQ-DOMAIN15 (IQD15) and a gene containing Domain of Unknown Function 966 (DUF966), hereafter referred to as *DUF966*, are strongly expressed in the first vascular cells of the globular stage embryo (Figure 4a, b, f, g). At early globular stage, *DUF966* is also weakly expressed in the first ground tissue cells (Figure 4a), possibly reflecting GFP protein inherited from its precursor cells. Notably, vascular expression of *DUF966* does not extend into the apical embryo region in heart stage embryos (Figure 4d), suggesting that *DUF996* expression might be root specific. In contrary, vascular expression of *IQD15* is ubiquitous and includes the apical embryo region (Figure 4i). Both genes are not expressed in the hypophysis in globular stage embryos (Figure 4a, f), but become expressed in hypophysis descendents (Figure 4b, h), although at slightly different time points. *DUF966* is expressed in both the apical and basal daughter cell of the hypophysis, while *IQD15* is only expressed in the apical daughter cell that will form the QC.

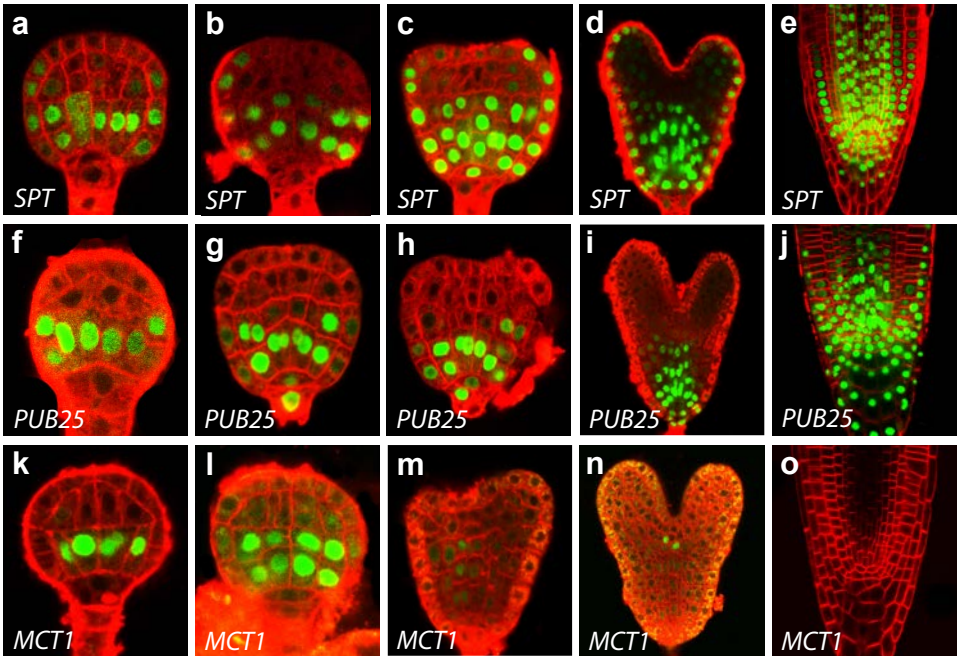

Figure 3. Expression pattern of putative MP target genes expressed in the future root meristem cells of the globular stage embryo. Expression of p*SPT-n3GFP* (a-e), p*PUB25-n3GFP* (f-j), and p*MCT1-n3GFP* (k-o) in the embryo at globular stage before (a, f, k) and after (b, g, l) division of the first vascular and ground tissue cells, transition stage (c, h, m), heart stage (d, i, n) and postembryonically in the root tip (e, j, o).

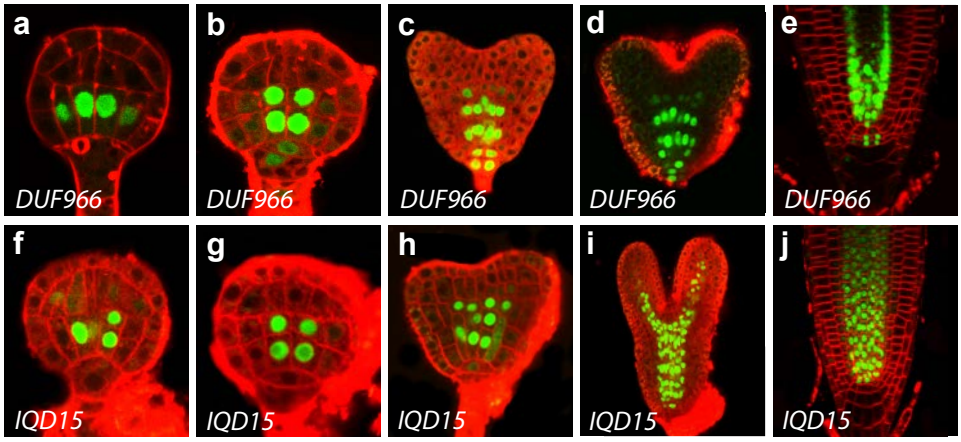

Figure 4. Expression pattern of putative MP target genes expressed in the first vascular tissue cells of the globular stage embryo. Expression of p*DUF966-n3GFP* (a-e) and p*IQD15-n3GFP* (f-j) in the embryo at globular stage before (a, f) and after (b, g) division of the first vascular tissue cells, transition stage (c, h), heart stage (d, i) and postembryonically in the root tip (e, j).

In the postembryonic root meristem, *DUF966* is only expressed in vascular cells in close proximity to the QC (Figure 4e). *DUF966* expression appears relatively uniform throughout the vascular bundle in cells closest to the QC, while slightly further away from the QC, *DUF966* expression seems highest in two separate strands. Postembryonically, *DUF966* appears not to be expressed in the QC, but is expressed in columella layers closest to the QC. The expression of *IQD15* is not limited to the vasculature in the postembryonic root meristem, but also found in endodermis and cortex cells, and in the QC (Figure 4j). The expression level of *IQD15* drops in cells that are displaced further away from the QC, but this occurs more gradually compared to *DUF966*. Based on their expression patterns, both *DUF966* and *IQD15* could be MP target genes involved in vascular tissue initiation in the embryonic root meristem.

Category D: Genes expressed in the first ground tissue cells of the globular stage embryo

We found one gene with specific expression in the first ground tissue cells of the globular stage embryo (Figure 5a, b, Table 2). This gene is a member of the Receptor Like Kinase (RLK) family, hereafter called *RLK*. It is also expressed in all daughter cells of the first ground tissue cells, although expression is stronger in the endodermis compared to the cortex (Figure 5b-d). Postembryonically, *RLK* expression is still, but weakly, detected in ground tissue cells closest to the QC, and in their daughter cells (figure 5e). The MYB domain-like gene of the SHAQKYF class (*MYB-LIKE*) is expressed in the first ground tissue cells of the early globular stage embryo (Figure 5f). In subsequent stages of embryogenesis, *MYB-LIKE* is also expressed in all daughter cells of the first ground tissue cell that will form the endodermis and cortex cell files (Figure 5g-i). *MYB-LIKE* is not expressed in the hypophysis (Figure 5f), but becomes expressed in both daughter cells after hypophysis division (Figure 5g). Postembryonically, MYB-LIKE is expressed in the QC, the first ground tissue cells, and in the cortex (Figure 5h). Both *RLK* and *MYB-LIKE* could be MP target genes involved in ground tissue specification, based on their expression patterns. However, expression of *MYB-LIKE* is not specific to the first ground tissue cells, suggesting that it might also be involved in other processes. *OVATE FAMILY PROTEIN8 (OFP8)* is expressed in the hypophysis (Figure 5k), suggesting that it is not a direct MP target gene as the latter is not expressed in the hypophysis. *OFP8* is not, or very weakly, expressed in the first ground tissue cells before they divide (Figure 5k, data not shown). When the first ground tissue cells have divided, *OFP8* is expressed in both the ground tissue initial and its daughter cells (Figure 5l). At heart stage of embryogenesis, *OFP8* is expressed in the QC, endodermis and cortex, and this expression pattern is unal-

tered in the postembryonic root (Figure 5n-o). Although hypophysis expression of *OFP8* is unlikely to be directly regulated by MP, the later expression of this gene, as well as that of *RLK* and *MYB-LIKE* may be controlled by MP.

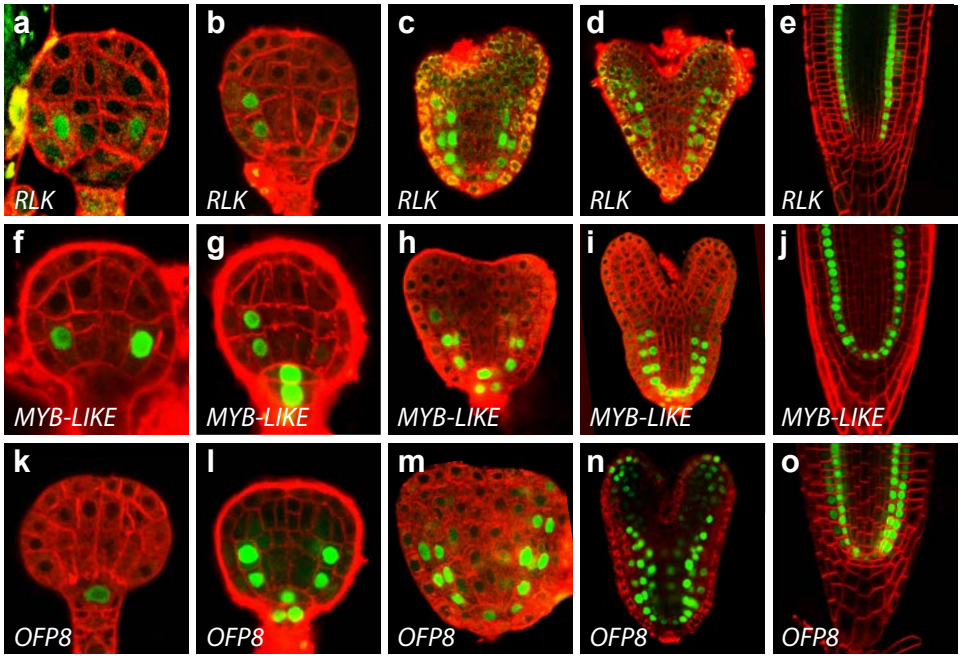

Figure 5. Expression pattern of putative MP target genes expressed in the first ground tissue cells of the globular stage embryo. Expression of p*RLK-n3GFP* (a-e), p*MYB-LIKE-n3GFP* (f-j), and p*OFP8-n3GFP* (k-o) in the embryo at globular stage before (a, f, k) and after (b, g, l) division of the first ground tissue cells, transition stage (c, h, m), heart stage (d, i, n) and postembryonically in the root tip (e, j, o).

MP-dependent expression of novel putative MP target genes

Embryo expression patterns of several down-regulated genes in the dataset on globular stage embryos fall within the domain of MP activity. This suggests that these genes could be MP target genes. However, down-regulation in Q0990-bdl embryos can be the result of several reasons other than MP inhibition. Other ARFs are co-expressed and to some extent redundant with MP (Hardtke *et al.*, 2004; Rademacher *et al.*, 2011), developmental progression may be altered in mutant embryos, or bdl may have ARF-independent effects. Therefore, to test if MP activity is required to promote expression of these genes, we analyzed their expression in *mp* mutant embryos. For this purpose, we analyzed expression of the fluorescent reporters in T4 generation embryos homozygous for the reporter, and segregating the *mp* mutation. To avoid ambiguity, expression was analyzed only

in embryos that were scored as mutant due to characteristic cell division defects in hypophysis or vascular or ground tissue cells. Therefore, although numbers are small, each observation represents a mutant individual.

We found that expression of at least four of the seven genes tested depends on MP activity (Figure 6). *DUF966* is strongly expressed in wild-type transition stage embryos (Figure 6a), but is nearly absent in *mp* mutant embryos in which the hypophysis has divided aberrantly (n=4; Figure 6b). *RLK* is weakly expressed in embryos, but MP-dependent gene expression could be reliably analyzed in early heart stage embryos. In these embryos, *RLK* was consistently expressed in wild-type embryos (Figure 6c), but not in any of the six *mp* mutant embryos that we observed (Figure 6d). *SPT* and *PUB25* were consistently and strongly expressed in wild-type late transition stage embryos (Figure 6e, g), while expression was absent or greatly reduced in at least five *mp* mutant embryos (Figure 6f, h). In addition, *SPT* expression appeared to be reduced already in late globular stage *mp* mutant embryos (n=3; data not shown). Importantly, for these four genes, we did not observe any *mp* mutant embryo with wild-type expression levels in the same developmental stage. Therefore, despite the limited number of *mp* mutant embryos that we observed, these genes are probably MP target genes. Further research is required to determine if these genes are directly or indirectly activated by MP.

Expression of three other genes does not obviously depend on MP activity. *IQD15* expression seems lost in several vascular cells in late globular stage *mp* mutant embryos (Figure 6i-j), but only two mutant embryos were observed. Furthermore, in early heart stage embryos, the expression pattern and level of *IQD15* appears similar in *mp* and wild-type embryos (Figure k-l). Together, these preliminary data suggest that MP might be required for initiation of *IQD15* expression at globular stage, but not for its maintenance at heart stage of embryogenesis. *OFP8* expression levels seem equally strong in *mp* mutant and wild-type globular stage embryos (n=2; Figure 6m-n). At heart stage, *OFP8* is strongly expressed in *mp* mutants with disturbed root meristem organization (n=5; Figure 6o-p). Similarly, *MYB-LIKE* is strongly expressed in *mp* mutants at transition (n=3) and heart stage (n=5) of embryogenesis (Figure 6q-t). Notably, both *OFP8* and *MYB-LIKE* are expressed in aberrantly dividing ground tissue cells of globular stage embryos (Figure 6n, r). On the contrary, *MYB-LIKE* expression is lost in late heart and torpedo stage *mp* mutant embryos (n=8; data not shown). However, this loss in expression in later stages of embryogenesis might be explained by severe defects in root meristem organization in *mp* embryos. MP-dependent expression of *MCT1* could not be analyzed because its expression in the wild-type root meristem is already down-regulated at the stage that *mp* mutants can be identified.

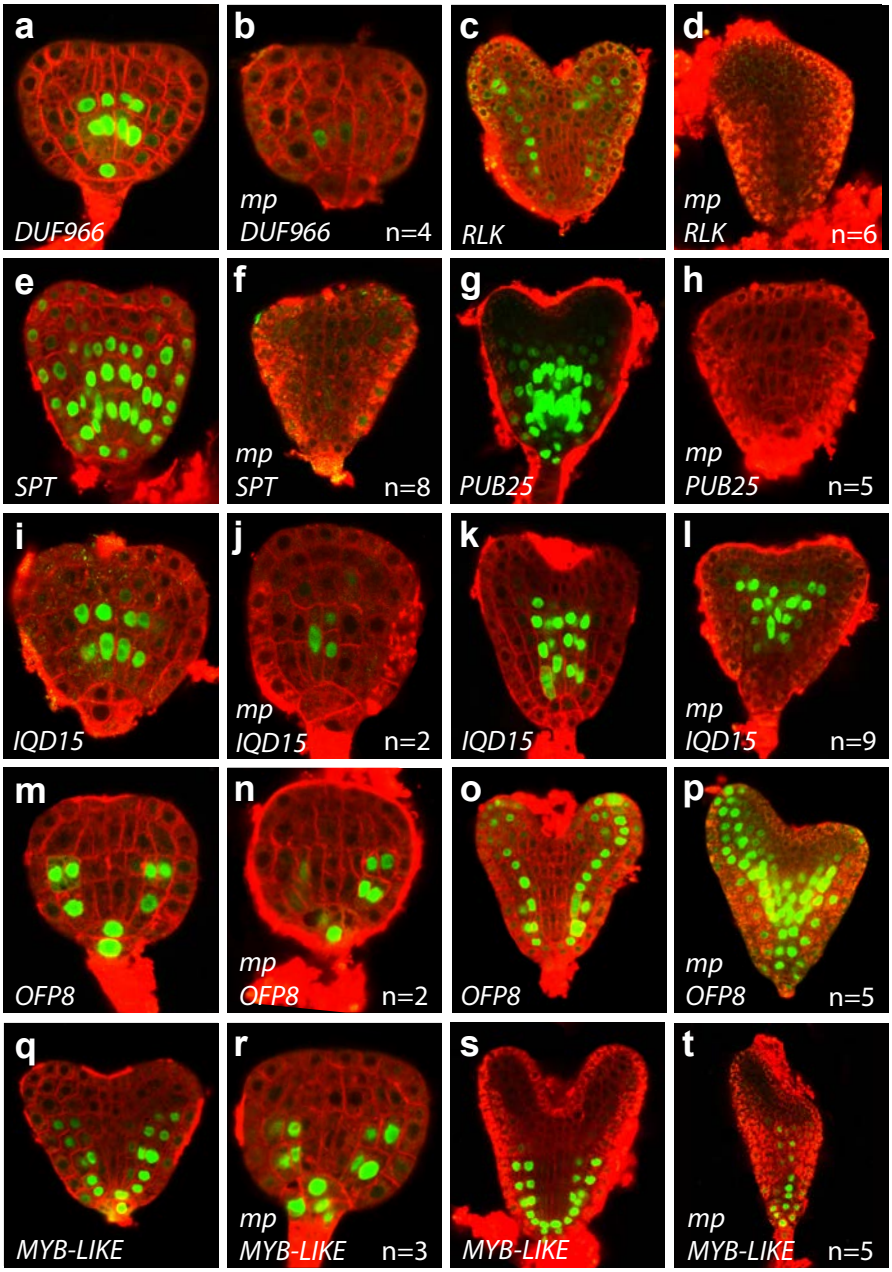

Figure 6. Expression of putative MP target genes in *mp* and wild-type embryos. Expression of p*DUF966-n3GFP* (a-b), p*RLK-n3GFP* (c-d), p*SPT-n3GFP* (e-f), p*PUB25-n3GFP* (g-h), p*IQD15-n3GFP* (i-l), p*OFP8-n3GFP* (m-p), and p*MYB-LIKE-n3GFP* (q-t) in transition (a, b, i, j, m, n, q, r) and heart (c-f, k, l, o, p, s, t) stage embryos. For each gene, identical confocal settings were used to compare gene expression levels in *mp* and wild-type for a given embryonic developmental stage. n is the number of *mp* embryos observed with similar expression.

Taken together, MP does not appear to be required for activating transcription of *OFP8* and *MYB-LIKE*. These genes are both expressed in the hypophysis, and could be down-regulated in the dataset as result of induced hypophysis defects in Q0990>>>bdl embryos. However, this analysis of reporter gene expression in *mp* mutant embryos is qualitative. It might not reveal a ~two-fold decrease in gene expression, as found in the microarray dataset on globular stage embryos. It is realistically possible that expression of *OFP8*, *IQD15* and *MYB-LIKE* are redundantly regulated by MP and other ARFs, and that, while bdl misexpression inhibits all these ARFs, redundant ARFs activate these genes in the *mp* mutant. Nonetheless, we have identified four novel MP target genes expressed in the first vascular or ground tissue cells in the early globular stage embryo, or in both.

Discussion

During plant development, various processes need to occur in the developing embryo to create a basic body plan with root and shoot meristems located at opposite sites. To initiate the root meristem during early embryo development, root tissues, stem cells and organizer cells need to be specified. Auxin signaling has been shown to be crucial to initiate root meristem formation. The MP transcription factor is the main executer of the auxin signal by regulating gene transcription. Previously, MP has been shown to activate members of several transcription factor families during early embryo development (Chapter 2). We performed a microarray on early globular stage embryos to find novel MP target genes involved in root initiation. We define MP targets here as genes that are cell-autonomously controlled by MP, and explicitly refrain from statements on whether this regulation is mediated by binding of MP to the regulatory elements within such target genes, or if regulation is indirect. MP activity was locally inhibited in the first vascular and ground tissue cells in the developing root meristem of early embryos. TMO7 was the most down-regulated gene in the dataset on globular stage embryos, validating our approach. We found a substantial enrichment of transcription factors and cell wall remodeling genes, suggesting that MP regulates many processes and plays a role in the extensive and dynamic cell shape changes in early embryo development. We identified four novel MP target genes that are expressed in either the first vascular or the first ground tissue cells in the early globular stage embryo, or in both. These cells are among the first cells of the embryonic root meristem, and will obtain stem cell identity. Therefore, we identified novel MP target genes that might be involved in vascular or ground tissue specification, and/or in stem cell identity. However, further research is needed to establish if these genes are direct MP target genes. These results suggest that MP is required for the initial formation

of vascular and ground tissue in the Arabidopsis embryo.
This study being based on micro-array and gene expression analysis, there are several critical issues related to the approach, selection of genes and method to determine gene expression. These have all been addressed in the previous section, where appropriate. We now turn the discussion to the genes that were newly identified as being MP-dependent, and what their identity and regulation can teach us about MP-dependent embryo development.

Initial specification of vascular and ground tissue in the early plant embryo
The mechanisms of initial tissue specification in the early embryo are largely unexplored. So far, the MP target gene *TMO5* is the only gene known to be expressed in the first vascular tissue cells of the root. We revealed another MP target gene that is expressed in the first vascular and columella cells in early embryos, and is limited to several vascular and columella cells in the proximity of the QC in postembryonic roots. *DUF966* expression is strongly reduced in *mp* mutant embryos, suggesting that MP is the main regulator of *DUF966* transcription. DUF966 might be involved in establishing vascular and columella tissue identity, or alternatively, in establishing and maintaining vascular and columella stem cells. However, without any functional data, we can only speculate about the role of *DUF966* in embryo development. The molecular function of *DUF966* is unknown, but the protein is predicted to be nuclear localized (http://suba.plantenergy.uwa.edu.au/), and the gene is plant-specific and conserved across all land plants (http://www.ebi.ac.uk/interpro/IEntry?ac=IPR010369). Arabidopsis has only five genes that contain a DUF966 domain, of which two are more than two-fold down-regulated in this microarray, and another one is ~1,5-fold down-regulated (http://www. phytozome.net/jalview). This suggests that MP is an important regulator of this small gene family. *IQD15* shows vascular-specific expression at early globular stage of embryogenesis, and this might be MP-dependent. IQD15 is a predicted calmodulin-binding protein with transcriptional activity (Abel *et al*., 2005). However, not much is known about the biochemical function of IQ-Domain proteins. *RLK* is specifically expressed in the first ground tissue cells in early embryos, and in all ground tissue daughter cells in subsequent root development. To our knowledge, this is the first report of a gene that is specifically expressed in ground tissue from early embryogenesis on. Therefore, *RLK* might be involved in specifying ground tissue identity in the early embryo. Alternatively, *RLK* might be expressed as result of ground tissue specification, and be involved in maintenance of ground tissue identity. *RLKs* constitute a large family in Arabidopsis with more than 600 members. However, the subclade that contains this specific *RLK* has only three members, characterized by an extracellular thaumatin domain, a central transmem-

brane spanning domain, and an intracellular serine/threonine kinase domain (Shiu *et al*., 2003). The thaumatin domain is related to proteins with known functions in pathogen defence, but for this *RLK* subclade this has not been shown (Wang *et al*., 1996). *RLKs* from the sizable leucine-rich repeat receptor-like kinases (LRR-RLKs) subclade have been shown to function in brassinosteroid signaling and SAM development (reviewed in Gish and Clark, 2011). In the latter case, CLE peptides have been shown to bind to LRR-RLKs to regulate the decision between cell proliferation and differentiation. Further research is required to determine the ligand for this RLK, and to determine the direction of signaling. A specific CLE peptide has been shown to promote MP-dependent proliferation of vascular cells (Whitford *et al.*, 2008). It is conceivable that this *RLK* mediates MP-dependent proliferation of ground tissue cells.

In any event, although the functional contribution of the newly identified genes to MP-dependent tissue and stem cell specification remain to be studied, these genes firmly demonstrate a role for MP in controlling these processes at transcriptional level. Not only does loss of MP activity lead to altered division in vascular initials, also the first expression of genes specific to these cells is affected. While this had previously been shown only for a few genes at low resolution (Chapter 2), we now expand the number of MP-dependent genes and the resolution at which their MP-dependence has been analyzed. Furthermore, the MP-dependent expression patterns provide insight into the timing of cell type-specification and as such present excellent molecular markers for early events in meristem initiation.

MP-dependent gradients in the root stem cell niche

Both *SPT* and *PUB25* are novel MP target genes expressed in the root stem cell niche from early embryogenesis on. Postembryonically, both genes are expressed in the putative stem cells and the QC, and show steep gradients similar to the *PLT* genes (Galinha *et al.*, 2007). *PLT* expression has been shown to be MP-dependent and auxin-inducible (Aida *et al.*, 2004). However, induction of *PLT* genes by auxin is very slow, suggesting that these are not direct MP targets. *SPT* and *PUB25* might be involved in parallel MP-dependent pathways to promote cell divisions in the stem cell niche, but this is purely speculative, and the role of both *SPT* and *PUB25* in embryo development is unknown. *SPT* is a bHLH transcription factor involved in growth regulation of carpel development (Alvarez and Smyth, 1999), but has been shown to play a role in several other processes as well. *SPT* was previously shown to be expressed in the root meristem region of heart stage embryos (Groszmann *et al*., 2010), but so far, *SPT* has not been assigned a role in embryo development. Nonetheless, *SPT* encodes a bHLH transcription factor and other family members including *TMO5* and *TMO7* are part of a MP-dependent regula-

tory pathway that controls embryonic root formation (Chapters 2 & 3). *PUB25* encodes an ubiquitin ligase with unknown function, but is related to the U-box protein PHOTOPERIOD RESPONSIVE 1 (PHOR1) that functions in gibberellin hormone signaling (Amador *et al*., 2001). PUB25 and PHOT1 both contain an Armadillo repeat shown to be responsible for nuclear import of armadillo repeat proteins in animals (Coates, 2003; Widelitz, 2005). PHOT1 is imported into the nucleus of tobacco cells by gibberellins, suggesting similarities with the armadillo repeat proteins in animals (Amador *et al.*, 2001). The latter are essential components of the *Wnt* signaling pathway involved in embryonic pattern formation, and interact with the *Tcf/LEF-1* family of transcription factors (reviewed in Widelitz, 2005). Interestingly, the basic residues responsible for this interaction are also found in PHOT1, suggesting the existence of a similar mechanism in plants (Amador *et al.*, 2001). Moreover, two related U-box proteins, *PUB22* and *PUB23*, have been shown to physically interact with a regulatory subunit of the 26S proteasome, and are involved in drought stress (Cho *et al.*, 2008). PUB25 might be involved in embryo development, and auxin could possibly mediate its nuclear import. It will be interesting to see in follow-up studies if the graded expression of *SPT* and *PUB25* has functional significance, and whether their activities are involved in defining the stem cell population in the root.
MP-dependent expression of *MCT1* has not been investigated due to its dynamic expression pattern in embryo development. The expression pattern of *MCT1* is similar to that of two closely related Terminal Ear-Like (TEL) *mei2*-like genes in Arabidopsis. A mutation in a homologous gene in maize results in altered patterns of leaf initiation in the SAM (Anderson *et al*., 2004). In view of embryonic *MCT1* expression in the root and shoot meristem at the time when these are specified, it is possible that *MCT1* has a role in specifying proximal stem cells. It is interesting to note that *MCT1* is expressed in stem cells closest to the organizing center cells in both the shoot and root meristem. To our knowledge, this is the first gene that has been shown to be transiently expressed in the root stem cell area and later in the shoot meristem. This pattern suggests that MCT1 might play a role in a singular event associated with activation of the meristems. However, as for all of the above discussed genes, further research is required to study their function in embryonic root initiation.

The number of genes known to be involved in root meristem formation or maintenance rapidly increases. Several gene families were not yet described at the time of our microarray analysis, and therefore not included in the expression analysis. *LONELY GUYs (LOGs)* encode cytokinin-activating enzymes required for root and shoot maintenance (Kuroha *et al.*, 2009; Tokunaga *et al.*, 2011). *LOG3* and *7*

are down-regulated in the dataset on globular stage embryos, suggesting that these are expressed in the embryo in an auxin-dependent manner. Postembryonically, *LOG3* was shown to be expressed in the vasculature of the root meristem, while *LOG7* is not expressed in the root meristem (Kuroha *et al.*, 2009). Moreover, small peptides called root meristem growth factors (RGFs) were recently shown to be required to maintain the root meristem (Matsuzaki *et al.*, 2010). RGF1 and 8 are down-regulated in the dataset on globular stage embryos, suggesting that they are expressed in the embryo, and possibly activated by MP. The tyrosylprotein sulfotransferase (TPST) enzyme, required for RGF activity, is first expressed in the QC area of heart stage embryos (Zhou *et al.*, 2010). However, *tpst* mutants lacking activity of all RGF members, exhibit normal embryo development. Auxin induces expression of RGF8 but not RGF1. However, in contrast to RGF1, RGF8 cannot rescue the proliferating activity of the root meristem in the *tpst* mutant. Therefore, whether *LOG* and *RGF* are involved in embryonic root initiation or not, and whether these are transcriptionally activated by MP or not, remain open questions.

We showed MP-dependent expression of genes in the first vascular and ground tissue cells in the early embryo, and found MP-dependent gradients in the postembryonic root meristem. The functional study of these putative MP target genes will probably reveal a lot about the mechanisms of embryonic root initiation. The domain structure of several genes, such as *RLK*, *PUB25* and *IQD15*, suggests that these are involved in intercellular signaling. It will be very interesting to reveal the network of signaling events required to specify the tissues, stem cells, and organizer cells in the embryonic root meristem. Recently, TMO7 has been identified as a mobile signal that is transported from the first vascular tissue cells into the precursor of the QC. In addition, SHR is known to signal form the vascular cells to the ground tissue cells and QC in the postembryonic root meristem, but it is so far unclear if this is also required in the embryo. Further research will also reveal if signaling towards the vascular cells from the surrounding cells is required to specify the embryonic root meristem, and if directionality in the timing of these signaling events is critical. These signaling events will most likely include hormonal crosstalk, and further research will probably show that auxin interacts with cytokinin and other hormones, as well as with small peptides like RGFs, in root initiation. This study suggests that MP is required for multiple aspects of root initiation, including vascular and ground tissue specification, and the specification of the embryonic root stem cells.

Material & Methods

Plant growth and Material

All seeds were surface sterilized, sown on solid MS plates and vernalized for one day before growing at a constant temperature of 22°C in a growth room. The *mp-B4149* allele in Columbia background and the *UAS*-bdl line were described in Weijers *et al.* (2006). The *Q0990-GAL4* enhancer trap line was generated by Jim Haseloff (University of Cambridge, UK) and obtained through the Arabidopsis Biological Resource Center (ABRC).

Microarray experiment

Q0990-GAL4 plants were crossed to UAS-bdl plants to locally inhibit ARF activity in the embryo and to wild-type plants to serve as a control. After three and six days, embryos from both crosses were separately isolated as described in Xiang *et al.*, 2011 using the dissecting microscope and fine forceps (Dumont 55 forceps, catalog no. 11295-55, Fine Science Tools). Total RNA was extracted from pooled embryos that were dissected three or six days after the crosses following the protocol of RNAqueous-micro kit (Ambion, catalog no. 1927). Each biological replicate contained 300-400 isolated embryos.

The mRNA was subsequently amplified prior to labeling to increase the quantity as described in Xiang *et al.*, 2011. Antisense RNA labeling was performed following the protocol of Wellmer *et al*. (2004).

The aRNA samples representing four biological replicates from experimental and control samples were labeled (two cy3 and two cy5) and hybridized to the microarray slides following the protocol described in http://ag.arizona.edu/microarray. The Arabidopsis 70-mer oligo array slides prepared by University of Arizona were used in all the microarray experiments (version ATV 3.7.2; http://ag. arizona. edu/microarray/). Hybridized slides were scanned sequentially for Cy3- and Cy5-labeled mRNA targets with a ScanArray 4000 laser scanner at a resolution of 10 μm. The image analysis and signal quantification were performed using the QuantArray program (GSI Lumonics). Limma Software (Smyth, 2004) was used to normalize and to determine the modulated genes from microarray data.

Cloning and plant transformation

All cloning was performed using a set of Ligation-Independent Cloning vectors according to procedures described previously (De Rybel *et al.*, 2011). Transcriptional fusions were generated by PCR-amplifying 2 kb fragments upstream of the ATG from genomic DNA using Phusion Flash polymerase (Finnzymes), and introducing them into the pGreenIIKAN:LIC:SV40: 3GFP:NOSt (pPLV04) vec-

tor. Primers used for amplifying promoter fragments are listed in Table 3. All promoter fusion constructs were transformed into wild-type Columbia and *mp-B4149* heterozygous plants by floral dip using the *Agrobacterium* strain GV3101(pSoup).

Microscopy

Differential interference contrast (DIC) microscopy and confocal microscopy were performed as described previously (Llavata *et al.*, 2012), using a Leica DMR microscope or a Zeiss LSM510 confocal microscope, respectively. Plant membranes of embryos and roots were stained using FM4-64 dye (Invitrogen), which is visible as the red signal in confocal pictures.

Acknowledgements

We acknowledge Willy van den Berg and Annemarie S. Lokerse for introducing Ligation Independent Cloning in the laboratory.

Tables

Table 1: List of down-regulated genes in the Q0990>>>bdl microarray on globular stage embryos. List of at least two-fold down-regulated genes from a microarray on early globular stage embryos. MP activity was locally inhibited in these embryos in the inner basal embryo cells that will acquire vascular and ground tissue identity, using the Q0990>>>bdl two component system (see Figure 1). The list shows genes that are significantly down-regulated in all four replicates (p= 0,05). Below the bold line are genes that were less than two-fold down-regulated or down-regulated in less than four replicates. The same experiment was performed with heart stage embryos. For each gene, the fold change in early globular stage embryos (FC glob) and in heart stage embryos (FC heart) is shown. Gene functions were categorized as transcription factors (TF), cell wall remodeling genes (CW), genes involved in signaling (S), degradation (D), cell cycle (CC), auxin signaling (A), cytokinin activation (CK) and ethylene signaling (ETH). Modulation of gene expression was compared to fold-changes in previously performed microarrays on dexamethasone inducible p*RPS5A*-bdl-GR seedlings (FC bdl-GR) and *mp* seedlings (FC *mp*) that were treated with auxin (Chapter 2). Enrichment of gene expression in embryo proper (EP) compared to gene expression in the suspensor (S) is arbitrarily defined as a ratio of absolute gene expression levels in S/EP equal or lower than 0,5. Gene expression levels in embryo proper and suspensor were obtained from a dataset of globular stage embryos from which the suspensor and embryo proper were isolated using Laser Capture Microdissection (LCM) (Le *et al.*, 2010). Genes that were selected to observe their expression (Expr. Obs.?) are shown, as well as closely related genes. * closest homolog. [a]Fold change is not significant (t-test, p>0,05). [b] Only three replicates, not significantly downregulated. [c] Only two replicates, not significantly downregulated. [d] Only one replicate, not significantly downregulated.

AT number	Gene name	Gene func.	FC glob	FC heart	FC bdl-GR	FC *mp*	Enriched in EP/S?	Expr. Obs.?	Closely related
AT1G74500	TMO7	TF	-8,80	-6,46	-2,81	-21,68	Yes		
AT1G05577	unknown, DUF966		-7,78	-2,18	1,10[a]	1,06[a]	Yes	Yes	Yes
AT2G30130	ASL5 (LBD12)	TF	-7,11	-5,98	-1,00[a]	-1,98	Yes	Yes	
AT5G34881	unknown, DUF784		-6,53	1,67[a]					
AT3G11260	WOX5	TF	-5,23	1,32[a]					
AT2G29350	SAG13, alcohol dehydrogenase		-4,98	-1,91	1,12[a]	1,20	Yes		
AT1G29270	unknown		-4,79	1,13[a]	-1,46	-2,20	Yes		
AT5G59760	unknown, DUF1635		-4,67	-2,81	1,08[a]	1,09[a]	No		
AT1G58270	ZW9		-4,29	1,32[a]	-1,04[a]	-86,99	No		
AT4G28720	YUC8	A	-4,09	1,41[a]	1,55[a]	-1,28	Yes	Yes	YUC1
AT2G01420	PIN4	A	-4,08	1,00	-2,81	-1,44	No		
AT2G03830	RGF8, secreted peptide	S	-3,99	1,43[a]	-1,32[a]	-1,25	No		RGF1
AT5G47440	PH/DUF828	S	-3,92	1,09[a]	-1,49[a]	3,98	No		
AT3G48970	copper-binding family protein		-3,45	1,45[a]	-2,49	-6,13	Yes		
AT5G37140	tRNA-splicing endonuclease		-3,33	1,38[a]	1,01[a]	1,26	No		
AT1G56010	NAC1	TF	-3,15	1,45[a]	1,44[a]	-1,76	No		
AT1G80840	WRKY40, class IIa	TF	-3,12	1,01[a]	-1,49[a]	2,30	Yes	Yes	
AT1G77145	unknown, DUF506		-3,09	-1,46[a]					
AT1G37140	MCT1		-3,03	1,29[a]	-1,06[a]	1,19[a]	Yes	Yes	
AT3G04070	NAC47	TF	-3,03	-1,08[a]	1,18[a]	-7,38	No	Yes	
AT5G57760	unknown protein		-3,01	1,36[a]	-1,78	-1,76	Yes		
AT3G19380	PUB25	D	-2,96	-1,87	-1,32[a]	-1,11[a]	No	Yes	PUB22
AT3G56770	bHLH106/TMO5-LIKE2	TF	-2,96	-1,16[a]					
AT2G01430	ATHB17	TF	-2,94	-1,63	-1,56[a]	3,54	No		AtHB31
AT2G21050	LAX2	A	-2,93	1,07[a]	-4,59	-3,34	Yes		
AT5G60810	RGF1, secreted peptide	S	-2,91	-1,19[a]					RGF8
AT2G37210	LOG3, cytokinin-activating enzyme	CK	-2,84	-2,77	-1,39	1,35	Yes		LOG7
AT3G13960	AtGRF5	TF	-2,83	-1,11[a]	1,01[a]	1,88	Yes		
AT3G13857	unknown protein		-2,81	-7,09					
AT3G26760	dehydrogenase		-2,81	-2,92	-3,29	-3,20	Yes		
AT2G18500	OFP7	TF	-2,81	1,48[a]	1,11[a]	1,31	Yes	Yes	OFP8*
AT2G42660	MYB-LIKE, SHAQKYF class	TF	-2,79	-3,00	-1,01[a]	1,06[a]	No	Yes	
AT5G06300	LOG7, cytokinin-activating enzyme	CK	-2,78	-1,56	-1,05[a]	-2,27	Yes		LOG3
AT3G52450	PUB22	D	-2,78	-1,20[a]	-1,29[a]	2,05	No	Yes	PUB25
AT1G76420	CUC3	TF	-2,78	1,35[a]	1,23[a]	1,59	Yes		
AT4G25390	kinase	S	-2,78	1,17[a]	-1,58[a]	-3,48	No		
AT1G16220	PP2C	S	-2,76	-1,16[a]	-1,00[a]	1,26	No		
AT5G05340	peroxidase	CW	-2,75	1,96[a]	1,17[a]	1,33	Yes		
AT1G05370	Sec14-like protein		-2,73	1,52	1,02[a]	1,13[a]	No		
AT1G12610	DDF1 (AP2)	TF	-2,73	1,25[a]	-1,01[a]	1,12[a]	No	Yes	TINYL
AT3G17680	Kinase interacting protein-like		-2,73	-3,06	-1,01[a]	2,45	Yes		
AT5G45480	unknown, DUF594		-2,71	1,14[a]	1,30[a]	-1,97	No		
AT4G37650	SHR	TF	-2,68	-2,26	-1,02[a]	-3,15	Yes		SCL28
AT4G37810	unknown		-2,68	1,30[a]					
AT5G15340	PPR containing protein		-2,68	1,46[a]	1,12[a]	1,14[a]	No		
AT5G28720	unknown		-2,62	1,00[a]	1,20[a]	1,19			
AT3G45450	Protease chaperone-like	D	-2,59	1,21[a]					
AT5G36960	unknown		-2,59	-1,05[a]	-1,06[a]	-1,02[a]	No		
AT1G03220	Extrecellular peptidase	CW	-2,56	-1,33[a]					
AT5G54020	DC1-domain Zn-finger	S	-2,56	-1,41[a]	-1,15[a]	-2,05	No		
AT2G35080	Aminoacyl tRNA synthetase		-2,54	-2,03	-1,05[a]	1,13[a]			
AT1G78860	Lectin	CW	-2,54	-3,59					
AT4G17240	unknown		-2,53	1,13[a]	1,55	-2,30	Yes		
AT3G54920	PMR6, pectate lyase	CW	-2,53	1,19[a]	-1,50	-1,11[a]	Yes		
AT5G67390	unknown		-2,53	-1,58	-1,07[a]	-1,60	Yes		

AT5G19650	OFP8	TF	-2,52	-1,76				Yes	OFP7*
AT1G03840	MGP	TF	-2,50	-1,95	-1,08[a]	-1,55	Yes		
AT2G23050	NPY4	A	-2,45	-3,35	-1,63[a]	-2,85	Yes		
AT5G28640	AN3 (GIF)	TF	-2,44	1,04[a]	-1,13[a]	-3,17	Yes		
AT1G02810	pectinesterase	CW	-2,44	-3,00	-1,02[a]	-14,83	No		
At3g08030	unknown, DUF642	CW	-2,41	1,00	-1,12[a]	-1,71	No		
AT4G32800	TINY-LIKE (AP2)	TF	-2,39	1,50[a]	1,03[a]	-1,01[a]	Yes		DDF1
AT3G62100	IAA30	TF/A	-2,39	-1,25[a]	-3,72	-1,07[a]	No		
AT3G57010	strictosidine synthase		-2,38	-1,72	-1,68	-1,04[a]	Yes		
AT4G02290	AtGH9B13, glycosyl hydrolase	CW	-2,37	-1,63	-1,05[a]	-3,52	Yes		
AT5G48940	RCH1, LRR-kinase	S	-2,37	-4,91	1,06[a]	-2,73	Yes		
AT1G63260	TET10		-2,36	-1,14[a]	1,12[a]	-1,13[a]	Yes	Yes	
AT5G48130	NPH3-like BTB-POZ	D/S	-2,35	-4,13	-1,02[a]	1,02[a]	No		
AT5G59790	unknown, DUF966		-2,35	-2,55					Yes
AT5G51450	RIN3, ubiquitin ligase	D	-2,34	1,14[a]					
AT4G32540	YUC1	A	-2,33	1,15[a]	1,11[a]	1,40	Yes		YUC8
AT4G22860	unknown		-2,33	1,24[a]	1,04[a]	4,63			
AT5G40630	ubiquitin	D	-2,32	-2,04	-1,39[a]	-1,42	Yes		
AT3G25100	CDC45	CC	-2,31	1,33[a]	-1,08[a]	1,26[a]	Yes		
AT2G27240	unknown		-2,30	1,40[a]	-1,01[a]	1,11[a]	No		
AT1G70560	TAA1	A	-2,30	-1,19[a]	1,67	-1,05[a]	Yes		
AT4G10640	IQD16	TF	-2,29	-1,82	-1,04[a]	-1,01[a]	Yes	Yes	IQD15*
AT2G45340	LRR RLK, LRR-IV	S	-2,29	-1,29[a]	1,56[a]	1,52	Yes		
AT1G01480	ACS2, ACC synthase	ETH	-2,28	1,06[a]	1,16[a]	1,07[a]	No		
AT2G28550	TOE1 (AP2)	TF	-2,28	1,24[a]	1,11[a]	1,54	No		
AT2G44660	Glycosyltransferase	CW	-2,28	1,66[a]	1,23[a]	1,08[a]	No		
AT3G62060	Pectinacetylesterase	CW	-2,27	1,25[a]	1,05[a]	1,14[a]	Yes		
AT3G17840	ORK1, RLK, LRR-III	S	-2,27	1,01[a]	-1,05[a]	1,20[a]	No		
AT2G34700	Extensin	CW	-2,24	1,25[a]	1,34[a]	-1,00[a]	No		
AT3G59200	LRR-F-box gene	D	-2,23	-1,05[a]					
AT2G45720	armadillo/beta-catenin repeat	S	-2,23	1,17[a]	-1,02[a]	-3,11	Yes		
AT1G33750	terpene synthase		-2,23	-2,38	-1,04[a]	-1,16[a]	No		
AT2G18340	LEA domain		-2,23	-3,23	1,22[a]	1,31	No		
AT2G25980	jacalin lectin	CW	-2,21	-5,03	-1,05[a]	-15,23	Yes		
AT2G06850	EXGT-A1, hydrolase	CW	-2,20	-1,35[a]	-1,02[a]	-1,79	Yes		
AT4G25240	SKS1, oxidoreductase	CW	-2,20	1,16[a]	1,19[a]	-1,99	Yes		
AT3G16490	IQD26	TF	-2,20	1,08[a]	1,10[a]	3,79	No		IQD15/16
AT4G29360	glycosyl hydrolase	CW	-2,19	1,14[a]	1,13[a]	2,31	Yes		
AT1G28400	unknown		-2,19	-1,87	-1,26[a]	-5,49	Yes		
AT1G18250	ATLP-1, thaumatin-like		-2,19	1,13[a]	1,08[a]	1,57	No		
AT3G16190	isochorismatase hydrolase		-2,18	1,21[a]	1,08[a]	1,75	No		
AT3G15170	CUC1	TF	-2,18	1,63	1,29[a]	1,15[a]	Yes		
AT5G35770	SAP	TF	-2,18	-1,01[a]	1,13[a]	1,30	Yes		
AT5G22860	serine carboxypeptidase	D/S	-2,17	1,26[a]	-2,21	-4,53	Yes		
AT1G53860	remorin		-2,17	-1,17[a]	1,08[a]	1,39	Yes		
AT4G37390	BRU6, GH3-2	A	-2,16	1,13[a]					
AT3G24650	ABI3	TF	-2,16	1,08[a]	1,14[a]	1,22	Yes		
AT4G03292	nucleic acid binding	TF	-2,16	1,29[a]					
AT2G18380	HANL1 (GATA20)	TF	-2,15	-1,13[a]	-1,52	-1,48	Yes		GATA8
AT5G10520	RBK1, Rop-binding kinase	S	-2,15	1,41[a]	-1,30[a]	-1,71	Yes		
AT2G47930	AGP26	CW	-2,14	1,11[a]	-1,05[a]	-1,56	Yes		
AT3G17970	atToc64-III		-2,13	1,41[a]	-1,04[a]	1,84	Yes		
AT4G31150	endonuclease		-2,13	1,44[a]	-1,04[a]	1,34	No		
AT2G17860	pathogenesis-related thaumatin		-2,13	1,19[a]	1,14[a]	1,08[a]	No		
AT3G15720	glycoside hydrolase	CW	-2,13	-2,28	2,80	1,27	Yes		
AT1G23000	heavy-metal-associated domain		-2,12	1,21[a]	1,26[a]	-1,26	No		
AT2G34650	PID	A	-2,11	-1,24[a]	-1,71	-1,69	Yes		
AT4G10630	glutaredoxin		-2,11	1,10[a]					
AT5G02070	kinase-related	S	-2,11	1,09[a]	-1,02[a]	1,11[a]	No		

AT5G48500	unknown protein		-2,10	-1,36[a]	1,27[a]	2,07	Yes		
AT4G19560	CYCT1	CC	-2,10	1,07[a]					
AT1G62420	Unknown, DUF506		-2,09	-1,74					
AT1G11130	SUB (RLK)	K/S	-2,09	1,03[a]	-1,04[a]	1,58	Yes		
AT3G15540	IAA19	TF/A	-2,09	-2,78	-7,32	-2,72	Yes		
AT3G17200	LTR Reverse Trancriptase-Like		-2,09	1,24[a]					
AT2G45190	FIL/YAB1	TF	-2,09	1,44[a]	-1,51	2,34	Yes		
AT4G22010	SKS4, oxidoreductase	CW	-2,08	1,12[a]	-1,07[a]	-1,94	No		
AT2G32280	unknown		-2,08	1,26[a]	-1,32[a]	-1,24	Yes		
AT1G63100	SCL28	TF	-2,08	1,08[a]	-1,16[a]	1,51	Yes		SHR
AT5G28646	WVD2, Microtubule-binding	S	-2,08	-1,74					
AT5G50890	lipase		-2,08	-1,02[a]	-1,28[a]	-1,18[a]	Yes		
AT5G43810	ZLL	S	-2,07	-1,09[a]	1,31[a]	1,30	Yes		
AT1G14440	AtHB31	TF	-2,07	1,55	2,28	2,45	Yes	Yes	AtHB17
AT1G34030	40S ribosomal protein S18		-2,06	1,18[a]	1,02[a]	-1,03[a]	Yes		
AT2G20515	unknown		-2,06	-4,49	-1,13[a]	-4,95	Yes		
AT5G50915	bHLH137	TF	-2,06	1,42[a]	1,35[a]	1,34	Yes	Yes	
AT1G28110	SCPL45, carboxypeptidase	CW	-2,05	-2,32	-1,99	-1,48	Yes		
AT4G07825	unknown		-2,05	1,12[a]					
AT4G23950	Galactose-binding like	CW	-2,04	1,28[a]	1,11[a]	1,81	No		
AT4G00390	GeBP-like transc. regulator	TF	-2,04	-1,51[a]	1,11[a]	1,57	No		
AT4G28100	GPI-anchored protein	CW	-2,04	1,26[a]	1,69	-1,53	Yes		
AT5G62890	AtNAT6, ascorbate transporter		-2,04	-1,01[a]	1,13[a]	1,38	No		
AT2G28510	TMO6-LIKE2 (Dof2.1)	TF	-2,03	1,99	-1,45[a]	-2,61	Yes	Yes	
AT5G55480	SVL1, phosphoric diester hydrolase		-2,03	1,01[a]	1,11[a]	1,14[a]	No		
AT5G01910	mannase	CW	-2,02	1,26[a]	1,21[a]	1,34	Yes		
AT2G28790	osmotin-like		-2,02	-1,18[a]	-1,35[a]	-1,93	No		
AT5G47230	ERF5 (AP2)	TF	-2,02	-1,65	-1,67	1,21	Yes	Yes	
AT1G04670	unknown		-2,01	-1,11[a]	1,06[a]	1,09[a]	No		
AT1G70510	KNAT2	TF	-2,01	-3,80	-1,03[a]	1,30	Yes	Yes	
AT3G29300	unknown		-2,00	1,04[a]	-1,05[a]	-1,00[a]	Yes		
AT3G16130	ROP-GEF13		-10,4[c]	1,59[a]	1,13[a]	1,35	No	Yes	
AT1G25310	MEE8 (bHLH108)	TF	-9,67[d]	-1,02[a]				Yes	
AT1G77730	pleckstrin homology domain		-8,13[c]	-1,58[a]	1,28[a]	-1,02[a]	Yes	Yes	
AT1G67520	lectin kinase		-6,17[c]	-2,33[a]				Yes	
AT1G32770	NAC12	TF	-6,05[c]	-1,02[a]	1,20[a]	1,07[a]	No	Yes	
AT2G24430	NAC38	TF	-4,36[d]	1,01[a]	1,22[a]	1,11[a]	Yes	Yes	CUC1
AT1G70250	receptor serine/threonine kinase	S	-4,21[c]	2,36[a]	1,06[a]	1,04[a]	Yes	Yes	
AT1G56030	Ubiquitin ligase	D	-3,80[c]	-2,40[a]	1,23[a]	1,08[a]	No	Yes	
AT5G44460	CML43	S	-3,60[c]	3,98[a]	1,26[a]	3,00	No	Yes	
AT3G49380	IQD15	TF	-3,12[b]	-1,88	-1,04[a]	1,02[a]	Yes	Yes	IQD16*
AT3G54810	BME3 (GATA8)	TF	-2,79[c]	1,44[a]	-1,10[a]	1,06[a]	No	Yes	GATA20
AT4G33880	bHLH85	TF	-2,75[c]	-1,50				Yes	
AT2G31215	bHLH138	TF	-2,44[c]	1,20[a]				Yes	
AT4G36930	SPT (bHLH24)	TF	-1,73	-1,19[a]	-1,65	9,56	No	Yes	
AT2G30590	WRKY21, class IId	TF	-1,72	-2,00	1,25[a]	-1,12[a]	No	Yes	WRKY17
AT2G24570	WRKY17, class IId	TF	-1,69	-1,28[a]	1,05[a]	-1,57	No	Yes	WRKY21
AT4G39410	WRKY13, class IIc	TF	-1,68[a]	-1,22[a]	1,07[a]	1,28	No	Yes	
AT4G00210	LBD31	TF	-1,63	-1,25[a]				Yes	

Table 2: Expression pattern analysis of putative MP target genes involved in root initiation. Schematic overview of embryo and root expression analysis of 37 putative MP target genes. Expression was visualized using transcriptional fusions consisting of 2 kb promoter fragments upstream of the ATG and nuclear localized triple GFP, and a confocal microscope. For simplicity, only expression in globular and heart stage embryos is shown. * Expression in apical embryo region. [a] Expression in L1 layer SAM. [b] no expression in root meristem but expression in differentiation zone of the root. [c] only lateral root cap and/or columella expression. [d] weak expression in root meristem and

stronger expression in differentiation zone. [e] very strong expression in vasculature of the root meristem. n.a., not analyzed. var, variable expression patterns between independently transformed lines of the same construct.

AT number	Gene name	Observed expression pattern in the embryo								Expression observed in postembryonic root meristem?
		Globular-stage				Heart-stage				
		hyp	VSC	GSC	ep	qc	vas	gt	ep	
A. Ubiquitous expression in globular stage embryo										
AT1G63260	*TET10*	X	X	X	X	X	X	X	X	n.a.
AT2G30590	*WRKY21*	X	X	X	X	X	X	X	X	X
B. Expression in VSC and GSC of globular stage embryo										
AT1G37140	*MCT1*		X	X						?
AT3G19380	*PUB25*	X	X	X	X	X	X	X	X	X
AT4G36930	*SPT (bHLH24)*		X	X	X	X	X	X	X	X
C. Expression in VSC of globular stage embryo										
AT1G05577	*DUF966*		X			X	X			X
AT3G49380	*IQD15*		X			X	X			X
D. Expression in GSC of globular stage embryo										
AT2G42660	*MYB-LIKE*	X		X		X		X		X
AT5G19650	*OFP8*	X		X		X		X		X
AT1G70250	Receptor kinase			X				X		X
E. Expression in hypophysis and epidermis										
AT3G54810	*GATA8*	X			X				X	X
AT4G10640	*IQD16*	X	X	X	X	X			X	n.a.
AT3G52450	*PUB22*	X			X	X			X	X
AT2G24570	*WRKY17*	X		X	X	X		X	X	X
F. Expression in apical embryo region										
AT1G14440	*ATHB31*				X*		X*		X*	n.a.
AT2G28510	*Dof2.1*						X*			X
AT1G70510	*KNAT2*								X*[a]	no
AT4G00210	*LBD31*								X*	X
G. Expression in differentiated columella cells of the torpedo stage embryo										
AT4G28720	*YUCCA8*									X[c]
H. Variable embryo expression among independently transformed plant lines										
AT4G33880	*bHLH85*	Variable expression pattern								X
AT5G50915	*bLH137 nakijken*	Variable expression pattern								?
AT2G31215	*bHLH138*	Variable expression pattern								no
AT3G04070	*NAC47*	Variable expression pattern								X[d]
I. No embryo expression observed										
AT5G44460	*CML43*	No expression								X
AT1G12610	*DDF1*	No expression								no
AT5G47230	*ERF5*	No expression								var
AT2G30130	*LBD12*	No expression								X[e]
AT1G67520	Lectin kinase	No expression								X[c]
AT1G25310	*MEE8 (bHLH108)*	No expression								n.a.
AT1G32770	*NAC12*	No expression								no[b]
AT2G24430	*NAC38*	No expression								no
AT2G18500	*OFP7*	No expression								X[d]
AT1G77730	PH domain	No expression								var
AT3G16130	*ROP-GEF13*	n.a.								no
AT1G56030	Ubiquitin ligase	No expression								no[b]
AT4G39410	*WRKY13*	No expression								no[b]
AT1G80840	*WRKY40*	No expression								n.a.

Table 3: Primers used for Ligation Independent Cloning

AT number	Gene name	Forward and reverse primer used for LIC cloning
AT1G14440	*ATHB31*	TAGTTGGAATGGGTTCGAAAACACATAACTTTCGATCCT TTATGGAGTTGGGTTCGAACTTTTTTAATTGGGTCTTCT

AT4G33880	*bHLH85*	TAGTTGGAATGGGTTCGAATTATTTTATCCATGGAACTTG TTATGGAGTTGGGTTCGAATTTTATATGTTTTGTTAACT
AT5G50915	*bLH137*	TAGTTGGAATGGGTTCGAATCTTAGAGTGAAGTAATGTA TTATGGAGTTGGGTTCGAAGAGAGAAGATTAAGGACTTG
AT2G31215	*bHLH138*	TAGTTGGAATGGGTTCGAATTGTTCAGAAGAAGAAGATC TTATGGAGTTGGGTTCGAAGAAGATGGTTCAATACTCTA
AT5G44460	*CML43*	TAGTTGGAATGGGTTCGAAAAACATGTAAATTTCATCGA TTATGGAGTTGGGTTCGAATGTTACTCTTCTTCTTAGTT
AT1G12610	*DDF1*	TAGTTGGAATGGGTTCGAAGTTTTTGAACAAAATAATCTTAAC TTATGGAGTTGGGTTCGAAAACTCAAAGTACCAAAAATTC
AT2G28510	*Dof2.1*	TAGTTGGAATGGGTTCGAAgcaagctcgctcatttcg TTATGGAGTTGGGTTCGAACCATGTAACAAAGGATCGAA
AT1G05577	*DUF966*	TAGTTGGAATGGGTTCGAACGTTCCGTGGTGAATCAATG TTATGGAGTTGGGTTCGAACTCTCTTTCTTTTTGTTTTGGTCT
AT5G47230	*ERF5*	TAGTTGGAATGGGTTCGAATCTCTGATTTGCTATATCAT TTATGGAGTTGGGTTCGAATGATAAAATTTTCAAAAAGC
AT3G54810	*GATA8*	TAGTTGGAATGGGTTCGAAtttacatttcttaattatc TTATGGAGTTGGGTTCGAAGTTTTACAATTATTGCAAGT
AT3G49380	*IQD15*	TAGTTGGAATGGGTTCGAAGTTTGCGATGGTAATTCTCT TTATGGAGTTGGGTTCGAACAAGATCGATCAACCTCGTC
AT4G10640	*IQD16*	TAGTTGGAATGGGTTCGAAGATCTACCAAGATCGAACAA TTATGGAGTTGGGTTCGAAATTGAATTAACGTTTTCTAAAAGC
AT1G70510	*KNAT2*	TAGTTGGAATGGGTTCGAATTTAGTATAGTAATCTCAAA TTATGGAGTTGGGTTCGAATAATGTGATCGTAGTGAGAT
AT2G30130	*LBD12*	TAGTTGGAATGGGTTCGAAtttaccatggttttgtctta TTATGGAGTTGGGTTCGAACTTCTACTATGATCGTGATT
AT4G00210	*LBD31*	TAGTTGGAATGGGTTCGAAtttcacaaatatttgaactt TTATGGAGTTGGGTTCGAACTTTTATGTCAAAGACGTAA
AT1G67520	Lectin kinase	TAGTTGGAATGGGTTCGAAAACAAAGAACAGAACAGAAG TTATGGAGTTGGGTTCGAAAGTTTCAGAAAGATGGATGA
AT1G37140	*MCT1*	TAGTTGGAATGGGTTCGAAGTTTTATGTTTCATGATGAT TTATGGAGTTGGGTTCGAAGGAAGCTAAAGAAACTAGGA
AT1G25310	*MEE8 (bHLH108)*	TAGTTGGAATGGGTTCGAATCTATATGTATTTGATTAAA TTATGGAGTTGGGTTCGAATCTTTTGATAGTTTTAAGTG
AT2G42660	*MYB-LIKE*	TAGTTGGAATGGGTTCGAAAGGAATTGTGAATGAAGTGTC TTATGGAGTTGGGTTCGAAGTCTCTCCGGCGAGAGTGTCTTT
AT1G32770	*NAC12*	TAGTTGGAATGGGTTCGAATCTTCTACATAACGATTTCT TTATGGAGTTGGGTTCGAATAACGAAGATAGCAATATAT
AT2G24430	*NAC38*	TAGTTGGAATGGGTTCGAATGATTATATATTACGTTTAT TTATGGAGTTGGGTTCGAATTTATATGATCTTTAGTTTA
AT3G04070	*NAC47*	TAGTTGGAATGGGTTCGAAAAGAAAACGTTAACTAGATC TTATGGAGTTGGGTTCGAATGTTTAAAGGAATGATATTT
AT2G18500	*OFP7*	TAGTTGGAATGGGTTCGAAtatttttaatgattaaacga TTATGGAGTTGGGTTCGAATTTTTTTTCTTTTCTTGTTT
AT5G19650	*OFP8*	TAGTTGGAATGGGTTCGAAagatatttagtctcttgctt TTATGGAGTTGGGTTCGAAGTTTAGAGAATATCGAGAGA
AT1G77730	PH domain	TAGTTGGAATGGGTTCGAAATTTCTTCAGATTGTACCAT TTATGGAGTTGGGTTCGAATGTTTGAAAACGTTCGAAGA
AT3G52450	*PUB22*	TAGTTGGAATGGGTTCGAACTTGGTCATGATTCTGGTCG TTATGGAGTTGGGTTCGAATTGACCCGCTCGAAAATATGAAAA
AT3G19380	*PUB25*	TAGTTGGAATGGGTTCGAATAAATAGAGACTATTTTCAT TTATGGAGTTGGGTTCGAATAAGAAACTTGAGAAACAGA
AT1G70250	Receptor kinase	TAGTTGGAATGGGTTCGAATCTACCGTCTCTAGCCCTGA TTATGGAGTTGGGTTCGAATTTTCTTTCTTGGTAAATGGTAATG
AT3G16130	*ROP-GEF13*	TAGTTGGAATGGGTTCGAATCAATAATCCATTAGATATGG TTATGGAGTTGGGTTCGAATTCCATGATTTTCTTAAATC
AT4G36930	*SPT (bHLH24)*	TAGTTGGAATGGGTTCGAATGCATATGTATTACGGAAAC TTATGGAGTTGGGTTCGAATACACCAACAACAAAAAAAAAGC
AT1G63260	*TET10*	TAGTTGGAATGGGTTCGAAATCTTCACAGTACCGTTTAT TTATGGAGTTGGGTTCGAATTTTTCAAGGTTGTTGCTTT
AT1G56030	Ubiquitin ligase	TAGTTGGAATAGGTTCATGGTGAAAAACTCCTATGTA AGTATGGAGTTGGGTTCTCAACGTCCCAACTCCTCAA
AT4G39410	*WRKY13*	TAGTTGGAATGGGTTCGAActtctaaatggataatgaaa TTATGGAGTTGGGTTCGAACTCGCAAAAGCTTGACGAAG

AT2G24570	*WRKY17*	TAGTTGGAATAGGTTCATGACCGTTGATATTATGCG AGTATGGAGTTGGGTTCTCAAGCCGAACCAAACACCA
AT2G30590	*WRKY21*	TAGTTGGAATGGGTTCGAAcaccaatatctagtattgga TTATGGAGTTGGGTTCGAACTAAGAACCCTAATTTTTTC
AT1G80840	*WRKY40*	TAGTTGGAATGGGTTCGAAaattcgaatatcaaatataa TTATGGAGTTGGGTTCGAAGTAAATATATGTAGGATGAA
AT4G28720	*YUCCA8*	TAGTTGGAATGGGTTCGAATATAATATTTTCTCTAATAT TTATGGAGTTGGGTTCGAATCTTTTTTTATAAGTTTCTT

References

Abel S, Savchenko T and Levy M. (2005). Genome-wide comparative analysis of the *IQD* gene families in *Arabidopsis thaliana* and *Oryza sativa*. BMC Evol Biol. 5: 72.

Aida M, Beis D, Heidstra R, Willemsen V, Blilou I, Galinha C, Nussaume L, Noh YS, Amasino R and Scheres B. (2004). The *PLETHORA* genes mediate patterning of the Arabidopsis root stem cell niche. Cell. 119(1): 109-120.

Amador V, Monte E, García-Martínez JL and Prat S. (2001). Gibberellins signal nuclear import of PHOR1, a photoperiod-responsive protein with homology to Drosophila armadillo. Cell. 106(3): 343-354.

Alvarez J and Smyth DR. (1999). *CRABS CLAW* and *SPATULA*, two Arabidopsis genes that control carpel development in parallel with *AGAMOUS*. Development. 126(11): 2377-2386.

Anderson GH, Alvarez ND, Gilman C, Jeffares DC, Trainor VC, Hanson MR and Veit B. (2004). Diversification of genes encoding mei2-like RNA binding proteins in plants. Plant Mol Biol. 54(5): 653-70.

Brady SM, Orlando DA, Lee JY, Wang JY, Koch J, Dinneny JR, Mace D, Ohler U and Benfey PN. (2007). A high-resolution root spatiotemporal map reveals dominant expression patterns. Science. 318(5851): 801-806.

Cheng Y, Dai X and Zhao Y. (2007). Auxin synthesized by the *YUCCA* flavin monooxygenases is essential for embryogenesis and leaf formation in Arabidopsis. Plant Cell. 19(8): 2430-2439.

Cho SK, Ryu MY, Song C, Kwak JM and Kim WT. (2008). Arabidopsis PUB22 and PUB23 are homologous U-Box E3 ubiquitin ligases that play combinatory roles in response to drought stress. Plant Cell. 20(7): 1899-914.

Coates JC. (2003). Armadillo repeat proteins: beyond the animal kingdom. Trends Cell Biol. 13(9): 463-471.

Cole M, Chandler J, Weijers D, Jacobs B, Comelli P and Werr W. (2009). *DORNRÖSCHEN* is a direct target of the auxin response factor MONOPTEROS in the Arabidopsis embryo. Development. 136(10): 1643-1651

De Rybel B, van den Berg W, Lokerse A, Liao CY, van Mourik H, Möller B, Peris CL and Weijers D. (2011). A versatile set of ligation-independent cloning vectors for functional studies in plants. Plant Physiol. 156(3): 1292-1299.

Di Laurenzio L, Wysocka-Diller J, Malamy JE, Pysh L, Helariutta Y, Freshour G, Hahn MG, Feldmann KA and Benfey PN. (1996). The *SCARECROW* gene regulates an asymmetric cell division that is essential for generating the radial organization of the Arabidopsis root. Cell. 86(3): 423-433.

Donner TJ, Sherr I and Scarpella E. (2009). Regulation of preprocambial cell state acquisition by auxin signaling in Arabidopsis leaves. Development. 136(19): 3235-3246.

Friml J, Vieten A, Sauer M, Weijers D, Schwarz H, Hamann T, Offringa R and Jürgens G. (2003). Efflux-dependent auxin gradients establish the apical-basal axis of Arabidopsis. Nature. 426(6963): 147-153.

Galinha C, Hofhuis H, Luijten M, Willemsen V, Blilou I, Heidstra R and Scheres B. (2007). PLETHORA proteins as dose-dependent master regulators of Arabidopsis root development. Nature. 449(7165): 1053-1057.

Gish LA and Clark SE. (2011). The RLK/Pelle family of kinases. Plant J. 66(1):117-127

Groszmann M, Bylstra Y, Lampugnani ER and Smyth DR. (2010). Regulation of tissue-specific expression of *SPATULA*, a bHLH gene involved in carpel development, seedling germination, and lateral organ growth in Arabidopsis. J Exp Bot. 61(5): 1495-1508.

Hamann T, Benkova E, Bäurle I, Kientz M and Jürgens G. (2002). The Arabidopsis *BODENLOS* gene encodes an auxin response protein inhibiting MONOPTEROS-mediated embryo patterning. Genes Dev. 16(13): 1610-1615.

Hardtke CS, Ckurshumova W, Vidaurre DP, Singh SA, Stamatiou G, Tiwari SB, Hagen G, Guilfoyle TJ and Berleth T. (2004). Overlapping and non-redundant functions of the Arabidopsis auxin response factors MONOPTEROS and NONPHOTOTROPIC HYPOCOTYL 4. Development. 131(5): 1089-1100.

Helariutta Y, Fukaki H, Wysocka-Diller J, Nakajima K, Jung J, Sena G, Hauser MT and Benfey PN. (2000). The *SHORTROOT* gene controls radial patterning of the Arabidopsis root through radial signaling. Cell. 101(5): 555-567.

Kuroha T, Tokunaga H, Kojima M, Ueda N, Ishida T, Nagawa S, Fukuda H, Sugimoto K and Sakakibara H. (2009). Functional analyses of LONELY GUY cytokinin-activating enzymes reveal the importance of the direct activation pathway in Arabidopsis. Plant Cell. 21(10): 3152-3169.

Le BH, Cheng C, Bui AQ, Wagmaister JA, Henry KF, Pelletier J, Kwong L, Belmonte M, Kirkbride R, Horvath S, Drews GN, Fischer RL, Okamuro JK, Harada JJ and Goldberg RB. (2010). Global analysis of gene activity during Arabidopsis seed development and identification of seed-specific transcription factors. Proc Natl Acad Sci U S A. 107(18): 8063-8070.

Llavata-Peris CI, Lokerse AS, Möller B, De Rybel B and Weijers D. (2012). Imaging of phenotypes, gene expression and protein localization during embryonic root formation in Arabidopsis. Meth Mol Biol. *in press*.

Matsuzaki Y, Ogawa-Ohnishi M, Mori A and Matsubayashi Y. (2010). Secreted peptide signals required for maintenance of root stem cell niche in Arabidopsis. Science. 329(5995): 1065-1070.

Megraw M, Baev V, Rusinov V, Jensen ST, Kalantidis K and Hatzigeorgiou AG. (2006). MicroRNA promoter element discovery in Arabidopsis. RNA. 12(9): 1612-9.

Rademacher EH, Möller B, Lokerse AS, Llavata-Peris CI, van den Berg W and Weijers D. (2011). A cellular expression map of the Arabidopsis *AUXIN RESPONSE FACTOR* gene family. Plant J. 68(4): 597-606.

Riechmann JL, Heard J, Martin G, Reuber L, Jiang C, Keddie J, Adam L, Pineda O, Ratcliffe OJ, Samaha RR, Creelman R, Pilgrim M, Broun P, Zhang JZ, Ghandehari D, Sherman BK and Yu G. (2000). Arabidopsis transcription factors: genome-wide comparative analysis among eukaryotes. Science. 290(5499): 2105-2110.

Sabatini S, Heidstra R, Wildwater M and Scheres B. (2003). SCARECROW is involved in positioning the stem cell niche in the Arabidopsis root meristem. Genes Dev. 17(3): 354-358.

Sarkar AK, Luijten M, Miyashima S, Lenhard M, Hashimoto T, Nakajima K, Scheres B, Heidstra R and Laux T. (2007). Conserved factors regulate signalling in *Arabidopsis thaliana* shoot and root stem cell organizers. Nature. 446(7137): 811-814.

Scheres B, Wolkenfelt H, Willemsen V, Terlouw M, Lawson E, Dean and Weisbeek P. (1994). Embryonic origin of the Arabidopsis primary root and root meristem initials. Development. 120(9): 2475-2487

Scheres B, Di Laurenzio L, Willemsen V, Hauser MT, Janmaat K, Weisbeek P and Benfey P. (1995). Mutations affecting the radial organization of the Arabidopsis root display defects throughout the embryonic axis. Development 121: 53-62

Shiu SH and Bleecker AB. (2003). Expansion of the receptor-like kinase/Pelle gene family and receptor-like proteins in Arabidopsis. Plant Physiol. 2003 Jun;132(2):530-543.

Smyth GK. (2004). Linear models and empirical bayes methods for assessing differential expression in microarray experiments. Stat Appl Genet Mol Biol. 3: Article3.

Staswick PE, Serban B, Rowe M, Tiryaki I, Maldonado MT, Maldonado MC and Suza W. (2005). Characterization of an Arabidopsis enzyme family that conjugates amino acids to indole-3-acetic acid. Plant Cell. 17(2): 616-627.

Stepanova AN, Robertson-Hoyt J, Yun J, Benavente LM, Xie DY, Dolezal K, Schlereth A, Jürgens G and Alonso JM. (2008). TAA1-mediated auxin biosynthesis is essential for hormone crosstalk and plant development. Cell. 133(1): 177-191.

Takada S and Jürgens G. (2007). Transcriptional regulation of epidermal cell fate in the Arabidopsis embryo. Development. 134(6): 1141-1150.

Tao Y, Ferrer JL, Ljung K, Pojer F, Hong F, Long JA, Li L, Moreno JE, Bowman ME, Ivans LJ, Cheng Y, Lim J, Zhao Y, Ballaré CL, Sandberg G, Noel JP and Chory J. (2008). Rapid synthesis of auxin via a new tryptophan-dependent pathway is required for shade avoidance in plants. Cell. 133(1): 164-176.

Tiwari SB, Wang XJ, Hagen G and Guilfoyle TJ. (2001). AUX/IAA proteins are active repres-

sors, and their stability and activity are modulated by auxin. Plant Cell. 13(12): 2809-2822.

Tokunaga H, Kojima M, Kuroha T, Ishida T, Sugimoto K, Kiba T and Sakakibara H. (2011). Arabidopsis lonely guy (LOG) multiple mutants reveal a central role of the LOG-dependent pathway in cytokinin activation. Plant J. doi: 10.1111/j.1365-313X.2011.04795.x.

Ugartechea-Chirino Y, Swarup R, Swarup K, Péret B, Whitworth M, Bennett M and Bougourd S. (2010). The *AUX1 LAX* family of auxin influx carriers is required for the establishment of embryonic root cell organization in *Arabidopsis thaliana*. Ann Bot. 105(2): 277-289.

Van den Berg C, Willemsen V, Hendriks G, Weisbeek P and Scheres B. (1997). Short-range control of cell differentiation in the Arabidopsis root meristem. Nature. 390(6657): 287-289.

Wang X, Zafian P, Choudhary M and Lawton M. (1996). The PR5K receptor protein kinase from Arabidopsis thaliana is structurally related to a family of plant defense proteins. Proc Natl Acad Sci U S A. 93(6): 2598-2602.

Weigel D and Jürgens G. (2002). Stem cells that make stems. Nature. 415(6873): 751-754.

Weijers D, Schlereth A, Ehrismann JS, Schwank G, Kientz M and Jürgens G. (2006). Auxin triggers transient local signaling for cell specification in Arabidopsis embryogenesis. Dev Cell. 10(2): 265-270.

Wellmer F, Riechmann JL, Alves-Ferreira M and Meyerowitz EM. (2004). Genome-wide analysis of spatial gene expression in Arabidopsis flowers. Plant Cell. 16(5): 1314-1326.

Whitford R, Fernandez A, De Groodt R, Ortega E and Hilson P. (2008). Plant CLE peptides from two distinct functional classes synergistically induce division of vascular cells. Proc Natl Acad Sci U S A. 105(47): 18625-30.

Widelitz R. (2005). Wnt signaling through canonical and non-canonical pathways: recent progress. Growth Factors. 23(2): 111-116.

Winter D, Vinegar B, Nahal H, Ammar R, Wilson GV and Provart NJ. (2007). An "Electronic Fluorescent Pictograph" browser for exploring and analyzing large-scale biological data sets. PLoS One. 2(8): e718.

Wysocka-Diller JW, Helariutta Y, Fukaki H, Malamy JE and Benfey PN. (2000). Molecular analysis of SCARECROW function reveals a radial patterning mechanism common to root and shoot. Development. 127(3): 595-603.

Xiang D, Venglat P, Tibiche C, Yang H, Risseeuw E, Cao Y, Babic V, Cloutier M, Keller W, Wang E, Selvaraj G and Datla R. (2011). Genome-wide analysis reveals gene expression and metabolic network dynamics during embryo development in Arabidopsis. Plant Physiol. 156(1): 346-356.

Zhou W, Wei L, Xu J, Zhai Q, Jiang H, Chen R, Chen Q, Sun J, Chu J, Zhu L, Liu CM and Li C. (2010). Arabidopsis Tyrosylprotein sulfotransferase acts in the auxin/PLETHORA pathway in regulating postembryonic maintenance of the root stem cell niche. Plant Cell. 22(11): 3692-7309.

Chapter 5

Early events in ground tissue formation in the Arabidopsis embryo are controlled by MONOPTEROS

Barbara Möller[1], Saiko Yoshida[1], Ikram Blilou[2] and Dolf Weijers[1]

[1]Laboratory of Biochemistry, Wageningen University, Dreijenlaan 3, 6703HA Wageningen, the Netherlands

[2]Molecular Genetics, Department of Biology, Faculty of Science, Utrecht University, Padualaan 8, 3584 CH Utrecht, The Netherlands

Abstract

The transcription factor MONOPTEROS (MP) is required to initiate the embryonic root in *Arabidopsis thaliana*. Root initiation involves the coordinated specification of tissues, stem cells and organizer cells in the root meristem. Recently, we showed that MP transcriptionally activates a *Receptor Like Kinase (RLK)* gene that is specifically expressed in the first ground tissue cells of the embryonic root meristem. This suggests that MP may be one of the elusive regulators of ground tissue initiation. Here, we further explore a potential role for MP in the embryonic ground tissue and show that MP is required for the asymmetric division of the first ground tissue cells in the early embryo. In contrast, the well-studied transcription factor SHORTROOT (SHR) regulates later cell divisions in ground tissue daughter cells to create distinct endodermis and cortex tissues. Moreover, MP activates *RLK* expression in a SHR-independent pathway. These results suggest that MP is initially required in embryonic ground tissue cells, while SHR acts later. Furthermore, our data suggest that MP activates *SHR* expression in the embryo. We show that several *SHR* homologs are co-expressed with SHR protein in the embryonic root meristem, which opens the possibility that SHR acts redundantly with these homologs to mediate MP-dependent specification of the first ground tissue cells.

Introduction

Vascular land plants have a characteristic radial arrangement of tissues in the root. Specification of these root tissues in a spatially and timely coordinated manner is crucial for plant growth. The establishment of this radial organization occurs during early embryo development, when the root meristem is initiated in the basal half of the embryo. Around the 16-cell stage of Arabidopsis embryogenesis, one cell is specified as precursor of the organizer cells of the root meristem, while other cells obtain tissue and stem cell identity, depending on their position. The organizer cells of the root meristem are called the quiescent center (QC), and have been shown to be required for stem cell maintenance (Van den Berg *et al.*, 1997). Stem cells surround the QC and produce daughter cells that will be incorporated in one of the different root tissues. Ground tissue is the middle one of three main root tissues in the proximal root meristem. It surrounds the vascular tissue and is enclosed by the epidermis. The first ground tissue cells of the embryonic root, which are closest to the QC, divide anticlinally (new cell wall perpendicular to embryo surface) at early globular stage to produce daughter cells. These daughter cells in turn divide periclinally (new cell wall parallel to embryo surface) around early heart stage of embryo development to generate separate endodermis and

cortex cell files that are collectively called ground tissue (Scheres *et al.*, 1994). Patterning of the ground tissue requires the activity of GRAS family transcription factors SHORTROOT (SHR) and SCARECROW (SCR). These are indispensable for the periclinal division of ground tissue daughter cells at heart stage of embryogenesis that generates separate endodermis and cortex layers (Benfey *et al*., 1993; Scheres *et al*., 1995, Di Laurenzio *et al.*, 1996). In agreement with this, SHR directly activates a *CyclinD6* gene that is specifically expressed in ground tissue daughter cells and is involved in the periclinal division (Sozzani *et al.*, 2010). SHR is also required for endodermis identity, illustrated by loss of endodermis identity in *shr* mutants, and the ability of SHR to ectopically induce endodermal fate in the epidermis (Helariutta *et al.*, 2000; Levesque *et al.*, 2006). SCR is required for asymmetry of division of ground tissue daughter cells, but not for the division itself (Heidstra *et al.*, 2004). Both *SHR* and *SCR* are expressed during embryogenesis from globular stage on (Wysocka-Diller *et al.*, 2000; Helariutta *et al.*, 2000). *SHR* is expressed in the stele but SHR protein moves into the adjacent endodermis and QC, where it interacts with SCR in the nucleus and activates *SCR* expression (Nakajima *et al.*, 2001; Sena *et al.*, 2004; Cui *et al.*, 2007). SCR keeps SHR in the nucleus, and thereby prevents further movement of SHR protein outside the endodermis (Cui *et al.*, 2007).

Besides the involvement of SHR and SCR, very little is known about embryonic ground tissue specification. So far, it is an open question what mechanisms control the initial specification of the first ground tissue cells in the early embryo. None of the plant hormones, including auxin, has been implicated in this specification step. The transcription factor MONOPTEROS (MP) is the main executer of auxin signaling in the embryo, and acts by regulating auxin response genes (reviewed in Chapter 1). It is involved in many aspects of embryonic root initiation, including specification of the precursor cell of the QC, and vascular stem cell specification (Chapters 2&3). We previously performed a microarray on embryos in which MP was locally inhibited in the first vascular and ground tissue cells of the early embryo (Chapter 4). We showed that a member of the *Receptor Like Kinase (RLK)* family, hereafter called *RLK*, is specifically expressed in the first ground tissue cells of the root meristem in the early embryo. Moreover, we showed that MP activates expression of this *RLK*, indicating that MP activity is required to promote gene expression in the first ground tissue cells. Here we further explore if MP is required in the first ground tissue cells in the early embryo, and show that MP activation of *RLK* does not depend on SHR activity. We found that MP but not SHR is required for the asymmetric anticlinal division of the first ground tissue cells in the early embryo. Furthermore, our data suggest that MP transcriptionally activates *SHR* and several homologous GRAS family genes that we found to be

expressed in the early embryo. We speculate that SHR and its homologs redundantly act downstream of MP to specify the first ground tissue cells in the early embryo. In conclusion, we show that MP is required to promote transcription and anticlinal divisions in the first ground tissue cells of the embryonic root meristem in a SHR-independent pathway.

Results

MP is required for the asymmetric division of the first ground tissue cells in the early embryo. During normal embryo development, the first vascular and ground tissue cells divide anticlinally to produce daughter cells for these tissues that will be incorporated into the root (Figure 1a). To determine if MP is involved in this first division, we examined early *mp* mutant embryos displaying aberrant hypophysis division. In these embryos, the first vascular cells frequently divided periclinally instead of anticlinally (Figure 1b, Table 1), as described in Chapter 3. Remarkably, we also found many *mp* embryos in which the first ground tissue cells divided abnormally (Figure 1c). In most cases, the ground tissue cells divided periclinally instead of anticlinally, but oblique divisions were also observed. In total, these aberrant ground tissue divisions were observed in ~50% of mutant embryos, in two independent *mp* alleles (Table 1). Since in our analyses, ground tissue cell division is always preceded by vascular cell division, it is possible that ground tissue cell division defects are a secondary consequence of a division defect in the adjacent vascular cell. We therefore investigated if aberrant divisions in vascular and ground tissue cells are correlated. We found all possible combinations of division defects: sometimes only the first vascular or ground tissue cells divided aberrantly (Figure 1b, c), while in other cases cells of both tissues showed division defects (Figure 1d). However, it should be noted that in this two-dimensional analysis, not all vascular and ground tissue cells of a given embryo can be observed. Therefore, even though there does not appear to be a correlation between ground tissue and vascular defects, more complex 3-dimensional correlations may exist. To exclude non cell-autonomous effects of MP outside of the ground tissue and vascular cells, we analyzed early embryos in which MP was locally inhibited in the first vascular and ground tissue cells, and found similar division defects in the ground tissue cells (Figure 1e). This suggests that MP activity is required in vascular or ground tissue cells to promote the asymmetric division of the first ground tissue cells. Previously, we showed that *RLK* expression in the first ground tissue cells is MP-dependent (Chapter 4). Together with the above results, this suggests that MP is required for the specification and subsequent division of the first ground tissue cells.

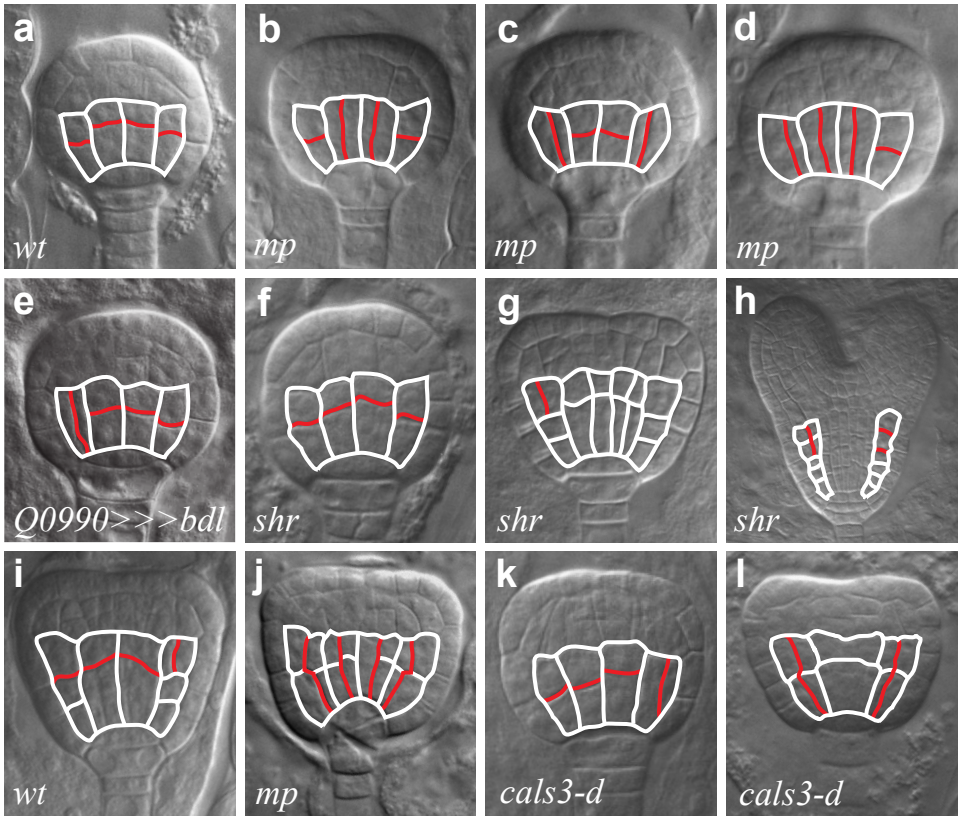

Figure 1. Aberrant vascular and ground tissue cell divisions in *mp*, *shr* and *cals3-d* mutant embryos. a, In wild-type globular stage embryos, both the hypophyis and first vascular and ground tissue cells divide transversally and asymmetrically. b-d, In *mp* mutant embryos showing abnormal hypophysis division, the first vascular and ground tissue cells frequently divide longitudinally instead of transversally. e, When MP activity is locally inhibited in the first vascular and ground tissue cells using the Q0990>>>bdl two component system (for details see Chapter 4), these cells often divide transversally. f-h, In *shr* mutant embryos, frequent division defects in the ground tissue layer are observed at heart stage, when the single ground tissue layer does not divide into seperate endodermal and cortex layers. Note that in this embryo, one side shows periclinal divisions in the ground tissue layer as in wild-type, while the other side shows the characteristic *shr* defect. i, In wild-type transition stage embryos, daughter cells of the first ground tissue cells divide longitudinally to separate the endodermis and cortex layer. j, In transition stage *mp* mutant embryos, the first ground tissue cell frequently divides abberrantly after a first correct, transverse division. k-l, Aberrant ground tissue cell divisions in *cals3-d* mutants at globular (k) and transition (l) stage of embryogenesis are identical to those in *mp* mutants.

SHORTROOT acts after the initial MP-dependent ground tissue formation

We next examined early embryos mutant for *SHR*, because of its role in endodermis specification from heart stage of embryogenesis on (Scheres *et al.*, 1995). In

shr mutants, the first vascular and ground tissue cells divided normally in globular and transition stage embryos (Figure 1f, g). The earliest defects were observed at heart stage, when ground tissue daughter cells fail to divide periclinally to separate endodermis and cortex layers (Figure 1h). It should be noted that, under our growth conditions, we observed partial penetrance of this defect (e.g. Fig. 1h) despite the proposed full knockout nature of the *shr-2* allele used (Helariutta *et al*., 2000). One other factor in the SHR pathway has been shown to contribute to embryonic ground tissue formation. *SCHIZORIZA (SCZ)* is a transcription factor involved in asymmetric cell divisions in the root meristem (Ten Hove *et al.*, 2010; Pernas *et al.*, 2010). However, similar to the *shr* mutant, the earliest defects in *scz shr* are observed in heart stage embryos (Ten Hove, 2010). Likewise, no globular stage defects have been reported for the *scr scz* double mutants (Pernas *et al.*, 2010). Thus, ground tissue division defects in *mp* mutants precede those in *shr* and other ground tissue mutants. This suggests that MP activity is required earlier in embryonic ground tissue cells than any other known factor in ground tissue specification.

MP-dependent regulation of *SHR* and its close homologs in the early embryo

SHR is ~three-fold down-regulated in the microarray on globular stage embryos in which MP is locally inhibited (Table 2; see Chapter 4 for details). In addition, the direct SHR target genes *SCR* and *MGP* are ~two-fold down-regulated (Levesque *et al.*, 2006; Table 2). These results suggest that *SHR* expression might be activated by MP in early embryos. We first investigated if *SHR* is expressed in early embryos, and if SHR protein is transported to the ground tissue layer at these early embryo stages. We found *SHR* to be expressed in vascular cells of the globular stage embryo (Figure 2a), while SHR protein also accumulates in nuclei of ground tissue cells and the hypophysis (Figure 2b). This demonstrates that SHR protein is already transported to the ground tissue layer in early embryos. Importantly, we already observed SHR movement before the first ground tissue cells had divided (data not shown), and hence at a stage far before a mutant phenotype is observed in the *shr* mutant (Fig. 1f-h). Thus, SHR is present in the first ground tissue cells at the time that these are specified in the early embryo. Likewise, the SHR target *SCR* is expressed in globular stage embryos (Figure 1c; Wysocka-Diller *et al.*, 2000), suggesting that SHR is active. To test if *SHR* expression is indeed MP-dependent, we analyzed *SHR* expression in T3 generation embryos segregating both the *mp* mutation and a p*SHR-ntdTomato* construct. We observed decreased or no *SHR* expression in the basal embryo region of heart stage mutant embryos (Figure 1e; n=3), whereas *SHR* was strongly expressed in the whole vasculature of wild-type embryos (Figure 1d; n=10). These data are preliminary due to the limited number

of *mp* mutant embryos observed, and need to be verified in T4 generation embryos homozygous for the p*SHR-ntdTomato* construct. Nonetheless, these data suggest that MP activates *SHR* expression in the basal embryo region. If this activation is direct also remains to be investigated, but transient inhibition of MP in seedlings does not result in reduced *SHR* expression (Table 2), suggesting that *SHR* might not be a direct MP target gene. In conclusion, based on our results, we hypothesize that *SHR* is a MP target gene that is activated prior to the specification of the first ground tissue cells.

Given the early MP-dependent expression of *SHR*, it is surprising that *shr* mutants only show defects later in embryo development. However, there is a large family of related GRAS genes, whose function or potential redundancy with *SHR* has not been explored. Interestingly, in addition to *SHR* and *SCR*, four other GRAS family genes are 1,5-2 fold down-regulated in the microarray dataset on globular stage embryos (Table 2). These are *SCARECROW-LIKE27 (SCL27)*, *28*, *31* and *32*. As a first step in exploring potential redundancy with SHR, we generated transcriptional fusions for these genes to investigate if they are expressed in the early embryo. As *SCL29* and *32* are the closest homologs of *SHR*, *SCL29* was included in the expression analysis although it was not down-regulated in the micro-array dataset. We observed ubiquitous *SCL28* expression in the basal embryo region and suspensor of globular stage embryos (Figure 2f, g). During later stages of embryo development, as well as in the postembryonic root, *SCL28* remained ubiquitously expressed in the root meristem (Figure 2h-j). *SCL31* shows a similar expression pattern to *SCL28* in early embryo development (Figure 2k, l). However, in transition and heart stage, *SCL31* expression is strongest in the inner basal embryo cells (Figure 2m, n). Postembryonically, *SCL31* expression is confined to the stem cell niche in the root (Figure 2o). *SCL32* is weakly expressed in early globular stage embryos (Figure 2p). *SCL32* expression appears to be stronger in apical embryo cells, but is detected in the root meristem throughout embryogenesis (Figure 2q-s). In the postembryonic root, *SCL32* expression is strongest in cortex and epidermis cell files, but is also observed in the endodermis layer (Figure 2t). *SCL27* and *SCL29* are not expressed in the embryo or the postembryonic root meristem, in accordance with previous observations and the documented function of SCL27 in the shoot apical meristem (Lee *et al.*, 2008; Schulze *et al.*, 2010) In conclusion, *SCL28*, *31* and *32* are expressed in the first ground tissue cells from early embryogenesis on, and in the postembryonic root. Thereby, these genes fulfill an important condition to be involved in specification of the first ground tissue cells. Moreover, based on their expression patterns, these genes could be activated by MP. These findings now allow genetic dissection of extended GRAS gene function in early ground tissue specification.

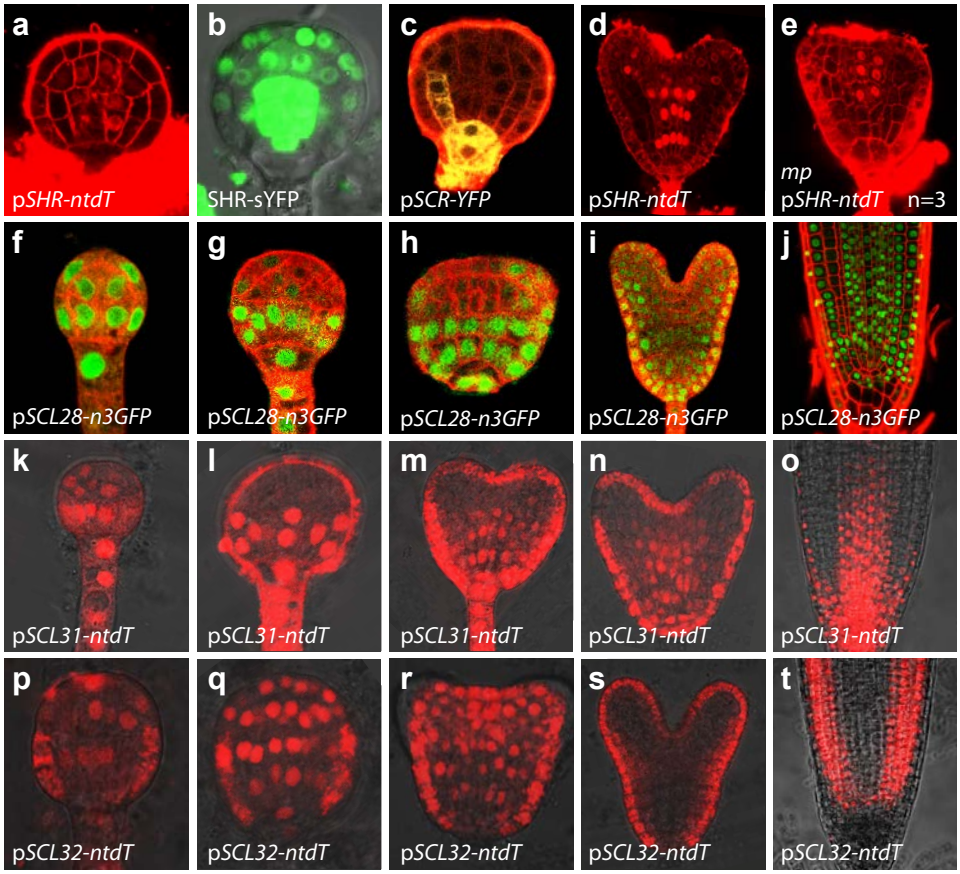

Figure 2. Embryo and root expression of GRAS family genes. a, *pSHR-ntdTomato* is expressed in vascular cells of the globular stage embryo. b, SHR-sYFP protein accumulates in vascular cells and nuclei of the hypophysis and ground tissue cells in the globular stage embryo. c, p*SCR-YFP* is expressed in the hypophysis daughter cells and ground tissue cells of the globular stage embryo. d, e, *pSHR-ntdTomato* expression in heart stage wild-type (d) and *mpB4149* (e) embryos. n is the number of *mp* embryos with similar expression. f-t, Expression of p*SCL28-n3GFP* (f-j), p*SCL31-ntdTomato* (k-o), and p*SCL32-ntdTomato* (p-t) in the embryo at globular stage before (f, k, p) and after (g, l, q) division of the first ground tissue cells, transition stage (h, m, r), heart stage (i, n, s), and postembryonically in the root tip (j, o, t).

MP activation of *RLK* in the ground tissue is SHR-independent

Previously, we showed that MP activates *RLK* that is expressed in the first ground tissue cells of the early embryo (Chapter 4). We investigated if MP-dependent expression of *RLK* is mediated by SHR activity. Therefore, *RLK* expression was examined in the root meristem of F2 generation seedlings segregating the p*RLK-n3GFP* construct and the *shr-2* mutant. Slightly stronger *RLK* expression was

observed in the root meristem of *shr* mutant seedlings (n=24, 75% roots with expression) compared to wild-type roots (n=14, 86% roots with expression; Figure 3a, b). This result indicates that MP activates *RLK* expression independently of SHR activity, and is in line with available microarray data on SHR target genes (Sozzani *et al.*, 2010). Thus, MP promotes transcription in the first ground tissue cells of the early embryo independently of SHR. This result confirms that (partial) ground tissue specification can occur in the absence of SHR.

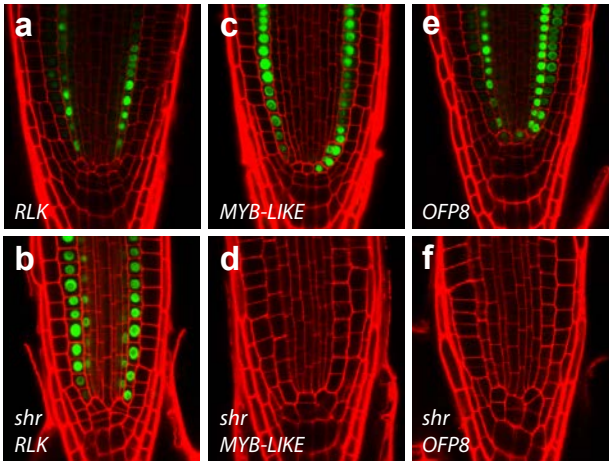

Figure 3. SHR transcriptionally regulates genes expressed in the ground tissue of the root meristem. Expression of p*RLK-n3GFP* (a-b), p*MYB-LIKE-n3GFP* (c-d), and p*OFP8-n3GFP* (e-f) in root meristems of wild-type (a, c, e) and *shr* (b, d. f) roots. For each gene, identical confocal settings were used to compare gene expression levels in *shr* and wild-type root meristems.

In Chapter 4, we showed that *OVATE FAMILY PROTEIN8 (OFP8)* and a *MYB-LIKE* transcription factor are expressed in the ground tissue cells and the quiescent center and its precursors from early embryogenesis on. We explored if expression of these genes is SHR-dependent in a similar manner as for *RLK*. Expression of both *OFP8* and *MYB-LIKE* is lost in the *shr* mutant (n=24 for each of both genes), indicating that their expression requires SHR function. *OFP8* and *MYB-LIKE* were not previously found to be regulated by SHR or SCR activity (Sozzani *et al.*, 2010 and Cui *et al.*, 2011), and thus represent novel potential SHR target genes expressed in the early embryo. Interestingly, in the postembryonic root, *OFP8* is mainly expressed in the endodermis, while *MYB-LIKE* is mainly expressed in the cortex. In conclusion, the SHR-independent activation of *RLK* by MP suggests the existence of a SHR-independent pathway in ground tissue specification in the early embryo.

Does MP act non cell-autonomously in vascular cells to specify the first ground tissue cells? We showed that MP is required for initial cell divisions in the ground tissue layer (see above), and to activate *RLK* expression in the first ground tissue cells of the early embryo (Chapter 4). Since MP acts through the mobile TMO7 signal to promote division of the QC precursor cell (Chapter 2), a key question is where MP is required to promote ground tissue initiation. If *SHR* is indeed a MP target gene mediating MP action in the first ground tissue cells, this suggests that MP activity is non cell-autonomously required in the first vascular cells to promote transcription of *SHR*. Several observations support this hypothesis. (1). The first vascular cells always divide earlier than the first ground tissue cells in wild-type globular stage embryos. This observation was made by analyzing late globular stage embryos. We never found embryos in which the first ground tissue cells but not the first vascular cells had divided (n=96). On the contrary, we counted multiple embryos in which the first vascular cells but not the first ground tissue cells had divided (n=20). Even though no correlation between cell division defects in vascular and ground tissue initials was observed (Fig 1b-d), the strict regulation of timing of the two divisions may be due to inductive signaling. (2). SHR protein has recently been shown to move from the vascular to the ground tissue cells through plasmodesmata (Vatén *et al.*, 2011). The gain of function mutant *callose synthase 3 (cals3-d)* accumulates excessive callose at the plasmodesmata, resulting in decreased aperture of the plasmodesmata (Vatén *et al.*, 2011). In globular stage *cals3-d* embryos, 97% of QC precursor cells divided abberantly (Table 1), indicating that intercellular signaling in embryonic root meristem is impaired. In addition, we found that ~10% of globular stage embryos showed aberrant ground tissue cell divisions (Figure 1k, Table 1). Moreover, we frequently observed transition stage *cals3-d* embryos in which the first ground tissue cells had divided anticlinally, but next performed an aberrant periclinal division (Figure 1l, compare to 1i). This defect was also frequently found in *mp* embryos (Figure 1j). The similar division defects in *mp* and *cals3-d* mutant embryos suggests that intercellular signaling through plasmodesmata is required for anticlinal division of the first ground tissue cells. MP activity is required in the first vascular or ground tissue cells to promote cell division planes in the latter (see above). This suggests that MP activity is non-cell autonomously required in vascular cells to signal to ground tissue cells. This scenario is similar to the non cell-autonomous MP action in the vascular cells of the embryonic root meristem to specify the adjacent QC precursor cell (Weijers *et al.*, 2006; Chapter 2). However, further research is required to determine if MP is indeed required in the vascular cells to specify the first ground tissue cells of the embryonic root meristem.

Discussion

The current knowledge about ground tissue specification in the embryonic root meristem of Arabidopsis is centered around SHR. This GRAS family transcription factor is required for endodermis specification and the periclinal division of ground tissue daughter cells. Several SHR targets have recently been identified (Levesque *et al.*, 2006, Sozzani *et al.*, 2010; Cui *et al.*, 2011). Among these is SCR that is also required for the asymmetric periclinal division of ground tissue daughter cells (Di laurenzio *et al.*, 1996; Heidstra *et al.*, 2004). However, nothing is known about upstream regulators of SHR. Also the mechanisms involved in specification of the first embryonic ground tissue cells are unclear. These first ground tissue cells in the early embryo divide anticlinally to produce ground tissue daughter cells. We show that MP activates *RLK* in the first ground tissue cells of the early embryo, and is required for anticlinal division of the first ground tissue cells. Furthermore, MP promotes *RLK* transcription independent of SHR activity. These results suggest that MP is required in the first ground tissue cells in a SHR-independent pathway. This pathway may precede SHR activity in ground tissue specification, as *shr* mutants show normal embryogenesis until heart stage. However, we showed that SHR protein is present in ground tissue cells of early globular stage embryos. In addition, three homologues GRAS family genes are also expressed in these cells. This suggests that SHR acts redundantly with homologues GRAS family genes to specify the first ground tissue cells. In line with this hypothesis, *WOX7* and a *MYB* transcription factor were recently identified as direct SHR targets, and are expressed in the first ground tissue cells in the postembryonic root meristem (Cui *et al.*, 2011). Furthermore, our results suggest that MP regulates *SHR* expression, as well as expression of several homologues GRAS family genes. In agreement with these results, Gardiner *et al* (2011) recently showed that *SHR* is strictly co-expressed with the MP target gene *ARABIDOPSIS THALIANA HOMEOBOX8 (ATHB8)* during leaf formation. If MP indeed activates SHR expression, this would be the first upstream regulator that has been found to control SHR transcription. In conclusion, we present evidence suggesting the existence of a MP-dependent pathway that specifies the first ground tissue cells in the early embryo.

In this study, we unambiguously showed that MP controls the orientation of the division plane in the first ground tissue cells. Whether MP is also required to specify the first ground tissue cells, or perhaps to regulate cell proliferation of the first ground tissue cells, will be the subject of further research. MP is required for the anticlinal, asymmetric division and specification of the QC precursor cell in the early embryo (Weijers *et al.*, 2006; Chapter 2). This suggests that MP controls

both aspects of cell identity in the first ground tissue cells in a similar fashion. Alternatively, the aberrant division planes could result from failure to specify the hypophysis and ground tissue cells. Analysis of the genetically unstable *shr-3* allele suggested that cell divisions in the ground tissue layer and specification of ground tissue cells can be uncoupled (Helariutta *et al*., 2000). Likewise, a more detailed analysis of different *mp* alleles might aid to distinguish between the possible involvement of MP in cell division orientation or specification of ground tissue cells. Another question is in which cells MP is required to promote transcription and anticlinal division planes in the first ground tissue cells. An elegant approach is to locally induce or eliminate MP activity in early embryos, using a clonal activation/deletion system (Heidstra *et al.*, 2004). Alternatively, analysis of ground tissue division defects in embryos in which MP activity is locally inhibited using the UAS-GAL4 system might also be instrumental.

MP is an executer of auxin signaling. Recently, SHR has been shown to directly activate *AUXIN RESPONSE FACTOR2 (ARF2)* and *Aux/IAA16* that are involved in auxin signaling (Cui *et al.*, 2011). If SHR is indeed a MP target gene, this suggests the existence of crosstalk between auxin signaling and SHR activity. Also gibberellins have been shown to be involved in growth of ground tissue cells in the root (reviewed in Miyashima and Nakajima, 2011). The GRAS family gene *SCL3* is a direct SHR target, but is also regulated by the so called DELLA subclade of GRAS family proteins that repress gibberellin signaling. Furthermore, SCL3 and DELLA proteins directly interact, thereby integrating multiple pathways in ground tissue regulation. Therefore, extensive interactions and transcriptional feedback loops among GRAS family genes exist, which complicates the study of these genes. *SCL28* was recently found to be a target of both SHR and SCR, and to be expressed in the first ground tissue cells or their daughter cells (Sozzani *et al.*, 2010). However, the embryo expression pattern of *SCL28* extends beyond the domains of SHR and SCR activity, suggesting that *SCL28* is only partly regulated by SHR and SCR. Further research is required to dissect the mechanisms of initial ground tissue specification in the embryonic root meristem. If SHR is indeed a MP target gene, it will be interesting to see if this activation is direct. It also needs to be verified if *SCR*, *SCL28*, *31* and *32* are regulated by MP, and if this regulation is direct. Furthermore, genetic studies should reveal if SHR redundantly acts with other GRAS family genes to specify ground tissue stem cells. Moreover, the role of *RLK* in specification of the first ground tissue cells needs to be investigated (discussed in Chapter 4). So far, only factors involved in specification of ground tissue daughter cells were known. Thus, this study is a starting point to reveal the mechanisms involved in ground tissue initiation in the early embryo. In conclusion, our data suggest that MP is required to specify the first ground tissue cells in

the early embryo in a SHR independent pathway. Thereby, these data provide the first link between auxin signaling and ground tissue specification.

Material & Methods

Plant growth and Material

All seeds were surface sterilized, sown on solid MS plates and vernalized for one day before growing at a constant temperature of 22°C in a growth room. The *mp-B4149* allele in Columbia background and the p*UAS*-bdl line were described in Weijers *et al.* (2006). The *mp-S319* allele corresponds to SALK_021319. The p*Q0990-GAL4* enhancer trap line was generated by Jim Haseloff (University of Cambridge, UK) and obtained through the Arabidopsis Biological Resource Center (ABRC). The *cals3-d* mutant is described in Vatén *et al* (2011), and the *shr-2* mutant is described in Benfey *et al* (1993) and obtained from dr. Ikram Blilou. The pGIIB:pSHR:SHR-YFP and pGIIB:pSCR:YFP constructs were also obtained from dr. Ikram Blilou. The pGIIB:pSHR:SHR-YFP construct contains 2525 bp of the *SHR* promoter upstream of first 38 bp before ATG, and the pGIIB:pSCR:YFP construct contains 2,4 kb of the *SCR* promoter upstream of the ATG.

Cloning

All cloning was performed using the LIC cloning system (De Rybel *et al.*, 2011). Transcriptional fusions were generated by PCR-amplifying ~2 kb fragments upstream of the ATG from genomic DNA using Phusion Flash polymerase (Finnzymes), and introducing them into the pGreenIIKAN:LIC: SV40:3GFP:NOSt vector. Primers used for amplifying promoter fragments are listed in Table 3 and in Table x of Chapter 4. All promoter fusion constructs were transformed into wild-type Columbia and *mp-B4149* heterozygous plants by floral dip using the *Agrobacterium* strain GV3101(pSoup).

Microscopy

Differential interference contrast (DIC) microscopy and confocal microscopy were performed as described previously (Llavata *et al.*, 2011), using a Leica DMR microscope or a Zeiss LSM510 confocal microscope, respectively. Plant membranes of embryos and roots were stained using FM4-64 dye (Invitrogen), which is visible as the red signal in confocal pictures.

Acknowledgements

We acknowledge the laboratory of prof. Ykä Helariutta for sharing the *cals3-d* mutant before publication and Yuchen Long for visualizing the accumulation of SHR protein in embryos.

Tables

Table 1. Percentage of embryos in which the putative first vascular and ground tissue cells has divided aberrantly in globular stage embryos. N is the number of embryos that are counted. ***** Percentage wrongly divided or not divided hypophysis cells in *dva* embryos is 96,8 % at globular stage (n=63)

	% aberrantly divided first vascular cells	N	% aberrantly divided first ground tissue cells	N
wild-type	0	86	0	57
mpB4149	88	50	46,9	49
mpS319	94,3	53	57,1	49
shr-2	1,8	55	2,4	41
*dva2-2**	12	50	10,1	69

Table 2: List of down-regulated GRAS family genes in the Q0990>>>bdl microarray on globular stage embryos. MP activity was locally inhibited in early globular stage embryos in the inner basal embryo cells that will acquire vascular and ground tissue identity, using the Q0990>>>bdl two component system (Weijers *et al.*, 2006; for details see Chapter 4). The list shows GRAS family genes that are significantly and at least 1,5-fold down-regulated in all four replicates (p= 0,05). Below the bold line are several direct SHORTROOT target genes shown. The same microarray experiment was performed with heart stage embryos. For each gene, the fold change in early globular stage embryos (FC glob) and in heart stage embryos (FC heart) is shown. Modulation of gene expression was compared to fold changes in previously performed microarrays on dexamethasone inducible p*RPS5A*-bdl-GR seedlings (FC bdl-GR) and *mp* seedlings (FC *mp*) that were treated with auxin (for details see Chapter 2). [a]Fold change is not significant (t-test, p>0,05). [b] Only three replicates, not significantly downregulated. [c] Only two replicates, not significantly downregulated. [d] Only one replicate, not significantly downregulated.

AT number	Gene name	FC glob	FC heart	FC bdl-GR	FC *mp*
AT4G37650	*SHR*	-2,70	-2,26	-1,02[a]	-3,15
AT1G63100	*SCL28*	-2,07	1,08[a]	-1,16[a]	1,51
AT3G54220	*SCR*	-2,00	-1,09[a]	1,23[a]	-1,02
AT2G45160	*SCL27*	-1,69	1,57	-1,27[a]	-1,53
AT1G55580	*SCL18*	-1,63[d]	-1,12[a]	1,10[a]	1,16
AT1G07520	*SCL31*	-1,59	-1,10[a]	-1,10[a]	-2,07
AT3G49950	*SCL32*	-1,53[c]	1,31[a]	1,10[a]	1,23
AT3G13840	*SCL29*	1,04[a]	1,05[a]	1,11[a]	1,19
AT1G03840	*MGP*	-2,50	-1,95	-1,08[a]	-1,55
AT5G44160	*NUC*	-6,66[d]	-1,40[b]	-1,17[a]	-1,59
AT2G29330	*TRI1*	1,56	-4,00	1,07[a]	-3,81
AT4G03270	*CYCD6;1*	-1,09[a]	-1,08[a]	-1,13[a]	-1,02[a]

Table 3: primers used for LIC cloning. *28 bp of coding sequence downstream of ATG are included in the promoter because the first bp upstream of the ATG are extremely AT rich, but the ATG is mutated in the reverse primer.

AT number	Gene name	Forward and reverse primer used for LIC cloning	Length promoter (bp)
AT4G37650	*SHR*	TAGTTGGAATGGGTTCGAAgcatacaggcatgcataacaacc TTATGGAGTTGGGTTCGAAGACTGACTAGTCTAAAGAGA GTATCCGTTTT	2847*
AT2G45160	*SCL27*	TAGTTGGAATGGGTTCGAAgcgtgatccatgttatgtcatcgag TTATGGAGTTGGGTTCGAACGCCTCCTCAACAACACAGAGTAAC	1989
AT1G63100	*SCL28*	TAGTTGGAATGGGTTCGAAtttagtctagtgattaacta TTATGGAGTTGGGTTCGAACCTCTACAAAATCTACCTAA	2000
AT3G13840	*SCL29*	TAGTTGGAATGGGTTCGAAgttcgagtgccttgtcggattcttc TTATGGAGTTGGGTTCGAATGAATAGATGATGAAAAAGGTATAA TTTGTGAGTAGG	2143
AT1G07520	*SCL31*	TAGTTGGAATGGGTTCGAActgttgatagtctctcgccaacacg TTATGGAGTTGGGTTCGAACCACACCTGAGTAATTCGATTCCTTCGTCC	2000
AT3G49950	*SCL32*	TAGTTGGAATGGGTTCGAAcgaacatgcccttatacgacaatttgaggcc TTATGGAGTTGGGTTCGAATTGAGTCTGGTTTTAGAGAGAAATGTACG	2085

References

Benfey PN, Linstead PJ, Roberts K, Schiefelbein JW, Hauser MT and Aeschbacher RA. (1993). Root development in Arabidopsis: four mutants with dramatically altered root morphogenesis. Development. 119(1): 57-70.

Cui H, Levesque MP, Vernoux T, Jung JW, Paquette AJ, Gallagher KL, Wang JY, Blilou I, Scheres B and Benfey PN. (2007). An evolutionarily conserved mechanism delimiting SHR movement defines a single layer of endodermis in plants. Science. 316(5823) :421-425

Cui H, Hao Y, Kovtun M, Stolc V, Deng XW, Sakakibara H and Kojima M. (2011). Genome-wide direct target analysis reveals a role for SHORT-ROOT in root vascular patterning through cytokinin homeostasis. Plant Physiol. 157(3): 1221-1231.

De Rybel B, van den Berg W, Lokerse A, Liao CY, van Mourik H, Möller B, Peris CL and Weijers D. (2011). A versatile set of ligation-independent cloning vectors for functional studies in plants. Plant Physiol. 156(3): 1292-1299.

Di Laurenzio L, Wysocka-Diller J, Malamy JE, Pysh L, Helariutta Y, Freshour G, Hahn MG, Feldmann KA and Benfey PN. (1996). The *SCARECROW* gene regulates an asymmetric cell division that is essential for generating the radial organization of the Arabidopsis root. Cell. 86(3): 423-433.

Gardiner J, Donner TJ and Scarpella E. (2011). Simultaneous activation of *SHR* and *ATHB8* expression defines switch to preprocambial cell state in Arabidopsis leaf development. Dev Dyn. 240(1): 261-270.

Heidstra R, Welch D and Scheres B. (2004). Mosaic analyses using marked activation and deletion clones dissect Arabidopsis SCARECROW action in asymmetric cell division. Genes Dev. 18(16): 1964-1969.

Helariutta Y, Fukaki H, Wysocka-Diller J, Nakajima K, Jung J, Sena G, Hauser MT and Benfey PN. (2000). The *SHORTROOT* gene controls radial patterning of the Arabidopsis root through radial signaling. Cell. 101(5): 555-567.

Lee MH, Kim B, Song SK, Heo JO, Yu NI, Lee SA, Kim M, Kim DG, Sohn SO, Lim CE, Chang KS, Lee MM and Lim J. (2008). Large-scale analysis of the GRAS gene family in *Arabidopsis thaliana*. Plant Mol Biol. 67(6):659-70.

Levesque MP, Vernoux T, Busch W, Cui H, Wang JY, Blilou I, Hassan H, Nakajima K, Matsumoto N, Lohmann JU, Scheres B and Benfey PN. (2006). Whole-genome analysis of the SHORTROOT developmental pathway in Arabidopsis. PLoS Biol. 4(5): e143.

Llavata-Peris CI, Lokerse AS, Möller B, De Rybel B and Weijers D. (2012). Imaging of phenotypes, gene expression and protein localization during embryonic root formation in Arabidopsis. Meth Mol Biol. *in press*.

Miyashima S and Nakajima K. (2011). The root endodermis: A hub of developmental signals and nutrient flow. Plant Signal Behav. 6(12).

Nakajima K, Sena G, Nawy T and Benfey PN. (2001). Intercellular movement of the putative transcription factor SHR in root patterning. Nature. 413(6853): 307-11.

Pernas M, Ryan E and Dolan L. (2010). SCHIZORIZA controls tissue system complexity in plants. Curr Biol. 20(9): 818-23.

Scheres B, Wolkenfelt H, Willemsen V, Terlouw M, Lawson E, Dean and Weisbeek P. (1994). Embryonic origin of the Arabidopsis primary root and root meristem initials. Development. 120(9): 2475-87

Scheres B, Di Laurenzio L, Willemsen V, Hauser MT, Janmaat K, Weisbeek P and Benfey P. (1995). Mutations affecting the radial organization of the Arabidopsis root display defects throughout the embryonic axis. Development 121: 53-62.

Schulze S, Schäfer BN, Parizotto EA, Voinnet O and Theres K. (2010). *LOST MERISTEMS* genes regulate cell differentiation of central zone descendants in Arabidopsis shoot meristems. Plant J. 64(4): 668-78.

Sena G, Jung JW and Benfey PN. (2004). A broad competence to respond to SHORT ROOT revealed by tissue-specific ectopic expression. Development. 131(12): 2817-2826.

Sozzani R, Cui H, Moreno-Risueno MA, Busch W, Van Norman JM, Vernoux T, Brady SM, Dewitte W, Murray JA and Benfey PN. (2010). Spatiotemporal regulation of cell-cycle genes by SHORTROOT links patterning and growth. Nature. 466(7302): 128-132.

Ten Hove CA, Willemsen V, de Vries WJ, van Dijken A, Scheres B and Heidstra R. (2010). *SCHIZORIZA* encodes a nuclear factor regulating asymmetry of stem cell divisions in the Arabidopsis root. Curr Biol. 20(5): 452-457.

Ten Hove CA. (2010). Regulation of cell fate and meristem maintenance in Arabidopsis root development. Thesis, Utrecht University, Utrecht, NL. ISBN 978-90-8559-951-7

Van den Berg C, Willemsen V, Hendriks G, Weisbeek P and Scheres B. (1997). Short-range control of cell differentiation in the Arabidopsis root meristem. Nature. 390(6657): 287-289.

Vatén A, Dettmer J, Wu S, Stierhof YD, Miyashima S, Yadav SR, Roberts CJ, Campilho A, Bulone V, Lichtenberger R, Lehesranta S, Mähönen AP, Kim JY, Jokitalo E, Sauer N, Scheres B, Nakajima K, Carlsbecker A, Gallagher KL and Helariutta Y. (2011). Callose Biosynthesis Regulates Symplastic Trafficking during Root Development. Dev Cell. 21(6): 1144-1155.

Wysocka-Diller JW, Helariutta Y, Fukaki H, Malamy JE and Benfey PN. (2000). Molecular analysis of SCARECROW function reveals a radial patterning mechanism common to root and shoot. Development. 127(3): 595-603.

Weijers D, Schlereth A, Ehrismann JS, Schwank G, Kientz M and Jürgens G. (2006). Auxin triggers transient local signaling for cell specification in Arabidopsis embryogenesis. Dev Cell. 10(2): 265-270.

Chapter 6

Towards the identification of MONOPTEROS-interacting proteins in the Arabidopsis embryo by mass spectrometry

Barbara Möller, Sjef Boeren and Dolf Weijers

Laboratory of Biochemistry, Wageningen University, Dreijenlaan 3, 6703HA Wageningen, the Netherlands

Parts of this chapter are published in:

Smith MR, Willmann MR, Wu G, Berardini TZ, Möller B, Weijers D and Poethig RS. (2009). Cyclophilin 40 is required for microRNA activity in Arabidopsis. Proc Natl Acad Sci U S A. 106(13): 5424-5429.

Zwiewka M, Feraru E, Möller B, Hwang I, Feraru MI, Kleine-Vehn J, Weijers D and Friml J. (2011). The AP-3 adaptor complex is required for vacuolar function in Arabidopsis. Cell Res. 21(12): 1711-1722.

Saiga S, Möller B, Watanabe A, Abe M, Weijers D, and Komeda Y. (2012). Control of embryonic meristem initiation in Arabidopsis by PHD finger protein complexes. Development. 139(8): 1391-1398.

Abstract

Embryonic root initiation involves the coordinated specification of several cell types that collectively create the root meristem. The MONOPTEROS (MP) transcription factor is involved in most of the specification events that result in the establishment of an embryonic root. Moreover, MP has been shown to activate several target genes that are involved in distinct aspects of root initiation. While MP protein accumulates in nearly the whole embryo, its target genes are activated in different subdomains. As a first step in dissecting the mechanisms of local MP-dependent gene regulation, we optimized an affinity purification protocol to investigate if MP could regulate distinct target genes through interaction with other factors. A collection of transgenic lines was generated in which MP was fused to different tags at different positions in the protein. The affinity purification protocol was optimized using siliques expressing the MP-GFP protein under the control of the native MP promoter. We optimized several steps in the procedure resulting in the reproducible recovery of MP protein in mass spectrometry analysis. However, these purifications did not identify any MP interacting protein. In contrast, this protocol can identify interacting transcription factors in the embryo for two other nuclear proteins. Therefore, further optimization of this procedure is an important step to identify the potentially transient or unstable MP protein complexes during embryonic root formation.

Introduction

In higher plants, the root is initiated in the early embryo by the coordinated specification of different cell types that collectively form the root meristem. Auxin signaling is required for root initiation, and its effects in the embryo mainly converge on the activity of the MONOPTEROS (MP) transcription factor (reviewed in Chapter 1). MP activates transcription of *TARGET OF MP (TMO)* genes (Chapter 2). Recently, novel MP target genes were identified that are expressed in the developing root meristem, although it is not clear if these genes are directly activated by MP (Chapter 4). Moreover, MP is involved in several aspects of embryonic root initiation that are mediated by MP target genes (Chapters 2&3). Thus it appears that MP controls distinct aspects of embryonic root initiation via the activation of distinct (sets of) target genes. So far, it is unclear how MP activates gene expression in spatially different domains of the early embryo. MP protein accumulates in most embryo cells of the globular stage embryo, while its - indirect and direct - target genes *TMO5*, *DUF966, RLK, SPT* and *PUB25* are only expressed in subsets of this domain (Figure 1). An unresolved question is how MP promotes gene

transcription in subsets of its activity domain. One possibility is that MP needs to interact with another transcription factor to activate a subset of target genes. The activity of this second protein should then be restricted to a certain cell type. Theoretically, this would allow MP to activate distinct sets of target genes by interacting with different transcription factors.

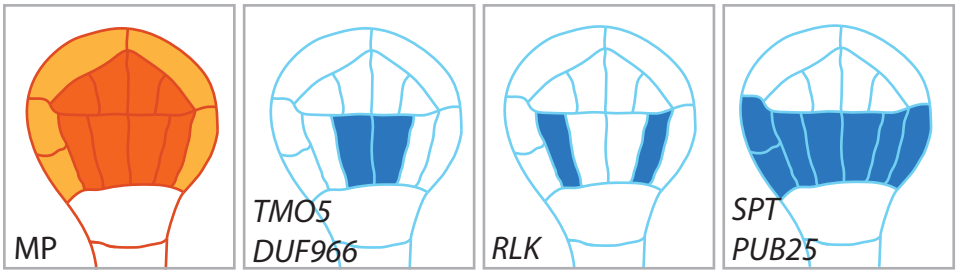

Figure 1. MP activates transcription in sub-domains of its region of activity. Schematic representation of domain of MP activity (dark orange: highest MP accumulation, lighter orange: lower MP accumulation) and expression pattern of MP target genes in the globular stage embryo.

The best candidates to interact with MP are proteins of the same transcription factor family called Auxin Response Factors (ARFs). MP/ARF5 interacts with ARF7 in yeast-two-hybrid experiments (Hardtke *et al.*, 2004). In addition, MP has been demonstrated to interact with several other ARFs when over-expressed in protoplasts in FRET-FLIM experiments (Cristina Llavata Peris and Alejandra Freire Rios, personal communication). Such experiments also showed that MP has the ability to homodimerize in protoplasts (Pascal van Oorschot, personal communication). However, it remains unclear if homo- and heterodimerization of ARFs is required for their function *in planta*. In addition to interacting with other ARFs, MP might bind proteins that belong to other transcription factor families. MP interacts with BODENLOS (BDL), which is a member of the Aux/IAA family of transcriptional repressors (Weijers *et al*., 2006; Hamann *et al*., 2002). Furthermore, ARF8 has been shown to interact with a bHLH transcription factor called BIGPETAL (BGP) (Varaud *et al.*, 2011), and several ARFs interact with a MYB transcription factor (Shin *et al.*, 2007). Both BGP and the MYB protein were shown to interact with ARFs by yeast-two-hybrid and bimolecular fluorescence complementation. However, MP has not been shown to interact with different transcription factor families other than the Aux/IAA proteins.

Our goal in this study is an unbiased search for putative MP interacting proteins. As discussed above, this could be important to understand how MP regulates gene expression. Several approaches can be taken that allow the proteome-wide identification of unknown binding partners for a given protein. The most common

techniques are yeast-two-hybrid screens and pull-down experiments in combination with mass spectrometry. In general, the low abundance of transcription factor complexes in plants and animals has hampered their identification. Nonetheless, several transcription factor complexes in yeast and mammalian cell lines were identified using these techniques (reviewed in Forde and McCutchen-Maloney, 2002; Tian, 2006). For instance, the mammalian GATA-1 transcription factor forms multiple different transcription factor complexes in mouse erythroleukemic cells (Grosveld *et al.*, 2005). Moreover, different GATA-1 complexes regulate distinct sets of GATA-1 target genes (Rodriguez *et al*., 2005). It is conceivable that in plants, transcription factors may employ similar mechanisms to control gene expression. In plants, yeast-two-hybrid screens identified interactions between members of different transcription factor families involved in hormone signaling (Bu *et al*., 2011; Chandler *et al*., 2007, 2009, Niu *et al*., 2011). Likewise, tandem affinity purification (TAP) on cell suspension cultures in combination with mass spectrometry identified novel interactions between transcriptional regulators involved in jasmonate signaling (Pauwels *et al*., 2010). In addition, *in planta* affinity purification in combination with mass spectrometry confirmed the existence of a MADS-box transcription factor complex, and showed that one of these transcription factors interacts with other types of transcription factors (Smaczniak *et al.*, 2012).

To date, immunoprecipitation followed by mass spectrometry has allowed the identification of interacting proteins in the most natural situation in the plant (reviewed in Kaufmann *et al*., 2011). Therefore, we decided to use this method to identify putative MP interacting proteins. A very brief protocol, consisting of a single purification step, had previously been optimized by Karlova *et al* (2006) for the identification of membrane complexes, including those encompassing SOMATIC EMBRYOGENESIS RECEPTOR-LIKE KINASE1 (SERK1) (Karlova *et al.*, 2006). Here, we show the optimization of an immunoprecipitation protocol for identifying nuclear protein complexes in seedlings, flowers and siliques. Although the results do not reveal any MP interacting protein, the procedure has been optimized such that several other tagged proteins have successfully been used to identify at least some of their interacting partners. Several possibilities that might explain why MP interacting factors are not found are discussed.

Results

Our goal in this study was an unbiased search for putative MP interacting proteins. We first performed a gel filtration experiment to examine if MP functions in a protein complex, or rather acts as monomer or dimer (Figure 2). In this experiment,

total protein extracts were prepared from seedlings expressing 6xHA-tagged MP under the control of the endogenous MP promoter (MP-6HA). These protein extracts were subsequently run on a size exclusion chromatography column to check the size of the MP protein complex *in planta*. We found that MP was present in a higher-order complex that ranged in size between 158 and 448 kDa. This size vastly exceeded the size of the monomer (105 kDa) or predicted dimer (210 kDa). Although size exclusion chromatography is not able to accurately determine the size of a protein complex, these results suggest that MP indeed resides in a protein complex. The following paragraphs discuss the optimization of an affinity purification protocol to find MP interacting proteins.

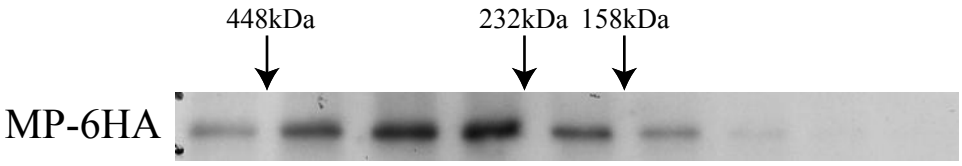

Figure 2: Size exclusion chromatography of MP-6HA expressing seedlings reveals the approximate size of the *in vivo* MP protein complex. MP-6HA was expressed under its native promoter in wild-type seedlings. The *in vivo* MP protein complex migrates between roughly 200-450 kDa on a Western blot. MP-HA protein is ~105 kDa and BDL protein is ~26 kDa.

Detection of MP protein on Western blot

Our aim was to find putative MP interacting proteins by performing affinity purification experiments with plants expressing MP fusion proteins. Several constructs were generated that consisted of the MP coding sequence fused to different tags – GREEN FLUORESCENT PROTEIN (GFP), biotin (De Boer *et al*., 2003), tandem StrepII and FLAG (Gloeckner *et al*., 2007) – each under the control of the MP promoter. Most of these tags were inserted into different places of the MP coding sequence to evaluate possible interference of the position of the tag in the MP protein with protein function. Nearly all constructs were shown to be functional as they rescued the strong *mpB4149* mutant phenotype (Table 1). Moreover, GFP fluorescence could be detected by confocal microscopy for all different MP-GFP lines (not shown). All different MP-GFP lines as well as some MP-biotin lines and the MP-FLAG line were used to perform affinity purification experiments followed by Western blotting (data not shown). Despite extensive efforts to optimize the Western blotting procedure (various antibodies and Western blotting procedures) and the successful detection of 6xHA-tagged MP on Western blot in the laboratory of prof. Gerd Jürgens (Tübingen, Germany, see above), MP could not be detected on Western blot in the Biochemistry Department at Wageningen University. Therefore the pTMO5-TMO5-3GFP line (Chapter 2) was used to ini-

tially optimize the protein extraction. Like MP-GFP, this fusion protein is nuclear and presumably also binds DNA (Chapters 2&3).

Table 1: MP fusion constructs with various tags and their functionality in plants as measured by the ability to rescue strong *mpB4149* mutant plants. The functionality of some fusion proteins has not yet been tested (-). For detailed description of these fusion constructs see Materials and Methods.

Tag	Tag insertion site relative to MP protein	Number of independent lines that show rescue of *mpB4149* mutant
eGFP	at N-terminus	3
eGFP	at C-terminus	3
eGFP	in coding sequence (EcoRI restriction site)	3
eGFP	in coding sequence (MscI restriction site)	1
biotin	at N-terminus	1
biotin	at C-terminus	-
biotin	in coding sequence (EcoRI restriction site)	1
double StrepII	at N-terminus	-
StrepII-FLAG	at N-terminus	-

Optimization of protein extraction

A brief affinity purification protocol was previously optimized for membrane proteins (Karlova *et al*., 2006). Here we show the results of the optimization of an affinity purification protocol for low abundant nuclear proteins. To efficiently extract nuclear proteins, such as MP and TMO5, the nuclear envelope must be disrupted. Two extraction methods with relatively short processing time were compared for efficient extraction of nuclear proteins. We reasoned that the short extraction time would help to keep the proteins in the extract intact, as proteins can be sensitive to degradation. One of these methods was previously used to extract membrane proteins (Karlova *et al*., 2006), while the other one used sonication to disrupt the nuclear envelope (De Folter *et al*., 2007). Sonicating the extract appears to be required to extract nuclear proteins because affinity purification experiments with TMO5-3GFP flowers showed only a band at the size of TMO5-3GFP on Western blot when the protein extract was sonicated (data not shown). Another factor that influenced the efficiency of extracting nuclear protein was the percentage of the detergent Nonidet P-40 (NP-40) in the extraction buffer. The protein extraction and subsequent affinity purification with TMO5 showed that 1% NP40 is required for efficient protein extraction (Figure 3). The amount of extracted TMO5 protein roughly decreased two-fold when the NP-40 percentage in the extraction buffer was 0.5% instead of 1%, and further decreased with lower NP-40 percentages.

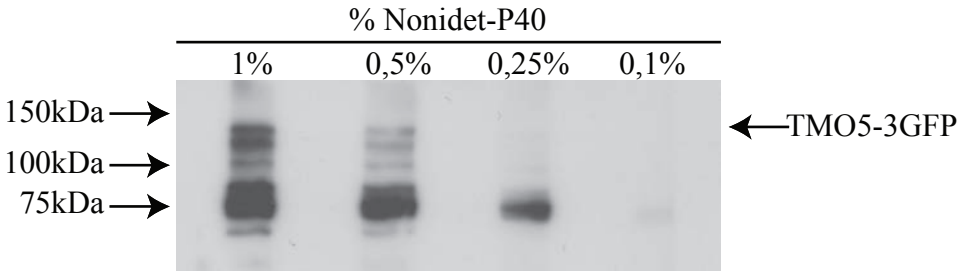

Figure 3: Efficiency of extracting a nuclear protein depends on the percentage of Nonidet P-40 in the extraction buffer. Total protein extracts of siliques expressing TMO5-3GFP under the endogenous TMO5 promoter were prepared using different percentages of NP-40 in extraction buffer: 1%, 0.5%, 0.25% and 0.1%. The protein extracts were subsequently used affinity purification with magnetic beads (Miltenyi). Ten per cent of each affinity purification was loaded on gel. Note that 1% NP-40 in the extraction buffer results in the highest extraction efficiency of TMO5-3GFP protein (~130 kDa, arrow).

Effect of antibody on purification efficiency

Although we could not detect MP on Western blot, MP can be detected by mass spectrometry after affinity purification (Table 2). The percentage of recovery of MP protein after affinity purification was used as readout to measure the purification efficiency. We optimized the affinity purification protocol using a MP-GFP line that showed the highest GFP fluorescence in confocal microscopy (GFP inserted in MscI restriction site of MP coding sequence). This MP-GFP line is in a homozygous *mp* mutant background to ensure that the tagged MP protein is active and binds putative interacting partners, and is not outcompeted with non-tagged MP protein. Several different antibodies and beads were used to optimize the affinity purification protocol with MP-GFP seedlings and siliques. The first antibody that was tested was a custom-made polyclonal anti-YFP antibody (Karlova *et al*., 2006) that was coupled to protein-A Sepharose beads. Using this antibody, a variable but low number of MP peptides was found in MP-GFP affinity purifications (Table 2 Exp. 1-6). However, the protein extraction method that was used in combination with this antibody was suboptimal for nuclear proteins (Table 2), which might have affected the purification efficiency. The second antibody that was tested was a monoclonal anti-GFP antibody coupled to magnetic beads (Miltenyi Biotec). These magnetic beads can bind to a column using a strong magnet (Miltenyi Biotec). This column was used to collect the beads after the incubation of the antibody with the protein extract. The results of pull-down experiments with this antibody were superior compared to the first antibody with respect to the coverage of MP protein (Table 2 Exp. 7-20, compare with Exp. 1-6). These better results probably also resulted from the small volume of the column that increased

the interaction chances of the antibody and the GFP-tagged protein. The third antibody that was tested was a commercially available polyclonal anti-YFP antibody (abcam) that was used in combination with ProteinA Agarose beads (Table 2 Exp. 20-22). Finally a GFP binding protein coupled to Agarose beads (GFP-Trap®-A, Chromotek) was tested (Table 2 Exp. 23; Rothbauer *et al*., 2008). The coverage of MP protein in affinity purification experiments with the last two antibodies was lower in comparison with the monoclonal anti-GFP antibody coupled to magnetic beads. In conclusion, affinity purification with the monoclonal anti-GFP antibody coupled to magnetic beads resulted in the highest coverage of MP protein after mass spectrometry analysis.

Effect of amount of plant material on purification efficiency

We used the monoclonal anti-GFP antibody to further optimize the affinity purification with siliques (Table 2 Exp. 7-17, 20). The amount of siliques that were used for the affinity purification appeared to affect the recovery of MP protein after mass spectrometry analysis. When one gram of siliques was used, the average coverage of MP protein between three independent experiments was 21.3% (Table 2 Exp. 7-9). When three grams of siliques were used, the average coverage of MP protein between five independent affinity purification experiments was 28.2% (Table 2 Exp. 10-14). When even more siliques were used, up to eight grams, the purification efficiency did not increase further (Table 2 Exp 16 and 17), suggesting that the maximum number of MP-GFP proteins was already bound to the beads using three grams of siliques. However, the ratio between plant material, available antibody and column volume probably determines how many MP proteins can be bound. Therefore, a general up scaling might result in higher purification efficiency. Not all affinity purifications were performed with siliques, as some experiments used flowers expressing GFP-tagged MP protein (Table 2 Exp. 18 and 19). Considering that only 0.5 gram of flowers was used, the coverage of MP protein from affinity purification with flowers is probably higher compared to siliques when equal amounts of plant material are used. In addition to the amount and type of plant material, the effect of several other factors on the purification efficiency was tested. These included (1) more extensive washing of the beads after affinity purification, (2) chemical elution of tagged protein from the beads, and (3) in gel digestion with trypsin before mass spectrometry analysis. However, none of these factors improved the purification efficiency.

Table 2: Optimization of an affinity purification procedure with pMP-MP-GFP seedlings, siliques and flowers. In all experiments the Nonidet P-40 percentage was 1% in the extraction buffer and 0.2-0.3% during the incubation of the supernatant of the protein extract with the antibody, except for experiment 15. n, number of different peptides (number of unique peptides), %, percentage coverage of protein, Sf, total score factor calculated by Bioworks v3.3.1.

Exp. #	Affinity purification procedure and antibody	MP peptides		
		n	%	Sf
Seedlings were ground in a mortar with liquid nitrogen, homogenised in extraction buffer and with a Potter followed by 10 minutes centrifugation at 4500 g at 4 ºC. The supernatant was pre-cleared with 50 µl CNBr - activated Sepharose 4B beads (GE Healthcare) with Tris-blocked active sites for 30 min., and subsequently incubated with 50 µl Sepharose 4B beads coupled to purified custum-made anti-YFP antibody (Eurogentec). The beads were washed twice with extraction buffer with 0.1% Triton and three times with 50 mM ammoniumcarbonate.				
1	4,7 gram seedling, overnight incubation with anti-YFP antibody	10	16	15
2	2,8 gram seedlings, 0,5 hour incubation with anti-YFP antibody	0	0	-
3	2,8 gram seedlings, 1 hour incubation with anti-YFP antibody	0	0	-
4	2,8 gram seedlings, 4 hour incubation with anti-YFP antibody	1	2.8	4.6
5	2,8 gram seedlings, overnight incubation with anti-YFP antibody	0	0	-
6	9,2 gram seedlings, 1 hour incubation with anti-YFP antibody	2	3.1	0.9
Plant material was ground in a mortar with liquid nitrogen before and after adding extraction buffer and sonicated with a probe sonicator followed by 2 x 10 minutes centrifugation at 10.000 g at 4 ºC. The supernatant was incubated with monoclonal anti-GFP antibody coupled to magnetic beads (Miltenyi) . The beads were washed four times with extraction buffer with 0.1% Triton and twice with 50 mM ammoniumcarbonate.				
7	1 gram siliques, 3 x centrifugation of cell lysate at 4500 g for 10 min. Incubation with 50 µl beads for 30 min. without rotation and 10 min. with rotation	12	17	11
8	1 gram siliques, 3 x centrifugation of cell lysate at 4500 g for 10 min. Incubation with 50 µl beads for 30 min. without rotation and 10 min. with rotation. Washing with larger volumes after antibody incubation compared to exp. 7	15	25	15
9	1 gram siliques. Incubation with 50 µl beads for 2 hours	15	22	13
10	3 gram siliques. Incubation with 100 µl beads for 2 hours	27	42	26
11	3 gram siliques. Incubation with 100 µl beads for 2 hours	20	29	20
12	3 gram siliques. Incubation with 100 µl beads for 2 hours	15	26	16
13	3 gram siliques. Incubation with 100 µl beads for 2 hours	13	19	10
14	3 gram siliques. Incubation with 100 µl beads for 2 hours	18	25	15
15	3 gram siliques. Incubation with 100 µl beads for 2 hours with 1% NP40 instead of 0,2%	0	0	0
16	6 gram siliques. Incubation with 100 µl beads for 2 hours	20	29	20
17	8 gram siliques. Incubation with 100 µl beads for 2 hours	19	30	19
18	0,5 gram flowers, 2 x centrifugation of cell lysate at 4500 g for 10 min. Incubation with 50 µl beads for 1 hour	19	28	15
19	0,5 gram flowers, 2 x centrifugation of cell lysate at 4500 g for 10 min. Incubation with 50 µl beads for 1 hour	9	15	8.4
Plant material was ground in a mortar with liquid nitrogen before and after adding extraction buffer and sonicated with a probe sonicator followed by 2 x 10 minutes centrifugation at 10.000 g at 4 ºC. The supernatant was incubated with 3 µl anti-GFP polyclonal antibody (Abcam) for 2 hours, followed by adding 25 µl packed agarose beads and another incubation for 1,5 hours. The beads were washed four times with extraction buffer with 0.1% Triton and twice with 50 mM ammoniumcarbonate.				
20	3 gram siliques. In gel digestion with trypsin.	4	4.8	3
21	3 gram siliques	9	15	7.7
22	0,75 gram flowers	0	0	0
Plant material was ground in a mortar with liquid nitrogen before and after adding extraction buffer and sonicated with a probe sonicator followed by 2 x 10 minutes centrifugation at 10.000 g at 4 ºC. The supernatant was incubated with 30 µl of GFP binding protein coupled to agarose beads (GFP-Trap®-A, Chromotek) for 2 hours. The beads were washed four times with extraction buffer with 0.1% Triton and twice with 50 mM ammoniumcarbonate.				
23	1 gram siliques, 2 x centrifugation of cell lysate at 12.000 g for 15 min.	8	13	6.5

Identification of interacting proteins in affinity purification experiments

After adjusting several factors that affect the purification efficiency, it seems that the protocol allows the reproducible recovery of MP protein after mass spectrometry analysis. We recovered up to 40 percent of the MP protein with the optimized protocol (Table 2 Exp. 10-14). To identify interacting proteins, we compared the mass spectrometry results of affinity purifications with tagged protein and the same wild-type plant material in multiple independent experiments. A protein was only designated as candidate interacting protein if it was present in plant material expressing the tagged protein and not in wild-type plant material in multiple independent experiments. Unfortunately, we did not reproducibly identify any MP-interacting protein in multiple independent affinity purification experiments. Moreover, we did not recover previously described interactions such as with BDL and MP itself (Weijers *et al*., 2006; Hamann *et al*., 2002). Even though the reasons are unknown, it is conceivable that MP complexes are not very stable, and that protein interactions are thus hard to detect. To test whether the optimized affinity purification procedure allows detection of *in vivo* protein complexes, we also performed affinity purification with other GFP-tagged proteins (Table 3). Affinity purification with seedlings over-expressing the cytosolic GFP tagged SQUINT (SQN) protein resulted in more than 60% recovery of the SQN protein (Figure 4), but did not identify any interacting protein (Smith *et al*., 2009). Affinity purification with the vacuolar ADAPTOR PROTEIN3β (AP3β) and δ identified nearly all subunits of the AP complex, as well as components of the clathrin and dynamin machineries (Table 3; Zwiewka *et al*., 2011). In addition, affinity purification with siliques expressing the GFP-tagged TMO5 transcription factor under the control of its endogenous promoter resulted in the identification of several interacting transcription factors (for details see Chapter 3). Moreover, we performed affinity purification experiments with siliques expressing the nuclear plant homeodomain finger protein OBERON1 (OBE1) under the control of its endogenous promoter. This resulted in the recovery of OBE1 and the identification of its three closest homologues (Table 3; Saiga *et al*., 2012). Furthermore, four of the six type IId WRKY transcription factors were identified (Eulgem, 2000).

Table 3: Identification of SQN, OBE1, AP3-β-GFP and AP3-δ-GFP and interacting proteins by immunoprecipitation. Two independent pull-down experiments have been performed with 5 day-old seedlings overexpressing SQN-GFP. No SQN interacting proteins could be found. To identify OBE1 interacting proteins, three independent pull-down experiments have been performed with one gram of siliques expressing OBE1-GFP under the control of its endogenous promoter. Experiments 1 and 2 were performed with 0.2% Nonidet-P40 during the incubation of the cleared protein extract with the anti-GFP antibody immobilized on magnetic beads, while the Nonidet-P40 percentage in experiment 3 was 1%. To identify AP3-bèta and AP3-delta interacting proteins two independent immunopreciptations of 5-day-old seedlings were performed for both AP3-bèta and AP3-delta expressed under their own promoter. n, number of different peptides (number of unique peptides), %, percentage coverage of protein, Sf, total score factor calculated by Bioworks v3.3.1. *Not distinguishable which of the two clathrin heavy chain proteins is identified.

AGI	Protein name	SQN-GFP											
		Exp. 1						Exp. 2					
		n		%		Sf		n		%		Sf	
At2g15790	SQN	19		60		23		15		63		26	
		OBE1-GFP											
		Exp. 1			Exp. 2			Exp. 3					
		n	%	Sf	n	%	Sf	n	%	Sf			
At3g07780	OBE1	40 (37)	62	40	43 (40)	62	39	26 (23)	45	21			
At5g48160	OBE2	8 (5)	17	4.8	7 (4)	13	5.3	4 (1)	6.3	2.7			
At1g14740	TTA1	17	24	14	17	25	14	5	6.8	3.2			
At3g63500	TTA2	22	26	17	25	23	19	10	9.0	6.9			
At4g24240	WRKY7	5	19	2.3	6	18	3.7						
At4g31550	WRKY11	3 (2)	14	2.5	4	17	2.8						
At2g30590	WRKY21	7	27	5.3	4	15	2.4						
At3g04670	WRKY39				5 (4)	20	3.8						
		AP3-β-GFP						AP3-δ-GFP					
		Exp. 1			Exp. 2			Exp. 1			Exp. 2		
		n	%	Sf	n	%	Sf	n	%	Sf	n	%	Sf
At3g55480	AP3-β	73	62	63	75	62	65	36	39	31	14	17	11
At1g48760	AP3-δ	37	51	31	38	55	34	45	53	40	41	44	31
At1g56590	AP3-μ	14	41	11	13	45	10	4	12	2.6			
At3g50860	AP3-σ	5	39	4.4	5	39	4.1						
At5g42080	ADL1A	10	20	8.4				16	32	11			
At1g14830	ADL1C	6 (3)	12	4.9				4 (3)	7.2	3.1			
At3g60190	ADL1E	4 (2)	5.1	2.9									
At1g59610	ADL3	18 (6)	22	15				19 (7)	24	14			
At1g10290	ADL6	17 (5)	21	13				15 (3)	18	10			
At3g11130, At3g08530*	Clathrin heavy chain				6	3.6	4.1						

The identification of protein complexes allowed us to optimize another factor that might affect the affinity purification. We used siliques expressing the GFP-tagged OBE1 protein to evaluate the effect of the percentage of detergent NP40 on the stability of protein interactions. Protein extracts from OBE1-GFP siliques were incubated in the presence of 1% or 0.2% NP40 during antibody incubation. More OBE1 interacting proteins – with higher coverage - were identified using 0.2% NP40 during antibody incubation compared to 1% NP40 (Table 3). This suggests

that higher detergent concentrations during antibody incubation disrupt protein interactions.

In conclusion, we optimized an affinity purification procedure for nuclear proteins and were able to recover up to 40 percent of the MP protein after mass spectrometry analysis, but did not find any MP interacting protein. Affinity purification with other nuclear GFP tagged proteins, including a transcription factor (Chapter 3) and a chromatin associated protein, identified several interacting transcription factors. Although it remains unclear why no MP interacting proteins were identified, these results suggest that the affinity purification procedure is optimized such that interacting proteins of nuclear tagged proteins can be identified.

MONOPTEROS (512/902 aa; 56.8%)
MMASLSCVEDKMKTSCLVNGGGTITTTTSQSTLLEEMKLLKDQSGTRKPVINSELWHACAGPLVCLPQVGSLVYYFSQGHSEQVA
VSTRRSATTQVPNYPNLPSQLMCQVHNVTLHADKDSDEIYAQMSLQPVHSERDVFPVPDFGMLRGSKHPTEFFCKTLTASDTSTHG
GFSVPRRAAEKLFPPLDYSAQPPTQELVVRDLHENTWTFRHIYRGQPKRHLLTTGWSLFVGSKRLRAGDSVLFIRDEKSQLMVGVR
RANRQQTALPSSVLSADSMHIGVLAAAAHATANRTPFLIFYNPRACPAEFVIPLAKYRKAICGSQLSVGMRFGMMFETEDSGKRRY
MGTIVGISDLDPLRWPGSKWRNLQVEWDEPGCNDKPTRVSPWDIETPESLFIFPSLTSGLKRQLHPSYFAGETEWGSLIKRPLIRVPD
SANGIMPYASFPSMASEQLMKMMMRPHNNQNVPSFMSEMQQNIVMGNGGLLGDMKMQQPLMMNQKSEMVQPQNKLTVNPSA
SNTSGQEQNLSQSMSAPAKPENSTLSGCSSGRVQHGLEQSMEQASQVTTSTVCNEEKVNQLLQKPGASSPVQADQCLDITHQIYQP
QSDPINGFSFLETDELTSQVSSFQSLAGSYKQPFILSSQDSSAVVLPDSTNSPLFHDVWDTQLNGLKFDQFSPLMQQDLYASQNICMS
NSTTSNILDPPLSNTVLDDFCAIKDTDFQNHPSGCLVGNNNTSFAQDVQSQITSASFADSQAFSRQDFPDNSGGTGTSSSNVDFDDCS
LRQNSKGSSWQKIATPRVRTYTKVQKTGSVGRSIDVTSFKDYEELKSAIECMFGLEGLLTHPQSSGWKLVYVDYESDVLLVGDDP
WEEFVGCVRCIRILSPTEVQQMSEEGMKLLNSAGINDLKTSVS

SQUINT (230/361 aa; 63.7%)
MGRSKCFMDISIGGELEGRIVIELYDDVVPKTAENFRLLCTGEKGLGPNTGVPLHYKGNRFHRVIKGFMIQGGDISANDGTGGESIY
GLKFDDENFELKHERKGMLSMANSGPNTNGSQFFITTRTSHLDGKHVVFGRVTKGMGVVRSIEHVSIEEQSCPSQDVVIHDCGEIP
EGADDGICDFFKDGDVYPDWPIDLNESPAELSWWMETVDFVKAHGNEHFKKQDYKMALRKYRKALRYLDICWEKEGIDEETSTA
LRKTKSQIFTNSAACKLKFGDAKGALLDTEFAMRDEDNNVKALFRQGQAYMALNNVDAAAESLEKALQFEPNDAGIKKEYAAV
MKKIAFRDNEEKKQYRKMFV

OBERON1 (399/566 aa; 70.5%)
MGTSSGSNLPHQMLPPRQQLQTSLSLVSSDPHLSRSNSGIVRESPAESASSQETWPTSKSIMGRKTDSGKTGPDSHDQHVIRHVSIAD
KVSLRDIARERLDIVAERMHRLPEEYLEELKNGLKAILEGNGAQPIDEFMFLQKFVQTRSDLTSKTLVRAHRVQLEVLVVINTGIQA
FLHPNINLSQSSLIEIFVYKRCRNIACQNELPADGCPCEICANRKGFCNLCMCVICNKFDFAVNTCRWIGCDVCSHWTHTDCAIRDG
EISMGVSPKSVSGMGEMLFKCRACNHTSELLGWVKDVFQHCAPNWDRESLMKELDFVSRIFRGSEDTRGRKLFWKCEELMEKIKG
GLAEATAAKLILMFFQEIELDSPKSLESGEGGGTIAPQDACNRIAEVVKETLRKMEIVGEEKTRMYKKARMGLEECEREVEEKAKQ
VAELQMERQKKKQQIEEVERIVRLKQAEAEMFQLKANEAKVEAERLERIVKAKKEKTEEEYASNYLKLRLSEAEAEKEYLFEKIKE
QESGGNGGEASQAVMYSKIREMLHGYNASSPRVDPRSNQRNPFRSNP

AP3-β (785/1115 aa; 70.4%)
MFNKFGSTSETLSKASAGLLRIGTDAHLYDDPEDVNIAPLLDSKFESEKCEALKRLLALIAQGFDVSNFFPQVVKNVASQSSEVKKL
VYLYLLQYAEKRPNEALLSINYFQKDLGDPNPLVRAWALRTMAGIRLHVIAPLALAAVSKCARDPAVYVRRCAANALPKLHDLRL
EEHASAIEELVGILLNDHSPGVVGAAAAAFTSICPNNFKLIGKNYKKLCQILPDVEEWGQILLIGTLLRYVVARHGLVRESLMLSIHG
TNSNGFCEKDGLGRDLTLDKEDGGKSDSFDVNLVSLVSKCYIQGPDEYLSRSSCTDTVSSAFDTKETTSIAHNEDVKILLQCTSPLL
WSNNSAVVLAAAGVQWIMAPLEDVKKIVKPLLFLLRSSSASKYVVLCNILVFAKAVPSLFAPHFENFFICSSDAYQVKAYKLEMLS
LIATTSSIASILREFEDYIKDPDRRFAADTVAAIGLCAKRLMTIPTTCLDGLLALVRQESFAGDFESADGEAGVLVQAVMSIQTMIER
DPLRHEKVLIQLFRSLDSIKVAAARATIIWMVGVYCSLGHIIPRMLTTITKYLAWSFKSEASETKLQILNTIAKVLISAEAGDFHMLKR
IVVYVFELGEYDLSYDIRDRTRFLKKLLSCKLASHEPAEDSVASQENIAAHVVEHVFGRKLKSVSPITLHNRFVYLPGSLSQIVLHAAP
GYEPLPKPCSFVYEEQDQLSDLDKQREAAADLDGSEESSETGDENGSSDYDSESSNGSDFSSEGDERTVSNDANDPAAPLIQISETSV
SADQEELRSRRALDLWLDDQPSTSNQTPSALNSNQSSYAKISIGDVGSRVKPKSYSLVDPGNGSGLKVDYAFLSEVSNVSPLHVCVE
VLFENSSAEPILEVNLEDEESMKVADSSEQTLVGKANASYNNIPTLIPMEEISCLEPHQSTKRLIQVRFHHHLLPMRLTLHYNEKKVP
VKLRPDLGYLVKPFSMSIEEFLATESRLPGMFEYSRRCTFDDHVKDSRTENGKDKFLSICESITLKVLSNSNLHLVSVDLPVANSLED
ATGLRLRFSSKILSSEIPLLITITVEGKCTEVLNLTVKINCEETVFGLNLLNRIANFMVEPSSSAT

AP3-δ (484/869 aa; 55.7%)
MSSSSTSIMDNLFQRSLEDLIKGFRLQLLGESNFISRAVEEIRREIKATDLSTKSTALHKLSYLAALHGVDMSWAAFHAVEVVSSSRF
QHKRIGYQAITQSFNDQTSVMLLITNQVRKDLNSANEYEVSLALECLSRIGTHDLARDLTPEVFTLLGSSKSFVKKKAIGVVLRVFE
KYHDAVKVCFKRLVENLETSDPQILSAVVGVFCELATKDPQSCLPLAPEFYKVLVDSRNNWVLIKVLKIFAKLALIEPRLGKKVAEP
ICEHMRRTVAKSLVFECVRTVVSSLSDNEAAVKLAVAKIREFLVEDDPNLKYLGLNALSIVAPKHLWAVLENKEVVVKAMSDEDP
NVKLEALHLLMAMVNEDNVSEISRILMNYALKSDPLFCNEIIFSVLSACSRNAYEIIVDFDWYLSLLGEMARIPHCQRGEDIEHQLIDI
GMRVRDARPQLVRVSWALLIDPALLGNLFLHPILSAAAWVSGEYVEFSKNPYETVEALLQPRTDLLPPSIKAIYIHSAFKVLVFCLGS
YFSSQEPTSSSLAQESSSGSLLVNVFTHESILSLVNVIELGLGPLSGYHDVEVQERAKNVLGYISVIKQEIAEQLNLQDNETEASRVTA
FMEDVFSEEFGPISATAQEKVCVPDGLELKENLGDLEEICGEHLKPVESDSVSYTDKISFSVSKLRIRDQQEATSSSSPPHEASSLLAE
HRKRHGMYYLTSQKEDQDSNGTSSDYPLANELANEISQDSFNPKRKPNQSKPRPVVVKLDDGDESRITPQAKTNIQTANDDESLSR
AIQSALLVKNKGKEKDRYEGNPNSGQQEKEESSRIENHQNSEKKKKKKKKKGEGSSKHKSRRQNEVASASEQVIIPDFLL

Figure 4: Sequence of MONOPTEROS, SQUINT, OBERON1, AP3-β and AP3-δ proteins with highlighted peptides (in grey) that have been identified in mass spectrometry analysis of at least one of three independent affinity purification experiments. Note that peptides are found from across the entire protein, indicating that intact proteins were precipitated.

Discussion

The aim of this study was to find MP interacting proteins involved in embryonic root initiation. For this purpose, we performed affinity purification on siliques expressing GFP-tagged MP protein under the control of the endogenous MP promoter. We optimized several steps in the affinity purification procedure, including the protein extraction, choice of antibody, and the amount of plant material used. Subsequent mass spectrometry analysis did not reveal any MP interacting protein. However, the affinity purification protocol was optimized such that the MP protein could be reproducible recovered. Furthermore, we identified several interacting transcription factors for the transcription factor TMO5 (Chapter 3) and the chromatin associated plant homeodomain finger protein OBE1 in siliques. This suggests that this optimized affinity purification protocol is suitable to identify nuclear protein complexes, as well as protein complexes in other parts of the cell. On the other hand, it is likely that technical limitations of the affinity purification procedure are the cause for not finding MP interacting proteins. One of the reasons could be that the protein extraction method is not efficient enough in extracting MP protein. Alternatively, the amount of MP protein in the embryo is so low that more than eight grams of plant material are needed to identify MP interacting proteins. It might be worthwhile to use nuclear extraction or expression in Arabidopsis cell suspension cultures to enhance the recovery of low abundant MP protein, although the latter does not identify *in planta* protein complexes (Cho *et al*., 2006; Van Leene *et al*., 2011). Another important obstacle to identify low abundant proteins is the non-specific binding of proteins to the antibody and beads. To reduce the interference of "background" proteins, a tandem affinity procedure might be instrumental (reviewed in Pflieger *et al*., 2011). It is also possible that the MP protein complex binds the DNA tightly and therefore the MP protein complex is precipitated together with the DNA while centrifuging the protein extract. However, Smaczniak *et al* (2012) showed that an unstable protein interaction becomes even more unstable by adding an endonuclease during affinity purification. This suggests that adding DNAse to the protein extract might not be a solution. Finally, another technical problem might be that the affinity of the antibody for the tagged protein is poor. Using other tags with higher affinities such as biotin or FLAG could be a solution (De Boer *et al*., 2003; Gloeckner *et al*., 2007). However, the

GFP-binding protein that we used resulted in low purification efficiencies (Rothbauer *et al*., 2008).

Another reason for not finding the MP protein complex could be that MP is present in many different transcription factor complexes. Each of these complexes could be present in only a few cells of the embryo. The limited number of cells with the same MP protein complex could result in not finding any MP interacting protein. This scenario is plausible because MP appears to have many distinct functions in different cell types of the embryonic root meristem. Each of these functions could be mediated by one or more target genes that are activated by a unique transcription factor complex. A possible solution to this problem is to perform cell sorting on embryos expressing GFP in a certain cell type. However, this technique demands intense training to achieve reproducible results, and the successful use of this technique is not yet reported. Yet another reason that could explain why no MP interacting proteins are found is that the protein complexes might be too unstable or transient to detect. It is unknown where transcription factor complexes assemble. They could assemble at the site of protein synthesis, in specific locations inside the cytoplasm or nucleus, or on the DNA and possibly on the promoters of target genes. If the putative MP protein complexes assemble on the DNA only shortly before transcription is initiated, the complex might be very transient. In addition, the transcription factor complex might easily dissociate when the cellular environment changes because of protein extraction. The affinity, stability and timing of transcription factor complexes might differ depending on the type of transcription factors involved. In addition, the MP protein itself might also be unstable and therefore we can possibly only detect a fraction of the MP protein in the mass spectrometry analysis. In line with the latter scenario, yeast-two-hybrid experiments suggest that MP binds to components of a CULLIN3 complex that possibly targets MP for degradation (Esther Lechner and Pascal Genschik, personal communication). A final, perhaps unlikely, reason that could explain why no MP interacting proteins are found is that there are no MP-interacting proteins.

In conclusion, the inability to find MP interacting proteins in this study illustrates that there are still many open questions about the time and place that putative MP protein complexes are assembled and active in the cell. Extensive further research needs to be performed to mechanistically unravel how MP precisely activates its target genes. MP is one of seven ARFs that are expressed in the globular stage embryo (Rademacher *et al*, 2011). Six of these ARFs are expressed in the proembryo at globular stage. However, combinations of MP with these other ARFs can not solely account for the observed expression patterns of MP target genes. Nonetheless, future experiments will learn if ARF heterodimers contribute to the expression of MP target genes. In summary, we have optimized an affinity purification

procedure that allows the identification of nuclear protein complexes in the embryo. This novel technique is an important step towards unraveling the molecular mechanisms involved in embryonic root initiation.

Material & Methods

Plant growth and Material

All seeds were surface sterilized, sown on solid MS plates and vernalized for one day before growing at a constant temperature of 22°C in a growth room. The *mp-B4149* allele in Columbia background and the pGreenIIBASTA:pMP-MP-6HA:NOSt construct were described in Weijers *et al.* (2006). The pGreenIIBASTA:pMP-MP-GFP:NOSt construct with eGFP inserted in the MscI restriction site in the coding sequence of MP was described in Chapter 2.

Cloning

All cloning was performed using conventional restriction sites. The MP cassette was generated by PCR-amplifying stretches of the genomic MP sequence and introducing them into the pGreeenIIBASTA:NOSt vector in a specific order: (1). 896 bp of the 3'UTR. (2). 3' region of the coding sequence containing exons and introns. (3). 5' region of the coding sequence containing exons and introns. (4). 4113 bp of the MP promoter upstream of the ATG. This resulted in a MP cassette with a XhoI restriction site directly upstream of the ATG, an EcoRI restriction site in the coding sequence (that encodes the variable middle region of ARF proteins), and a SpeI restriction site directly upstream of the stop codon. Primers with restriction sites are listed in Table 4. Subsequently, different tags were inserted in the restriction sites of the MP cassette. eGFP was PCR-amplified and inserted into the XhoI, EcoRI and SpeI restriction sites. To generate biotin-tagged MP constructs with the coding region of the *Escherichia coli* birA protein ligase gene, we first PCR-amplified 3xHA-tagged birA containing the nuclear localization signal SV40 from the pGEM-SD2 plasmid 706-0034 (John Strouboulis, Department of Cell Biology, Erasmus MC) using primers with EcoRI restriction sites and introduced this fragment into the pGreenIIKAN:35S:NOSt construct. We subsequently PCR-amplified 35S-sv40-birA-HA-tNOS using primers with KpnI restriction sites and introduced this fragment into the MP cassette. Next, we annealed two 5' phosphorylated primers containing the biotin sequence (De Boer *et al*., 2003) with overhangs for XhoI, EcoRI or SpeI restriction sites and introduced them into the MP cassette containing the birA sequence. The double StrepII-tagged MP construct was generated by annealing two 5' phosphorylated primers contain-

ing the tandem StrepII sequence (Gloeckner *et al*., 2007) with overhangs for the SpeI restriction sites and introducing them into the MP cassette. Likewise, the FLAG-StrepII-tagged MP construct was generated by annealing four different 5' phosphorylated primers containing the FLAG-StrepII sequence (Gloeckner *et al*., 2007) with overhangs for the SpeI restriction sites and introducing them into the MP cassette. All fusion constructs were transformed into *mp-B4149* heterozygous plants by floral dip using the *Agrobacterium* strain GV3101(pSoup).

Western blotting and gel filtration

For Western blotting we used several different antibodies: two polyclonal anti-GFP antibodies (ab290, abcam; 11814460001, Roche), a monoclonal anti-GFP-HRP antibody (130-091-833, Miltenyi), a custom-made polyclonal anti-GFP antibody (Eurogentec), a monoclonal anti-FLAG antibody (A 8592, SIGMA), a streptavidin-peroxidase polymer (S 2438, SIGMA) two different monoclonal anti-HA antibodies (sc57592, Santa Cruz; HA.11 Covance), and secondary anti-rabbit-HRP (A 0545 SIGMA) and anti-mouse-HRP (A 9917 SIGMA) antibodies. For gel filtration analyses, protein extracts were prepared from 7-day-old Arabidopsis seedlings in protein extraction buffer (20 mM Tris-HCl, pH 7.4, 200 mM NaCl, 10% glycerol, 1 mM PMSF, and 1 mM ß-mercaptoethanol) as previously described in Dohmann *et al* (2005). Size exclusion chromatography of 300 µg of protein extract was performed using a Superose 6 HR column (Amersham Pharmacia, Freiburg, Germany) as previously described (Schwechheimer and Deng, 2002). We used monoclonal anti-HA antibody (sc57592, Santa Cruz) to detect MP-6HA on Western blot.

Affinity purification and mass spectrometry analysis

The affinity purification procedure with Sepharose 4B beads coupled to purified custum-made anti-YFP antibody (Eurogentec) was previously described in Karlova *et al* (2006). In affinity purification procedure with monoclonal anti-GFP antibody (Miltenyi) coupled to magnetic beads, between 0.5 and 8 grams of siliques, seedlings or flowers were ground in a mortar with liquid nitrogen. The powder was homogenised in extraction buffer (50 mM Tris-HCl, 150 mM NaCl, 1% Nonidet P-40 [NP40], protease inhibitors mix cocktail [Roche, 1 tablet per 50 ml]). After grinding, the protein extract was sonicated 3 x 15 seconds with a probe sonicator (MSE) at half-maximal power and incubated on ice for 30 min. The NP40 in the protein extract was then diluted to 0.2%, followed by 2 x 15 min centrifugation at 20.000 rpm at 4 ºC. The supernatant was incubated for 2 h at 4°C with rotation with 100 µl magnetic beads coupled to a monoclonal anti-GFP antibody (Miltenyi). µColumns on a MACS MultiStand (Miltenyi) were equilibrated

with 200 µl extraction buffer containing 0.1% NP40, then the supernatant was passed through the µColumn. The column was subsequently washed with 4 x 200 µl extraction buffer containing 0.1% NP40 and 2 x 500 µl 50 mM ammoniumcarbonate. The beads were eluted from the column into Low Bind tubes (Eppendorf AG) with 50 µl 50 mM ammoniumcarbonate that was heated to 95°C.
For MS measurements, 1 µl 50 mM DTT in 50 mM NH_4HCO_3 was added to the beads and incubated at 37 ºC. After two hours 1 µl 100 mM iodocetamide in 50 mM NH_4HCO_3 was added and incubated two hours at room temperature in the dark. Subsequently 1 µl 200 mM cysteine in 50 mM NH_4HCO_3 and 1 µl trypsin sequencing grade (0.5 µg/µl in1 mM HCl) were added and the beads were incubated over night at 20ºC while shaking. The following day 1.2 µl trifluoro acetic acid (TFA) was added to adjust to approximately pH 3 and the beads were centrifuged 3 minutes at maximum speed. The supernatant was subjected to nLC-MS/MS analysis using a LTQ-Orbitrap. Data was analyzed using the Bioworks software package version 3.1.1 (Thermo Scientific). The in gel digestion protocol was previously described in Mravec *et al* (2011).

Acknowledgements

We would like to thank Walter van Dongen for technical advice concerning the optimization of the affinity purification procedure.

Tables

Table 4. primers used for cloning of MP fusion proteins. Primers contain restriction sites that were used for cloning. * restriction sites in primers used to amplify GFP and biotin are not shown as these sequences were amplified with overhangs for three different restriction sites (XhoI, EcoRI and SpeI).

Amplified region	Restriction site	Sequence
Promoter MP cassette	KpnI XhoI	CAGGTACCGACGTGTGTGAATTACC GTCTCGAGCATCATACAGAGAGATTTTTC
5′ region of coding sequence MP cassette	XhoI EcoRI	GACTCGAGGCTTCATTGTCTTGTGTTG CTGAATTCTGGATCAGACTGTGGTTGG
3′ region of coding sequence MP cassette	EcoRI SpeI	CCGAATTCATAAATGGATTCTCTTTCC CCACTAGTTGAAACAGAAGTCTTAAGATCG
Downstream region MP cassette	SpeI SstI	GCACTAGTTAAATGTAACAATATAAAAATGATCTCATG CTGAGCTCCACCCATAACTCATATTCC
Green Fluorescent protein	XhoI/EcoRI/SpeI*	atggtgagcaagggcgaggagc CTTGTACAGCTCGTCCATGCCG
Biotin (annealed 5′ phosphorylated primers)	XhoI/EcoRI/SpeI*	gcttctttctcttagacaaatccttgattctcaaaagatggagtggagatctaacgctggaggatctc AGATCCTCCAGCGTTAGATCTCCACTCCATCTTTTGAGAATCAAGGATTT GTCTAAGAGAAGAAGCC
SV40-BirA-HA	EcoRI EcoRI	GAATTCATGGCTCCAAAGAAGAAGAGAAAGGTTAAGGATAACACCGTGC CACTG GAATTCTCAAGCATAATCAGGAACATCATAAGGATATTTTTCTGCACTAC GCAGGG
Tandem StrepII (annealed 5′ phosphorylated primers)	SpeI SpeI	ctagtTGGTCTCATCCTCAATTTGAGAAAGGTGGAGGTTCTGGAGGGGGTTC GTGGTCTCATCCACAGTTCGAGAAGa ctagtCTTCTCGAACTGTGGATGAGACCACGAACCCCCTCCAGAACCTCCAC CTTTCTCAAATTGAGGATGAGACCAa
StrepII-FLAG (annealed 5′ phosphorylated primers)	SpeI	ctagtTGGTCTCATCCTCAATTTGAGAAAGGTGGAGGTTCAGGTGGTGGAT CAGGAGGTGGTTCATGGTCTCATCCACAGTTCGAGAAGGGTGCATCAGG TGAGGATTATAAGGATGACGATGACAAGa AACTGTGGATGAGACCATGAACCACCTCCTGATCCACCACCTGAACCTCC ACCTTTCTCAAATTGAGGATGAGACCAa ctagtCTTGTCATCGTCATCCTTATAATCCTCACCTGATGCACCCTTCTCG

References

Bu Q, Castillon A, Chen F, Zhu L and Huq E. (2011). Dimerization and blue light regulation of PIF1 interacting bHLH proteins in Arabidopsis. Plant Mol Biol. 77(4-5): 501-511.

Chandler JW, Cole M, Flier A and Werr W. (2009). BIM1, a bHLH protein involved in brassinosteroid signalling, controls Arabidopsis embryonic patterning via interaction with DORNRÖSCHEN and DORNRÖSCHEN-LIKE. Plant Mol Biol. 69(1-2): 57-68.

Chandler JW, Cole M, Flier A, Grewe B and Werr W. (2007). The AP2 transcription factors DORNRÖSCHEN and DORNRÖSCHEN-LIKE redundantly control Arabidopsis embryo patterning via interaction with PHAVOLUTA. Development. 134(9): 1653-1662.

Cho YH, Yoo SD and Sheen J. (2006). Regulatory functions of nuclear hexokinase1 complex in glucose signaling. Cell. 127(3): 579-589.

De Boer E, Rodriguez P, Bonte E, Krijgsveld J, Katsantoni E, Heck A, Grosveld F and Strouboulis J. (2003). Efficient biotinylation and single-step purification of tagged transcription factors in mammalian cells and transgenic mice. Proc Natl Acad Sci U S A. 100(13): 7480-5.

De Folter S, Urbanus SL, van Zuijlen LG, Kaufmann K and Angenent GC. (2007). Tagging of MADS domain proteins for chromatin immunoprecipitation. BMC Plant Biol. 7: 47.

Dohmann EM, Kuhnle C and Schwechheimer C. (2005). Loss of the CONSTITUTIVE PHOTOMORPHOGENIC9 signalosome subunit 5 is sufficient to cause the *cop/det/fus* mutant phenotype in Arabidopsis. Plant Cell. 17(7): 1967-1978.

Eulgem T, Rushton PJ, Robatzek S and Somssich E. (2000). The *WRKY* superfamily of plant transcription factors. Trends Plant Science. 5(5): 199-206.

Forde CE and McCutchen-Maloney SL. (2002). Characterization of transcription factors by mass spectrometry and the role of SELDI-MS. Mass Spectrom Rev. 21(6): 419-439.

Gloeckner CJ, Boldt K, Schumacher A, Roepman R and Ueffing M. (2007). A novel tandem affinity purification strategy for the efficient isolation and characterisation of native protein complexes. Proteomics. 7(23): 4228-4234.

Grosfeld F, Rodriguez P, Meier N, Kripc S, Pourfarzad F, Papadopoulos P, Kolodziej K, Patrinos GP, Hostert A and Strouboulis J. (2005). Isolation and characterization of hematopoietic transcription factor complexes by in vivo biotinylation tagging and mass spectrometry. Ann N Y Acad Sci. 1054: 55-67.

Hamann T, Benkova E, Bäurle I, Kientz M and Jürgens G. (2002). The Arabidopsis *BODENLOS* gene encodes an auxin response protein inhibiting MONOPTEROS-mediated embryo patterning. Genes Dev. 16(13): 1610-1615.

Hardtke CS, Ckurshumova W, Vidaurre DP, Singh SA, Stamatiou G, Tiwari SB, Hagen G, Guilfoyle TJ and Berleth T. (2004). Overlapping and non-redundant functions of the Arabidopsis auxin response factors MONOPTEROS and NONPHOTOTROPIC HYPOCOTYL 4. Development. 131(5): 1089-1100.

Karlova R, Boeren S, Russinova E, Aker J, Vervoort J and De Vries S. (2006). The Arabidopsis SOMATIC EMBRYOGENESIS RECEPTOR-LIKE KINASE1 protein complex includes BRASSINOSTEROID-INSENSITIVE1. Plant Cell. 18(3): 626-638

Kaufmann K, Smaczniak C, de Vries S, Angenent GC and Karlova R. (2011). Proteomics insight into plant signaling and development. Proteomics. 11(4): 744-755.

Mravec J, Petrášek J, Li N, Boeren S, Karlova R, Kitakura S, Pařezová M, Naramoto S, Nodzyński T, Dhonukshe P, Bednarek SY, Zažímalová E, de Vries S and Friml J. (2011). Cell plate restricted association of DRP1A and PIN proteins is required for cell polarity establishment in Arabidopsis. Curr Biol. 21(12): 1055-1060.

Niu Y, Figueroa P and Browse J. (2011). Characterization of JAZ-interacting bHLH transcription factors that regulate jasmonate responses in Arabidopsis. J Exp Bot. 62(6): 2143-2154**.**

Pauwels L, Barbero GF, Geerinck J, Tilleman S, Grunewald W, Pérez AC, Chico JM, Bossche RV, Sewell J, Gil E, García-Casado G, Witters E, Inzé D, Long JA, De Jaeger G, Solano R and Goossens A. (2010). NINJA connects the co-repressor TOPLESS to jasmonate signalling. Nature. 464(7289): 788-791.

Pflieger D, Bigeard J and Hirt H. (2011). Isolation and characterization of plant protein complexes by mass spectrometry. Proteomics. 11(9): 1824-33. doi: 10.1002/pmic.201000635.

Rodriguez P, Bonte E, Krijgsveld J, Kolodziej KE, Guyot B, Heck AJ, Vyas P, de Boer E, Grosveld F and Strouboulis J. (2005). GATA-1 forms distinct activating and repressive complexes in erythroid cells. EMBO J. 24(13): 2354-2366.

Rothbauer U, Zolghadr K, Muyldermans S, Schepers A, Cardoso MC and Leonhardt H. (2008). A versatile nanotrap for biochemical and functional studies with fluorescent fusion proteins. Mol Cell Proteomics. 7(2): 282-289.

Rademacher EH, Möller B, Lokerse AS, Llavata-Peris CI, van den Berg W and Weijers D. (2011). A cellular expression map of the Arabidopsis *AUXIN RESPONSE FACTOR* gene family. Plant J. 68(4): 597-606.

Saiga S, Möller B, Watanabe A, Abe M, Weijers D, and Komeda Y. (2012). Control of embryonic meristem initiation in *Arabidopsis* by PHD finger protein complexes. Development. *In press.*

Smaczniak C, Immink RG, Muiño JM, Blanvillain R, Busscher M, Busscher-Lange J, Dinh QD, Liu S, Westphal AH, Boeren S, Parcy F, Xu L, Carles CC, Angenent GC and Kaufmann K. (2012). Characterization of MADS-domain transcription factor complexes in Arabidopsis flower development. Proc Natl Acad Sci U S A. e-pub ahead of print doi: 10.1073/pnas.1112871109

Smith MR, Willmann MR, Wu G, Berardini TZ, Möller B, Weijers D and Poethig RS. (2009). Cyclophilin 40 is required for microRNA activity in Arabidopsis. Proc Natl Acad Sci U S A. 106(13): 5424-5429.

Shin R, Burch AY, Huppert KA, Tiwari SB, Murphy AS, Guilfoyle TJ and Schachtman DP. (2007). he Arabidopsis transcription factor MYB77 modulates auxin signal transduction. Plant Cell. 19(8): 2440-2453.

Tian Q. (2006). Proteomic exploration of the Wnt/beta-catenin pathway. Curr Opin Mol Ther. 8(3): 191-197.

Van Leene J, Eeckhout D, Persiau G, Van De Slijke E, Geerinck J, Van Isterdael G, Witters E and De Jaeger G. (2011). Isolation of transcription factor complexes from Arabidopsis cell suspension cultures by tandem affinity purification. Methods Mol Biol. 754: 195-218.

Varaud E, Brioudes F, Szécsi J, Leroux J, Brown S, Perrot-Rechenmann C and Bendahmane M. (2011). AUXIN RESPONSE FACTOR8 regulates Arabidopsis petal growth by interacting with the bHLH transcription factor BIGPETALp. Plant Cell. 23(3): 973-983.

Weijers D, Schlereth A, Ehrismann JS, Schwank G, Kientz M and Jürgens G. (2006). Auxin triggers transient local signaling for cell specification in Arabidopsis embryogenesis. Dev Cell. 10(2): 265-270.

Zwiewka M, Feraru E, Möller B, Hwang I, Feraru MI, Kleine-Vehn J, Weijers D and Friml J. (2011). The AP-3 adaptor complex is required for vacuolar function in Arabidopsis. Cell Res. 21(12): 1711-1722.

Chapter 7

General Discussion

Barbara Möller

Laboratory of Biochemistry, Wageningen University, Dreijenlaan 3,
6703HA Wageningen, the Netherlands

Embryonic root initiation in *Arabidopsis thaliana* involves the coordinated specification of several cell types in the early embryo that will jointly establish the root meristem. The MONOPTEROS (MP) transcription factor is the main executer of auxin signaling in the early embryo, and is required for root meristem formation (reviewed in Chapter 1). The results described in this thesis collectively show that MP activity is involved in diverse aspects of embryonic root initiation, and suggest that MP is required to specify nearly all cell types that form the embryonic root meristem. MP activates transcription of downstream genes in cells that will contribute to the early embryonic root meristem. These downstream factors are in turn involved in distinct aspects of embryonic root initiation. By combining the results of the individual thesis chapters, novel mechanisms of embryonic root initiation emerge. In this last chapter, I will discuss these novel mechanisms that MP employs to set up the root meristem in the early embryo.

MP controls diverse aspects of embryonic root initiation

The embryonic root is initiated when cells in the basal half of the early embryo adopt the different cell identities that constitute a root meristem. The cell types that form the root meristem are the mitotically inactive Quiescent Center (QC) cells and the surrounding tissue-specific stem cells that continuously divide to supply new cells for the different tissue types. Until recently, not much was known about root meristem initiation in the early embryo besides the requirement for auxin signaling and MP action (reviewed in Chapter 1). It was known that MP activity is essential to regulate the cell division plane of the hypophysis cell - the precursor of the QC - in the globular stage embryo (Berleth and Jürgens, 1993; Hardtke and Berleth, 1998). MP specifies the hypophysis in part by promoting auxin transport into the hypophysis cell via regulation of *PIN1* expression in the first vascular cells (Weijers *et al*., 2006). Furthermore, a microarray on seedlings identified four novel *TARGET OF MONOPTEROS (TMO)* genes that are all transcription factors expressed in the early embryo (Chapter 2). In this thesis, we further explored the role of MP in embryonic root initiation and found that MP controls diverse aspects of root meristem specification. We showed that MP directly activates *TMO7* expression and that the TMO7 protein moves to the hypophysis cell where it contributes to the specification of this cell (Chapter 2). Thus, both the transport of auxin and the TMO7 protein into the hypophysis depend on MP activity. Several observations indicate that MP, in addition to its role in hypophysis specification, is involved in the specification of the first vascular and ground tissue cells of the embryonic root meristem. (1). We found that MP activates transcription specifically in the first vascular and ground tissue cells of the embryonic root meristem (Chapters 2&4). (2). MP is required to orient the division plane in the first vascular and

ground tissue cells of the embryonic root meristem. Importantly, MP activity does not seem to be required for the general progression of cell division in these cells, indicating that MP specifically regulates the plane of division. (Chapters 3&5). (3). *TMO5* and its closest homologues are required downstream of MP to activate proliferation of vascular cells in the embryonic and postembryonic root meristem (Chapter 3). Regulation of gene transcription, cell proliferation and proper cell division planes are different aspects of cell identity, and surprisingly, these all seem to be controlled by MP. Even more unexpectedly, MP appears to control aspects of cell identity in nearly all cell types that contribute to the embryonic root meristem, including the hypophysis and the first vascular and ground tissue cells.

The general role of MP in embryonic root meristem initiation might reveal some of the molecular mechanisms involved. First, the coordinated regulation of transcription, cell division planes, and proliferation activity within one cell type by a single transcription factor suggests that these processes are intimately connected at the molecular level. However, based on our results, it can not be explained how these processes are intertwined. Several processes involved in establishing aspects of cell identity might be causally related, or alternatively, parallel pathways controlling distinct aspects of cell identity might operate in the embryonic root meristem. An interesting observation in this context is the requirement of a functional *TMO5* subclade acting downstream of MP for the activation of cell proliferation and for proper cell division planes in the first vascular cells of the embryonic root meristem. Similarly, TMO7 is required to specify the embryonic root meristem and to regulate the proper division plane of the hypophysis. These results suggest that one level downstream of MP activity, several aspects of cell identity can still be controlled by one factor. Perhaps this reflects the position of MP at the summit of a "molecular hierarchy", as is also suggested by the high number of transcription factors that are regulated by MP (Chapters 2&4). Another outcome of the results in this thesis is that MP appears to initiate specification of nearly all cells that form the embryonic root. The specification of cell types that constitute the root meristem probably occurs simultaneously or shortly after each other in embryo development, and this is probably crucial for the development of the embryonic root. Thus, the presence of a master regulator of early embryonic root initiation might ensure the coordinated specification of different cell types within the root meristem. MP activity does not seem to be generally required for root formation *per se*, as MP is not required for root initiation in embryos mutant for the GATA transcription factor *HANABA TARANU (HAN)* or the corepressor *TOPLESS (TPL)*, and in lateral roots (Nawy *et al.*, 2010; Long *et al.*, 2002; De Smet *et al.*, 2010). Interestingly, root meristem formation in *han* mutants is severely delayed and shifted towards the apical embryo region as result of a delay

and upward shift of the generation of an auxin maximum. These findings suggest that in some cases, other factors can induce embryonic root formation in the absence of MP. As auxin signaling seems to be essential for root formation in different contexts (Nawy *et al.*, 2010; De Smet *et al.*, 2010), redundant AUXIN RESPONSE FACTORs (ARFs; Rademacher *et al*., 2011) are obvious candidates. However, MP action in the embryo could be required for the proper timing of root initiation.

The crucial role of MP in embryonic root initiation makes it extremely important that MP is active in the early embryo, and that its activity is robustly regulated. Recently, several findings have suggested that the activation and maintenance of *MP* transcription in the embryo could be robust. Lau *et al* (2011) showed that MP directly activates both its own transcription and that of its inhibitor *BODENLOS (BDL)* that is co-expressed with *MP* throughout embryo development. Auxin stimulates BDL degradation and thereby enhances the transcriptional activity of MP. Modeling suggests that auxin can thus trigger an autoregulatory feedback loop with a switch-like behavior, such that MP only becomes active above a threshold concentration of auxin (Lau *et al.*, 2011). Following the initial activation of *MP* expression in the early embryo, this autoregulatory feedback loop could be sufficient to stably maintain MP activity in the embryo throughout embryo development (Lau *et al.*, 2012). Furthermore, *SHORT SUSPENSOR (SSP)* expression in the suspensor is another safety mechanism to restrict *MP* expression to the embryo proper (Rademacher *et al.*, 2012). *MP* is first expressed in the apical daughter cell of the zygote that will develop into the embryo proper. *MP* expression in the apical cell could be activated by the transport of auxin into this cell by PIN7 in the presence of just a few zygotic *MP* transcripts. However, regulation of PIN7 expression and localization is unknown. Further research is required to carefully dissect the mechanisms of MP regulation at the transcriptional and post-translational level, and this will certainly contribute to a better understanding of embryonic root initiation.

In summary, the results described in this thesis show that MP controls diverse aspects of cell identity in nearly all cells that contribute to the embryonic root meristem. Therefore, these results reveal novel mechanisms that auxin employs to specify the root meristem in the early embryo. Moreover, the results in this thesis allow a refinement of the current paradigm of the hypophysis as the root meristem founder cell, as embryonic root formation seems to start with specification of the inner basal embryo cells rather than the hypophysis.

Embryonic root meristem formation requires multiple specification steps

MP instructs basal embryo cells of the globular stage embryo to adopt the cell identities that shape the root meristem. In later stages of embryo development, several other transcription factors are known to be required to specify or maintain at least one of the cell types in the root meristem (Aida *et al.*, 2004; Scheres *et al.*, 1995. Wysocka-Diller *et al.*, 2000, Sarkar *et al.*, 2007). This shows that embryonic root meristem specification involves multiple subsequent specification steps. Root initiation in the early embryo is controlled by MP, while later steps of embryonic root formation as well as root meristem maintenance are at least partly regulated by other developmental pathways. The stepwise specification of cell types in the root meristem can be illustrated by several results from this thesis. (1). MP is required in the early embryo to specify the hypophysis cell, which is the precursor of the QC (Chapter 2). In subsequent stages of embryo development, the transcription factors *SCARECROW (SCR)*, *SHORTROOT (SHR)* and *PLETHORA (PLT) 1* and *2* are indispensable to create and maintain the QC (Wysocka-Diller *et al.*, 2000; Scheres *et al.*, 1995; Aida *et al.*, 2004). (2). MP is required to specify aspects of the identity of the first vascular and ground tissue cells in the developing root meristem (Chapters 3-5). Later, around heart stage of embryo development, SHR and SCR are required to control ground tissue patterning (Wysocka-Diller *et al.*, 2000; Scheres *et al.*, 1995). These findings suggest the existence of multiple auxin-dependent pathways in root meristem specification, similar to the sequential action of auxin in lateral root initiation (De Smet *et al.*, 2010). In both processes, auxin seems to control root formation at multiple stages in time. However, in contrast to lateral root initiation, not all transcription factors involved are ARFs. It is possible that *PLT*, *SHR* and *SCR* genes are required to maintain the embryonic root meristem rather than to specify this stem cell niche (Scheres, 2007). However, this seems unlikely in light of the results presented above, and would imply the transient activation of cell identities in embryos mutant for these genes, which has not yet been reported.

PLT expression at least partly depends on MP activity and is slowly induced by auxin, and *SHR* transcription might also be regulated by auxin in the embryonic root meristem (Aida *et al.*, 2004; Chapter 5). Furthermore, MP affects auxin distribution via activation of *PIN1* and possibly *PIN4* and *LAX2* expression in the early embryo, while PLTs activate *PIN4* expression during embryo development (Chapters 2&4; Friml *et al.*, 2003; Ugartechea-Chirino *et al.*, 2010; Blilou *et al.*, 2005). It is possible that MP – and other ARFs like ARF7 - indirectly activate the *PLT* and *SHR* genes to ensure that these are active when their action is required (Aida *et al.*, 2004). This would link the early events in root meristem specification to the establishment of a system for root meristem maintenance at heart stage of

embryo development. Moreover, these results show that multiple positive feedback loops ensure the generation and maintenance of an auxin maximum in the embryonic root meristem. MP is still expressed at heart stage of embryo development, and is particularly strongly expressed in the QC (Hamann *et al.*, 2002), but it is not clear if MP is still required at these later embryo stages to maintain root meristem integrity and to maintain transcription of its target genes. It would be interesting to see how the root meristem develops if MP activity is eliminated in embryos from heart stage of embryogenesis onwards. Future research might also reveal additional roles for the *PLT* genes in later steps of stem cell specification. Together, all these findings should result in an integrated molecular framework for embryonic root initiation including sequential specification steps.

MP-dependent intercellular communication shapes the embryonic root meristem. Despite the organized cell division patterns in Arabidopsis embryo development, cell identities inside the root meristem are largely determined by positional information (Van den Berg *et al.*, 1995). This implies extensive intercellular communication, and laser ablation studies indeed revealed signaling between almost all cells that are in direct contact within the postembryonic root (Van den Berg et al., 1995, 1997). Several intercellular signaling pathways that are active in root and shoot meristem maintenance have been revealed, and these include the activity of secreted peptides, mobile transcription factors and small RNAs (reviewed in Van Norman *et al.*, 2011; Meng, 2012). In both meristems, CLE peptides bind to receptor-like kinases to restrict the expression of related homeobox transcription factors that in turn inhibit differentiation of surrounding stem cells (Sarkar *et al.*, 2007; De Smet *et al.*, 2008; Stahl *et al.*, 2009). In addition to these CLE peptides, another class of small peptides called root meristem growth factors (RGFs) were recently shown to be required to maintain QC and stem cell identity in the root meristem (Matsuzaki *et al.*, 2010; Zhou *et al.*, 2010). The expression of two of these RGF peptides might be activated by MP (Chapter 4). However, mutants lacking activity of all RGF members exhibit normal embryo development (Matsuzaki *et al.*, 2010).

In this thesis, we add several novel MP-dependent ways of intercellular communication that are active in root meristem specification. We observed movement of TMO7 protein from the first vascular cells where its transcription is activated by MP to the adjacent hypophysis cell (Chapter 2). Here, TMO7 contributes to the asymmetric division of the hypophysis. In addition to TMO7, SHR is another mobile transcription factor known to be involved in the specification of the embryonic root meristem (reviewed in Van Norman *et al.*, 2011). Interestingly, MP might also induce transcription of SHR in the embryonic root meristem, and thus

promote ground tissue specification in the root meristem (Chapter 5). Multiple MP-dependent intercellular signaling pathways involved in ground tissue specification could exist in the embryonic root meristem, as MP appears to activate transcription of a receptor-like kinase specifically in the first ground tissue cells of the embryonic root (Chapter 4). Other receptor-like kinases operate in root and shoot maintenance, and seem to be required for protoderm specification in the early embryo (reviewed in Lau *et al.*, 2012). Therefore, local signaling of neighboring cells inside the embryonic root meristem seems to be fundamental for its proper development, and further research should identify multiple signaling modules involved in this process.

The role of chromatin remodeling in root initiation

Epigenetic control over gene transcription represents another level of complexity in plant development. It plays a role in establishing expression patterns through the inheritance of epigenetic marks in daughter cells of dividing cells, such as stem cells. Recent findings suggest that chromatin modifications are also involved in embryonic root initiation, as mutations in the SWI-SNF chromatin remodeling complex result in arrested embryo development at globular stage (reviewed in Reyes, 2006; Jarillo *et al.*, 2009). PLANT HOMEODOMAIN (PHD) finger proteins are involved in the recognition and translation of the histone code into patterns of gene expression. These proteins bind to trimethylated lysine on histone H3 (H3K4), which is a typical mark of active chromatin (Mellor, 2006). Recent publications combined with results in this thesis suggest that MP could direct root initiation by recruiting the activity of the PHD finger proteins OBERON1 (OBE1) and 2. The latter are required for root initiation, and *obe1 obe2* double mutants show aberrant hypophysis division similar to *mp* mutants (Saiga *et al.*, 2008). Moreover, expression of the *PLT1*, *SCR* and *WOX5* transcription factors that are involved in root formation, is lost in the *obe1 obe2* double mutant. In contrast, *MP* is still expressed in *obe1 obe2* double mutants, and genetic analysis suggests that *MP* is epistatic over *OBE1* (Saiga *et al.*, 2008; Thomas *et al.*, 2009). These results suggest that cell identity specification in *obe1 obe2* mutants is compromised downstream of MP activity. Transcript profiling showed that a large number of genes involved in auxin signaling is altered in the *obe1 obe2* double mutant (Thomas *et al.*, 2009). These results suggest that the PHD finger proteins OBE1 and 2 bind to the chromatin associated with genes involved in auxin signaling to affect their transcription.

Recently, Saiga *et al* (2012) showed that expression of *TMO5* and *7* is lost in the embryonic root meristem of *obe1 obe2* double mutants, and that OBE1 directly binds to the *TMO7* promoter. Although MP does not activate *OBE1* expression,

the binding of OBE1 to the *TMO7* promoter could indirectly be the result of MP action, perhaps mediated by type IId *WRKY* transcription factors (Saiga *et al.*, 2008; Eulgem *et al.*, 2000). In the embryo, OBE1 protein interacts with nearly all WRKY transcription factors of type IId, including WRKY7,11, 21, and 39 (Chapter 6). These type IId *WRKY* transcription factors are all down-regulated in a microarray on embryos in which MP activity was inhibited (Chapter 4; data not shown). The expression pattern of *WRKY21* is strikingly similar to that of *MP* in embryo development (Chapter 4). Therefore, MP might activate class IId *WRKY* transcription factors that in turn interact with the OBERON protein complex to affect gene transcription. Interestingly, type III WRKYs bind to HISTONE DEACETYLAE 19 (HDA19) in plants, suggesting a similar interaction for type IId WRKYs (Kim *et al.*, 2008). Surprisingly, type III WRKYs function as transcriptional activators in plant cells, but their activity is counteracted by HDA19 (Kim *et al.*, 2008). A similar mechanism might operate in embryonic root initiation to fine tune the transcriptional activity downstream of MP. Possibly, an OBE-WRKY-HDA complex both modifies and recognizes the acetylation status of several genes involved in embryonic root formation to regulate their transcription. However, further research is required to understand the details of this process, and to identify the targets of the WRKY-OBE complex. Recently, a WRKY has been shown to activate transcription of a *WUSCHEL HOMEOBOX RELATED (WOX)* transcription factor that is required for early embryo development (Ueda *et al.*, 2011). Type IId WRKYs are characterized by a calmodulin binding domain, but the function of this domain is not understood (Kim *et al.*, 2008). Interestingly, MP might both activate and repress TMO7 transcription via direct binding to the TMO7 promoter and the WRKY-OBE-HDA complex, suggesting that precise control over TMO7 protein levels is important for hypophysis specification.

In conclusion, this thesis describes several novel mechanisms that are involved in embryonic root initiation, including several inductive signaling events and a possible role for epigenetic control. Also putative connections to signaling by other plant hormones are revealed by the identification of *LONELY GUYs (LOGs)* and *PLANT U-BOX25 (PUB25)* as putative MP target genes (Chapter 4; Kuroha *et al.*, 2009; Tokunaga *et al.*, 2011; Amador *et al*., 2001). *LOGs* are cytokinin-activating enzymes and *PUB25* is involved in gibberellin signaling. The putative activation of *LOG* transcription by MP corresponds with the reported requirement for local cytokinin signaling in the early embryo to specify the root meristem (Müller and Sheen, 2008). MP is highly expressed in the apical daughter cell after hypophysis division, and this might contribute to active cytokinin signaling specifically in these cells via activation of *LOG* transcription. In addition, auxin negatively

regulates cytokinin signaling in the basal daughter cell of the hypophysis (Müller and Sheen, 2008), and this might be achieved by other ARFs. Further research should unravel the extent of hormone crosstalk during embryonic root formation. In summary, the results in this thesis indicate a major role for auxin signaling during early stages of embryo development, and show that MP employs many strategies to influence root initiation. Importantly, this work showed that MP not only specifies the hypophysis, but also the first vascular and ground tissue cells of the embryonic root initiation. Further research might reveal how the role of MP in embryonic root initiation is integrated in other signaling pathways.

References

Aida M, Beis D, Heidstra R, Willemsen V, Blilou I, Galinha C, Nussaume L, Noh YS, Amasino R and Scheres B. (2004). The *PLETHORA* genes mediate patterning of the Arabidopsis root stem cell niche. Cell. 119(1): 109-120.

Amador V, Monte E, García-Martínez JL and Prat S. (2001) Gibberellins signal nuclear import of PHOR1, a photoperiod-responsive protein with homology to Drosophila armadillo. Cell. 106(3): 343-354.

Berleth T and Jürgens G. (1993). The role of the *MONOPTEROS* gene in organizing the basal body region of the Arabidopsis embryo. Development. 118: 575-587.

Blilou I, Xu J, Wildwater M, Willemsen V, Paponov I, Friml J, Heidstra R, Aida M, Palme K and Scheres B. (2005). The PIN auxin efflux facilitator network controls growth and patterning in Arabidopsis roots. Nature. 433(7021): 39-44.

De Smet I, Lau S, Voss U, Vanneste S, Benjamins R, Rademacher EH, Schlereth A, De Rybel B, Vassileva V, Grunewald W, Naudts M, Levesque MP, Ehrismann JS, Inzé D, Luschnig C, Benfey PN, Weijers D, Van Montagu MC, Bennett MJ, Jürgens G, Beeckman T. (2010). Bi-modular auxin response controls organogenesis in Arabidopsis. Proc Natl Acad Sci U S A. 107(6): 2705-2710.

De Smet I, Vassileva V, De Rybel B, Levesque MP, Grunewald W, Van Damme D, Van Noorden G, Naudts M, Van Isterdael G, De Clercq R, Wang JY, Meuli N, Vanneste S, Friml J, Hilson P, Jürgens G, Ingram GC, Inzé D, Benfey PN and Beeckman T. (2008). Receptor-like kinase ACR4 restricts formative cell divisions in the Arabidopsis root. Science. 322(5901): 594-597.

De Smet I, Voss U, Jürgens G and Beeckman T. (2009). Receptor-like kinases shape the plant. Nat Cell Biol. 11(10): 1166-1173.

Eulgem T, Rushton PJ, Robatzek S and Somssich E. (2000). The WRKY superfamily of plant transcription factors. Trends Plant Science. 5(5): 199-206.

Friml J, Vieten A, Sauer M, Weijers D, Schwarz H, Hamann T, Offringa R and Jürgens G. (2003). Efflux-dependent auxin gradients establish the apical-basal axis of Arabidopsis. Nature.

426(6963): 147-53.

Galinha C, Hofhuis H, Luijten M, Willemsen V, Blilou I, Heidstra R and Scheres B. (2007). PLETHORA proteins as dose-dependent master regulators of Arabidopsis root development. Nature. 449(7165): 1053-7.

Hamann T, Benkova E, Bäurle I, Kientz M and Jürgens G. (2002). The Arabidopsis *BODENLOS* gene encodes an auxin response protein inhibiting MONOPTEROS-mediated embryo patterning. Genes Dev. 16(13): 1610-5.

Hardtke CS and Berleth T. (1998). The Arabidopsis gene *MONOPTEROS* encodes a transcription factor mediating embryo axis formation and vascular development. EMBO J. 17(5):1405-1411.

Jarillo JA, Piñeiro M, Cubas P, Martínez-Zapater JM. (2009). Chromatin remodeling in plant development. Int J Dev Biol. 53(8-10):1581-1596.

Kim KC, Lai Z, Fan B and Chen Z. (2008). Arabidopsis WRKY38 and WRKY62 transcription factors interact with histone deacetylase 19 in basal defence. Plant Cell. 20(9): 2357-2371.

Kuroha T, Tokunaga H, Kojima M, Ueda N, Ishida T, Nagawa S, Fukuda H, Sugimoto K and Sakakibara H. (2009). Functional analyses of LONELY GUY cytokinin-activating enzymes reveal the importance of the direct activation pathway in Arabidopsis. Plant Cell. 21(10): 3152-69.

Lau S, De Smet I, Kolb M, Meinhardt H and Jürgens G. (2011). Auxin triggers a genetic switch. Nat Cell Biol. 13(5): 611-615.

Lau S, Slane D, Herud O, Kong J and Jürgens G. (2012). Early Embryogenesis in Flowering Plants: Setting Up the Basic Body Pattern. Annu Rev Plant Biol. 2011 May 4. [Epub ahead of print]

Long JA, Woody S, Poethig S, Meyerowitz EM and Barton MK. (2002). Transformation of shoots into roots in Arabidopsis embryos mutant at the *TOPLESS* locus. Development. 129(12):2797-2806.

Mellor J. (2006). It takes a PHD to read the histone code. Cell. 126(1): 22-24.

Meng L. (2012). Roles of secreted peptides in intercellular communication and root development. Plant Sci. 183: 106-114.

Matsuzaki Y, Ogawa-Ohnishi M, Mori A and Matsubayashi Y. (2010). Secreted peptide signals required for maintenance of root stem cell niche in Arabidopsis. Science. 329(5995): 1065-1067.

Müller B and Sheen J. (2008). Cytokinin and auxin interaction in root stem-cell specification during embryogenesis. Nature. 453(7198): 1094-1097**.**

Nawy T, Bayer M, Mravic J, Friml J, Birnbaum KD and Lukowitz W. (2010). The GATA factor HANABA TARANU is required to position the proembryo boundary in the early Arabidopsis embryo. Dev Cell. 19(1): 103-113.

Van Norman JM, Breakfield NW and Benfey PN. (2011). Intercellular communication during plant development. Plant Cell. 23(3): 855-64.

Rademacher EH, Lokerse AS, Schlereth A, Llavata-Peris CI, Bayer M, Kientz M, Freire Rios A, Borst JW, Lukowitz W, Jürgens G and Weijers D. (2012). Different auxin response machineries control distinct cell fates in the early plant embryo. Dev Cell. 22(1): 211-222.

Rademacher EH, Möller B, Lokerse AS, Llavata-Peris CI, van den Berg W and Weijers D. (2011). A cellular expression map of the Arabidopsis *AUXIN RESPONSE FACTOR* gene family. Plant J. 68(4): 597-606.

Reyes JC. (2006). Chromatin modifiers that control plant development. Curr Opin Plant Biol. 9(1): 21-27.

Sarkar AK, Luijten M, Miyashima S, Lenhard M, Hashimoto T, Nakajima K, Scheres B, Heidstra R and Laux T. (2007). Conserved factors regulate signalling in *Arabidopsis thaliana* shoot and root stem cell organizers. Nature. 446(7137): 811-814.

Scheres B, Di Laurenzio L, Willemsen V, Hauser MT, Janmaat K, Weisbeek P and Benfey P. (1995). Mutations affecting the radial organization of the Arabidopsis root display defects throughout the embryonic axis. Development 121: 53-62.

Scheres B. (2007). Stem-cell niches: nursery rhymes across kingdoms. Nat Rev Mol Cell Biol. 8(5):345-354.

Saiga S, Furumizu C, Yokoyama R, Kurata T, Sato S, Kato T, Tabata S, Suzuki M and Komeda Y. (2008). The Arabidopsis *OBERON1* and *OBERON2* genes encode plant homeodomain finger proteins and are required for apical meristem maintenance. Development. 135(10): 1751-1759.

Saiga S, Möller B, Watanabe A, Abe M, Weijers D, and Komeda Y. (2012). Control of embryonic meristem initiation in *Arabidopsis* by PHD finger protein complexes. Development. *In press*.

Stahl Y, Wink RH, Ingram GC and Simon R. (2009). A signaling module controlling the stem cell niche in Arabidopsis root meristems. Curr Biol. 19(11): 909-914.

Thomas CL, Schmidt D, Bayer EM, Dreos R and Maule AJ. (2009). Arabidopsis plant homeodomain finger proteins operate downstream of auxin accumulation in specifying the vasculature and primary root meristem. Plant J. 59(3): 426-436.

Tokunaga H, Kojima M, Kuroha T, Ishida T, Sugimoto K, Kiba T and Sakakibara H. (2011). Arabidopsis lonely guy (LOG) multiple mutants reveal a central role of the LOG-dependent pathway in cytokinin activation. Plant J. doi: 10.1111/j.1365-313X.2011.04795.x.

Ugartechea-Chirino Y, Swarup R, Swarup K, Péret B, Whitworth M, Bennett M and Bougourd S. (2010). The *AUX1 LAX* family of auxin influx carriers is required for the establishment of embryonic root cell organization in *Arabidopsis thaliana*. Ann Bot. 105(2): 277-289.

Ueda M, Zhang Z and Laux T. (2011). Transcriptional activation of Arabidopsis axis patterning genes *WOX8/9* links zygote polarity to embryo development. Dev Cell. 20(2): 264-270.

Van den Berg C, Willemsen V, Hage W, Weisbeek P and Scheres B. (1995). Cell fate in the Arabidopsis root meristem determined by directional signalling. Nature. 378(6552): 62-65.

Van den Berg C, Willemsen V, Hendriks G, Weisbeek P and Scheres B. (1997). Short-range control of cell differentiation in the Arabidopsis root meristem. Nature. 390(6657): 287-289.

Weijers D, Schlereth A, Ehrismann JS, Schwank G, Kientz M and Jürgens G. (2006). Auxin triggers transient local signaling for cell specification in Arabidopsis embryogenesis. Dev Cell. 10(2): 265-270.

Wysocka-Diller JW, Helariutta Y, Fukaki H, Malamy JE and Benfey PN. (2000). Molecular analysis of SCARECROW function reveals a radial patterning mechanism common to root and shoot. Development. 127(3): 595-603.

Zhou W, Wei L, Xu J, Zhai Q, Jiang H, Chen R, Chen Q, Sun J, Chu J, Zhu L, Liu CM and Li C. (2010). Arabidopsis Tyrosylprotein sulfotransferase acts in the auxin/PLETHORA pathway in regulating postembryonic maintenance of the root stem cell niche. Plant Cell. 22(11): 3692-3709.

Summary

Plants produce a basic body plan during embryo development with root and shoot meristems located at opposite ends. These meristems consist of organizing cells and the surrounding tissue-specific stem cells that continuously supply new tissue cells during plant life. In **Chapter 1** we discussed the specification events that result in this basic body plan, with emphasis on the prominent role of the plant hormone auxin in most of these patterning steps.

The AUXIN RESPONSE FACTOR5/MONOPTEROS (ARF5/MP) transcription factor is the main executer of auxin signaling during embryo development. MP is required to specify the precursor of the organizer cell - called hypophysis - in the embryonic root meristem in part by promoting the transport of auxin into this cell, but its direct targets had until recently not been identified. In **Chapter 2** we performed microarray-based transcript profiling on seedlings and identified four *TARGET OF MP (TMO)* genes. These *TMO* genes encode transcription factors that contribute to MP-dependent embryonic root formation. We show that the TMO7 protein is transported from the proembryo to the hypophysis cell where it contributes to the specification of this cell. The identification of this novel intercellular signal explains part of the non cell-autonomous action of MP in root initiation.

In **Chapter 3** we investigated the role of the bHLH transcription factor TMO5 in embryonic root initiation. We showed that TMO5 and its closest homologues are redundantly required for formative divisions of vascular cells in the embryonic and postembryonic root meristem. Members of the TMO5 subclade interact *in vivo* with the distantly related LONESOME HIGHWAY (LHW) bHLH transcription factor and its closest homologue. The accumulation of TMO5 and LHW protein overlaps in a small subpopulation of vascular cells in the root meristem that are close to the organizing center, and could represent a stem cell pool. Indeed, co-misexpression of TMO5 and LHW results in ectopic stem cell-like divisions in non-vascular tissues. Our data suggest that the TMO5/LHW dimer defines a vascular stem cell population that is required for indeterminate growth.

In **Chapter 4** we extended our transcript profiling in search of MP target genes by performing a microarray experiment on embryos in which MP activity was locally inhibited in cells that contribute to the future root meristem. We identified several genes that are specifically expressed in either the first vascular or ground tissue cells of the developing root meristem in the early embryo. Furthermore, we

showed that MP activates expression of these genes in the embryo. These results suggest a role for MP to specify the first vascular and ground tissue cells of the embryonic root and identifies genes that may mediate MP function in this process.

In **Chapter 5** we further explored a potential role for MP in the first ground tissue cells of the embryonic root meristem that was suggested by the MP-dependent expression of genes in the first ground tissue cells (Chapter 4). We showed that MP is required for the asymmetric division of the first ground tissue cells in the early embryo, while the well-studied transcription factor SHORTROOT (SHR) regulates later cell divisions in ground tissue daughter cells. Moreover, we show that MP activates transcription specifically in the embryonic ground tissue cells in a SHR-independent pathway. These results suggest that MP is required prior to the requirement for SHR to activate transcription and to regulate cell divisions in the ground tissue cells of the early embryo.

The spatially different expression patterns of genes that are activated by MP in the early embryo suggest that MP could function in one or more protein complexes to locally regulate gene transcription. In **Chapter 6** we optimized an affinity purification procedure to identify putative MP-interacting proteins in the embryo. Despite extensive optimization, we did not identify any MP interacting protein, whereas we could identify interacting proteins for several other nuclear proteins. Therefore, further optimization of this procedure is required to identify the potentially transient or unstable MP protein complexes during embryonic root formation.

In **Chapter 7** we discuss novel insights into the mechanisms of embryonic root initiation that emerge from the results described in this thesis. These results collectively show that MP activity is involved in diverse aspects of embryonic root initiation, and suggest that MP is required to specify nearly all cell types that form the embryonic root meristem.

Nederlandse samenvatting

De ontwikkeling van een plant begint met de bevruchting van een eicel in het zaad, dat zich in het vruchtbeginsel bevindt. De eicel begint vervolgens te delen en vormt zo een embryo met aan de uiteinden de groeitoppen (meristemen) voor wortel en scheut. Beide meristemen bevatten stamcellen die gedurende het hele leven van de plant blijven delen. De stamcellen genereren nieuwe cellen voor de verschillende weefseltypes van de wortel en scheut, en zorgen ervoor dat de plant kan blijven groeien. De organiserende cellen liggen centraal in het meristeem en zorgen ervoor dat de stamcellen hun eigenschappen behouden. In **Hoofdstuk 1** wordt besproken wat er bekend is over de moleculaire processen die nodig zijn om een embryo te vormen met stamcellen en organiserende cellen. Het lijkt erop dat de positie van cellen in het vroege embryo bepaalt welke eigenschappen deze cellen verkrijgen, en dit kan sterk verschillen al naar gelang de positie van de cel in het vroege embryo. Dit proces waarbij cellen verschillende identiteiten aannemen tijdens de embryonale ontwikkeling van een organisme, wordt patroonvorming genoemd. Het plantenhormoon auxine speelt een sturende rol bij de patroonvorming in het vroege plantenembryo.

In het vroege embryo stuurt het plantenhormoon auxine allerlei processen aan door het activeren van AUXINE RESPONS FACTOR5 (ARF5), ook wel MONOPTEROS (MP) genoemd. MP is een transcriptiefactor. Dit houdt in dat MP de transcriptie van andere genen aanstuurt, en zo bepaalt welke processen er in een cel plaatsvinden. Het is bekend dat de activiteit van MP noodzakelijk is om een embryonale wortel te vormen. Om precies te zijn is de activiteit van MP vereist om de identiteit van de hypofyse cel vast te leggen die iets later tijdens de embryogenese de organiserende cellen van het meristeem zal genereren. MP doet dit onder andere door ervoor te zorgen dat auxine naar deze cel wordt getransporteerd vanuit de naastgelegen cellen. Echter, op basis van eerder onderzoek was duidelijk dat auxine alleen niet voldoende is om de identiteit van de hypofyse te bepalen. Tot nu toe was echter nog niet bekend welke genen MP direct aanstuurt. In **Hoofdstuk 2** laten we zien dat MP vier *TARGET OF MONOPTEROS (TMO)* genen aanschakelt. Deze *TMO* genen coderen zelf ook voor transcriptiefactoren die een bijdrage leveren aan embryonale wortelvorming. Verder laten we zien dat het TMO7 eiwit wordt getransporteerd naar de hypofyse cel, en hier bijdraagt aan het vastleggen van de identiteit van deze cel. Aangezien MP zelf niet actief is in de hypofyse cel, verklaart dit ten dele hoe MP de eigenschappen van de naastgelegen cel kan aansturen.

In **Hoofdstuk 3** hebben we onderzocht wat de rol is van de bHLH transcriptie factor TMO5 tijdens de embryonale wortelvorming. We hebben laten zien dat TMO5 samen met drie andere, verwante, eiwitten nodig is voor celdelingen in het vaatweefsel van het embryonale en post-embryonale meristeem in de wortel. TMO5 en zijn drie naaste homologen binden aan de LONESOME HIGHWAY bHLH transcriptiefactor en zijn naaste homoloog. De hoogste concentraties TMO5 en LHW eiwit komen samen in vaatweefselcellen die het dichtst bij de organiserende cellen van het wortelmeristeem liggen. Deze cellen reguleren mogelijk alle celdelingen in het vaatweefsel, en zouden mogelijk de stamcelpopulatie van dit weefsel kunnen zijn. Wanneer de activiteit van zowel TMO5 en LHW experimenteel wordt aangeschakeld in cellen buiten het vaatweefsel, worden er formatieve celdelingen (delingen waarbij nieuwe cellagen ontstaan) waargenomen in andere weefseltypes. Alle resultaten samen suggereren dat de TMO5/LHW dimeer nodig is voor zowel de aanleg van het vaatweefsel in het embryo, als voor het in stand houden van dit weefsel in de groeiende wortel.

In **Hoofdstuk 4** hebben we een genoom-brede aanpak gebruikt om nieuwe genen te vinden die door MP worden aangeschakeld in het vroege embryo. Hiervoor hebben we de activiteit van MP specifiek geremd in die cellen van het vroege embryo die het wortel meristeem gaan vormen, en vervolgens gekeken van welke genen de transcriptie verandert. Op deze manier hebben we genen kunnen vinden die specifiek tot expressie komen in het vaatweefsel of grondweefsel van het vroege embryo. Verder hebben we laten zien dat de expressie van deze genen in het vroege embryo daadwerkelijk afhangt van de activiteit van MP. Deze resultaten suggereren dat MP nodig is voor het vastleggen van de identiteit van de eerste vaatweefsel- en grondweefsel cellen in het vroege embryo.

De MP-afhankelijke expressie van genen in de eerste grondweefsel cellen van het vroege embryo suggereert dat MP betrokken is bij de aanleg van deze cellen (Hoofdstuk 4). In **Hoofdstuk 5** zijn we hier verder op ingegaan. We hebben laten zien dat de activiteit van MP nodig is om de eerste grondweefsel cellen van het embryonale wortelmersiteem correct te laten delen. Bovendien lijkt de SHORTROOT (SHR) transcriptiefactor, waarvan bekend is dat deze de identiteit van het grondweefsel controleert, pas later nodig tijdens de embryogenese om de delingen van grondweefsel dochtercellen te reguleren. Verder hebben we laten zien dat MP de transcriptie van één gen specifiek activeert in de eerste grondweefsel cellen en daarbij geen activiteit van SHR nodig heeft. Tezamen suggereren deze resultaten dat de activiteit van MP vroeger vereist is dan die van SHR om de celdeling te reguleren en de transcriptie te activeren in de eerste grondweefsel cellen van het

vroege embryo.

In **Hoofdstuk 6** hebben we een procedure geoptimaliseerd met als doel om interactoren te vinden van MP in het embryo. Ondanks succesvolle optimalisatie en zeer goede resultaten met verschillende andere GFP-gemarkeerde eiwitten, is het zelfs na vele pogingen niet gelukt om interactoren van GFP-gemarkeerd MP te vinden. Verdere optimalisatie van de procedure is nodig om de wellicht onstabiele of vluchtige interacties die MP aangaat met andere eiwitten bloot te leggen.

In **Hoofdstuk 7** wordt besproken tot welke nieuwe inzichten in de embryonale wortelvorming de resultaten in dit proefschrift hebben geleid. Het was al bekend dat MP nodig is voor het vastleggen van de identiteit van cellen die de organiserende cellen van het wortelmeristeem gaan vormen. De resultaten uit dit proefschrift suggereren dat MP waarschijnlijk nodig is voor het vastleggen van de identiteit van vrijwel alle celtypes van het wortelmeristeem in het vroege embryo.

Publications

De Rybel B*, **Möller B***, Yoshida S, Grabowicz I, Barbier de Reuille P, Boeren S, Smith RS, Borst JW and Weijers D. Genetic control of stem cell specification in the plant embryo. Under revision.
* These authors contributed equally

Saiga S, **Möller B**, Watanabe A, Abe M, Weijers D, and Komeda Y. (2012). Control of embryonic meristem initiation in Arabidopsis by PHD finger protein complexes. Development. 139(8): 1391-1398.

Llavata-Peris CI, Lokerse AS, **Möller B,** De Rybel B and Weijers D. (2012). Imaging of phenotypes, gene expression and protein localization during embryonic root formation in Arabidopsis. Meth Mol Biol. *In press*.

Rademacher EH*, **Möller B***, Lokerse AS*, Llavata-Peris CI, van den Berg W and Weijers D. (2011). A cellular expression map of the Arabidopsis *AUXIN RESPONSE FACTOR* gene family. Plant J. 68(4): 597-606.
* These authors contributed equally

Zwiewka M, Feraru E, **Möller B**, Hwang I, Feraru MI, Kleine-Vehn J, Weijers D and Friml J. (2011). The AP-3 adaptor complex is required for vacuolar function in Arabidopsis. Cell Res. 21(12): 1711-1722.

De Rybel B, van den Berg W, Lokerse A, Liao CY, van Mourik H, **Möller B**, Peris CL and Weijers D. (2011). A versatile set of ligation-independent cloning vectors for functional studies in plants. Plant Physiol. 156(3): 1292-1299.

De Rybel B, Vassileva V, Parizot B, Demeulenaere M, Grunewald W, Audenaert D, Van Campenhout J, Overvoorde P, Jansen L, Vanneste S, **Möller B**, Wilson M, Holman T, Van Isterdael G, Brunoud G, Vuylsteke M, Vernoux T, De Veylder L, Inzé D, Weijers D, Bennett MJ and Beeckman T. (2010). A novel aux/IAA28 signaling cascade activates GATA23-dependent specification of lateral root founder cell identity. Curr Biol. 20(19): 1697-1706.

Schlereth A, **Möller B**, Liu W, Kientz M, Flipse J, Rademacher EH, Schmid M, Jürgens G and Weijers D. (2010). MONOPTEROS controls embryonic root initiation by regulating a mobile transcription factor. Nature. 464(7290): 913-916.

Möller B and Weijers D. (2009). Auxin control of embryo patterning. Cold Spring Harb Perspect Biol. 1(5):a001545.

Smith MR, Willmann MR, Wu G, Berardini TZ, **Möller B**, Weijers D and Poethig RS. (2009). Cyclophilin 40 is required for microRNA activity in Arabidopsis. Proc Natl Acad Sci U S A. 106(13): 5424-5429.

Education Statement of the Graduate School
Experimental Plant Sciences

The Graduate School EXPERIMENTAL PLANT SCIENCES

Issued to: Barbara Möller
Date: 1 June 2012
Group: Laboratory of Biochemistry, Wageningen University & Research Centre

1) Start-up phase	date
First presentation of your project	
Transcriptional targets of the MONOPTEROS protein complex during embryonic root formation	Jun 07, 2007
Writing a review or book chapter	
Bookchapter "Auxin control of embryo patterning", Cold Spring Harb. Perspect. Biol. 2009; 1: a001545	2009
Subtotal Start-up Phase	*6.5 credits**

2) Scientific Exposure	date
EPS PhD student days	
EPS PhD student day, Wageningen University	Sep 13, 2007
EPS PhD Joint Retreat, Wageningen University	Oct 02-03, 2008
EPS PhD student day, Naturalis Leiden	Feb 26, 2009
EPS theme 1 'Developmental Biology of Plants', Wageningen University	Oct 11, 2007
EPS theme 1 'Developmental Biology of Plants', Leiden University	Jan 30, 2009
EPS theme 1 'Developmental Biology of Plants', Wageningen University	Jan 28, 2010
NWO Lunteren days and other National Platforms	
ALW meeting 'Experimental Plant Sciences', Lunteren	Apr 02-03, 2007
ALW meeting 'Experimental Plant Sciences', Lunteren	Apr 07-08, 2008
ALW meeting 'Experimental Plant Sciences', Lunteren	Apr 06-07, 2009
ALW meeting 'Experimental Plant Sciences', Lunteren	Apr 19-20, 2010
Netherlands Proteomics Centre Progress Meeting, Utrecht	Feb 19, 2007
Netherlands Proteomics Centre Progress Meeting, Utrecht	Jan 26, 2009
Seminars (series), workshops and symposia	
Thursday Seminars Biochemistry in 2008: Maarten Jongsma (NL), Delphine Chinchilla (Switserland), Niko Geldner (Switserland), Jan Lohmann (Germany), Anna Koltunow (Australia)	2008
EPS Flying Seminars in 2008: Richard Vierstra, Simon Gilroy, Zhenbiao Yang	2008
Minisymposium Biochemistry Department	Feb 21, 2008
Joint Meeting groups prof. Sacco de Vries and prof. Gerco Anganent	May 28, 2008
Thursday Seminars Biochemistry in 2009: Cyril Zipfel (UK), Dorus Gadella (NL), Bruno Müller (Switserland), Klaus Harter (Germany)	2009
Joint Meeting groups dr. Dolf Weijers and prof. Ben Scheres, Utrecht	Jun 22, 2009
Thursday Seminars Biochemistry in 2010: Maarten Merkx (NL), M. Ubbink (NL), Roeland Boer (Spain), Teva Vernoux (France), Dirk Bosch (NL), Richard Smith (Switzerland), Yoselin Benitez Alfonso (UK), Saiko Yoshida (Switzerland)	2010
Expectations Career Day	Nov 19, 2010
Thursday Seminars Biochemistry in 2011: Renier van de Hoorn (Germany), Joakim Palovaara (Sweden), S. Kepinski (UK), W. Lukowitz (USA)	2011
Joint Meeting groups dr. Dolf Weijers and prof. Ben Scheres, Utrecht	Feb 11, 2011
Seminar plus	
Seminar plus with prof. Richard Vierstra and prof. Zhenbiao Yang	Apr & Jun, 2008
International symposia and congresses	
SFB Symposium, Max Planck Institute Cologne (Germany)	Sep 03-04, 2007
Symposium Max Planck Institute Tübingen (Germany)	May 02-03, 2008
Auxin conference 2008, Marrakech (Morocco)	Oct 05-09, 2008
Auxins and Cytokinins in Plant Development (ACDP), Prague (Czech Republic)	Jul 11-14, 2009
Plant Growth Biology and Modeling 2011, Elche (Spain)	Sep 19-21, 2011
Presentations	
Poster presentation at NWO Lunteren days 2007	Apr 02-03, 2007
Oral presentation at joint meeting groups prof. Sacco de Vries and prof. Gerco Angenent	May 28, 2008
Poster presentation at Auxin Conference 2008, Marrakech	Oct 05-09, 2008
Oral presentation at EPS theme I symposium 2009, Leiden	Jan 30, 2009
Poster presentation at ACPD 2009, Prague	Jul 11-14, 2009
Oral presentation at ACPD 2009, Prague	July 11-14, 2009
Poster presentation at PGBM 2011, Spain	Sep 19-21, 2011
IAB interview	Dec 04, 2009
Excursions	
Scientific PhD Excursion group prof. Sacco de Vries, Barcelona	Apr 21-25, 2009
PhD excursion Monsanto site Wageningen	Jan 27, 2010
PCDI Life Sciences Company visit	Jun 23, 2011
Subtotal Scientific Exposure	*23.6 credits**

3) In-Depth Studies	date
EPS courses or other PhD courses	
PhD Summerschool 'Environmental Signaling', Utrecht University	Aug 27-29, 2007
Journal club	
Participation in a literature discussion group	2007-2011
Subtotal In-Depth Studies	*3.9 credits**

4) Personal development	date
Skill training courses	
PhD presentation skills	October 06 and 20, 2009
Teaching and supervising thesis students	Feb 22-23, 2010
Scientific Writing	Mar 10-Apr 28, 2010
Teaching methodology and skills for PhD students	Jan 20-21 & Apr 04-05, 2011
Subtotal Personal Development	*5.2 credits**

TOTAL NUMBER OF CREDIT POINTS*	**39,2**

Herewith the Graduate School declares that the PhD candidate has complied with the educational requirements set by the Educational Committee of EPS which comprises of a minimum total of 30 ECTS credits

** A credit represents a normative study load of 28 hours of study.*

The research presented in this thesis was performed at the Biochemistry Department, Wageningen University, and was financially supported by the Netherlands Organization for Scientific Research (NWO; ALW-VIDI 864.06.012).

Cover design by Bas Smits
Layout by Barbara Möller

Printed by Wöhrmann Print service B.V. Zutphen, the Netherlands